

**ADVANCED CONTROL STRATEGIES FOR
AUTOMATIC DRUG DELIVERY TO
REGULATE ANESTHESIA DURING SURGERY**

YELNEEDI SREENIVAS

NATIONAL UNIVERSITY OF SINGAPORE

2009

**ADVANCED CONTROL STRATEGIES FOR
AUTOMATIC DRUG DELIVERY TO
REGULATE ANESTHESIA DURING SURGERY**

YELNEEDI SREENIVAS

(M.Tech., Indian Institute of Technology Madras, India)

(B.Tech., Andhra University Engineering College, India)

A THESIS SUBMITTED

FOR THE DEGREE OF DOCTOR OF PHILOSOPHY

DEPARTMENT OF CHEMICAL & BIOMOLECULAR ENGINEERING

NATIONAL UNIVERSITY OF SINGAPORE

2009

ACKNOWLEDGMENTS

I am highly indebted to my thesis advisors, A/Prof. Lakshminarayanan S. and Prof. Rangaiah G.P. for their endless commitment to directing research, and the affection they showed me for all these years. They have provided me excellent guidance to work enthusiastically and develop critical thinking abilities. I am extremely thankful to them for their invaluable suggestions and constant encouragement. I learned many other things apart from technical matters which will definitely help me in achieving my future career goals. I grateful by acknowledge their hard work and the professional dedication to the field of 'Process Systems Engineering' .

I would like to convey my sincere thanks to A/Prof. Chen Fun Gee Edward (Head of the Department) and A/Prof. Ti Lian Kah, Department of Anaesthesia, National University Hospital, Singapore for their valuable help in providing access to surgical theaters, providing clinical data and feedback on the simulation results.

I am extremely thankful to my thesis committee members, A/Prof. Chiu Min-Sen and Dr. Lee Dong-Yup for their insightful comments and suggestions.

I would like thank my parents and sister Sandhya for their everlasting affection, love and constant support throughout my life.

I am extremely thankful to my beloved wife - Surekha who always encouraged and supported me with her deepest love and affection all these days.

I gratefully acknowledge the *National University of Singapore* which has provided me excellent research facilities and financial support for my doctoral studies in the form of scholarship for all these four years.

Many thanks to Mr. Boey, Mdm. Koh and other technical staff of the Department of Chemical & Biomolecular Engineering for their kind assistance in providing the necessary laboratory facilities and computational resources.

Last but not the least, I am lucky to have many friends who always helped me and kept me cheerful. I would like to thank my labmates Sundar Raj Thangavelu, Raghuraj Rao, Sukumar Balaji, May Su Tun, Rohit Ramachandran, Lakshmi Kiran Kanchi, Melissa Angeline Setiawan, Loganathan and Prem Krishnan for their valuable technical discussions and kind support. My sincerest thanks to my close friends Sreenivasa Reddy Punireddy, Saradhibabu Daneti and Ramarao Vemula for the concern they showed me all these days. I am immensely thankful to all my flatmates and roommates Venkateswarlu Ayineedi, Ramprasad Poturaju, Sumanth Karnati, Vijay Butte, Satyanarayana Tirunahari, Vempati Srinivasa Rao, Anjaiah Nalaparaju and Nanda Kishore for sharing the joy of togetherness. I am thankful to my friends Mekapati Srinivas, Sudhakar Jonnalagadda, Sudhir Hulikal Ranganath, N.V.S.N. Murthy Konda, Naveen Agarwal, Suresh Selvarasu for spending the time together in tea-time and technical discussions. Special thanks to Satyen Gautam, and the couple Vivek Vasudevan & Karthiga Nagarajan for spending joyful time during a US conference trip. I am also thankful to my friends Umamaheswara Rao, Raajan, Bhaskar, Ravi Khambam, Madan, Sonti Sreeram, Venu, Mukta Bansal, Sendhil Kumar Poornachary, Thaneer Malai Perumal, Sridharan Srinath, Sudaramurthy Jayaraman, Sivasangari Jnanasambhandam, Babarao Ravichandar, and Raju Gupta for their good company. Also, I am extremely thankful to one of the nice couples I have seen, B.T.V. Ramana and Deepthi for their kind support in many ways.

TABLE OF CONTENTS

	Page
Summary	ix
List of Tables	xi
List of Figures	xiii
Abbreviations	xvii
Nomenclature	xix
1 Introduction	1
1.1 Anesthesia and its Regulation	1
1.2 Drugs and their Effect during Anesthesia	4
1.2.1 Anesthetics	4
1.2.2 Analgesics	6
1.2.3 Neuromuscular blocking agents	7
1.3 Measuring and Monitoring of Anesthesia	8
1.3.1 Measuring and monitoring of hypnosis	9
1.3.2 Measuring and monitoring of analgesia	11
1.4 Conducting the Anesthesia Process	11
1.4.1 Induction	11
1.4.2 Maintenance	12
1.4.3 Emergence	14
1.5 Modeling Anesthesia	14
1.6 Automatic Control Strategies to Regulate Anesthesia	17
1.7 Motivation and Scope of the Work	19
1.8 Organization of the Thesis	22
2 Literature Review	26
2.1 Feedback Control in Anesthesia	26
2.2 Feedback Control for Hypnosis	27
2.3 Feedback Control for Analgesia	31

	Page
2.4 Feedback Control for Simultaneous Regulation of Hypnosis and Analgesia	33
2.5 Summary	37
3 Evaluation of PID, Cascade, Model Predictive and RTDA Controllers for Regulation of Hypnosis with Isoflurane	39
3.1 Introduction	39
3.2 The Mathematical Model	40
3.2.1 Model for the breathing system	42
3.2.2 Pharmacokinetic model	43
3.2.3 Pharmacodynamic model	44
3.3 Patient Model Variability Analysis	45
3.4 Controller Design	48
3.4.1 PI controller design	48
3.4.2 PID controller design	49
3.4.3 Cascade controllers design	50
3.4.4 Model predictive controller (MPC) design	52
3.4.5 Robustness, set-point tracking, disturbance rejection, aggressiveness (RTDA) controller design	56
3.5 Evaluation of Controllers	59
3.6 Performance of Controllers	64
3.7 Controller Performance in the Absence of BIS Signal	71
3.8 Conclusions	76
4 A comparative study of three advanced controllers for the regulation of hypnosis with isoflurane	77
4.1 Introduction	77
4.2 Patient Model - Modeling Hypnosis	78
4.3 Controller Design	78
4.3.1 Cascade internal model controller (CIMC) Design	78
4.3.2 Cascade modeling error compensation (CMEC) controller design	79
4.3.3 Model predictive controller (MPC) design	80
4.4 Results and Discussion	80

	Page
4.4.1	Tuning of MPC 81
4.4.2	Comparison of the performances of MPC, CIMC and CMEC controllers 82
4.4.3	Robustness comparison 84
4.4.4	Performance comparison for a step change in BIS and sudden disturbance in Q_0 during the surgery 88
4.4.5	Performance comparison for measurement noise in BIS signal during the surgery 92
4.5	Conclusions 94
5	Advanced control strategies for the regulation of hypnosis with propofol 95
5.1	Introduction 95
5.2	Mathematical Model for BIS Response to Propofol 96
5.2.1	Pharmacokinetic model 97
5.2.2	Pharmacodynamic model 99
5.3	Controller Design 100
5.3.1	Proportional-integral-derivative (PID) controller 101
5.3.2	Internal model controller (IMC) 101
5.3.3	Modeling error compensation (MEC) controller 102
5.3.4	Model predictive controller (MPC) 103
5.4	Results and Discussion 104
5.4.1	Closed-loop performance 105
5.4.2	Robustness comparison 109
5.4.3	Performance comparison for disturbances and measurement noise in the BIS signal 116
5.4.4	Performance comparison for set-point changes in BIS during surgery 124
5.5	Comparison of the performance with the RTDA Controller 130
5.5.1	Performance comparison for a step change in BIS during surgery 131
5.5.2	Robustness comparison 133
5.5.3	Performance comparison for a sudden disturbance in BIS signal 134
5.6	Conclusions 136

	Page
6 Simultaneous Regulation of Hypnosis and Analgesia Using Model Predictive Control	137
6.1 Introduction	137
6.2 Modeling Hypnosis and Analgesia	138
6.2.1 Pharmacokinetic model	140
6.2.2 Pharmacodynamic interaction model for BIS response to propofol and remifentanil	141
6.2.3 Pharmacodynamic model for MAP response to remifentanil	145
6.3 Controllers Studied	145
6.3.1 Model predictive controller (MPC)	145
6.3.2 Proportional-integral-derivative (PID) controller	148
6.4 Results and Discussion	149
6.4.1 Tuning of controllers	150
6.4.2 Performance of MPC and PID for step type set-point changes in BIS and MAP during surgery	156
6.4.3 Performance of MPC and PID for disturbance rejection in BIS and MAP during surgery	166
6.5 Conclusions	170
7 Conclusions and Recommendations	171
7.1 Conclusions	171
7.2 Recommendations for Future Work	174
7.2.1 Simultaneous control of hypnosis, analgesia and skeletal muscle relaxation	174
7.2.2 Fault-tolerant control	175
7.2.3 Nonlinear model-based control	176
7.2.4 Clinical validation	176
References	177
Appendix A Presentations and Publications of the Author	193
Appendix B Curriculum Vitae of the Author	195

SUMMARY

Patients undergoing surgery must be maintained at a certain anesthetic state (loss of sensation) in order to prevent the awareness of pain and to attenuate the body's stress response to injury. In order to provide safe and adequate anesthesia, the anesthesiologist must guarantee hypnosis and analgesia (pain relief). Hypnosis, referred to as depth of anesthesia, is a general term indicating unconsciousness and absence of postoperative recall of events. Generally, anesthesiologists use bispectral index (BIS) and mean arterial pressure (MAP) as the indirect measurements of hypnosis and analgesia, respectively. Anesthetics (or hypnotics) and opioids are administered to regulate hypnosis and analgesia, respectively in the patient during the surgery.

Automation of anesthesia is very useful as it will provide more time and flexibility to anesthesiologists to focus on critical issues that may arise during the surgery. Until now, much of the research in this area has dealt with the automatic manipulation of single drug and manual administration of other drugs. Also, there have been only a few studies on using model predictive control (MPC) for anesthesia regulation. The objective of this work is to develop the MPC control strategies for regulation of hypnosis with various drugs and thoroughly evaluate and compare MPC controller's performance with the performance of other control structures. The second objective of this study is to develop and evaluate the MPC control structure to find the best infusion rates of the anesthetic and analgesic drugs by considering drug interaction for simultaneous regulation of hypnosis and analgesia such that the patient's anesthetic state is well regulated even as the side effects (due to overdose) are minimized. This assures cost reduction as a result of minimized drug consumption and shortened postoperative recovery.

Specifically, MPC was designed for regulation of hypnosis using BIS as the controlled variable by manipulating the inhalational drug isoflurane. Because of potential patient-model mismatch, several simulations are conducted to check the robustness of the MPC controller. The performance of the proposed MPC scheme has also been tested for several set-point changes, various disturbances in the form of surgical stimuli, noisy measurement signals and loss of measurement signal which can occur during the surgery. The performance of the proposed MPC scheme for the above mentioned scenarios is comprehensively compared with that of PI, PID, PID-P, PID-PI, and RTDA (Robustness, set-point tracking, disturbance rejection, aggressiveness) controllers which were also designed for regulation of hypnosis with isoflurane using BIS as the controlled variable. Next, the performance of the proposed MPC scheme is compared with that of cascade internal model controller (CIMC) and cascade controller with modeling error compensation (CMEC) which are available in the literature.

Next, control strategies such as MPC, IMC, MEC and PID were extended to regulate hypnosis by infusing intravenous drug propofol with BIS as the controlled variable. The performance of the advanced, model based controllers (MEC, IMC and MPC) is comprehensively compared with that of PID controller for the robustness, set-point changes, disturbances and noise in the measured BIS.

Finally, MPC strategy was extended for the simultaneous regulation of hypnosis and analgesia by infusing propofol and remifentanyl. The infusion rates of both drugs are determined according to the hypnosis level and the surgical stimulus leading to a satisfactory regulation of the patient hypnotic and analgesic state. The performance of the MPC is compared with that of decentralized PID controllers developed for simultaneous regulation of hypnosis and analgesia. Results show the lesser usage of hypnotic drug when compared to the controllers designed to regulate hypnosis alone because of synergistic interaction with the analgesic drug.

LIST OF TABLES

Table	Page
3.1 Rate constants and volumes of the different compartments of the PK model (Yasuda et al. 1991)	43
3.2 Sixteen PPs and their associated PK and PD parameters	47
3.3 Tuning rules and the PI controller settings	49
3.4 Tuning rules and their associated PID controller settings	50
3.5 Cascade controller settings using the method of Chen & Seborg (2002) for the slave controller and the IMC method (Chien & Fruehauf 1990) for the master controller	51
3.6 Series of intraoperative set-point changes	64
3.7 Controller performance of various controllers for the maintenance period ($t = 100 - 350 \text{ min}$)	66
3.8 Controller performance of various controllers for the surgical stimuli period ($t = 100 - 160 \text{ min}$)	67
3.9 Estimated EC_{50} values for selected PPs for all six controllers	73
4.1 Performance of different controllers	85
5.1 Rate constants and volumes of the different compartments of the PK model (Marsh model) (Marsh et al. 1991)	98
5.2 Values of the parameters for the 17 patient sets arranged in the decreasing order of their BIS sensitivity to propofol infusion	110
6.1 Rate constants and volumes of the different compartments (Marsh et al. 1991, Minto et al. 1997) of the PK model	141
6.2 Tuning Parameters	151
6.3 Decentralized PID controller settings	155
6.4 Series of intraoperative set-point changes for BIS and MAP	156
6.5 Performance of MPC and PID for nominal patient for the set-point changes during the maintenance period	157
6.6 Variation in parameters in PK/PD models	161
6.7 28 patients and their associated PK and PD parameters	162

Table	Page
6.8 Performance of MPC and PID for sensitive and insensitive patients for the set-point changes during the maintenance period	163
6.9 Average performance of MPC and PID for the set-point changes during the maintenance period, for 28 patients	164
6.10 Performance of MPC and PID controllers during disturbances for sensitive, nominal and insensitive patients	167
6.11 Average performance of MPC and PID controllers during disturbances for the 28 patients	169

LIST OF FIGURES

Figure	Page
1.1 Schematic representation of triad combination of anesthesia	1
1.2 Schematic representation of combined respiratory, PK and PD models	16
1.3 Input/Output (I/O) representation of the anesthesia problem . .	17
3.1 Schematic representation of combined respiratory, PK and PD models	41
3.2 Comparison of open-loop responses of all 972 patients (represented by black lines) with the 16 selected patients (represented by thick red lines)	46
3.3 Schematic representation of the MPC scheme for regulation of BIS	52
3.4 Schematic representation of basic concept of MPC	54
3.5 Setup of a feedback controller for hypnosis regulation	60
3.6 BIS response with PI controller for all 16 patients for a set-point change from 100 to 50	61
3.7 Disturbance profile (adopted from Struys et al. (2004))	64
3.8 IAE values for the maintenance period for six controllers on 16 patients	65
3.9 Percentage of the time that BIS is ± 5 units outside its set-point during the maintenance period	68
3.10 Performance of (a,b) PID, (c,d) MPC and (e,f) RTDA controllers for PP 1, PP 4 (nominal) and PP 13	69
3.11 Performance of (a,b) PID, (c,d) MPC and (e,f) RTDA controllers for the nominal (PP 4) and highly insensitive (PP 15 and PP 16) patients	70
3.12 Effect of PD parameters on closed-loop performance during the loss of BIS signal ($t = 120 - 200 \text{ min}$): (a) effect of EC_{50} , (b) effect of γ and (c) effect of k_{e0}	72
3.13 BIS response and controller output in the absence of BIS signal from $t = 120 - 200 \text{ min}$ for PP 3, using (a,b) MPC and (c,d) RTDA . .	74
3.14 Performance of MPC and RTDA controllers in the absence of BIS signal in the period of $t = 120 - 200 \text{ min}$: (a,b) transient profiles for PP 1, PP 7, and PP 13 using MPC, (c,d) transient profiles for PP 1, PP 7, and PP 13 using RTDA and (e) IAE comparison for all patient models	75

Figure	Page
4.1 Schematic representation of the CIMC structure	78
4.2 Schematic representation of the CMEC scheme	79
4.3 Comparison of the best performances of the MPC, CIMC and CMEC controllers	83
4.4 Comparison of the performance of the proposed MPC controller for several patient parameters	87
4.5 Comparison of the performance of the MPC, CIMC and CMEC controllers to a sudden step change in BIS and to disturbance in Q_0 for the nominal patient	89
4.6 Comparison of the performance of the MPC, CIMC and CMEC controllers to a sudden step change in BIS and to disturbance in Q_0 for insensitive patient	90
4.7 Comparison of the performance of the MPC, CIMC and CMEC controllers to a sudden step change in BIS and to disturbance in Q_0 for sensitive patient	91
4.8 Performance of the MPC, CIMC and CMEC controllers for measurement noise in the BIS feedback signal during the surgery: BIS profiles	93
5.1 Schematic representation of propofol delivery circuit with PK and PD models	96
5.2 BIS vs effect-site concentration C_e for different values of γ	100
5.3 Schematic representation of the IMC structure	102
5.4 Schematic representation of the MEC scheme	103
5.5 Performance of MPC, IMC, MEC and PID controllers for the Marsh model	108
5.6 Performance of MPC controller for 17 patients	112
5.7 Performance of IMC controller for 17 patients	113
5.8 Performance of MEC controller for 17 patients	114
5.9 Performance of PID controller for 17 patients	115
5.10 IAE for all the 17 patients for set-point change from 100 to 50	116
5.11 Performance of the MPC controller for measurement noise and disturbances during the surgery	118
5.12 Performance of the IMC controller for measurement noise and disturbances during the surgery	120
5.13 Performance of the MEC controller for measurement noise and disturbances during the surgery	121

Figure	Page
5.14 Performance of the PID controller for measurement noise and disturbances during the surgery	122
5.15 IAE for all the 17 patient models for noise and disturbances in BIS signal	123
5.16 Percentage of the time output BIS value is outside ± 10 units of the set-point for all 17 patient models for disturbances in the BIS signal	123
5.17 Performance of the MPC controller for different set-point changes in BIS during the surgery	125
5.18 Performance of the IMC controller for different set-point changes in BIS during the surgery	126
5.19 Performance of the MEC controller for different set-point changes in BIS during the surgery	127
5.20 Performance of the PID controller for different set-point changes in BIS during the surgery	128
5.21 IAE for all the 17 patient models for set-point changes	129
5.22 Percentage of the time output BIS value is outside ± 10 units from the set-point for all 17 patient models for different set-point changes	129
5.23 FOPTD model fit to true patient model response	130
5.24 Performance of the RTDA controller for different values of θ_T . . .	131
5.25 Performance of the RTDA, MPC and PID controllers for different set-point changes during the surgery	132
5.26 Robust performance of the RTDA controller for different sets of patient model parameters	133
5.27 IAE for all the 17 patient models for BIS set-point 50	134
5.28 Performance of the RTDA, MPC and PID controllers for disturbance during the surgery	135
6.1 Schematic representation of propofol and remifentanil delivery circuit with PK and PD models	139
6.2 Nonlinear PD interaction between propofol and remifentanil . . .	144
6.3 Schematic representation of the MPC scheme for simultaneous regulation of BIS and MAP	146
6.4 Schematic representation of the PID controller scheme for simultaneous regulation of BIS and MAP	148
6.5 Performance of the MPC controller for different weights (see Table 6.2)	153
6.6 Performance of the decentralized PID controller for different tuning parameters (see Table 6.3)	154

Figure	Page
6.7 Performance of MPC and PID controllers for set-point changes during the maintenance period $t = 30 - 280 \text{ min}$: BIS, predicted propofol concentration in the plasma and propofol infusion rate	158
6.8 Performance of MPC and PID controllers for set-point changes during the maintenance period $t = 30 - 280 \text{ min}$: MAP, predicted remifentanil concentration in the plasma and remifentanil infusion rate	159
6.9 Performance of MPC and PID for all the 28 patients for set-point changes during the maintenance period $t = 30 - 280 \text{ min}$	165
6.10 Performance of MPC and PID controllers for disturbance rejection	168
6.11 Performance of MPC and PID for all the 28 patients for disturbances in BIS and MAP	169

ABBREVIATIONS

AEP	Auditory Evoked Potential
ARX	Autoregressive model with Exogenous input
BIS	Bispectral Index
BP	Blood Pressure
CIMC	Cascade Internal Model Control
CMEC	Cascade control with Modeling Error Compensation
CNS	Central Nervous System
CO	Cardiac Output
CV	Controlled Variable
EEG	Electroencephalogram
EMG	Electromyogram
FG	Fat Group
FO	First-Order Model
FOPTD	First-Order-Plus-Time-Delay Model
FSR	Finite Step Response Model
HR	Heart Rate
HRV	Heart Rate Variability
IAE	Integral of Absolute Error
IMC	Internal Model Control
ITAE	Integral of the Time-weighted Absolute Error
MAP	Mean Arterial Pressure
MDAPE	Median Absolute Performance Error
MDPE	Median Performance Error
MEC	Modeling Error Compensation Control

MEF	Median Edge Frequency
MF	Median Frequency
MG	Muscle Group
MIMO	Multiple Input-Multiple Output
MLAEP	Midlatency Auditory Evoked Potential
MPC	Model Predictive Control
NMB	Neuromuscular Block
PCA	Patient-Controlled Analgesia
PD	Pharmacodynamics
PE	Performance Error
PI	Proportional-Integral Control
PID	Proportional-Integral-Derivative Control
PK	Pharmacokinetics
PP	Patient Profile
RE	Response Entropy
RTDA	Robustness, Set-point Tracking, Disturbance Rejection, and Aggressiveness Control
SD	Standard Deviation
SE	State Entropy
SEF	Spectral Edge Frequency
SISO	Single Input-Single Output
SQI	Signal Quality Index
SSE	Sum of Squared Error
TCI	Target-Controlled Infusion
TIVA	Total Intravenous Anesthesia
TV	Total Variation
VRG	Vessel-Rich Group

NOMENCLATURE

Chapters 1 & 2

k_{12} & k_{21}	drug transfer rates between the auxiliary and central compartments (min^{-1})
k_{20}	elimination rate constant (min^{-1})
k_{e0}	equilibration constant for the effect-site (min^{-1})
u	infusion rate of either inhalational or intravenous drug

Chapters 3 & 4

C_0	concentration of the anesthetic in the fresh gas ($vol.\%$)
C_1	alveolar concentration or end tidal concentration, measured as volume percent of the breathing mixture ($vol.\%$)
C_e	concentration of drug at the effect-site ($vol.\%$)
C_{insp}	concentration of the drug in the inspired gas ($vol.\%$)
C_j ($j = 2$ to 5)	concentration of drug in auxiliary compartments ($vol.\%$)
EC_{50}	concentration of drug at half maximal effect ($vol.\%$)
f_R	respiratory frequency (min^{-1})
k_{ij} ($i, j = 1$ to 5)	drug transfer rate constants between auxiliary and central compartments (min^{-1})
k_{20}	elimination rate constant (min^{-1})
k_{e0}	equilibration constant for the effect-site (min^{-1})
Q_0	fresh gas flow entering the respiratory circuit (ℓ/min)
ΔQ	losses from the breathing circuit through the pressure-relief valves (ℓ/min)
V	volume of the respiratory system (ℓ)
V_1	volume of the central compartment (ℓ)

V_j ($j = 2$ to 5)	volume of the auxiliary compartments (ℓ)
V_T	tidal volume (ℓ)
Δ	physiological dead space (ℓ)
γ	degree of nonlinearity (dimensionless)
Chapters 5 & 6	
C_1	concentration of drug in plasma compartment (propofol - $\mu g/ml$, remifentanil - ng/ml)
C_e	concentration of drug at the effect-site (propofol - $\mu g/ml$, remifentanil - ng/ml)
C_j ($j = 2, 3$)	concentration of drug in auxiliary compartments (propofol - $\mu g/ml$, remifentanil - ng/ml)
EC_{50}	concentration of drug at half maximal effect (propofol - $\mu g/ml$, remifentanil - ng/ml)
k_{ij} ($i, j = 1$ to 3)	drug transfer rate constants between auxiliary and central compartments (min^{-1})
k_{10}	elimination rate constant (min^{-1})
k_{e0}	equilibration constant for the effect-site (min^{-1})
u	normalized drug infusion rate with respect to patient weight (propofol - $mg/kg/hr$, remifentanil - $\mu g/kg/min$)
U	drug infusion rate (propofol - ml/hr , remifentanil - ml/min)
V_1	volume of the central compartment (ℓ)
V_j ($j = 2, 3$)	volume of the auxiliary compartments (ℓ)
w	subject's weight (kg)
α	normalization constant (propofol - min/hr , remifentanil - min/min)
γ	degree of nonlinearity (dimensionless)
ρ	available drug concentration (propofol - mg/ml , remifentanil - ng/ml)

Chapter 1

INTRODUCTION

1.1 Anesthesia and its Regulation

Clinical anesthesia is a reversible pharmacological state which can be defined as a balance between the triad combination of hypnosis, analgesia and muscle relaxation of the patient (see Figure 1.1). In clinical practice, anesthesiologists administer drugs and adjust several infusion devices to achieve desired anesthetic state in the patient (Linkens & Hacisalihzade 1990) and also to compensate for the effect of surgical stimulation while maintaining the important vital functions of the patient.

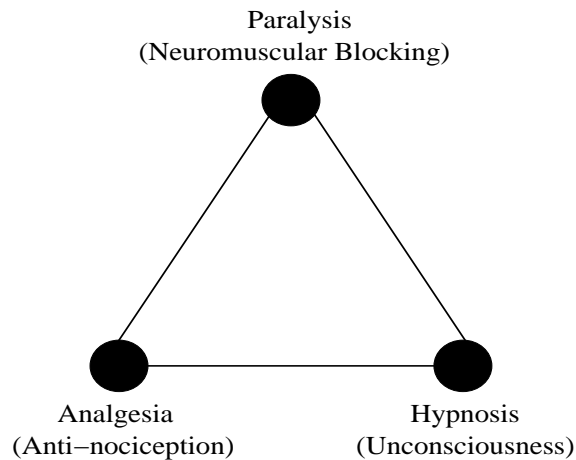


Fig. 1.1. Schematic representation of triad combination of anesthesia

Hypnosis describes a state of anesthesia which is not only related to unconsciousness of the patient but also to the disability of the patient to recall (amnesia) events that occurred during surgery. The disability to recall is important because during surgery, when the patient is intubated and ventilated artificially, he/she might

feel pain and be aware of the surgical procedures but cannot “communicate”. This awareness can be a traumatic experience, which should be avoided by maintaining sufficient hypnosis level in the patient. Hypnosis is provided by administration of hypnotic agents, which are either inhalational (e.g., isoflurane) or intravenous (e.g., propofol). An acceptable metric to quantify the depth of hypnosis is the bispectral indexTM (BIS) (Rampil 1998).

Analgesia describes the disability of the patient to perceive pain (antinociception). Surgical procedures are painful and can discomfort the patient. Analgesia is provided by administration of analgesics (opioids). A stable analgesia state is partially responsible for a stable hypnosis and vice versa. Therefore, it is important to have a “balance” between hypnosis and analgesia. At present, there are no specific measures to quantify pain intraoperatively and mean arterial pressure (MAP) is often used as an indirect measure.

Muscle relaxation (relaxing skeletal muscles) is a standard practice during induction of anesthesia to facilitate the access to internal organs and to depress movement responses to surgical stimulations. Many surgical procedures require skeletal muscle relaxation to improve surgical conditions or to reduce surgical risks caused by movements of the patients. Relaxation is provided by administration of neuromuscular blocking agents (NMBs) and can be assessed by measuring the force of thumb adduction induced by stimulation of the ulnar nerve or by single twitch force depression (STFD).

In addition to maintaining the balanced anesthetic depth, the anesthesiologist is also responsible to maintain vital functions of the patient throughout the surgery. The main vital functions are heart rate (HR) and blood pressure (BP) which are continuously monitored. These are considered as the principal indicators for hemodynamic stability and are maintained by administration of anesthetics and/or replacement of blood volume by isotonic solutions or (rarely) by blood transfusions. As

spontaneous breathing is suppressed by several anesthetics, the patient is ventilated artificially to ensure sufficient blood oxygenation and carbon dioxide elimination.

The anesthesiologist's tasks are usually routine in nature. However, critical incidents (e.g., sudden changes in blood pressure, cardiac arrest etc.) occur during the surgery and the anesthesiologist needs to be prepared for such critical incidents and minimize subsequent negative effects on the patient. The importance of automation is therefore in reducing the workload of the anesthesiologist's routine tasks and allow him/her to monitor and deal with critical aspects of the surgery. Automated systems have the advantage of not being subject to distraction or fatigue, thus they maintain the same vigilance level throughout the surgical procedure. Continuous regulation of physiological variables by an automatic control system in combination with supervision by the anesthesiologist should obviously reduce critical incidents and reduce patient risk. Other patient benefits include faster recovery, reduction in postoperative care, and fewer side effects due to improved stability of the controlled parameters. Also, because of automatic control, drug consumption will be minimized and lead to the reduction in health care costs. The motivation for designing automatic control system that infuses drugs based on patient's anesthetic level relies on the following facts:

- Better anesthetic depth is achieved compared to manual administration because the controlled variables are sampled more frequently leading to active adjustment of the delivery rate of suitable drugs (O'Hara et al. 1992, Glass & Rampil 2001).
- High quality of anesthesia can be obtained by providing drug administration guidelines, which pursue multiple control objectives such as tracking of reference signals, disturbance compensation, handling of input and output constraints and drug minimization.

- A well-designed drug administration policy should suppress the inter- and intra-individual variability thus avoiding both overdosages and underdosages. It must also compensate for differences in surgical procedures and anesthetic regimes (Bailey & Haddad 2005).
- A well-designed automatic control system can tailor the drug dosage based on the patient's response. This leads to minimal drug consumption, less intra-operative awareness and shorter recovery times, thereby decreasing the cost of surgery and also the cost of postoperative care. Overall, this improves the patient's rehabilitation and safety during and after the surgery (Mortier et al. 1998, Absalom et al. 2002, Bailey et al. 2006).

1.2 Drugs and their Effect during Anesthesia

During the surgical process, anesthesiologists administer a combination of anesthetics, opioids, and neuromuscular blocking (NMBs) drugs by adjusting respective infusion devices to maintain an adequate level of anesthetic depth (a triad combination of hypnosis, analgesia and muscle relaxation). The development of safer and more potent agents with faster onset of effect and, in certain cases, shorter duration of action, has greatly impacted anesthesia practice. Nowadays, small drug quantities used in appropriate combination can produce a balanced state of anesthesia while minimizing side-effects.

1.2.1 Anesthetics

Inhalation gases like isoflurane are still the anesthetic agents on which standard practice is based. However, intravenous agents like propofol are increasingly employed in the operating room. Currently, administration of intravenous agents is geared towards facilitating intubation, compensating for undesirable changes in patient's state and also in anticipation of painful surgical stimuli.

Inhalation anesthetics

Commonly used inhaled anesthetics are isoflurane, desflurane, and sevoflurane in conjunction with nitrous oxide. All these drugs induce a decrease in MAP (analgesic effect) when administered to healthy subjects. A major advantage with inhaled anesthetics is that the drug uptake in the arterial blood stream can be precisely titrated by measuring the difference between the inspired and expired concentrations. Hence, inhaled gases are extensively used in the maintenance phase of anesthesia process.

Intravenous anesthetics

Intravenous anesthetics are also called as hypnotics as they do not provide analgesic effects like inhaled anesthetics at normal clinical concentrations. However, they are strongly synergistic when used in conjunction with opioids, both in terms of hypnosis and analgesia. Propofol is a commonly used intravenous anesthetic drug for induction and maintenance of anesthesia process. Its higher lipid solubility permits ready penetration of the blood brain barrier resulting in rapid induction, fast redistribution and metabolism. Hence, it can be easily used in infusion schemes as it provides very fast emergence compared to most other drugs used for the rapid intravenous induction of anesthesia. This is one of the most important advantages of propofol compared to other intravenous anesthetic drugs.

Inhalation versus intravenous anesthetics

Inhaled anesthetics are used by many anesthesiologists for the maintenance of anesthesia while the intravenous anesthetics are used at the start of the surgical procedure as they provide rapid induction of anesthesia. Inhaled anesthetics have both hypnotic and analgesic properties while intravenous anesthetics have hypnotic property only. Inhalational anesthetic concentrations in the brain can be easily measured as they are closely related to the exhaled vapor concentration. The lung

partial pressures of inhaled anesthetics are closely related to the vapor concentration in the brain, and the control problem is significantly simplified since additional states are measurable. On the other hand, the concentration of intravenous drug in the brain is not easily measurable. As a result, anesthesiologists face more challenges in titration of these drugs as they do not have any feedback on plasma drug concentration (which is directly related to concentration of drug in the brain). However, since intravenous agents are more specific than inhaled anesthetics, they give more flexibility in separately controlling the functional components of anesthesia. Also, the short acting characteristic of intravenous drugs result in too strong effects over too short periods of time when they are administered as boluses. The inability to measure the plasma concentration of intravenous drugs makes it difficult for anesthesiologists to set precise rates of infusion. The result is that they usually rely on experience as well as on infusion regimens published in medical journals. Such estimations can lead to error, and the resulting titration might not correspond to the actual needs of the patient.

1.2.2 Analgesics

Morphine, fentanyl, alfentanil, remifentanyl, sufentanil analgesics (opioids) are unique in the sense that they provoke analgesia without loss of touch, temperature and consciousness, when administered in small doses. They act as agonist at specific receptors within the central nervous system (CNS) and to a much lesser extent in peripheral tissues outside the CNS. Their principal effect may be the inhibition of neurotransmitter release, resulting in a significant analgesic effect.

Unlike most anesthetics, opioids do not depress the heart and are thus particularly suitable for cardiac anesthesia. Opioids can produce unconsciousness when used in very large doses. This observation has led some authors to believe that opioids should be considered to be anesthetics. However, the state of unconsciousness

brought by opioids is not reliable. It has been shown, for instance, that they cannot fully replace inhaled vapors to provoke an adequate state of hypnosis. However, their use can reduce the requirements of inhaled anesthetics by up to 50%. Also, the sedative effect of opioids is opposed by the presence of acute pain. Hence, even though patients in severe pain receive very large amount of opioids, they can remain aware. In current practice, therefore, opioids are almost always supplemented by other anesthetics.

Five opioid compounds are used in clinical anesthesia: morphine, hydromorphone, fentanyl, sufentanil and remifentanil. While they all have similar effects, their characteristics differ tremendously due to large differences in their lipid-solubility. Of particular interest is remifentanil, a relatively new agent introduced in the mid 1990s. Remifentanil is used mostly to provide the analgesic component of general anesthesia. The potency of remifentanil is twice that of fentanyl and its effect-site equilibration time is slightly smaller than that of alfentanil ($\approx 1.1 \text{ min}$). The main characteristics of remifentanil are: brevity of action, rapid onset, noncumulative effects in inactive tissues and rapid recovery after termination of the infusion. Its brevity of action allows patients to recover rapidly from undesirable opioid-induced side-effects such as ventilatory depression.

1.2.3 Neuromuscular blocking agents

Neuromuscular blocking agents (NMBs) block transmission of nerve impulses at the neuromuscular junction, causing paralysis of the affected skeletal muscles. Because NMBs may also paralyze muscles required for breathing, mechanical ventilation should be given to maintain adequate respiration. These are used together with hypnotics and/or analgesics to produce skeletal muscle relaxation to facilitate intubation of the trachea and to provide optimal surgical conditions. NMBs do not have any hypnotic or analgesic properties but may sometimes cause transient hy-

potension. Also, these do not interact in a clinically significant way with anesthetics and opioids. NMBs such as Vecuronium, mivacurium and rocuronium are normally used when a longer effect is desired.

1.3 Measuring and Monitoring of Anesthesia

Measuring the state of anesthesia is still a grey area. Advances have been made towards the use of the electroencephalogram, usually in its processed forms (e.g., bispectral index, wavelet index, auditory evoked potentials), for correlated measures of consciousness. Some interesting work has also been done in the field of analgesia monitoring where surrogate measures have shown some potential. Nevertheless, the major problem faced by most of these sensors is the established correlation accuracy between their output and consciousness. While extensive studies have been conducted to demonstrate such properties, the reality is that only directly measurable vital signs have a true meaning. Such measurements are already used by anesthesiologists (BIS, MAP, BP, HR and respiratory rate etc.) in their practice, but still these are indirect measurements. The argument that favors the use of surrogate measures is their ability to remove delays and time constants from the normally used vital signs. This is emphasized by the existence of sensors working better than others when it comes to the estimation of the anesthetic state. Continuous responses, reduced delay and time constant in the determination of the consciousness/analgesia level will favor the use of that particular sensor.

Another limiting factor on current sensors is their sampling frequency. The performance limitations generated by a slow sensor can be overwhelming, e.g., the inability of the controller to correct for fast transients (Bibian et al. 2003).

More important than the accessibility of the measurement is the reliability of the sensor to the rough environment of the operating room that is valued highly. The sensor needs to cope with artificially created (e.g., electrocautery, x-ray, move-

ment) and patient generated (e.g., muscular, neural) artifacts. Surrogate measures can also be influenced by other factors such as the administration of other drugs (e.g., pre-medicants), blood loss, etc., which will result in unreliable measurements. It is therefore mandatory to establish a therapeutic window and normal working conditions for each sensor.

All these issues indicate the need to spend significant effort toward improving the sensors. The other direction of development is the combined use of surrogate measures with measurable vital signs for better estimation of the anesthetic state.

1.3.1 Measuring and monitoring of hypnosis

Until recently, no direct measure of hypnosis was available and arterial blood pressure has been used as an indirect indicator. In 1996, an EEG derived parameter (Bispectral Index (BIS), Aspect Medical Systems) was introduced, which correlates with the hypnotic component of anesthetic state. More recently, few promising monitors (NeuroWave by CleveMed, Ohio, 2003) have been released. These recent monitors have yet to establish a significant market share. Description of few measures for hypnosis are given below. However, this thesis work considers only BIS as a measure of hypnosis.

Bispectral analysis

A commercial monitor (approved by U.S. Food and Drug Administration (FDA)) from Aspect Medical systems (Newton, MA, USA), is available to measure the depth of hypnosis in terms of Bispectral IndexTM (BIS). It is an electroencephalogram (EEG) derived variable that quantifies the power and phase couplings of the EEG at different frequencies (Sigl & Chamoun 1994). Multivariate statistics have been used to combine the different features into a single indicator as BIS (Rampil 1998). Values of BIS lie in the range 0-100. A value in the range 90-100 represents a fully

awake state, whereas values around 60-70 represents light hypnotic state and 40-50 represents moderate hypnotic state. BIS has been found to be a reliable measure of sedation irrespective of the kind of anaesthetic drug, and has been successfully tested for isoflurane, propofol and midazolam (Glass et al. 1997).

Power spectrum analysis

- Median edge frequency (MEF) is the frequency below which 50% of the signal power is present *i.e.*, it splits the power spectrum distribution into two parts of equal power.
- Spectral edge frequency (SEF) is the frequency below which 95% of the signal power is present (Schwilden et al. 1987, 1989).

Wavelet analysis

The wavelet transform is a computationally effective signal processing method and the wavelet coefficients derived from the EEG can be used to derive a univariate descriptor of the depth of hypnosis (Bibian et al. 2001). WAV_{CNS} (wavelet based anesthetic value for central nervous system) is used as a measure to quantify (on a 100-0 scale like BIS) cortical activity. The WAV_{CNS} technology is currently being used in NeuroSENSETM Monitor (CleveMed NeuroWave Inc., Ohio, 2003).

Entropy analysis

Entropy analysis is used to quantify the complexity of EEG and (Electromyogram) EMG signals. Datex-Ohmeda EntropyTM Module (Datex-Ohmeda Division, Instrumentarium Corp., Helsinki, Finland) (Vierti-Oja et al. 2004) is available to measure hypnotic depth in terms of state entropy (SE) and response entropy (RE).

Quantitative evoked potentials

Midlatency auditory evoked potentials (MLAEP) are the specific features of EEG, which are extracted from transitory oscillatory signals generated by auditory, visual or tactile stimulation. Distinct shape of this feature enables to distinguish between different unconsciousness levels of the patient. However, poor signal to noise ratio limit the usage of this feature. Recently, a new method was developed for extracting auditory evoked potential waves from the EEG signal by employing an autoregressive model with an exogenous input (ARX) adaptive model (Struys et al. 2002, 2003). Devices based on such features/models have yet to become universally accepted in surgical environment.

1.3.2 Measuring and monitoring of analgesia

There is no direct measure to quantify analgesia when the patient is in an unconscious state. The widely accepted indirect measures are the hemodynamic variables like mean arterial pressure (MAP) (Gentilini et al. 2002, Mahfouf et al. 2003) and heart rate variability (HRV) (Pomfrett 1999).

1.4 Conducting the Anesthesia Process

The general anesthesia process is a combination of three distinct phases which are induction, maintenance and emergence.

1.4.1 Induction

This phase is the most critical part of the anesthesia process because patient's state will be changed from alert to an anesthetized state. This can generally be achieved by bolus intravenous injection of drugs (such as propofol) that work rapidly. Normally, inhalational agents are not used to induce anesthesia because of their

slower onset. With the intravenous agents, respiratory and cardiovascular reflexes are depressed with the sudden onset of unconsciousness.

In addition to the anesthetic drug, a bolus dose of opioid must be given to most of the patients. Hypnotic drugs and opioids work synergistically to induce anesthesia. These opioids help in reducing the undesirable responses like increase of blood pressure and heart rate which may occur because of endotracheal intubation and incision of the skin.

It is to be noted that these drugs induce respiratory depression which in turn reduces the spontaneous breathing. If surgery requires NMBs, the respiratory depression is even more. Thus, securing of the airway is the crucial step in the induction process and artificial ventilation is important for the patient.

This induction process usually lasts for only a few minutes.

1.4.2 Maintenance

This phase is the most stable part of anesthesia process. At this point, the effect of propofol infused during induction phase begins to wear off, and the patient must be kept anesthetized with a maintenance agent. This is usually done with the infusion of inhalational anesthetic agents such as isoflurane, desflurane etc. into the lungs of the patient. These may be inhaled as the patient breathes himself or delivered under pressure during each mechanical breath of the ventilator.

However, appropriate levels of anesthesia must be chosen based on the surgical procedure. Also, before any surgical incision or any other stimulating surgical event, infusion of a small bolus dose of opioid is required. The inhalational agent also acts as an analgesic, hence care must be taken when infusing opioid as higher doses can lead to cardiac arrest. This maximizes patient safety and rehabilitation. In some

cases, propofol is also infused continuously during the maintenance period along with inhalational agents. This is because intravenous agents give faster onset and also has fewer side effects compared to inhalational agents. A major drawback with the intravenous agents is the unavailability of plasma drug concentration. In recent years, total intravenous anesthesia (TIVA) is practiced by many anesthesiologists because of their faster onset and the real time plasma drug concentrations are obtained through pharmacokinetic (PK) models. But, large inter- and intra-patient variability limits their usage in practice.

Irrespective of whether inhalational or intravenous agents are used, the desired level of anesthesia should be maintained by giving the minimum amount necessary for the planned surgical event. This needs a reliable measurement of anesthetic depth and some of the available measures based on EEG were discussed earlier in section 1.3.

If muscle relaxants are not required for the surgery, inadequate anesthesia becomes easily noticeable. The patient will move or cough if the anesthetic is too light for the stimulus being given. If muscle relaxants are required for the surgery, then the patient is unable to demonstrate any of these phenomena. Hence, anesthesiologist must rely on careful observation of measures of EEG, autonomic phenomena such as MAP, tachycardia, sweating, and capillary dilation to decide on the required actions to achieve the correct anesthetic depth. This requires experience and sound judgment – failure to recognize such signs can lead to tragic consequences for the patient. On the other hand, excessive anesthetic is associated with decreased heart rate and blood pressure, and can be fatal if carried to extremes. Also, excessive depth caused by higher usage of the drug results in more side effects and slower awakening of the patient which leads to more time required for the postoperative care. This increases medical care costs.

1.4.3 Emergence

Towards the end of the surgical procedure, anesthesiologists are also responsible to plan for patient's emergence from anesthesia. This is achieved by decreasing the infusion of the anesthetic or by entirely switching off the drug infusion and allow time for them to be exhaled by the lungs. This is usually done during skin closure so that patient wakes up faster at the end of the surgery. Also, adequate analgesic may be given to keep the patient comfortable in the recovery room. If artificial ventilation is used, the patient is restored to breathing by self as anesthetic drugs dissipate and the patient emerges to consciousness.

1.5 Modeling Anesthesia

The design of an automatic controller for regulating anesthesia requires a reliable mathematical model of the patient to represent anesthesia (hypnosis and analgesia) dynamics and also appropriate hardware devices to measure and monitor the depth of anesthesia. The mathematical model should accurately represent the relationship between administered anesthetic dose and its effect on the patient in terms of hypnosis and analgesia.

Various methods are available for modeling biological systems for the distribution of drugs and their effect. The pharmacology of anesthetic drugs includes linear pharmacokinetic (PK) effects as well as nonlinear pharmacodynamic (PD) effects. Pharmacokinetics (PK) represent the dynamic process of drug distribution in the body while pharmacodynamics (PD) represents the description of the effect of the drug on the body. Empirical, compartmental and physiological models are the three main forms to model the anesthesia process.

Empirical models are black box models, and relate the inputs to outputs by analytical expressions, such as the sums of exponentials. Compartmental models are

formulated on the basis of the minimal number of compartments that adequately fits observed data. Physiologically based models are the most realistic representation of drug kinetics, because the parameters relate directly to physiology, anatomy and biochemistry.

Compartmental models are subdivided into simple, catenary and mammillary models. The simple model can be viewed as a special case of the other two model types. The peripheral compartments of the mammillary model are arranged around a central compartment. All peripheral compartments are linked via micro rate constants to the central compartment. The compartments of the catenary model are on the other hand arranged in the form of a chain (Bibian et al. 2001).

In general, mammillary compartmental models are widely used in the PK-PD modeling of inhalational and intravenous administered drugs (Parker et al. 1999, Bibian et al. 2005). A typical structure is shown in Figure 1.2. The pharmacokinetics is described by one central compartment (compartment 1 in Figure 1.2) and one or more peripheral compartments, which are linked to the central compartment (compartment 2 in Figure 1.2). Drug distribution is described by the micro rate constants (k_{12} & k_{21}) and by the elimination rate constant (k_{10}). The pharmacodynamics are described by an additional dynamic compartment, the effect-site compartment (E) and a static dose-effect nonlinearity (fractional E_{max} model). The identification of PK/PD model is normally a two step approach.

1. The pharmacokinetics are identified on the basis of input-output data sequences. A drug bolus, u is administered (either as inhalational or intravenous dose) and the time course is measured by taking blood samples. The infusion time of the bolus is generally neglected and therefore the response can be viewed as an approximation of an impulse response. For inhalational drug, lungs compartment and for intravenous drug, the “blood” (or more appropriately, “plasma”) compartments are used as central compartment (compartment

ment 1). Depending on the characteristics of the drug, one or more peripheral compartments (compartments 2, 3, 4, 5 etc.) are added.

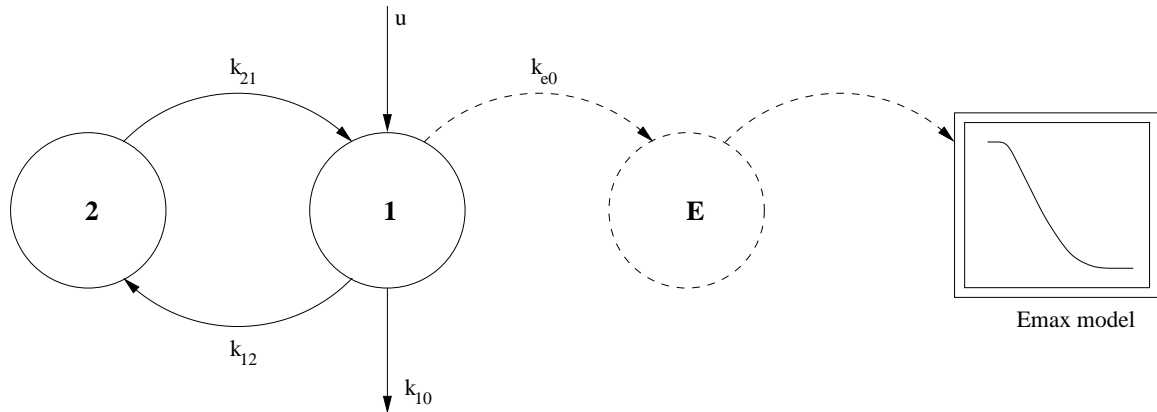


Fig. 1.2. Schematic representation of combined respiratory, PK and PD models

Typically, the concentration in the central compartment versus the drug effect shows a time lag. In pharmacology, this is often referred as “hysteresis” because a plot showing drug concentration after a bolus versus drug effect looks similar to a hysteresis. Moreover, the peripheral compartments are used to describe the characteristic time course of drug concentration in the central compartment. Generally, the time course of drug effect will differ from the time course in any of the compartments.

2. To describe this time lag, an effect-site compartment (compartment E in Figure 1.2) is added to the PK model. The effect-site concentration is only used to account for the time lag between drug concentration and drug effect. A standard fractional sigmoid E_{max} model (PD model) relating concentration at the effect-site to drug effect is added.

1.6 Automatic Control Strategies to Regulate Anesthesia

Measurement and control of anesthesia during surgery is one of the important problems in biomedical field (Morari & Gentilini 2001, Bibian et al. 2003, Dua & Pistikopoulos 2005). In clinical practice, anesthesiologists administer drugs (either inhalational or intravenous) by adjusting several infusion devices to achieve desired anesthetic state in the patient (Linkens & Haciasalihzade 1990). Figure 1.3 depicts the Input/Output (I/O) representation of the anesthesia process during surgery. The components of anesthesia (hypnosis, analgesia and muscle relaxation) are unmeasurable and they must be assessed by correlating them to available physiological measurements like BIS (extracted from EEG), MAP, blood pressure, and heart rate etc.

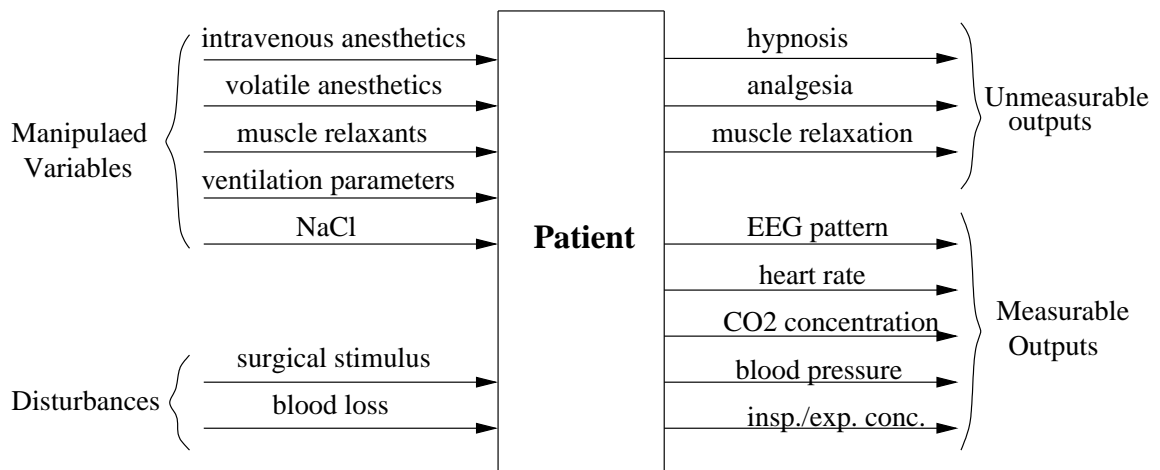


Fig. 1.3. Input/Output (I/O) representation of the anesthesia problem

The above discussion concludes that the anesthesiologist is acting as a manual feedback controller. It is difficult to tailor the drug administration to the needs of each patient in time because of the considerable inter-patient variability (based on patient's weight, age, sex etc.) that exists. Moreover, it will be more challenging for the anesthesiologist to adjust the infusion rates of several drugs simultaneously for regulation of several variables (BIS, MAP etc).

In clinical anesthesia, automatic regulation, *i.e.*, closed-loop control of infusion of drugs has been shown to provide more benefits when compared to manual administration (O'Hara et al. 1992). Drug delivery using the automatic control system clinically adjusts the rate of anesthetic uptake according to a patient's status by monitoring changes in BIS, MAP, blood pressure and heart rate etc. Also, closed-loop system would precisely titrate infusion agents according to the patients' needs, resulting in lesser intra and postoperative side-effects. In addition, by judiciously selecting the set-points, the patient will be quickly driven into an appropriate anesthetic depth according to the requirements of the surgery and the anesthesiologist's judgment. Also, to be on safe side, anesthesiologists administer large amounts of drugs than required to reduce the chances of intraoperative awareness in the patient. Even though, this this is not a major health risk, overdosing is one of the main reasons for patients' discomfort (nausea, vomiting) and slow recovery. Closed-loop systems based on new state-of-the-art monitors of the anesthetic state can significantly reduce drug consumption and lessen recovery times. Overall, this improves patient rehabilitation and also reduces the costs associated with drugs and postoperative care (Bailey & Haddad 2005). One more important issue that motivates the design of automatic drug infusion systems is that it can impose bounds on dosages and infusion rates to avoid underdosing and overdosing while keeping monitored variables within bounds.

Drugs are often combined for anesthesia during surgery because they interact synergistically to create the desired anesthetized state. For example, induction of anesthesia may consist of intravenous administration of a benzodiazepine before induction, a hypnotic to achieve loss of consciousness, and an opioid to blunt the response to noxious stimulation. Because of the synergistic interaction between the drugs, the anesthesiologist faces difficulty in adjusting the amount of infused drugs to get the desired level of hypnosis and analgesia. Closed-loop controllers can overcome this difficulty by titrating suitable doses of the drugs to tightly maintain

the variables at desired set-point. Also, with automatic controllers, the degree of drug interaction of different drugs can be quantified by assessing the differences in drug consumption. Hence, adequate anesthesia can be obtained by maintaining several variables at their desired levels by infusing several drugs and from the control engineering point of view, it can be inferred as a multi input-multi output (MIMO) problem.

All the above mentioned favorable characteristics of automatic drug infusion systems have motivated researchers to propose several automatic closed-loop control strategies for regulation of anesthesia. The control strategies applied for regulation of several variables by infusing various drugs in clinical anesthesia will be discussed in detail in chapter 2. Most of the closed-loop systems are still under development and in testing phase only. Wide use of closed-loop systems in clinical anesthesia will happen only when the developed systems pass all the requirements suggested by anesthesiologists. These requirements include the achievement of robust and stable performance in spite of considerable variability existing among the patients (inter-patient variability).

Despite the advantages mentioned above, there are considerable challenges associated in the design of closed-loop systems for anesthesia. Some of the important challenges addressed in this work are listed in section 1.7.

1.7 Motivation and Scope of the Work

The purpose of current research project is to investigate how modern multivariate model based control techniques can be effectively applied to clinical anesthesia. Following are the specific issues that provide motivation for this thesis work.

Challenges in automatic control of anesthesia

- Patient variability results from differences in the way the drug distributes and eliminates by the body's renal and liver function, cardiac output, patient's age, body mass and also from how drug affects the corresponding state of the patient. Genetic differences and enzyme activity might also alter the mechanism of action of the drug. Also, some patients might be hypo-reactive (insensitive patients) and some may be hyper-reactive (sensitive patients). Due to significant inter- and intra-patient variability, there is considerable uncertainty in dose-response models obtained from population based studies. The designed feedback controller must be stable and perform satisfactorily in spite of considerable variability in the patients.
- When using different drugs in combination to regulate several components of anesthesia, synergistic interactions among the drugs play an important role. Synergistic effect means that the resulting effect is greater than what could be expected from simple superposition. Synergism often appears when using hypnotics in combination with opioids. From a control point of view, such interactions between drugs tend to generate an important cross-coupling. Only very few models of such coupling have been discussed in the literature (Vuyk 1997, Vuyk et al. 1997, Minto et al. 2000, Vuyk 2001). These models are mainly mathematical expressions that describe drug interactions at steady state. There is a need for developing closed-loop feedback controllers in a multivariable framework by accounting for the cross coupling introduced by the PD interactions of the drugs. This would be useful for optimizing the drug dosages while not compromising on patient's comfort and safety during and after the surgery.
- Constraints on drug delivery rate and maximum amount of drug infused are most important for patient safety. Hence, these constraints should be explicitly included in the designed closed-loop feedback controller algorithm.

- Better regulation of anesthetic depth is possible by regulating as many number of variables as possible with the automatic controllers. This mainly depends on the success of measuring the key variables during the surgery. For example, on-line concentration measurement is possible with inhalational drugs (alveolar concentration) whereas this is not the case with intravenous drugs (concentration in blood plasma). Hence, predicting the concentrations and also at the same time updating the assumed nominal PD model parameters with some of the key predicted parameters would be helpful for better regulation of the anesthetic depth. This would be more helpful in the design of fault tolerant controllers *i.e.*, if any one of the feedback signals accidentally disconnects or gets corrupted by artifacts (highly noisy environment), the feedback controller can still rely on other reliable measurements for effectively controlling the anesthetic depth.
- Set-point changes are often made in the variables during the surgery depending on the surgical procedure being performed. The controller should perfectly respond to these changes without any considerable delay in the response. Also, disturbances of varying magnitudes occur during the surgery depending on the strength of the surgical stimuli. The designed controller should satisfactorily guarantee the required anesthetic depth in the patient despite these disturbances.
- Success of feedback controllers for anesthesia largely depends on the sensors that measure the different components of anesthesia. Hypnosis and analgesia are the result of different mechanisms and there are no universally accepted metrics to quantify them. Even though it is not possible to assess them directly, indirect measures like BIS for hypnosis and MAP for analgesia have been used by anesthesiologists over the past several years. These signals are more prone to noise because of electromyographic (EMG) inference caused by movement of the patient and also electromagnetic inference caused by other

monitors or sensors. The designed feedback controller should consider these limitations associated with sensors and should perform satisfactorily.

1.8 Organization of the Thesis

The above mentioned issues and challenges are considered in this thesis. A detailed description of the scope of the present work and organization of the thesis is given below.

An extensive review about various control strategies applied in clinical anesthesia has been covered in chapter 2.

Several clinical studies comparing closed-loop to manual anaesthesia control performance have been reported (Schwilden & Schuttler 1995, Kenny & Mantzaridis 1999, Struys et al. 2006). These studies used proportional-integral-derivative (PID) controllers as well as model based controllers. However, there is a need for comprehensive evaluation of closed-loop systems to establish their safety, reliability and efficacy for anesthesia regulation. This requires a detailed evaluation of promising and/or recent controllers for a range of patients and conditions via simulation. The study in chapter 3 investigates the performance of single-loop PI, PID, cascade PID-P, PID-PI, MPC and RTDA (robustness, set-point tracking, disturbance rejection, aggressiveness) controllers for closed-loop regulation of hypnosis using isoflurane with BIS as the primary controlled variable. MPC is a popular control scheme used in process industries over the past three decades for complex multivariable constrained processes (Ogunnaike & Ray 1994, Qin & Badgwell 2003). The MPC scheme employs an identified model to predict the future behavior of the system over an extended prediction horizon and computes the optimal manipulated variable moves to achieve the desired process states (Morari & Lee 1999). An important issue in the design of drug infusion systems is the need to impose bounds on dosages and infusion rates to avoid underdosing and overdosing (Rao et al. 2001). While

most control strategies handle such constraints in an ad hoc manner, the primary advantage of MPC is its ability to handle constraints explicitly. Its optimization-based framework allows computation of the optimal infusion rates subject to input and output constraints. For example, constraints on drug infusion rates and output variables (such as maintaining BIS and/or MAP above a minimum value) can be explicitly specified and the resulting control actions will satisfy them. RTDA is the most recent control scheme used for single input-single output (SISO) systems (Ogunnaike & Mukati 2006). This controller design combines the simplicity of PID controller with the advantages of MPC. Extensive simulations are carried out using a model that simulates patient responses to the drug, surgical stimuli and sudden failure of the feedback signals which can happen anytime during the surgery. Results of this comprehensive evaluation show that model predictive and RTDA controllers provide better regulation of BIS compared to the other controllers tested.

In chapter 4, the performance of the designed MPC controller is comprehensively compared with the performances obtained with other controllers available in literature such as cascade internal model controller (CIMC) and cascade controller with modeling error compensation (CMEC). The proposed MPC uses the approximate linear PK-PD model in the controller design and regulates patient's BIS and endtidal concentration by manipulating the infusion rate of isoflurane. Because of potential patient-model mismatch, several simulations are conducted to check the robustness of the MPC controller. The proposed MPC scheme has also been tested for disturbance rejection and noisy measurement signals.

The above studies are limited to closed-loop regulation of hypnosis with the inhalational drug isoflurane. The study in chapter 5 investigates the performance of MPC, IMC, MEC and PID controllers for closed-loop regulation of hypnosis using intravenous drug propofol with BIS as the primary controlled variable. The main

objective in chapter 5 is to comprehensively compare the performance of MPC, IMC, MEC and PID controllers for hypnosis control. Cascade control structure is impractical for propofol-based hypnosis regulation because of unavailability of continuous propofol concentration measurement. Hence, MEC and IMC strategies (and not their cascade versions) are employed here. The performance of the advanced, model based controllers (MEC, IMC and MPC) is comprehensively compared with that of PID controller. Extensive simulations are then conducted to test the robustness of the four controllers, by considering parameter variations in the selected model to account for patient-model mismatch. The four controllers are tested for set-point changes, disturbances and noise in measured BIS. Results of these simulations point to the choice of the best controller(s).

While studies in chapters 3, 4 and 5 are limited to regulation of hypnosis by infusing either isoflurane or propofol, the study in chapter 6 investigates the simultaneous closed-loop regulation of hypnosis and analgesia by infusing intravenous drugs propofol and remifentanyl. BIS and MAP are indirect measurements for hypnosis and analgesia respectively. The objective in chapter 6 is to determine the best infusion rates of the hypnotic and analgesic drugs such that the patient's anesthetic state (*i.e.*, BIS and MAP) is well regulated and the side effects (due to overdose) are minimized. A MPC strategy that incorporates a PK model and a PD interaction model is devised for the simultaneous administration of both the drugs. The infusion rates of the drugs are determined according to the BIS and MAP measurements which can be disturbed by noise and surgical stimuli. The performance obtained is compared with the performance of decentralized PID controllers developed for simultaneous regulation of hypnosis and analgesia. Results of these simulations indicate that the MPC performs better. The simulation results are also used to compare the amount of drugs infused with the controller designed to regulate hypnosis alone.

Conclusions from the present work and key areas identified for future work are presented in chapter 7.

Chapter 2

LITERATURE REVIEW

2.1 Feedback Control in Anesthesia

Biomedical applications of process control have been attracting attention of researchers for several years now (O'Hara et al. 1992, Doyle et al. 2007, Marchetti et al. 2008). As seen in chapter 1, automatic feedback control of anesthesia is an important and challenging biomedical problem. During surgery, anesthesiologists infuse several drugs by adjusting respective infusion devices to maintain an adequate level of anesthetic depth (a triad combination of hypnosis, analgesia and muscle relaxation) (Linkens & Hacisalihzade 1990). Hypnosis is related to unconsciousness and also to the inability of the patient to recall events (amnesia). An automatic controller that infuses drugs based on patient's anesthetic level may provide several benefits. One of the significant benefit is it will reduce the anesthetist's workload during the surgery and allow him/her to monitor and deal with other critical aspects of the surgery such as blood loss and sudden blood pressure change etc.

However, to design a feedback controller for controlling anesthesia (hypnosis and analgesia), a reliable mathematical model of the patient to represent anesthesia is required. In addition, appropriate hardware devices to measure and monitor the level of anesthesia are mandatory (Schwilden et al. 1989). In general, mammillary compartmental models are widely used to describe the pharmacokinetics (PK) and pharmacodynamics (PD) of inhaled and intravenously administered drugs (Bibian et al. 2005). The mathematical model employed in recent studies on hypnosis and/or analgesia control is a series combination of a linear PK model and

a nonlinear PD model. A theoretical effect compartment is also attached to the central compartment to represent the time-lag between observed effect and the central (plasma) concentration. The values for parameters used in the PK and PD models are the population mean values; consequently, the “patients” would have parameters that are different from the nominal values used in the controller design. The PK model parameters can be approximately estimated through covariate adjustments of weight, age and sex, but it is not possible to estimate the PD parameters. The designed controller should be robust and result in stable responses for all patients characterized by a range of PD parameters (Grieder et al. 2001). Hence, the controller design should take into consideration inter- and intra-patient variability and provide robust performance against uncertainties like modeling errors, noisy measurements and signal failure. In the following paragraphs, a literature survey on the feedback control of hypnosis and analgesia is provided.

2.2 Feedback Control for Hypnosis

The concept and implementation of closed-loop anesthesia have been investigated via numerous attempts by controlled titration of various anesthetic drugs through feedback control. As stated earlier, BIS is a measure derived from EEG to measure the depth of anesthesia. BIS accurately predicts the return of consciousness (Doi et al. 1997, Glass et al. 1997), and it has been developed and verified based on the EEG recordings of about 5000 subjects. More than 600 peer-reviewed articles and abstracts describe the clinical evaluation of BIS as specified in the literature (www.aspectmedical.com). More than 2.5 million patients (around the globe) have been monitored with BIS.

Anesthesiologists have a choice of administering different combinations of drugs to maintain the required anesthetic depth in the patient during surgery. Though specific drugs may belong to the same class of drugs (e.g., opioids), they have different

properties. An extensive review of the anesthetic drugs is available in the literature (Stoelting & Hillor 2006). Generally, for regulation of hypnosis, inhalational drug isoflurane and intravenous drug propofol are most commonly used.

Schwilden et al. (1987) and Schwilden & Schuttler (1995), tested a model-based adaptive controller by infusing methohexital and isoflurane, respectively using median edge frequency (MEF) as a controlled variable. Adaptation was done if the system output diverged too far from its reference. Results on volunteers have shown that a constant excitation is necessary to guarantee the reliability of the feedback quantity (otherwise the volunteers were drifting from a drug-induced unconsciousness into a natural sleep). This technique also works for opioids (alfentanil). The controlled drug was used as the only anesthetic agent during the maintenance phase.

Propofol is a common intravenous anesthetic drug and is widely used for both induction and maintenance of general anesthesia during surgical operations because of its favorable pharmacokinetic (PK) profiles and inhibition of postoperative nausea and vomiting (Huang et al. 1999). Many closed-loop feedback systems for propofol infusion have been proposed in the literature. Schwilden et al. (1989) developed a model-based adaptive controller using the median frequency of the EEG as the controlled variable. A linear two-compartmental PK model was used to describe the relation between infusion rate of propofol and its plasma concentration. A closed-loop proportional-integral (PI) controller was developed by Kenny & Ray (1993, 1995) and Kenny & Mantzaridis (1999) to control the depth of anesthesia using auditory evoked potential index (AEP_{index}), a parameter derived from EEG, as the controlled variable. The AEP_{index} is used to determine the target blood concentration of propofol required to induce and maintain general anesthesia. They observed that there was no incidence of intraoperative awareness and only minimal patient movement during surgery. Cardiovascular stability and overall control of anesthesia were satisfactory. Nayak & Roy (1998) and Huang et al. (1999) also used

AEP_{index} as the controlled variable by infusing halothane and propofol. They used a fuzzy rule-based control system regulating either the vaporizer or giving reference to a target-controlled infusion (TCI) device. These works mostly emphasize the hypnosis index derived from midlatency auditory potentials using wavelet analysis. Due to the extensive averaging needed, a value quantifying the level of hypnosis was calculated every 3 *min*.

After the commercial availability of BIS monitor in 1998, Mortier et al. (1998) developed a model based adaptive closed-loop feedback system for propofol infusion based on BIS as a controlled variable for spinal anesthesia. Later, the designed model-based adaptive control system was tested for general anesthesia (Struys et al. 2001). They used a lookup table of the drug pharmacodynamic model to set the target plasma concentration of a target controlled infusion device in order to reach and maintain a given hypnotic reference. The authors concluded that the closed-loop system worked better than the manual administration of propofol in a clinical setting. Sakai et al. (2000) proposed a closed-loop PID control system for propofol administration using BIS as the controlled variable. They concluded that their system provided intraoperative hemodynamic stability and a prompt recovery from the sedative-hypnotic effects of propofol. Morley et al. (2000) also investigated the performance of a PID controller for administering propofol using BIS as the target for control. They claimed that the closed-loop systems offered no performance advantage over conventional, manual anesthetic administration. They defined performance based on intraoperative conditions and initial recovery characteristics. Absalom et al. (2002) developed a similar closed-loop PID controller using BIS as the controlled variable, and a propofol targeting central plasma concentration-controlled infusion system as the control actuator. The authors concluded that further studies are required to determine if control performance could be improved by changing the proportional gains of the PID controller or by using an effect-site-targeted propofol controlled infusion system. Later, they modified their control algorithm to a

target-controlled infusion (TCI) system which regulates effect-site concentration, and proved it to be more efficient. However, the PID controller still faced some stability problems (Absalom & Kenny 2003).

Struys et al. (2004) proposed a simulation methodology to test the performance of the two published controllers (PID and model based controllers). They modeled a disturbance signal which is caused by stimulation during the surgery. This disturbance signal together with random noise was added to the original BIS signal. Simulations were then carried out by feeding back this combined BIS signal to the controller. This study concluded that model-based controller outperformed (lower median absolute prediction error for BIS targets 30 and 50) the conventional PID controller. In a recent review, Struys et al. (2006) noted the need for further evaluation of existing closed-loop systems to establish their safety, reliability and efficacy for anesthesia regulation. This requires a comprehensive evaluation of promising and/or recent controllers for a range of patients and conditions via simulation.

The closed-loop control system proposed by Gentilini et al. (2001a) emphasize that the problem is far from being solved due to the challenges posed by the intra- and inter-patient variability. They used the cascade internal model controller (CIMC) to regulate the level of hypnosis by infusing isoflurane. The cascade type control structure has a master controller which controls BIS and a slave controller that regulates the endtidal concentration (concentration of isoflurane in the exhaled breathing gas). The basic approach in IMC framework is to invert the minimum phase components of the plant model and multiply it with the filter transfer function to get the controller proper (Morari & Zafiriou 1989, Brosilow & Joseph 2002). In the work of Gentilini et al. (2001a), the PK model is linear and minimum phase, and hence directly invertible. However, the PD model is nonlinear and the inversion is not straightforward. Therefore the PD model was linearized and then inverted. The designed controller thus has the inverted plant model and this compensates for the

plant dynamics. The tuning of the IMC filter is relatively easy with the filter time constant as the only tunable parameter. Inter-patient variability can be handled by selecting the filter time constant appropriate to each patient. The clinical results provided by Gentilini (2001c) showed that the CIMC strategy worked well when compared to manual drug administration.

Recently, Puebla & Alvarez-Ramirez (2005) proposed an adaptive feedback controller for regulation of hypnosis based on modeling error compensation (MEC) approach by infusing isoflurane. They used the BIS as the measure of level of hypnosis and employed it as the controlled variable. They also used the cascade control configuration along with the MEC approach. The central idea in the MEC-based approach is to lump input-output uncertainties into a term whose trajectory is estimated and compensated via a suitable algorithm (Alvarez-Ramirez et al. 2002). This approach automatically takes care of the inter-patient and intra-patient variability to achieve stable control of BIS. Several tuning parameters characterize the MEC-based cascade control scheme. Puebla & Alvarez-Ramirez (2005) suggest values for these tuning parameters. An important feature of the MEC-cascade scheme is that the linearization of the PD model is not required and that the model need not be minimum phase. The adaptive nature of this control strategy has the potential to minimize the effect of disturbances and patient-model mismatch. The cascade MEC controller (CMEC) performed better than the CIMC controller (Puebla & Alvarez-Ramirez 2005).

2.3 Feedback Control for Analgesia

Opiates are used for intraoperative and postoperative pain treatment. In the postoperative setting, the drug infusion rate is adjusted according to the patient's pain level. With patient-controlled analgesia (PCA), the patient can regulate the

administration of opiates without supervision of the medical staff (Liu & Northrop 1990, Johnson & Luscombe 1992).

The intraoperative administration of opiates is not directly related to pain treatment, since no specific measures of pain are available when the subject is unconscious (Habibi & Coursin 1996). The International Association for the Study of Pain defines pain as an “unpleasant sensory and emotional experience associated with actual or potential tissue damage”. Consequently, it may even be improper to speak about “pain” during general anesthesia when the patient experiences unconsciousness.

Several feedback controllers have been proposed in the literature for analgesia. For analgesia, where no reliable measure exists, it was noted that the patient’s autonomic responses to painful stimulations are present both in the awake state and with hypnotic and analgesic agents (Pinskier 1986). An acceptable task would be to deliver the sufficient amount of drugs to reduce the effect of pain. Hemodynamic variables such as mean arterial pressure (MAP), cardiac output (CO) and heart rate (HR) have been considered as the measures to represent pain (Isaka & Sebald 1993, Rao et al. 2000). Surgical stimulation causes increase in MAP and HR - these reactions must be minimized during surgery (Prys-Roberts 1987). Generally, these reactions can be decreased by infusing opiates which can decrease autonomic stress reactions to surgical stimulation (Ausems et al. 1988, Kaplan 1993). MAP control is also crucial during surgery to improve surgical visibility and to guarantee adequate perfusion to internal organs (Furutani et al. 1995).

Several open- and closed-loop approaches have been investigated to improve the intraoperative administration of analgesics. Ausems et al. (1986) titrated opiate infusion to several clinical endpoints such as MAP and HR, somatic responses, and autonomic signs of inadequate anesthesia, such as sweating and lacrimation. In their

clinical validation, infusion rate of alfentanil was gradually decreased in the absence of signs of inadequate analgesia as a remedy to prevent overdosing.

Schwilden & Stoeckel (1993) tested a closed-loop controller which administers alfentanil to maintain the patient's median frequency (MF) of the electroencephalogram (EEG) at 2-4 Hz. Despite the adequate performance of the control system, it is questionable to look at the MF of EEG as the clinical end-point for analgesic drugs. Further, if used in combination with analgesics, hypnotics compromise the reliability of MF by inducing burst-suppression episodes in the EEG (Rampil 1998). Moreover, from clinical data, it is not clear whether and how noxious stimuli affect the EEG (Rampil & Laster 1992, Kochs et al. 1994).

Recently, Gentilini et al. (2002) proposed a model predictive control (MPC) strategy for the regulation of analgesia by infusing alfentanil with MAP as the controlled variable. They claimed that the proposed control worked well in the clinical setting. The above studies are encouraging because they confirm the possibility of achieving good hemodynamic control with opiates. They also suggest that an optimal closed-loop system aiming at the regulation of MAP with opiates must include a way to minimize the drug consumption and must offer some degree of freedom to adjust the infusion rate based on other qualitative signs of inadequate analgesia.

2.4 Feedback Control for Simultaneous Regulation of Hypnosis and Analgesia

Drugs are routinely combined to regulate several states of anesthesia during surgical process. Some drug combinations interact synergistically to create the desired anesthetic state. The goal of combining these synergistic interacting drugs is to decrease toxicity by minimizing the overdosage while maintaining or increasing efficacy of the drugs (Rosow 1997). Generally, anesthesia is maintained with a com-

bination of a hypnotic (e.g., propofol, isoflurane) to achieve loss of consciousness (reduce BIS levels) and an analgesic or opiate (e.g., remifentanil, alfentanil, nitrous oxide) to blunt the response to noxious stimulation (reduce MAP and HR) (Vuyk 1997). There are several studies conducted by researchers for simultaneous automatic regulation of anesthetic drugs. Linkens (1992, 1994) was probably among the first to attempt the control of distinct anesthesia components simultaneously (analgesia and areflexia) using different agents (atracurium and isoflurane) by using expert systems and fuzzy logic. An in-depth analysis of such cases reveals the need for strong knowledge of the patient model. The intra- and inter-patient variability makes the establishment of *a priori* rules very difficult.

Several studies reported that propofol-remifentanil combination improved the speed of induction and also lower propofol concentrations are sufficient for loss of consciousness in the presence of high remifentanil concentrations (Bouillon et al. 2004, Schraag et al. 2006). Propofol is a common intravenous hypnotic drug while remifentanil is a short acting opioid, provides hemodynamic stability and rapid post-anesthetic emergence and recovery. Although higher remifentanil concentrations may enhance the control of somatic and autonomic responses, there is a threshold on it, *i.e.*, further increase in its concentration may not decrease the concentration of hypnotic needed for the desired unconscious state. Also, as the opioid decreases the spontaneous ventilation of the patient, it should not increase beyond the threshold associated with adequate spontaneous ventilation, otherwise recovery is delayed. Hence, hypnotic propofol and analgesic remifentanil dosages should be administered optimally by taking the synergistic interaction between these two drugs into consideration. This will help to achieve the objectives of a stable intra-operative course and rapid recovery to consciousness with adequate spontaneous ventilation (Glass 1998). Hence, drug interactions provide additional challenges for optimal drug dosing strategies during anesthesia and also play an important role in the regulation of the anesthetic states.

In general, propofol-remifentanyl anesthesia is associated with the most rapid return of consciousness after any infusion duration compared with fentanyl, sufentanyl or alfentanyl (Egan 2000, Epple et al. 2001). Another benefit of remifentanyl is that, even at suboptimally high remifentanyl concentrations, return of consciousness is postponed marginally only. Remifentanyl reduces the propofol dose requirement because of its synergistic interaction with propofol and this may lead to hemodynamic stability during the surgical process (Mertens et al. 2003). In elderly patients, or patients with cardiovascular instability, high remifentanyl/low-propofol anesthesia may be associated with increased hemodynamic stability during induction of anesthesia (Kern et al. 2004, Johnson et al. 2008). Also, the level of postoperative pain experienced by the patient is not only influenced by the type of surgery but also by the propofol-remifentanyl concentrations used intraoperatively. When propofol is given in high concentrations, the need for intraoperative opioids are low. At the end of the surgery, when propofol infusion is discontinued, the opioid concentration may then appear to be insufficient for adequate postoperative analgesia. To prevent this from happening, in anticipation of severe nociception, intraoperative low opioid concentrations may be avoided (Lichtenbelt et al. 2004). These aspects should be taken care when designing an automatic control protocol for Total Intravenous Anesthesia (TIVA), *i.e.*, to optimize intravenous delivery of these two synergistically interacting drugs.

Several studies in the literature have considered the simultaneous administration of propofol and remifentanyl to regulate hypnosis and analgesia, and supported their favorable synergistic interactions (Bouillon et al. 2004, Mertens et al. 2003). Generally, these works consider a closed-loop feedback approach for administration of propofol and open-loop administration of remifentanyl or both drugs by open-loop administration (Struys et al. 2006). Schraag et al. (2006) clinically supported their synergistic interaction by considering automatic administration of propofol and manual administration of remifentanyl in 45 subjects. Milne et al. (2003) considered

the closed-loop PID (proportional-integral-derivative) control of propofol by using auditory evoked potential index (AEP_{index}) as the controlled variable and manual administration of remifentanyl. This work concluded that there is a synergistic interaction between propofol and remifentanyl because propofol requirement considerably decreased with the use of remifentanyl to get the same level of unconsciousness. Mendonca et al. (2006) considered adaptive predictive control strategy for the regulation of BIS by automatic control of propofol and manual administration of remifentanyl. This single input-single output (SISO) controller design takes care of interaction between the drugs which is modeled using a response surface.

Very few works in the literature have reported the closed-loop control of both hypnosis and analgesia by simultaneous administration of hypnotic and analgesic intravenous drugs. Zhang et al. (1998) reported a closed-loop system for TIVA by simultaneously administering propofol and fentanyl. They studied the interaction between propofol and fentanyl for loss of response to surgical stimuli using an unweighted least squares nonlinear regression analysis of human data. A look-up table of optimal and awakening combinations of concentrations was built and used to determine the fentanyl set-point according to propofol set-point. This approach was limited to the control of the plasma concentration of propofol and fentanyl in dogs, where the set-points were chosen to minimize the wake up time. Mahfouf et al. (2005) considered the multivariable fuzzy control strategy for simultaneous regulation of hypnosis and analgesia with propofol and remifentanyl. The hybrid patient model with the use of fuzzy concept they developed in another work (Nunes et al. 2005) was used for this closed-loop control. This model relates the HR, the systolic arterial pressure and the AEP features to the effect concentrations of propofol and remifentanyl. Later, Nunes et al. (2006) improved the developed model by including the effect of surgical stimulus. They demonstrated that the developed control algorithm optimally administers these two drugs simultaneously in the operating theater during surgery. Further, Cardoso & Lemos (2008) considered MPC strategy for the

regulation of BIS by automatic control of propofol, taking the remifentanil dose (used to regulate analgesia) as a disturbance to BIS because of synergistic effect of remifentanil and propofol on hypnosis. This SISO controller design also takes care of interaction between the drugs which is modeled using a response surface.

As an overall remark, it seems that, while the previous attempts were promising, the researchers did not design controllers that completely account for inter-patient variability and drug interactions. The results reported in the literature involve healthy population and very few “patients”. As a consequence, these closed-loop achievements did not manage to convince practicing anesthesiologists about the viability of the proposed methods. The work presented in the following chapters answers some of the above mentioned issues by designing controllers which are able to handle inter-patient variability as well as drug interactions.

2.5 Summary

Anesthesiologists have succeeded in making anesthesia a safe procedure. However, despite many studies and potential benefits, closed-loop control of anesthesia is not yet accepted for routine use. It is therefore natural to ask if automation in clinical anesthesia is a valuable research endeavor. The reality is that, efforts in fast acting drug development, sensor design and robust control complemented by changes in the current anesthesia practice, are paving the way to closed-loop anesthesia control. Based on the literature (Kissin 2000, Glass & Rampil 2001, Mahfouf 2006), the control of anesthesia cannot be done based on a single feedback quantity. It is necessary to consider all functional components of anesthesia when setting the controller specifications and requirements. To respect the current balanced anesthesia practice, a first step would be the regulation of both a hypnotic agent (e.g., such as an inhalational anesthetic or intravenous anesthetic) and an opioid, in order to

reach an adequate anesthetic state. Such a system would be directly usable in most elective surgeries, where the use of neuromuscular blocking agent is not required.

From a control point of view, the challenges are many. First, such a controller will need to account for inter- and intra-patient variability. Also, models linking the infusion of drugs and their effects will need to be developed in a multivariable framework so as to account for the interactions introduced by their PK and PD dynamics. Finally, the nonlinear nature of the models developed and of the sensors used to provide the feedback measurements will have to be included in the design. On the way to such high level goals, the purpose of current research project is to investigate how modern advanced control techniques like model predictive control (MPC) strategy, can be effectively applied to clinical anesthesia. The resulting closed-loop system would precisely titrate the infusion rate according to the patients' needs, resulting in lesser intra- and postoperative side effects. Hence, MPC for anesthesia control is studied and presented in the next 4 chapters.

Chapter 3

EVALUATION OF PID, CASCADE, MODEL PREDICTIVE AND RTDA CONTROLLERS FOR REGULATION OF HYPNOSIS WITH ISOFLURANE

3.1 Introduction

Several clinical trials on closed-loop hypnosis regulation with isoflurane using BIS as the controlled variable have already been conducted and reported in the literature (Morley et al. 2000, Gentilini et al. 2001a, Locher et al. 2004). These studies used the ubiquitous proportional-integral-derivative (PID) controllers, as well as advanced model-based controllers. Because of the potential risks of such clinical trials, they are often conducted on young, healthy patients undergoing noncritical surgical procedures. As such, the efficacy of controllers in the presence of extreme patient sensitivities (e.g., that of a young child or an elderly person) and unexpected surgical events (e.g., sudden loss of feedback signal) cannot be fully evaluated. Without extensively validating the performance of controllers under these scenarios, the application of such closed-loop systems remains limited. Recently reported simulation studies for regulation of hypnosis with isoflurane are limited to the nominal patient (Dua & Pistikopoulos 2005, Puebla & Alvarez-Ramirez 2005). Therefore, it is important to conduct a comprehensive evaluation of promising and/or recent controllers for a range of patients and conditions via simulation (Struys et al. 2006, Beck et al. 2007).

The present chapter has two main objectives. One objective is to apply and evaluate the promising model predictive control (MPC) and the recent RTDA (Robustness, set-point Tracking, Disturbance rejection, Aggressiveness) approaches for hypnosis regulation using BIS as the controlled variable by manipulating isoflurane infusion. MPC is a popular control scheme that has been used by process industries since many years, for the optimal, constrained control of complex multivariable processes (Ogunnaike & Ray 1994, Qin & Badgwell 2003). Recently, this controller has been used for the regulation of hypnosis with propofol (Furutani et al. 2005). RTDA is the most recent control scheme used for single input-single output (SISO) systems (Ogunnaike & Mukati 2006). Another objective is to extensively assess and compare the performance of single-loop PID, cascade, MPC and RTDA controllers for hypnosis control. The performance comparison of six controllers is conducted by testing the robustness (considering parameter variations in the patient model to account for patient-model mismatch), set-point changes, and disturbances during the surgery. For realistic assessment, measurement noise is added to the BIS signal in the simulations. The study and findings described in this chapter have been reported in Sreenivas et al. (2009b).

3.2 The Mathematical Model

The model developed for hypnosis consists of three interacting parts: a respiratory system model to describe the inhalation and exhalation of isoflurane, a PK model for the distribution of isoflurane in the internal organs, and a PD model to describe the effect of drug on the physiological variable, *i.e.*, BIS (Gentilini et al. 2001a, Yasuda et al. 1991). Figure 3.1 presents a schematic of the respiratory system - comprising of the isoflurane delivery circuit, and the PK and PD models.

A fresh flow of anesthetic-breathing mixture delivered by the pump combined with the cleaned exhaled gas is sent to the patient's lungs. The pump stays at rest during

the patient's expiration. Circulation of the gases in the system and prevention of the

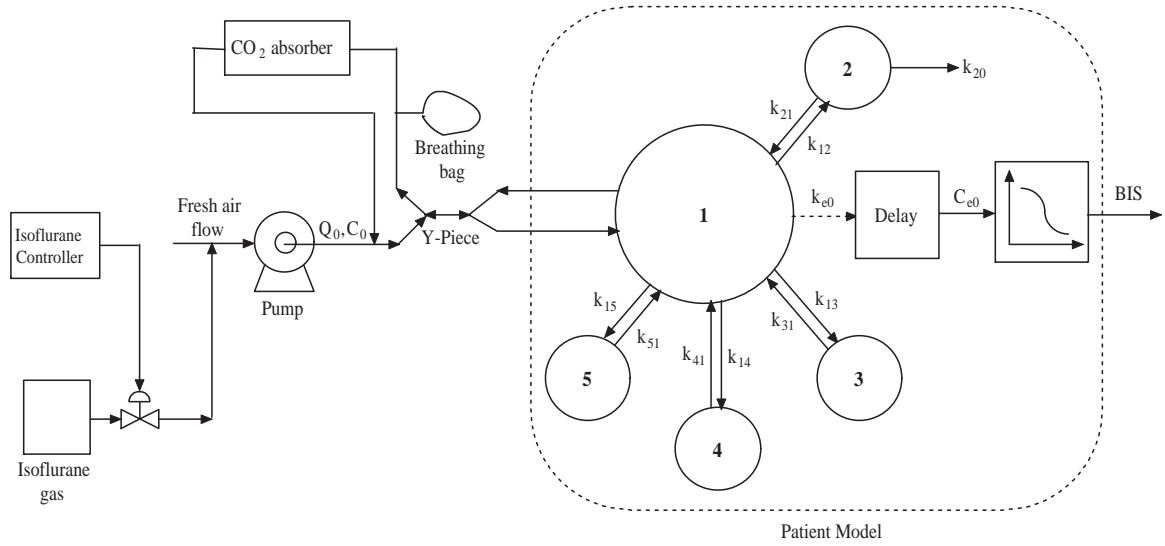


Fig. 3.1. Schematic representation of combined respiratory, PK and PD models

patient from rebreathing the exhaled gases is guaranteed by unidirectional and pressure relief valves. The breathing bag maintains positive pressure ventilation during manual ventilation and compensates for excessive pressure during artificial ventilation. The CO₂ absorber uses soda-lime to remove CO₂ from the exhaled breath and this cleaned exhaled gas is added to the fresh gas flow, Q_0 . The combined gas compensates for the uptake of anesthetic gases, O₂, and the gas exhausted from the pressure relief valve. The inhaled gas has the drug isoflurane which is taken into the lungs from where it diffuses into the blood and carried to all parts of the body before finally distributing into various tissues (compartments). The mammillary compartment model, *i.e.*, PK model for the distribution of isoflurane is adopted from Yasuda et al. (1991). The compartments are also depicted in Figure 3.1. Here, the first compartment is the central compartment which represents lungs, second compartment indicates the vessel-rich group (VRG), third compartment indicates the muscle group (MG), and fourth and fifth compartments indicate the fat group (FG). Also, the metabolism of the drug is assumed to occur in the second compart-

ment, *i.e.*, in VRG (liver). The PD part assumes some delay between the inhalation of isoflurane by lungs and the dissolving of isoflurane in brain tissue thereby affecting the hypnosis level. This effect on hypnosis level is represented by a nonlinear equation relating the state variables and other system variables to BIS.

3.2.1 Model for the breathing system

The breathing system is approximated as a well-stirred tank (Gentilini et al. 2001a). The relation between inspired anesthetic drug concentration C_{insp} (vol.%) to the fresh anesthetic gas concentration C_0 (vol.%) and parameters of the breathing system is given by the following equation:

$$V \frac{dC_{insp}}{dt} = Q_0 C_0 - (Q_0 - \Delta Q) C_{insp} - f_R (V_T - \Delta) (C_{insp} - C_1) \quad (3.1)$$

where V (ℓ) is the volume of the breathing system, C_1 (vol.%) is the alveolar concentration or endtidal concentration, measured as volume percent of the breathing mixture, f_R (min^{-1}) is the frequency of respiration, V_T (ℓ) is the tidal volume (volume of each breath), Δ (ℓ) is the physiological dead space, ΔQ (ℓ/min) represents losses of the breathing circuit through the pressure relief valves, and Q_0 (ℓ/min) is the flow rate of fresh gas entering the breathing system. C_0 (vol.%) is the manipulated variable.

Typical ranges for the parameters of the respiratory system are (Gentilini 2001c): $Q_0 = 1 - 10 \ell/min$, $f_R = 4 - 25 min^{-1}$, $V_T = 0.3 - 1.2 \ell$, $V = 4 - 6 \ell$, $\Delta = 0.1 - 0.2 \ell$, and $\Delta Q = 0.1 - 0.5 \ell/min$. The nominal values for the above parameters are (Yasuda et al. 1991, Gentilini et al. 2001a): $Q_0 = 1 \ell/min$, $f_R = 10 min^{-1}$, $V_T = 0.6 \ell$, $V = 5 \ell$, $\Delta = 0.15 \ell$, and $\Delta Q = 0.2 \ell/min$.

3.2.2 Pharmacokinetic model

The PK model for distribution of drug is described by a mass balance between the five compartments which are attached to the central compartment. The main assumption here is that the distribution of isoflurane is not affected by the presence of other drugs. Hence, the resulting mass balance for isoflurane in the central compartment is given by equation (3.2).

$$\frac{dC_1}{dt} = \sum_{j=2}^5 \left(k_{j1} C_j \frac{V_j}{V_1} - k_{1j} C_1 \right) + \frac{f_R(V_T - \Delta)}{V_1} (C_{insp} - C_1) \quad (3.2)$$

For all the remaining compartments (except second compartment), the corresponding mass balance is

$$\frac{dC_j}{dt} = k_{1j} C_1 \frac{V_1}{V_j} - k_{j1} C_j \quad (3.3)$$

Table 3.1

Rate constants and volumes of the different compartments of the PK model (Yasuda et al. 1991)

Parameter	Value	Parameter	Value
k_{12}	$1.26 \pm 0.024 \text{ min}^{-1}$	k_{41}	$0.00304 \pm 0.00169 \text{ min}^{-1}$
k_{13}	$0.402 \pm 0.055 \text{ min}^{-1}$	k_{51}	$0.0005 \pm 0.000119 \text{ min}^{-1}$
k_{14}	$0.243 \pm 0.072 \text{ min}^{-1}$	V_1	$2.31 \pm 0.71 \text{ l}$
k_{15}	$0.0646 \pm 0.0414 \text{ min}^{-1}$	V_2	$7.1 \pm 2.5 \text{ l}$
k_{20}	$0.0093 \pm 0.0137 \text{ min}^{-1}$	V_3	$11.3 \pm 5.6 \text{ l}$
k_{21}	$0.210 \pm 0.082 \text{ min}^{-1}$	V_4	$3.0 \pm 0.7 \text{ l}$
k_{31}	$0.023 \pm 0.0156 \text{ min}^{-1}$	V_5	$5.1 \pm 4.1 \text{ l}$

Because metabolism of the drug occurs in the second compartment, the mass balance is

$$\frac{dC_2}{dt} = k_{12} C_1 \frac{V_1}{V_2} - k_{21} C_2 - k_{20} C_2 \quad (3.4)$$

where k_{20} is the hepatic metabolism rate constant. Values of the parameters in equations (3.2) – (3.4) are summarized in Table 3.1.

3.2.3 Pharmacodynamic model

The above PK model is limited to the representation of distribution kinetics of isoflurane into different compartments. A PD model is required to relate the effect of drug and the hypnotic level (BIS). The PK model is attached to an effect-site compartment model which represents the time lag between the distribution of drug and its effect on BIS which is given by the nonlinear Hill equation (Beck et al. 2007). The effect-site compartment accounts for the equilibration time between endtidal concentration and concentration of drug in the central nervous system (brain). The effect-site concentration and endtidal concentration are related by a first-order lag given by:

$$\frac{dC_e}{dt} = k_{e0}(C_1 - C_e) \quad (3.5)$$

where k_{e0} is used to describe the time course of equilibration between the endtidal and the effect-site. The effect-site concentration is related to BIS as (Hill equation) (Bibian et al. 2005):

$$\Delta\text{BIS} = \Delta\text{BIS}_{\text{MAX}} \frac{C_e^\gamma}{C_e^\gamma + EC_{50}^\gamma} \quad (3.6)$$

where

$$\Delta\text{BIS} = \text{BIS} - \text{BIS}_0 \quad (3.7)$$

and

$$\Delta\text{BIS}_{\text{MAX}} = \text{BIS}_{\text{MAX}} - \text{BIS}_0 \quad (3.8)$$

where EC_{50} is the concentration of drug at half-maximal effect and represents the patient's sensitivity to the drug, and γ is a dimensionless parameter that determines the degree of nonlinearity. BIS has the range between 0 and 100, where $\text{BIS}_0 = 100$ denotes a fully conscious state and $\text{BIS}_{\text{MAX}} = 0$ denotes nil cerebral electrical activ-

ity, *i.e.*, deep coma. By substituting equations (3.7) and (3.8) into equation (3.6), it can be written as:

$$\text{BIS} = 100 - 100 \frac{C_e^\gamma}{C_e^\gamma + EC_{50}^\gamma} \quad (3.9)$$

The nominal values of the parameters $k_{e0} = 0.3853 \text{ min}^{-1}$, $EC_{50} = 0.7478 \text{ vol.}\%$ and $\gamma = 1.534$ are obtained from the pooled analysis (Gentilini et al. 2001a).

3.3 Patient Model Variability Analysis

Patient variability in drug responses was simulated by varying important parameters in the PK and PD models. Open-loop simulations (by varying each parameter independently) showed that the dominant PK parameters are breathing frequency (f_R), tidal volume (V_T) and lung volume (V_1). In the PD model, all three PD parameters (EC_{50} , k_{e0} , and γ) were determined to be important. Hence, these three PK and three PD parameters were varied in three levels (except V_T , which was varied over four levels) within their ranges reported in Yasuda et al. (1991) and Gentilini et al. (2001a), and then combined to give many PK and PD models with different drug sensitivities. From these, 16 patient profiles (PPs) with different combinations of the PK and PD models were chosen, based on decreasing sensitivity to the drug. Figure 3.2 shows the open-loop responses of all 972 (4×3^5) patients, along with those of the 16 selected PPs. These data are for a step change of $0.7068 \text{ vol.}\%$ in the input C_0 , which takes the nominal patient model to a BIS value of 50. This step change is small compared to the C_0 value that is used to induce hypnosis in a patient, and, hence, a long time is required to attain steady state. Larger step changes in C_0 results in the final BIS value being well below 50.

Figure 3.2 clearly shows that the 16 selected PPs cover the open-loop dynamics of the 972 patients. The values of the PK and PD parameters for these 16 selected PPs are given in Table 3.2, which also includes the steady-state gain of each PP to the step change of $0.7068 \text{ vol.}\%$ in the input C_0 value used for Figure 3.2. These gains are

calculated based on the ratio of the difference between the initial value and the final steady-state value of the output (BIS) to the given step input (C_0 , in units of *vol.%*). A high gain value in Table 3.2 indicates a sensitive patient and a low gain indicates an insensitive patient. In the set of 16 profiles constructed, more emphasis is placed on insensitive patients, because controller performance is expected to degrade with decreased sensitivity. Notably, PP 15 and PP 16 represent extremely insensitive patients who are atypical, and controller performance is expected to be poor when tested on these PPs.

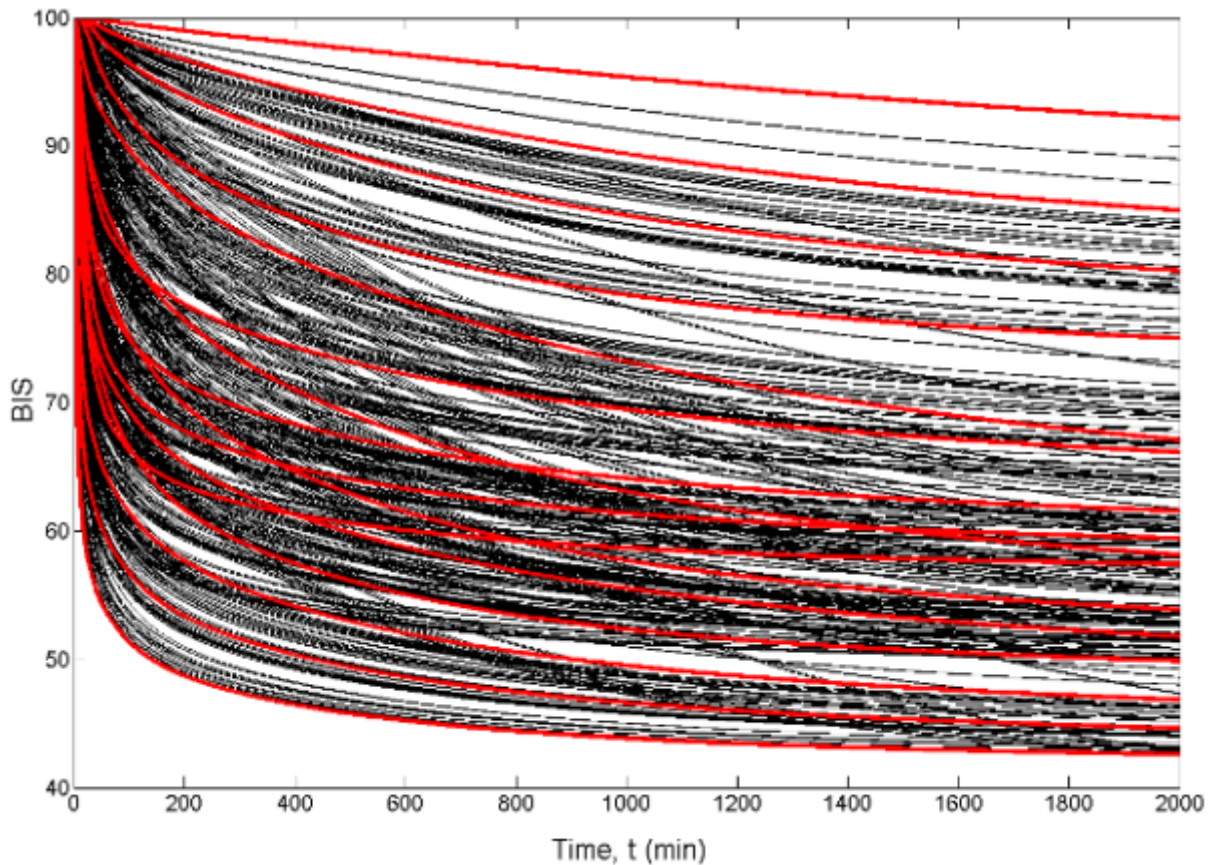


Fig. 3.2. Comparison of open-loop responses of all 972 patients (represented by black lines) with the 16 selected patients (represented by thick red lines)

Because of the uncertainty in the model parameters, it is useful to perform controllability, observability, and robustness analysis. These analyses were performed on the linearized patient model (linearized at the operating point, $BIS = 50$). For all 16

patient profiles, all seven states were determined to be controllable and observable. Furthermore, controllability analysis shows that the output (BIS) is controllable for all the patient profiles. Robustness analysis of the closed-loop system of the patient model with the proportional-integral (PI) controller shows that the system is robustly stable for the deviations in the parameters considered. It furthermore shows that the system is more sensitive to the parameters f_R and EC_{50} , which is consistent with the open-loop sensitivity analysis.

Table 3.2
Sixteen PPs and their associated PK and PD parameters

Patient Profile No.	PK Parameters			PD Parameters			Steady State Gain
	f_R (min^{-1})	V_T (ℓ)	V_1 (ℓ)	k_{e0} (min^{-1})	EC_{50} ($\text{vol.}\%$)	γ	
1	25	1.2	1.60	3.4890	0.5146	0.7915	82.8
2	25	1.2	1.60	0.3853	0.7478	1.5340	81.1
3	10	0.6	2.31	3.4890	0.5146	0.7915	74.1
4 (nominal)	10	0.6	2.31	0.3853	0.7478	1.5340	70.7
5	4	0.8	3.02	0.3853	0.7478	1.5340	67.0
6	4	0.8	3.02	3.4890	0.5146	0.7915	66.5
7	4	0.3	3.02	0.3853	0.7478	1.5340	62.2
8	4	0.3	3.02	3.4890	0.5146	0.7915	61.9
9	10	0.6	2.31	0.0804	1.0940	2.9130	60.2
10	25	1.2	1.60	0.0804	1.0940	0.7915	58.8
11	25	1.2	1.60	0.0804	1.0940	2.9130	58.3
12	10	0.6	2.31	0.0804	1.0940	0.7915	54.2
13	4	0.8	3.02	0.0804	1.0940	2.9130	40.1
14	4	0.8	3.02	0.0804	1.0940	0.7915	35.1
15	4	0.3	3.02	0.0804	1.0940	0.7915	30.1
16	4	0.3	3.02	0.0804	1.0940	2.9130	20.9

3.4 Controller Design

The controller has to maintain BIS between 40 and 60 during the surgery. Initially it is assumed that the patient is in a fully conscious state ($BIS \cong 100$) and then the controller is turned on to bring the patient to the surgical operating range (*i.e.*, $BIS \cong 50$) and maintained there for the duration of the surgery. Also, C_1 (*vol.%*) is the endtidal concentration which can be measured online. C_0 is the manipulated variable which is restricted between 0 and 5 *vol.%* (Gentilini et al. 2001b, Puebla & Alvarez-Ramirez 2005). The upper bound for C_0 is 5 *vol.%* because high isoflurane concentration may lead to hypnotic crisis, cardiac arrhythmia, or even cardiac arrest. The minimum bound on $C_0 = 0$ *vol.%* reflects the impossibility to administer negative concentrations of isoflurane.

Six controllers - identified as PI, PID, cascaded PID-P, cascaded PID-PI, MPC, and RTDA - were designed for closed-loop administration of isoflurane to regulate hypnosis. All these controllers were tuned for minimal integral of absolute error (IAE) and smaller undershoot in BIS response in the induction period $t = 0 - 100$ *min* for the nominal patient. The performance of all the controllers was then checked for the maintenance period (*i.e.*, for $t = 100 - 350$ *min*) and was determined to be satisfactory, before further testing and evaluation. Thus, controllers were designed not just for the induction period but also for the maintenance period. PI(D) and cascade controllers were designed with specific tuning rules and later were fine-tuned, whereas MPC and RTDA controllers were tuned via a direct search optimization algorithm.

3.4.1 PI controller design

For the PI controller, the nonlinear patient system was approximated by a linear first-order (FO) model. Time delay was neglected due to the large time constant of the open-loop response. Linear approximation was performed near the operating

point of the system (*i.e.*, when BIS is near its intraoperative range of 40 – 60), to facilitate the design of a controller that can respond quickly to changes in BIS set-point and reject disturbances during the surgical period. Model parameters ($K = -53.3 \text{ vol.}\%^{-1}$, $\tau = 317.5 \text{ min}$) were determined by minimizing the sum of squared error (SSE) between the actual BIS response and the FO model response.

For FO systems with negligible time delay, three tuning rules are applicable: internal model control (IMC) tuning, which was proposed by Chien & Fruehauf (1990); the tuning method of Chen & Seborg (2002); and that of Haeri (2005). Of these, the PI controller settings obtained by the method of Chen & Seborg (2002) were determined to be better. These controller settings gave oscillatory response for safe application (because of the nonlinear nature of the patient system), and therefore the proportional gain was first lowered, to reduce both proportional and integral actions. The integral action was then independently increased, to hasten the response that had become too sluggish. The initial and final settings of the PI controller are compared in Table 3.3. Similar fine-tuning was applied to design other controllers that are studied in this chapter.

Table 3.3
Tuning rules and the PI controller settings

	K_c	τ_I
Tuning rules (Chen & Seborg 2002)	$(2\tau\tau_c - \tau_c^2)/(K\tau_c^2)$	$(2\tau\tau_c - \tau_c^2)/\tau$
Original settings	-0.46	48.0
Final settings (with fine-tuning)	-0.09	12.0

3.4.2 PID controller design

For the PID controller, the tuning methods of Wojsznis et al. (1999) and Friman & Waller (1997), which are based on the ultimate gain and frequency of the system, were used. Using P-only control, the ultimate gain and period of the nominal PP

were determined to be $-0.55 \text{ vol.}\%^{-1}$ and 12.7 min , respectively. The PID controller was such that the derivative (D) action acted solely on the filtered BIS measurement, while proportional (P) and integral (I) actions acted on the error in BIS. This is to avoid sudden spikes in the controller output that are due to step changes in set-point. Of the two methods attempted, the settings obtained by Wojsznis et al. (1999) were determined to be better. The tuning rules of Wojsznis et al. (1999) and the PID controller settings obtained are reported in Table 3.4.

Table 3.4
Tuning rules and their associated PID controller settings

	K_c	τ_I	τ_D
Tuning rules (Wojsznis et al. 1999)	$0.38K_{cu}$	$1.2P_{cu}$	$0.18P_{cu}$
Original settings	-0.21	15.2	2.29
Final settings (with fine-tuning)	-0.08	11.5	0.30

3.4.3 Cascade controllers design

For the cascade controllers, the inner and outer controllers were tuned sequentially. The inner process that related the endtidal concentration (C_1) to the isoflurane input was approximated by a FO model, and the model parameters ($K = 1.06 \text{ vol.}\%^{-1}$, $\tau = 432.5 \text{ min}$) were determined by minimizing the SSE value. The controller settings were determined using the tuning method of Chen & Seborg (2002), and their values are as reported in Table 3.5. With the inner loop closed, the open-loop response of BIS to set-point changes in C_1 was approximated by a FO-plus-time-delay (FOPTD) model.

Table 3.5

Cascade controller settings using the method of Chen & Seborg (2002) for the slave controller and the IMC method (Chien & Fruehauf 1990) for the master controller

Setting	Slave Controller		Master Controller		
	K_c	τ_I	K_c	τ_I	τ_D
PID-PI					
Original	5.5	14	-0.020	5.4	0.4
Final (Set 1)	5.5	14	-0.018	6.0	0.1
Final (Set 2)	5.5	14	-0.018	12.0	0.1
PID-P					
Original	5.5	-	-0.018	6.0	0.1
Final	4	-	-0.025	6.0	0.05

Note: IMC tuning for a PID controller is given as follows: $K_c = (\tau + \theta/2)/[K(\tau_c + \theta/2)]$, $\tau_I = (\tau + \theta/2)$ and $\tau_D = \tau\theta/(2\tau + \theta)$.

Here, the action of the inner loop resulted in faster dynamics of the outer loop, and the time delay became significant when compared to the small time constant. Using the model parameters that have been determined ($K = -53.0 \text{ vol.}\%^{-1}$, $\tau = 5.0 \text{ min}$ and $\theta = 0.77 \text{ min}$), the controller settings were calculated using the IMC tuning method (Chien & Fruehauf 1990) (see Table 3.5). Simulations showed that two sets of settings (set 1, for PPs 1–14, and set 2, for PPs 15 and 16) are required for PID-PI to guarantee satisfactory performance; only one parameter of the master controller (τ_I) was adjusted for easier implementation. Two sets need to be chosen because the patient models 15 & 16 are very insensitive and the set 1 which is designed based on the nominal model is not giving the satisfactory performance for these two patients. Further, PID-P controller settings were obtained by fine-tuning the PID-PI settings with the integral action removed.

3.4.4 Model predictive controller (MPC) design

This section describes the design of a MPC for the regulation of BIS. This control scheme offers more advantages than the other control schemes; of these, the most important one is that the constraints on inputs, input rates and outputs can be considered in a systematic manner (Camacho & Bordons 2004). The MPC scheme can prevent violations of input and output constraints, drive some output variables to their optimal set-points while maintaining other outputs within specified ranges, and prevent excessive movement of the input variables (Bequette 2003, Seborg et al. 2004). These properties make the MPC, the most attractive out of all the advanced control schemes available presently.

In MPC scheme shown in Figure 3.3, the patient model is used to predict the current value of the output variable (BIS). The difference between the measured BIS from the patient and the model output (residual), serves as the feedback signal to the prediction block. With this residual and input variable, the prediction block predicts the future values of output BIS. On the basis of these predicted BIS values, the controller calculates the future input moves of which only first input move is implemented by the controller at current sampling instant. The linear MPC uses a linear step response model to make the future predictions.

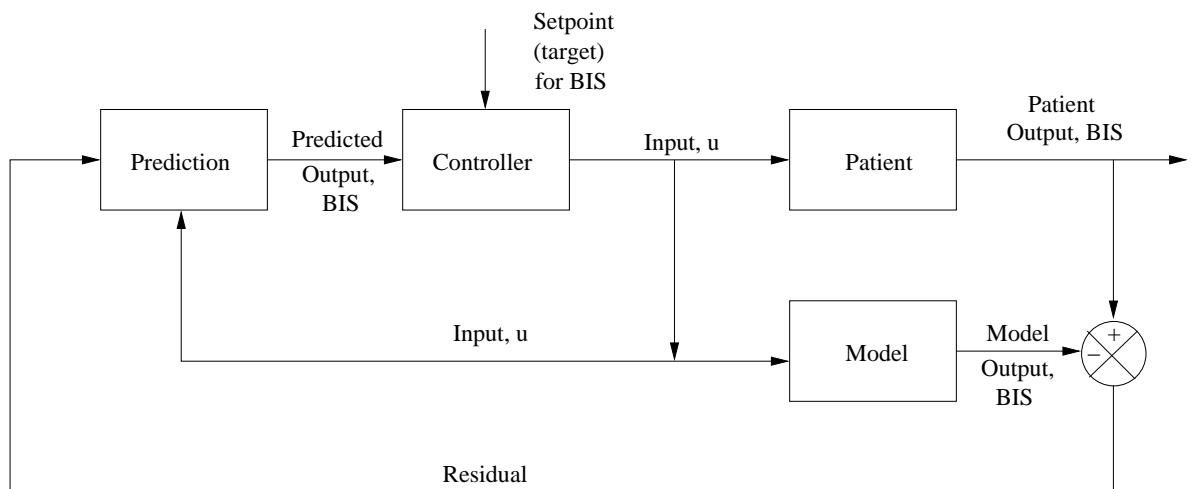


Fig. 3.3. Schematic representation of the MPC scheme for regulation of BIS

The basic objective of MPC as shown in Figure 3.4 is to determine the sequence of M future control moves (*i.e.*, manipulated input variable changes) such that the sequence of P predicted responses (output variables) are close to the set-point. Even though M control moves are calculated at each sampling instant, of which only the first input move will be implemented, and the optimization procedure repeats for the next sampling instant based on the updated measurements of the output variables.

The expression for quadratic objective function for the proposed MPC scheme is

$$\min_{\Delta u_k, \Delta u_{k+1}, \dots, \Delta u_{k+M-1}} J(P, M) = \sum_{i=k+1}^{k+P} e_i^T S e_i + \sum_{i=k}^{k+M-1} \Delta u_i^T R \Delta u_i \quad (3.10)$$

subject to absolute and rate constraints on the manipulated variable

$$\begin{aligned} u_{min} &\leq u_i \leq u_{max} && \text{(for } i = k, k + 1, \dots, k + M - 1) \\ u_{i-1} - \Delta u_{max} &\leq u_i \leq u_{i-1} + \Delta u_{max} && \text{(for } i = k, k + 1, \dots, k + M - 1) \end{aligned}$$

where, at each sampling instant i , $\Delta u_i = u_{i+1} - u_i$ is the vector of manipulated variable deviations, $e_i = r_i - y_i$ is the vector of predicted errors, r_i is the desired set-point for BIS and y_i is the vector of future BIS values those are predicted using the linear model. The length of these vectors depends on the prediction (output) horizon P and control (input) horizon M . Also, S and R are the weighting matrices for BIS and input rate, respectively. These weighting matrices can be used to tune the MPC controller to achieve the desired tradeoff between output performance and manipulated variable movement. The prediction horizon P is chosen on the basis of open-loop settling time, whereas control horizon M is chosen on the basis of tradeoff between faster response (large value of M) and robustness (small value of M). Generally, the chosen value for M is very small, compared to P . To reject constant disturbances that are due to patient-model mismatch, the patient model is augmented by the output disturbance model, which is an integrator that is driven

by white noise. The measurement noise is modeled as Gaussian noise, having zero mean and unit variance.

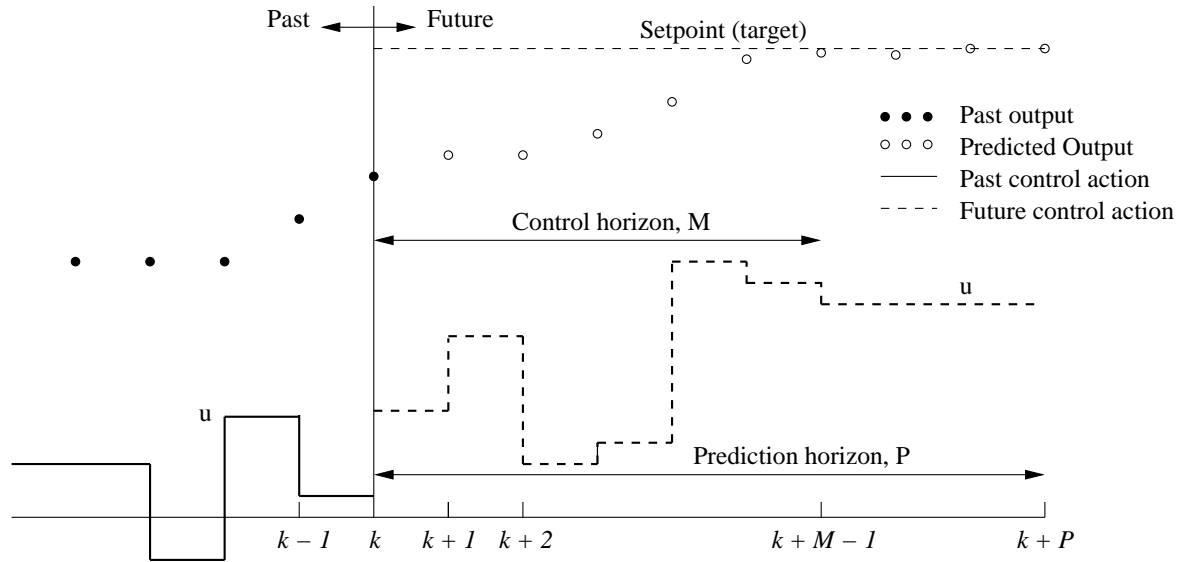


Fig. 3.4. Schematic representation of basic concept of MPC

A linear MPC requires an internal linear time-invariant model (e.g., a linear step response model) to estimate the future output values using past and future values of the inputs. Here, the overall dynamic system for the patient model is a combination of respiratory system, PK and PD models, which are physically represented as a series connection from vaporizer setting to concentration at the effect-compartment in series with the BIS measurement as shown in Figure 3.1. Since, a mathematical representation of the system is necessary to implement the MPC scheme, the above physical system can be represented mathematically as a series cascade of two linear time-invariant systems followed by a static nonlinear system (which provides the BIS values). The two linear time-invariant systems lead to two SISO models, where the anesthetic gas (isoflurane) concentration C_0 & the endtidal concentration C_1 are the input & output of the first model, and the endtidal concentration C_1 & effect-compartment concentration C_e are the input & output of the second model. The above two SISO models are in series with the nonlinear model which has effect-

compartment concentration C_e as input and BIS as output. These combined linear time-invariant systems and the linearized form of the nonlinear subsystem can be represented in state-space form. The combined state-space model is given in equations (3.11) – (3.13).

$$\begin{aligned} \dot{x} &= Ax + Bu \\ y &= Cx \end{aligned} \quad (3.11)$$

i.e.,

$$\begin{bmatrix} \dot{C}_{insp} \\ \dot{C}_1 \\ \dot{C}_2 \\ \dot{C}_3 \\ \dot{C}_4 \\ \dot{C}_5 \\ \dot{C}_e \end{bmatrix} = \begin{bmatrix} -k_R & k_{1R} & 0 & 0 & 0 & 0 & 0 \\ k_{10} & -k_1 & k_{21} \frac{V_2}{V_1} & k_{31} \frac{V_3}{V_1} & k_{41} \frac{V_4}{V_1} & k_{51} \frac{V_5}{V_1} & 0 \\ 0 & k_{12} \frac{V_1}{V_2} & -k_{20} - k_{21} & 0 & 0 & 0 & 0 \\ 0 & k_{13} \frac{V_1}{V_3} & 0 & -k_{31} & 0 & 0 & 0 \\ 0 & k_{14} \frac{V_1}{V_4} & 0 & 0 & -k_{41} & 0 & 0 \\ 0 & k_{15} \frac{V_1}{V_5} & 0 & 0 & 0 & -k_{51} & 0 \\ 0 & k_{e0} & 0 & 0 & 0 & 0 & -k_{e0} \end{bmatrix} \begin{bmatrix} C_{insp} \\ C_1 \\ C_2 \\ C_3 \\ C_4 \\ C_5 \\ C_e \end{bmatrix} + \begin{bmatrix} \frac{Q_0}{V} \\ 0 \\ 0 \\ 0 \\ 0 \\ 0 \\ 0 \end{bmatrix} \begin{bmatrix} C_0 \end{bmatrix} \quad (3.12)$$

where, $k_R = \frac{[Q_0 - \Delta Q + f_R(V_T - \Delta)]}{V}$,
 $k_{1R} = \frac{f_R(V_T - \Delta)}{V}$,
 $k_{10} = \frac{f_R(V_T - \Delta)}{V_1}$,
 $k_1 = k_{10} + k_{12} + k_{13} + k_{14} + k_{15}$.

$$\begin{bmatrix} BIS \\ C_1 \end{bmatrix} = \begin{bmatrix} 0 & 0 & 0 & 0 & 0 & 0 & k_m \\ 0 & 1 & 0 & 0 & 0 & 0 & 0 \end{bmatrix} \begin{bmatrix} C_{insp} & C_1 & C_2 & C_3 & C_4 & C_5 & C_e \end{bmatrix}^T \quad (3.13)$$

where, k_m is the linearization constant (equation (3.14)) obtained via linearization of equation (3.9) around the reference concentration $C_e = EC_{50}$. Using the values of $k_{e0} = 0.3853 \text{ min}^{-1}$, $EC_{50} = 0.7478 \text{ vol.}\%$ and $\gamma = 1.534$, k_m is calculated to be -51.28.

$$k_m = -\frac{100\gamma}{4EC_{50}} \quad (3.14)$$

As discussed above, in equation (3.13), BIS is a controlled variable and C_1 is a measured variable. In the present chapter, a step response model obtained from the above state-space model is used in the MPC design. However, the state-space model itself can be used directly in the MPC design (Wang 2004, Wang & Young 2006). The MPC parameters that have been determined using direct search optimization for hypnosis regulation are output (BIS) weight, $S = 10$; input rate (isoflurane) weight, $R = 1$; prediction (output) horizon, $P = 25$; control (input) horizon, $M = 2$; and sampling interval of 5 *sec*.

3.4.5 Robustness, set-point tracking, disturbance rejection, aggressiveness (RTDA) controller design

RTDA controller involves a novel control scheme that is sufficiently simple to implement and can achieve better control (Mukati & Ogunnaike 2004, Ch'ng & Lakshminarayanan 2006, Ogunnaike & Mukati 2006). Each of its four tuning parameters (θ_R , θ_T , θ_D and θ_A) is normalized between 0 and 1 (with 0 being aggressive and 1 denoting conservative settings) and is related directly to one performance attribute (namely, robustness, set-point tracking, disturbance rejection, and aggressiveness). Hence, it is possible to tune each parameter independently to obtain the optimum for the corresponding performance attribute. Thus, the RTDA controller avoids the tuning problems that are associated with PID and MPC controllers. Furthermore, RTDA controller uses simple linear MPC strategy based on the model approximated as FOPTD as like in the design and tuning of PID controllers. The main features of the RTDA controller for the control of hypnosis are described as follows.

The FOPTD model can be written as:

$$y(s) = \frac{K e^{-\alpha s}}{\tau s + 1} u(s) \quad (3.15)$$

where y , u , K , α and τ represents process output, input, time delay, time constant, and gain, respectively.

Since, RTDA controller is designed in digital form, the discretised form of equation (3.15) is given by:

$$\hat{y}(k+1) = a\hat{y}(k) + bu(k-m); \quad k = 0, 1, 2, \dots \quad (3.16)$$

where $a = e^{-\frac{\Delta t}{\tau}}$; $b = K \left(1 - e^{-\frac{\Delta t}{\tau}}\right)$; $m = \text{round}\left(\frac{\alpha}{\Delta t}\right)$ and Δt is the sampling time. Control strategy is implemented as at each time instant k , the computation of current control move $u(k)$ required to bring the predicted process output as close as possible to the reference trajectory to be held over the prediction horizon, N beyond the delay period, m . Based on this strategy, predicted process output is given by:

$$\hat{y}(k+m+i) = a^{m+i}\hat{y}(k) + a^{i-1}b\mu(k, m) + b\eta_i u(k) \quad (3.17)$$

$1 \leq i \leq N$, with $\mu(k, m) = \sum_{i=1}^m a^i u(k-i)$, and $n_i = \frac{1-a^i}{1-a}$. Because of the use of a FOPTD model in the place of original model, results in modeling error between the actual process output and the model predicted output, $e(k) = y(k) - \hat{y}(k)$. The modeling error, $e(k)$ can be grouped into two types of estimates $e_m(k)$ and $e_D(k)$ as given by:

$$e(k) = e_m(k) + e_D(k) \quad (3.18)$$

where $e_m(k)$ represents the inherent modeling uncertainties and $e_D(k)$ represents the effects of unmeasured disturbances. By using Bayesian estimation procedure, $e_D(k)$ can be estimated as:

$$\hat{e}_D(k) = \theta_R \hat{e}_D(k-1) + (1 - \theta_R) e(k) \quad (3.19)$$

where θ_R , ($0 < \theta_R < 1$), serves as the tuning parameter for robustness of the controller. With the current error estimate, the future error is then estimated to update the model prediction. This can be written as:

$$\hat{e}_D(k+j|k) = \hat{e}_D(k) + \frac{(1-\theta_D)}{\theta_D} [1 - (1-\theta_D)^j] \nabla \hat{e}_D(k) \quad (3.20)$$

for $m+1 \leq j \leq m+N$, where,

$$\nabla e_D(k) = e_D(k) - e_D(k-1) \quad (3.21)$$

and θ_D , ($0 < \theta_D < 1$), serves as the tuning parameter for disturbance rejection. Using the above outlined error estimation, the future prediction of $y(k+m+i)$ over the N -step prediction horizon is given by updating the model prediction in equation (3.17) with equation (3.20) is represented as:

$$\tilde{y}(k+m+i) = \hat{y}(k+m+i) + \hat{e}_D(k+m+i|k) \quad (3.22)$$

For the purpose of set-point (y_d) tracking, a desired set-point trajectory (y^*) needs to be defined. The control action is computed based on at each instant k , the single control move, $u(k)$, is determined to minimize the error between predicted output from the desired set-point trajectory, y^* , over the next N discrete steps in the future. The desired set-point trajectory for the set-point, y_d , is given by:

$$y^*(k+j) = \theta_T^j y^*(k) + (1 - \theta_T^j) y_d(k); \quad 1 \leq j \leq \infty \quad (3.23)$$

with θ_T , ($0 < \theta_T < 1$), serves as the tuning parameter for set-point tracking. The tuning parameter for overall controller aggressiveness, θ_A , depends on the value of N and which is given by:

$$\theta_A = 1 - e^{-\left(\frac{(N-1)\Delta t}{\tau}\right)} \quad (3.24)$$

Having defined a reference trajectory and derived the model prediction with error correction, the current control action $u(k)$ may now be solved for to obtain the least deviation from the trajectory. Thus, the analytical solution for the optimization problem is given by:

$$u(k) = \frac{1}{b} \frac{\sum_{i=1}^N \eta_i \psi_i(k)}{\sum_{i=1}^N \eta_i^2} \quad (3.25)$$

where:

$$\psi_i(k) = y^*(k+i) - a^{m+i} \hat{y}(k) - a^{i-1} b \mu(k, m) - \hat{e}_D(k+m+i|k)$$

For the present application, the values for RTDA parameters are found to be $\theta_R = 0.7675$, $\theta_T = 0.9884$, $\theta_D = 0.5033$ and $\theta_A = 0.6130$ by using direct search optimization algorithm.

3.5 Evaluation of Controllers

For realistic evaluation of controllers, white noise with zero mean and standard deviation (SD) of ± 3 and $\pm 0.045 \text{ vol.}\%$ was added to the BIS and C_1 , respectively, in all simulations. The SD value of ± 3 in BIS was used in the study of Struys et al. (2004) and is also employed here. This value is consistent with our observations in the local hospital. The SD value of C_1 is not known, and so we used 0.045% , which is 6% of the nominal value (similar to the SD value of BIS). For PI, PID, MPC, and RTDA controllers, the BIS measurement was passed through a filter with a time constant of 5 min , whereas, for cascade controllers, the BIS and C_1 measurements were passed through a filter with time constant of 1 and 5 min , respectively. For cascade control, the inner slave controller led to faster dynamics of the outer BIS loop, requiring a smaller filter time constant to avoid introducing too much lag into the closed-loop response. Lower and upper limits of 0 and $5 \text{ vol.}\%$ (Gentilini et al. 2001a) were also placed on the controller outputs for all six controllers.

Figure 3.5 shows the schematic representation of the closed-loop setup for regulating hypnosis that uses BIS as the controlled variable. Figure 3.6 shows the BIS response for all the patient sets reported in Table 3.2 with the PI controller (with settings in Table 3.3) for a set-point change from 100 to 50. From this figure, one can clearly observe that the second half of the PPs (PP 9–16) are more insensitive (mainly because of lower f_R , k_{e0} and higher EC_{50}) compared to the first half (PP 1–8). Furthermore, responses in case of PP 9, 11, 13 and 16 are oscillatory, because of the higher γ value that is associated with these patient profiles. The settling time, for the case of the most sensitive patient (PP 1), is ~ 30 min, compared to 250 min for the case of the most insensitive patient (PP 16).

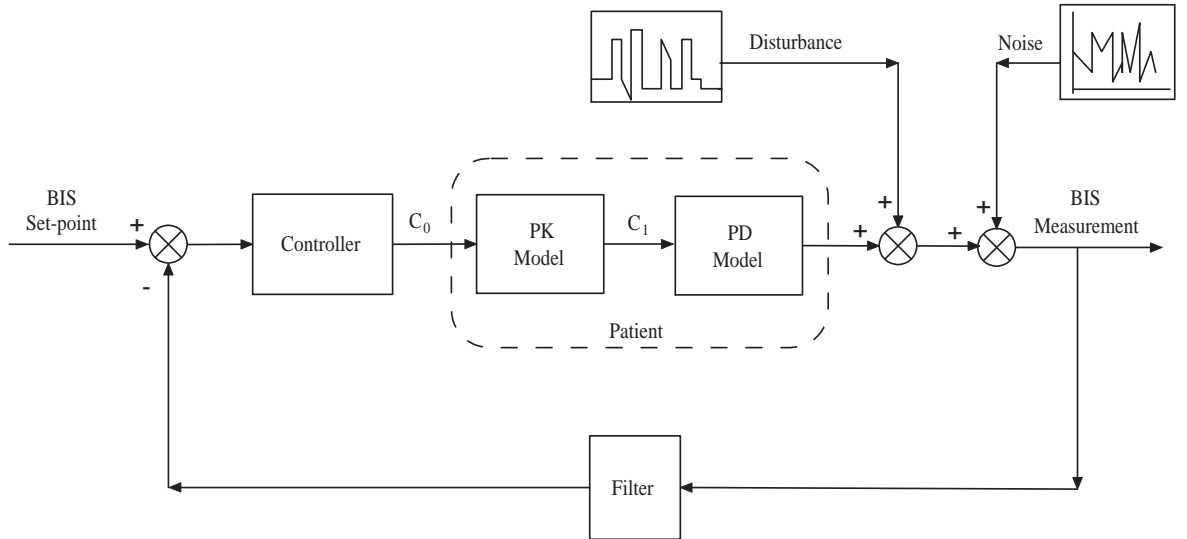


Fig. 3.5. Setup of a feedback controller for hypnosis regulation

The IAE was used as the main performance criterion, and this value was calculated by integrating the absolute difference (error, e) between the BIS set-point and its measurement.

$$\text{IAE} = \int_0^t |e(t)| dt \quad (3.26)$$

Large IAE values indicate responses that are more sluggish and less desirable. However, they do not indicate the amount of oscillatory behavior. The performance

criterion based on the performance error (PE), which was used by Struys et al. (2004), was also employed.

$$PE = \left(\frac{\text{Measured Value} - \text{Target Value}}{\text{Target Value}} \right) \times 100 \quad (3.27)$$

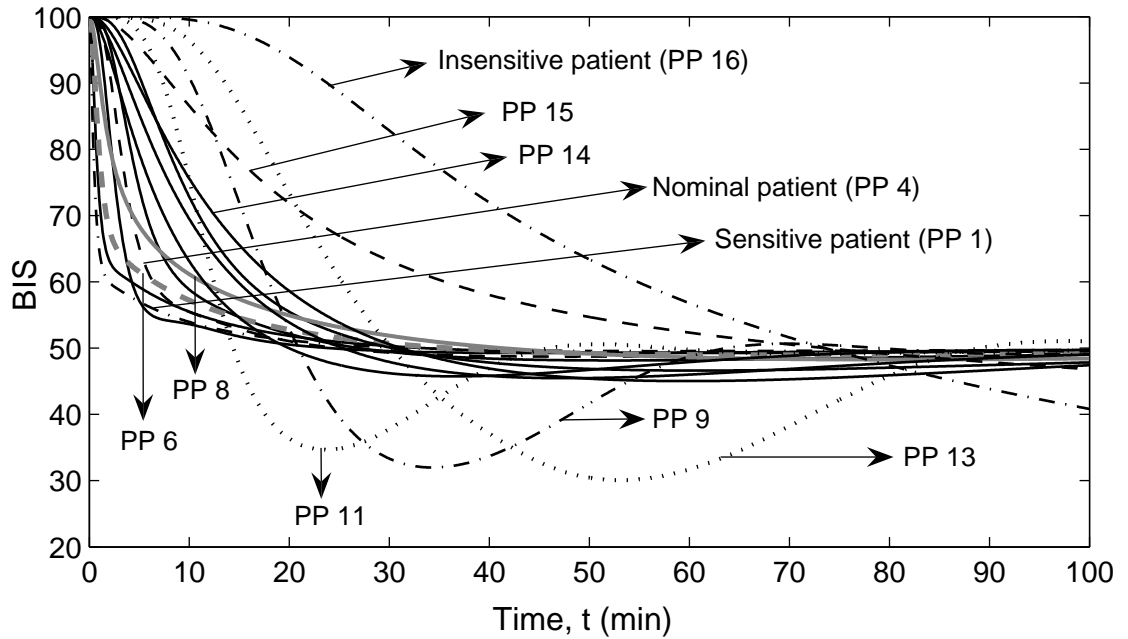


Fig. 3.6. BIS response with PI controller for all 16 patients for a set-point change from 100 to 50

The median performance error (MDPE) is a measure of bias and indicates if the measured value is systematically above or below the set-point. MDPE can be calculated from the expression

$$MDPE = \text{Median}\{PE_i, i = 1, 2, \dots, N\} \quad (3.28)$$

where N is the number of PE values obtained for that particular subject. MDPE is a signed value and therefore represents the direction of PE. It does not reveal either the oscillatory behavior or the amplitude of possible oscillations in the output (Struys et al. 2004). On the other hand, the median absolute performance error

(MDAPE), gives the magnitude of control inaccuracy, with larger MDAPE values being indicative of poorer closed-loop performance.

$$\text{MDAPE} = \text{Median}\{|PE_i|, i = 1, 2, \dots, N\} \quad (3.29)$$

Wobble is an index of time-related changes in performance; it measures the degree of intra-patient variability in PEs. It also gives an indication of the degree of oscillatory behavior.

$$\text{Wobble} = \text{Median}\{|PE_i - MDPE|, i = 1, 2, \dots, N\} \quad (3.30)$$

Large wobble values indicate large variability in PE values and, thus, signify a more oscillatory response.

In summary, conventional measures (such as IAE) indicates the controller performance, in terms of sluggishness in response. These measures do not indicate the oscillatory behavior in the response. On the other hand, MDPE indicates whether the measured values are systematically above or below the specified set-point. MDAPE reflects the magnitude of the control inaccuracy, similar to IAE. Finally, wobble is an index of oscillatory behavior of the output response.

All the above criteria characterize only the output performance of the controller. Because controller design invariably involves tradeoff between input and output performance, another measure of controller performance - an input performance criterion (total variation, TV) - is also used. The required control effort is computed by calculating the TV of the manipulated input, u :

$$\text{TV} = \sum_{i=0}^{\infty} |u_{i+1} - u_i| \quad (3.31)$$

The TV value of $u(t)$ is the sum of all the up and down control moves. Thus, it is a good measure of the smoothness of the manipulated input. The TV value should be as small as possible.

Controller performance was evaluated mainly for the surgical stimuli and the maintenance phase of the surgery. Less emphasis was placed on the induction period during which a patient is brought into a hypnotic state. Induction is typically conducted using open-loop intravenous injection of hypnotics to avoid the undesirable slow-acting characteristic of volatile hypnotics such as isoflurane. In fact, in clinical trials to evaluate controller performance, such as those conducted by Morley et al. (2000) and Struys et al. (2001), the induction of anaesthesia was done in open-loop and the controller was switched on only after induction. The surgical stimuli period in the present chapter spans time range of $t = 100 - 160 \text{ min}$, during which period the disturbance profile (Figure 3.7) adopted from Struys et al. (2004) was introduced into the patient system by adding a pulse input of different strengths to the BIS output from the PD model (see Figure 3.5). In Figure 3.7, stimulus A mimics the response to intubation; B represents surgical incision, followed by a period of no surgical stimulation (e.g., waiting for pathology result); C represents an abrupt stimulus after a period of low level stimulation; D shows onset of a continuous normal surgical stimulation; E, F, and G simulate short-lasting, larger stimulation within the surgical period; and H simulates the withdrawal of stimulation during the closing period (Struys et al. 2004).

The maintenance period refers to the entire intraoperative period during which the surgery proceeds and a desired level of hypnosis must be guaranteed and maintained. In the simulations, the maintenance period spanned a time period of $t = 100 - 350 \text{ min}$ and, hence, included disturbances that were due to both surgical stimuli (*i.e.*, $t = 100 - 160 \text{ min}$) and intraoperative set-point changes (*i.e.*, $t = 200 - 350 \text{ min}$). The set-point changes and their time of introduction are given in Table 3.6. These

do not include the BIS set-point change from 100 to 50 at $t = 10 \text{ min}$, for the induction.

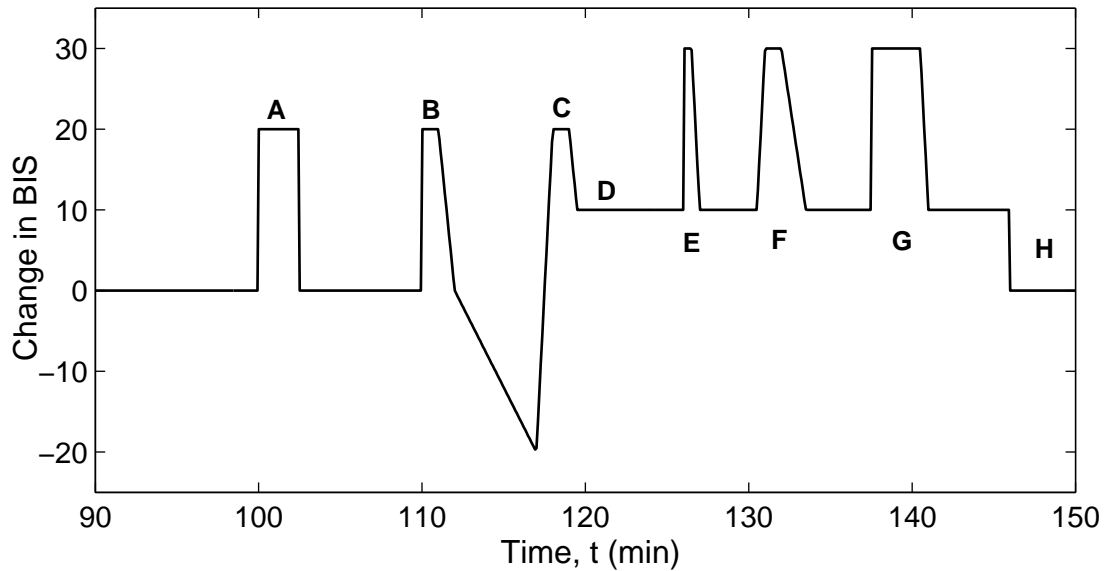


Fig. 3.7. Disturbance profile (adopted from Struys et al. (2004))

Table 3.6
Series of intraoperative set-point changes

Time, t (min)	BIS set-point change
200	50 to 60
250	60 to 40
300	40 to 50

3.6 Performance of Controllers

Figure 3.8 shows IAE values obtained during the maintenance period for all six controllers when implemented on the 16 PPs. Advanced controllers were determined to give better closed-loop control, with reductions of up to 13%, 27%, and 33% in the mean IAE value for cascade, MPC, and RTDA controllers, respectively, compared to PI/PID controllers (see Table 3.7). The additional integral action in the inner loop of the PID-PI controller seems to have made the closed-loop system perform poorly,

with the IAE value for PP 16 and PP 15 deviating up to 400% and 125% from that of the nominal patient, even when different controller settings were used. PID-P gave better control for PP 16, with an IAE value of 3375, compared to a value of 5087 for PID-PI. The performance of PID-PI is inferior to that of PID-P for PP 13 to PP 16 (see Figure 3.8). This could be due to the slow dynamics of the inner loop, which result from the small value of f_R (see Table 3.2) and because disturbances are in the outer loop in hypnosis regulation. Both these are uncommon in chemical process applications of cascade control. Finally, MPC and RTDA gave the best robust performance with coefficient of variance (SD/mean) values of 0.174 and 0.180, compared to 0.385 and 0.349 for PID-P and PI (best performing cascade and single loop controller), respectively. This indicates that MPC and RTDA controllers have the least dependence on the patient's sensitivity to the drug.

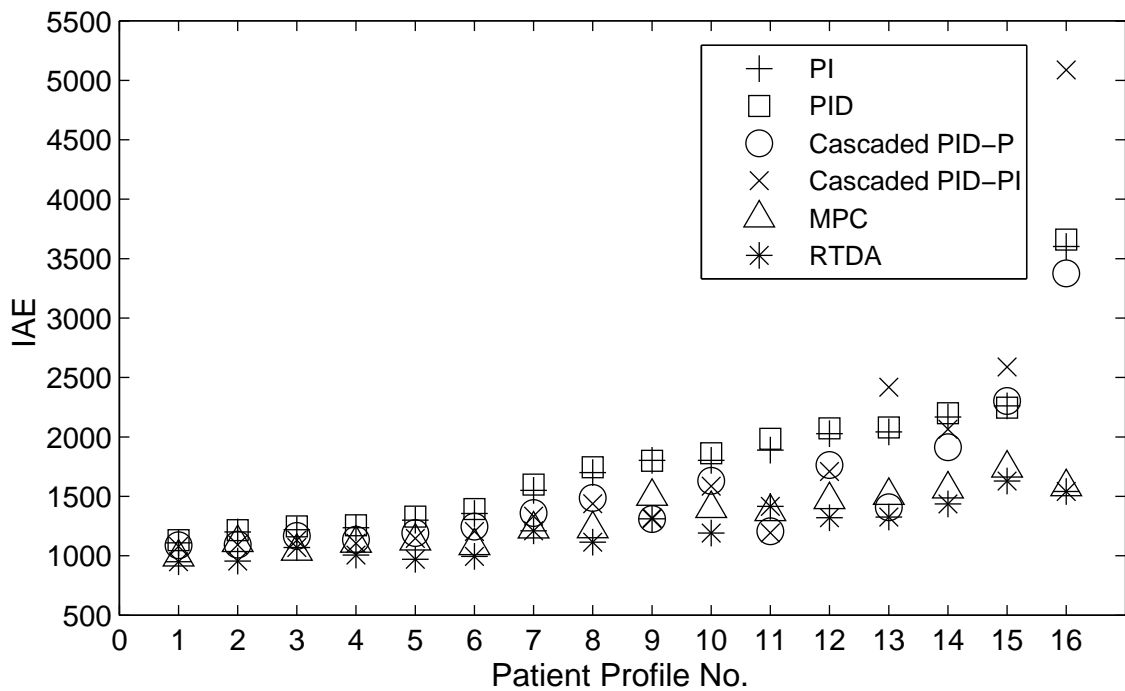


Fig. 3.8. IAE values for the maintenance period for six controllers on 16 patients

Tables 3.7 and 3.8 summarize the performance, in terms of the mean and standard deviation of each performance criterion, of all six controllers during the maintenance and surgical stimuli period, respectively. The MDPE values for all controllers were

negative, which indicated a consistent tendency for the measured BIS to be less than the set-point. This means that the controllers had a tendency to slightly overdose, and this observation can be explained by the asymmetric control operation that is performed by the controllers. They govern only the infusion, but not the elimination, of drugs from the body, which is a slower process (Struys et al. 2004).

Table 3.7
Controller performance of various controllers for the maintenance period ($t = 100 - 350 \text{ min}$)

Performance Criterion	Value for the Controller ^a					
	PI	PID	PID-P	PID-PI	MPC	RTDA
IAE	1767 (617)	1801 (624)	1542 (593)	1719 (1017)	1314 (229)	1215 (219)
MDPE	-3.29 (4.38)	-3.54 (4.46)	-2.95 (3.43)	-4.11 (10.8)	-0.87 (0.61)	-0.79 (0.60)
MDAPE	11.5 (5.79)	11.8 (5.98)	9.41 (4.95)	10.8 (9.67)	7.40 (1.80)	6.59 (1.71)
Wobble	10.2 (4.11)	10.3 (4.01)	8.62 (4.30)	8.51 (3.59)	7.24 (1.71)	6.95 (1.64)
% time outside ± 10 BIS	24.6 (12.2)	25.4 (12.5)	19.4 (12.2)	22.2 (18.1)	15.3 (4.20)	13.5 (3.85)
% time outside ± 5 BIS	51.4 (16.3)	52.4 (16.0)	43.6 (16.2)	43.8 (18.5)	37.2 (9.71)	34.6 (8.56)
TV	45.42 (9.35)	44.66 (8.99)	53.56 (9.67)	47.58 (9.48)	60.16 (11.49)	63.25 (12.11)

^aNote: The mean and standard deviation (shown in brackets) of the criterion are given for each controller.

Results in Tables 3.7 and 3.8 further confirm that cascade, MPC, and RTDA controllers outperform PI and PID controllers for hypnosis regulation, with reference to other performance criteria besides IAE. In particular, for the maintenance period (see Table 3.7), the use of MPC and RTDA resulted in reductions of $\sim 37\%$ and $\sim 44\%$ in MDAPE and $\sim 30\%$ and $\sim 33\%$ in wobble, respectively, compared to PI/PID controllers, indicating better control and less oscillation. A significant improvement in the percentage of time for which measured BIS value was within ± 5 and ± 10 from the set-point is also observed for the MPC and RTDA controllers, which indi-

cates tighter control over the BIS output (see Figure 3.9). However, improvement in surgical stimuli rejection alone is less with PID-P, MPC, and RTDA controllers, giving a reduction of $\sim 9\% - 19\%$ in MDAPE and $14\% - 23\%$ in wobble, respectively, compared to PI/PID controllers (see Table 3.8). The performance of PID-PI controller is disappointing, despite the cascaded setup, giving $<10\%$ improvement in the performance, compared to PI/PID controller (see Tables 3.7 and 3.8).

Table 3.8
Controller performance of various controllers for the surgical stimuli period ($t = 100 - 160 \text{ min}$)

Performance Criterion	Value for the controller ^a					
	PI	PID	PID-P	PID-PI	MPC	RTDA
IAE	618 (55)	622 (62)	569 (49)	618 (200)	571 (45)	545 (41)
MDPE	-1.77 (5.38)	-1.86 (5.31)	-2.90 (5.00)	-0.21 (9.76)	-3.16 (5.10)	-2.85 (4.56)
MDAPE	18.5 (2.35)	18.7 (3.09)	16.0 (2.35)	17.4 (5.42)	16.8 (2.41)	15.2 (2.25)
Wobble	17.9 (2.13)	18.3 (2.88)	15.3 (2.55)	16.7 (6.52)	15.5 (2.57)	14.1 (2.41)
% time outside ± 10 BIS	45.2 (6.64)	45.6 (7.52)	39.4 (6.13)	41.3 (8.97)	41.7 (5.77)	37.2 (5.42)
% time outside ± 5 BIS	72.1 (3.58)	71.8 (4.64)	68.7 (5.53)	69.1 (6.06)	69.2 (6.2)	64.8 (5.6)
TV	22.96 (6.64)	21.89 (6.72)	30.41 (7.61)	23.1 (9.49)	30.75 (7.96)	33.29 (11.85)

^aNote: The mean and standard deviation (shown in brackets) of the criterion are given for each controller.

The last row in Tables 3.7 and 3.8 compare the input performance (*i.e.*, control effort (TV)) for all the six controllers. These results show that the better control performance of MPC and RTDA, compared to other controllers, is accompanied by greater control effort, which may still be acceptable. This clearly shows the aggressive nature of these two controllers, compared to the remaining four controllers.

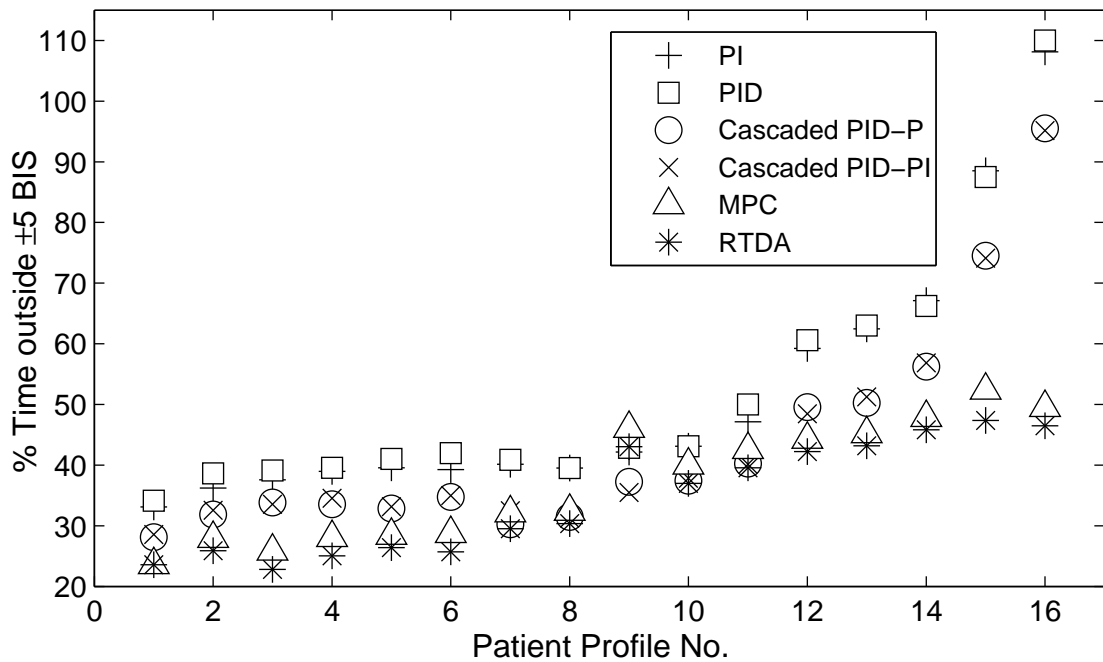


Fig. 3.9. Percentage of the time that BIS is ± 5 units outside its set-point during the maintenance period

It is worth mentioning that the performance of all six controllers was determined to have a greater dependence on PD parameters than PK parameters. Although not presented here, all of them had been determined to give consistent and acceptable performance in the presence of PK variation only (*i.e.*, with PD parameters kept at nominal values). PK parameters affect the uptake and distribution of drugs, whereas PD parameters describe the drug effect and degree of nonlinearity in the patient system. Hence, variations in PD parameters are expected to have greater influence on the closed-loop performance, especially because linear controllers were employed.

The closed-loop performance of the PID controller for a few patient models is compared to that of MPC and RTDA controllers in Figures 3.10 and 3.11. Generally, regardless of the controller, the closed-loop performance became more sluggish with decreasing drug sensitivity (which can be observed for PP 15 and PP 16 in Figure 3.11). However, MPC and RTDA gave tighter control of BIS for different PPs

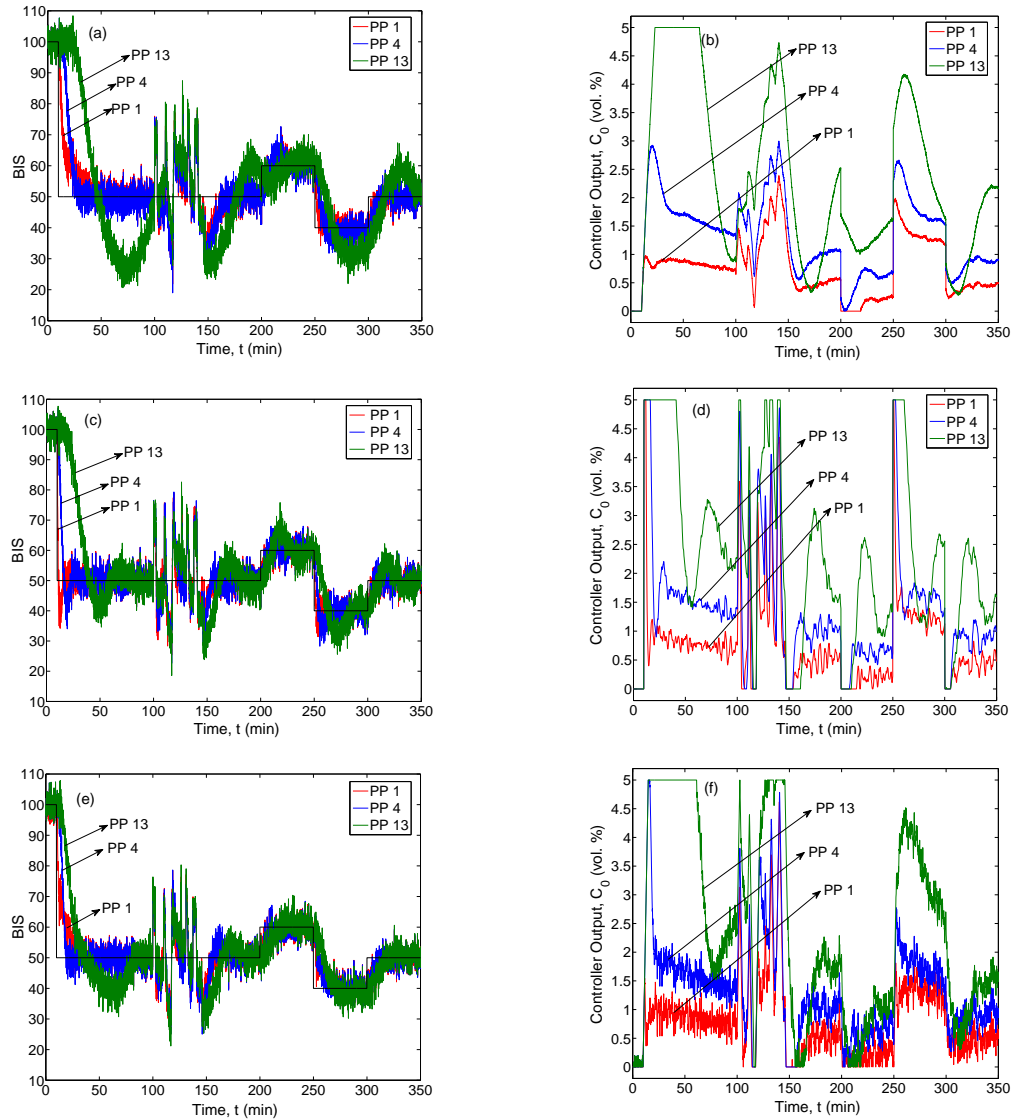


Fig. 3.10. Performance of (a,b) PID, (c,d) MPC and (e,f) RTDA controllers for PP 1, PP 4 (nominal) and PP 13

(*i.e.*, from PP 1 to PP 16), as can be seen from Figures 3.8 and 3.9, which indicates a weaker dependence of their performance on the drug sensitivity of patients. Despite the sluggishness, these controllers tracked the intraoperative set-point changes and also rejected the disturbances, for PP 13 (a considerably insensitive patient), PP 15 and PP 16 (highly insensitive patients).

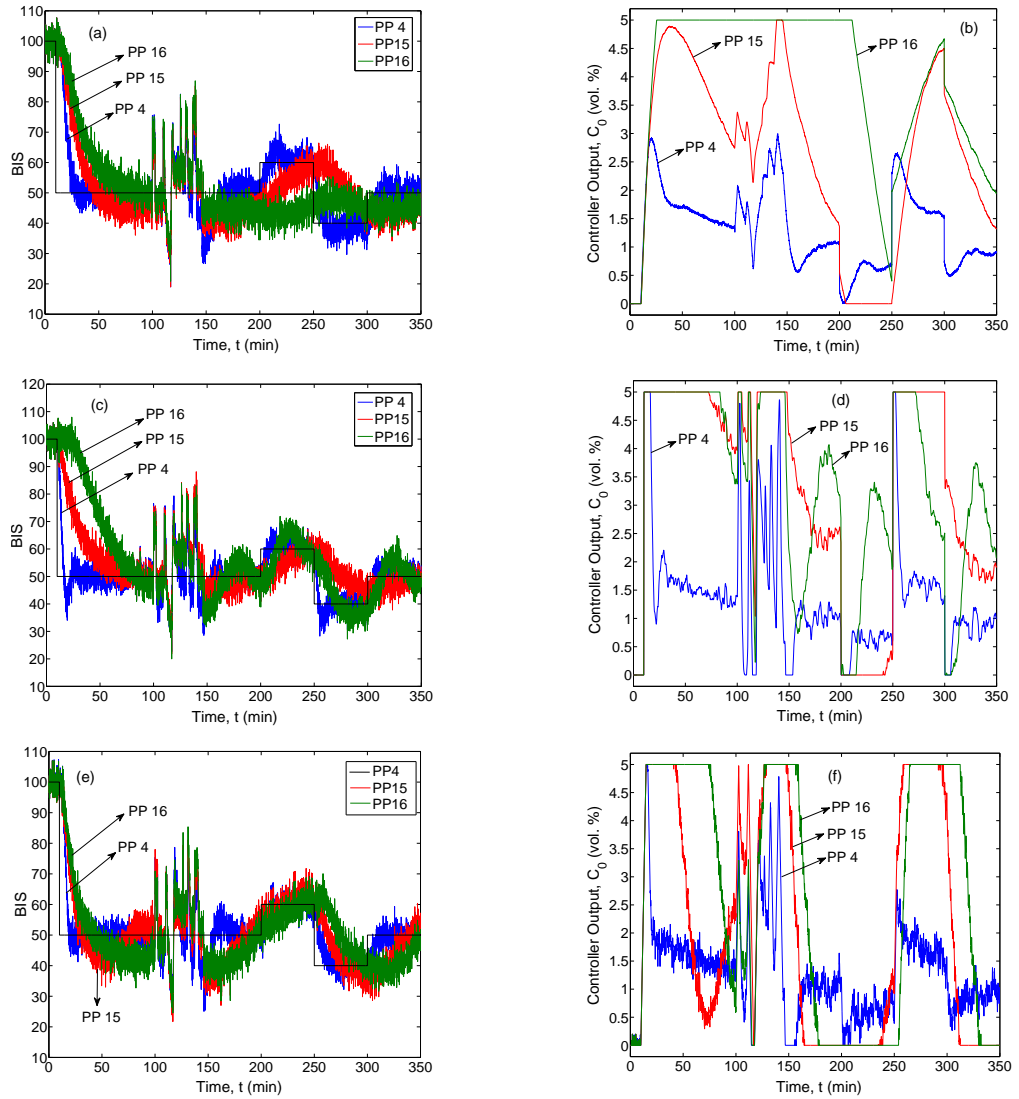


Fig. 3.11. Performance of (a,b) PID, (c,d) MPC and (e,f) RTDA controllers for the nominal (PP 4) and highly insensitive (PP 15 and PP 16) patients

3.7 Controller Performance in the Absence of BIS Signal

The measured BIS and C_1 are sometimes corrupted with artifacts; BIS artifacts may come from the high impedance of the electrodes, corruption of the EEG with the electromyography (EMG) signal and accidental disconnection of electrodes from the patient's head (Gentilini et al. 2001a), whereas C_1 artifacts result from device calibration errors and disconnection of sample lines. The present section focuses on evaluating controller performance during the loss of BIS feedback signal, because of its higher likelihood of occurrence and the higher risks involved.

When BIS signal is lost, the controllers are designed to use an estimated BIS value as subsequent feedback until the disconnection of electrodes is rectified. BIS may be estimated using the last BIS measurement or using the measured C_1 and the nominal PD model. We propose a modification of the latter method using a patient-specific EC_{50} value, together with nominal k_{e0} and γ values in the PD model for BIS estimation. The problem with estimating BIS value based on a nominal PD model (which uses a nominal EC_{50} value of 0.7478 *vol.%*) arises when the patient has a different EC_{50} value. Simulations by varying each PD parameter independently were conducted, and the results (with noise removed for clarity) are shown in Figure 3.12. In these simulations, each patient PD parameter was varied individually, and the PID controller performance using the nominal PD model for BIS estimation during the loss of BIS signal was observed. The results reflect that only EC_{50} has a drastic effect (as proven by robustness analysis) on the accuracy of BIS prediction (Figure 3.12); therefore, only this parameter must be known accurately and the remaining PD parameters can be taken as their nominal values for BIS estimation.

The patient-specific EC_{50} value can be estimated by averaging all C_1 concentrations (during the induction, $t = 0 - 100 \text{ min}$) that correspond to BIS within ± 6 units (*i.e.*, within $\pm 2\text{SD}$ of BIS measurements) from $\text{BIS} = 50$. Table 3.9 summarizes the

estimated EC_{50} for all six controllers when implemented on PP 1, PP 7, and PP 13. All the EC_{50} estimates are very close to the true values (within a deviation of 3% from the actual EC_{50} value) because, C_1 measurements are used for the estimation and these measurements directly reflect the patient's sensitivity to the drug.

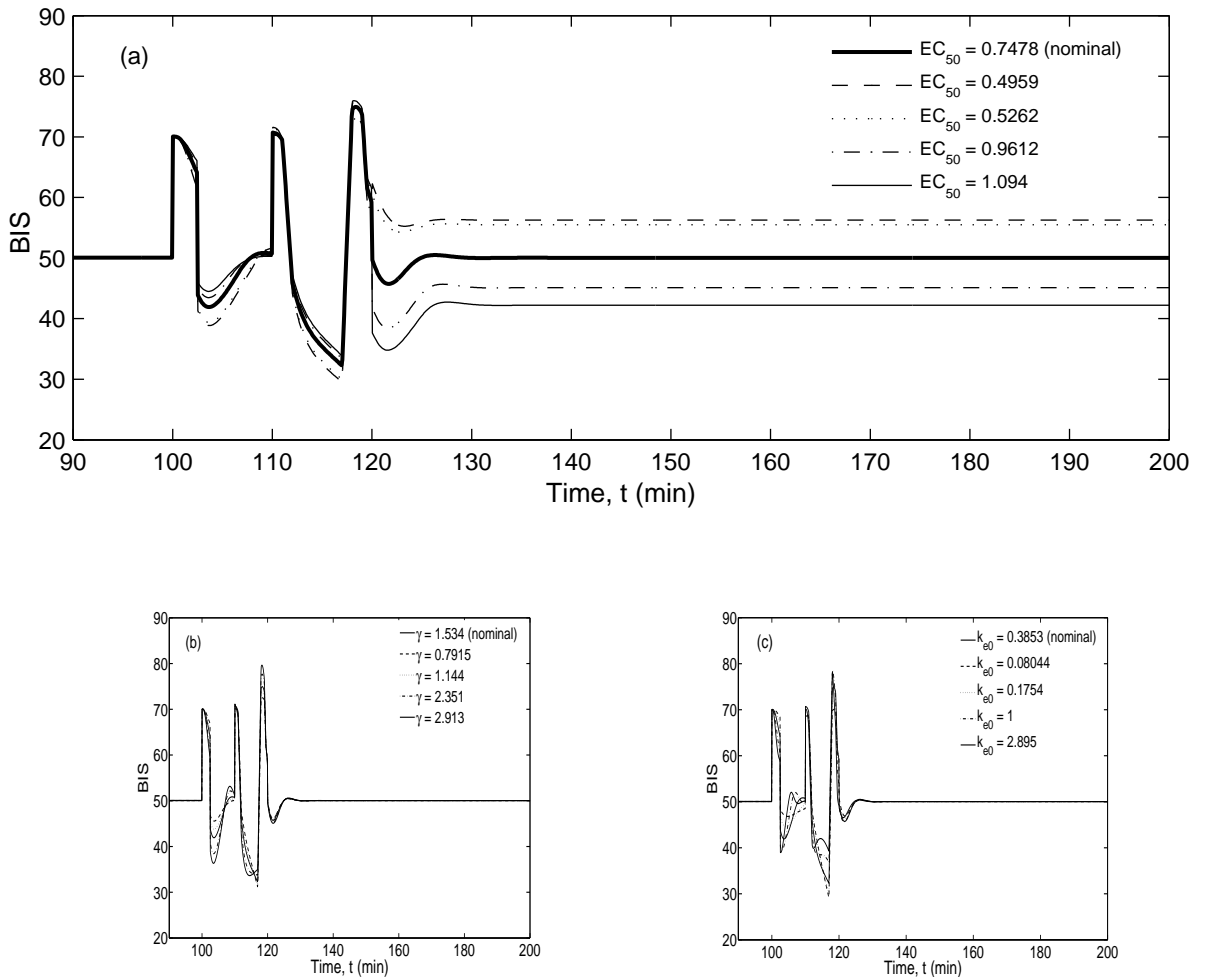


Fig. 3.12. Effect of PD parameters on closed-loop performance during the loss of BIS signal ($t = 120 - 200 \text{ min}$): (a) effect of EC_{50} , (b) effect of γ and (c) effect of k_{e0}

The loss of BIS signal was simulated by breaking the BIS loop at $t = 120 \text{ min}$ during the occurrence of extreme surgical stimuli to test the controllers in the most difficult scenario. When the electrodes attached to the patient's head get disconnected, BIS falls sharply to 0, and an estimated BIS value is automatically used as feedback. Furthermore, prolonged loss of BIS signal (such as when the disconnec-

tion of electrodes goes unnoticed) was assumed. For PP 3, using MPC and RTDA controllers, Figures 3.13(a) and 3.13(c) show that BIS cannot be maintained at its set-point of 50 by simply using the last BIS measurement recorded or BIS estimated from the nominal PD model as feedback. On the other hand, using the patient-specific EC_{50} value that was estimated from the measurements in the induction period resulted in significantly improved closed-loop performance.

Table 3.9
Estimated EC_{50} values for selected PPs for all six controllers

	PP 1 (actual $EC_{50} = 0.5146$)	PP 7 (actual $EC_{50} = 0.7478$)	PP 13 (actual $EC_{50} = 1.0940$)
	Estimated EC_{50}	Estimated EC_{50}	Estimated EC_{50}
PI	0.4986	0.7285	1.1105
PID	0.4975	0.7196	1.1226
PID-P	0.4752	0.7289	1.1195
PID-PI	0.4786	0.7205	1.1235
MPC	0.5055	0.7401	1.0885
RTDA	0.5085	0.7425	1.0902

The calculation of EC_{50} is patient-specific; therefore, this method of BIS estimation during the loss of feedback signal is expected to be robust for a wide range of patient sensitivities. The results in Figure 3.14 confirm this for MPC and RTDA. Similar trends were observed for all other controllers studied in this chapter. Figure 3.14(e) shows the comparison of performance, in terms of IAE for the 16 patients for MPC and RTDA controllers; RTDA shows slightly better performance than MPC.

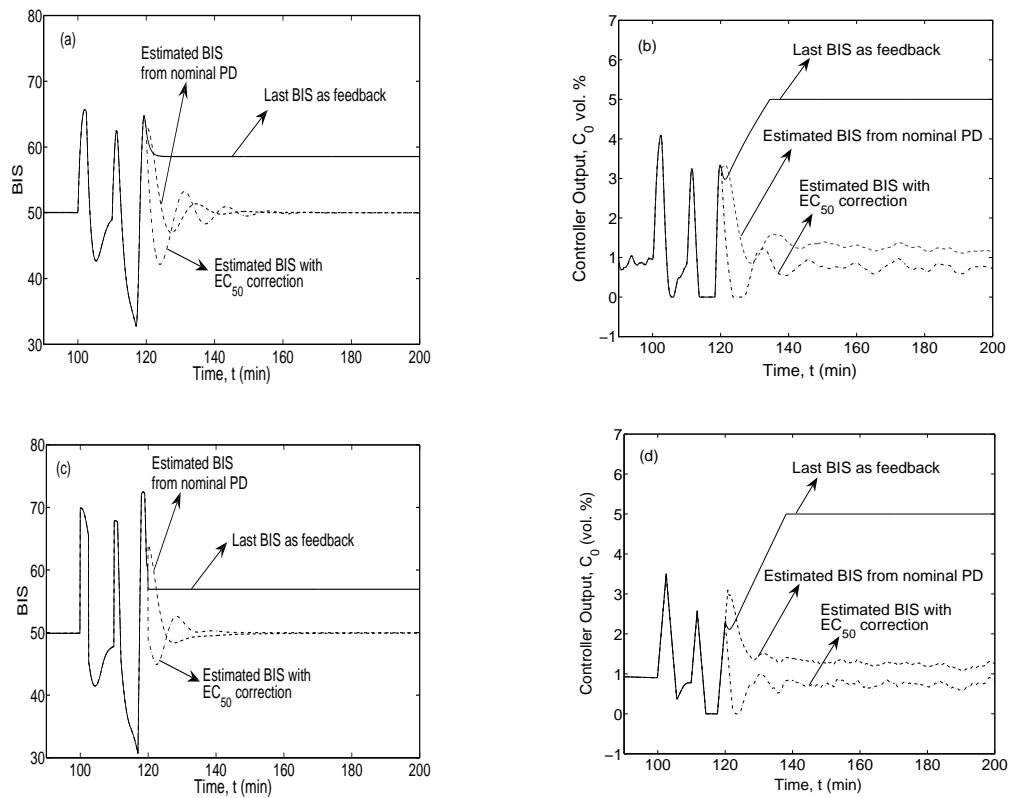


Fig. 3.13. BIS response and controller output in the absence of BIS signal from $t = 120 - 200$ min for PP 3, using (a,b) MPC and (c,d) RTDA

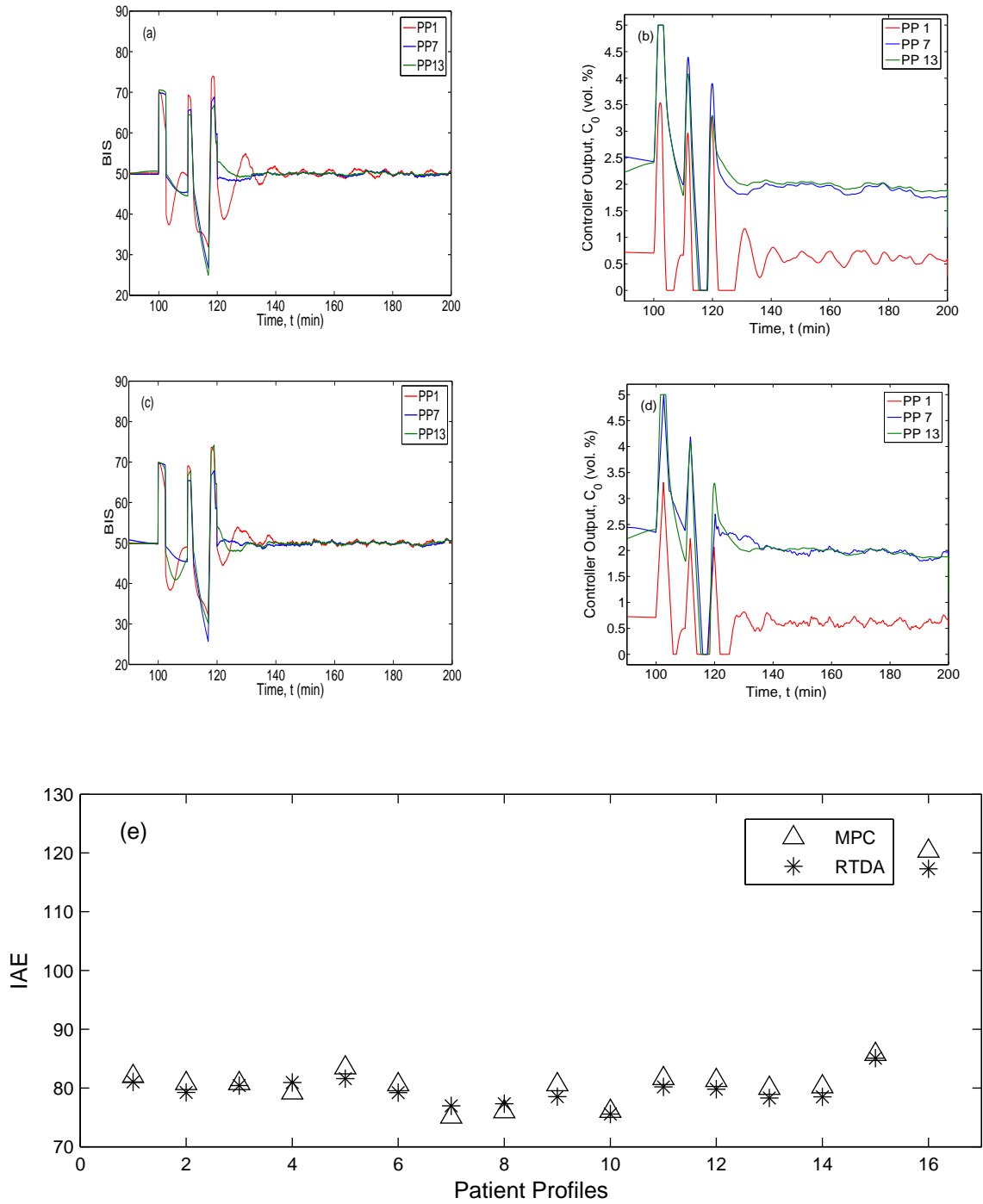


Fig. 3.14. Performance of MPC and RTDA controllers in the absence of BIS signal in the period of $t = 120 - 200 \text{ min}$: (a,b) transient profiles for PP 1, PP 7, and PP 13 using MPC, (c,d) transient profiles for PP 1, PP 7, and PP 13 using RTDA and (e) IAE comparison for all patient models

3.8 Conclusions

The efficacy of PI, PID, PID-PI, PID-P, MPC and RTDA controllers was evaluated and compared for a range of patient drug sensitivities and extreme surgical scenarios. For this purpose, after analyzing the effect of PK and PD model parameters, a set of 16 patient profiles was constructed to represent patients with different drug sensitivities. MPC and RTDA controllers are capable of improving hypnosis regulation by up to 40%, compared to PI/PID controllers, and also display better robustness when implemented on different patient profiles. Cascade controllers provide an improvement of up to 20% in performance, compared to PI/PID, but they exhibit less robustness than MPC and RTDA. To cope with the possible loss of BIS signal during surgery, estimation of a patient-specific EC_{50} value (based on BIS and endtidal concentration measurements in the induction period) and its use for estimating BIS for subsequent feedback was proposed, and its effectiveness was shown via simulation.

Chapter 4

A COMPARATIVE STUDY OF THREE ADVANCED CONTROLLERS FOR THE REGULATION OF HYPNOSIS WITH ISOFLURANE

4.1 Introduction

The contribution of this chapter is to demonstrate the control of hypnosis using model predictive controller (MPC), and to comprehensively compare its performance with CIMC and CMEC approaches (Gentilini et al. 2001a, Puebla & Alvarez-Ramirez 2005). The proposed MPC uses the approximate linear PK-PD model in the controller design, which will regulate patient's BIS by manipulating the infusion rate of isoflurane. Because of potential patient-model mismatch, several simulations are conducted to check the robustness of the MPC controller. The proposed MPC scheme has also been tested for disturbance rejection and noisy measurement signals. The performance obtained with the MPC controller is compared with the performances of the CIMC and CMEC. Extensive numerical simulations showed that the proposed MPC algorithm performed considerably better when compared to these two control strategies previously reported in the literature (Gentilini et al. 2001a, Puebla & Alvarez-Ramirez 2005). The study and the findings described in this chapter have been reported in Sreenivas et al. (2009a).

4.2 Patient Model - Modeling Hypnosis

The response of a patient to the hypnotic drug, isoflurane is modeled with a pharmacokinetic (PK) – pharmacodynamic (PD) model and is detailed in section 3.2.

4.3 Controller Design

The three control strategies mentioned above for the regulation of hypnosis are described briefly in this section.

4.3.1 Cascade internal model controller (CIMC) Design

The CIMC structure to regulate BIS is depicted in Figure 4.1. In this figure, the blocks P_2 (obtained from equations (3.2) – (3.4)) and P_1 (obtained from equation (3.5)) together with the nonlinear equation block (equation (3.9)) represents the patient's pharmacokinetics and pharmacodynamics, respectively. The corresponding parallel models are \tilde{P}_2 and \tilde{P}_1 together with the linearization constant k_m . Here, \tilde{P}_2 is a sixth order transfer function, \tilde{P}_1 is a first order transfer function and k_m is a linearization constant as given by equation (3.14) and its value calculated to be -51.28. Also, Q_2 and Q_1 are the IMC controller blocks which are the filtered inverses

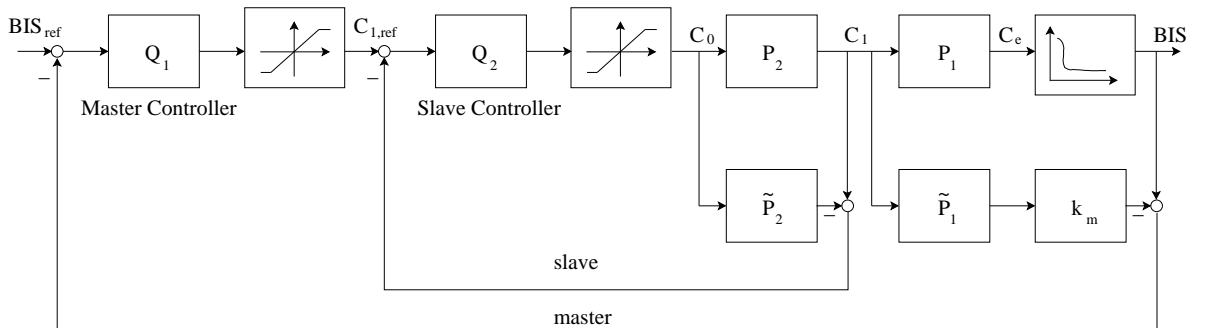


Fig. 4.1. Schematic representation of the CIMC structure

of the nominal patient models \tilde{P}_2 and \tilde{P}_1 with k_m , respectively. The master controller Q_1 regulates the BIS and the slave controller Q_2 regulates C_1 (endtidal concentration). Because controllers Q_2 and Q_1 are the filtered inverses of the nominal patient models, the tuning of the IMC controller depends on the filter time constants (λ_2 & λ_1 , respectively) and order of the filters (n_2 & n_1 , respectively). Because IMC structure cannot handle the manipulated variable constraints, the constraints on the maximum and minimum infusion rates are effected by placing saturation blocks (see Figure 4.1).

4.3.2 Cascade modeling error compensation (CMEC) controller design

As in CIMC, here also, the master controller regulates BIS and slave controller regulates C_1 as depicted in Figure 4.2. The master closed-loop observer estimates the modeling error which is a function of estimated time constant for the master loop, τ_{eM} and the error, e_M which is the difference between measured BIS and the set-point for BIS. With these findings, the master controller generates the reference value for the endtidal concentration, $C_{1,ref}$ which is a function of master closed-loop

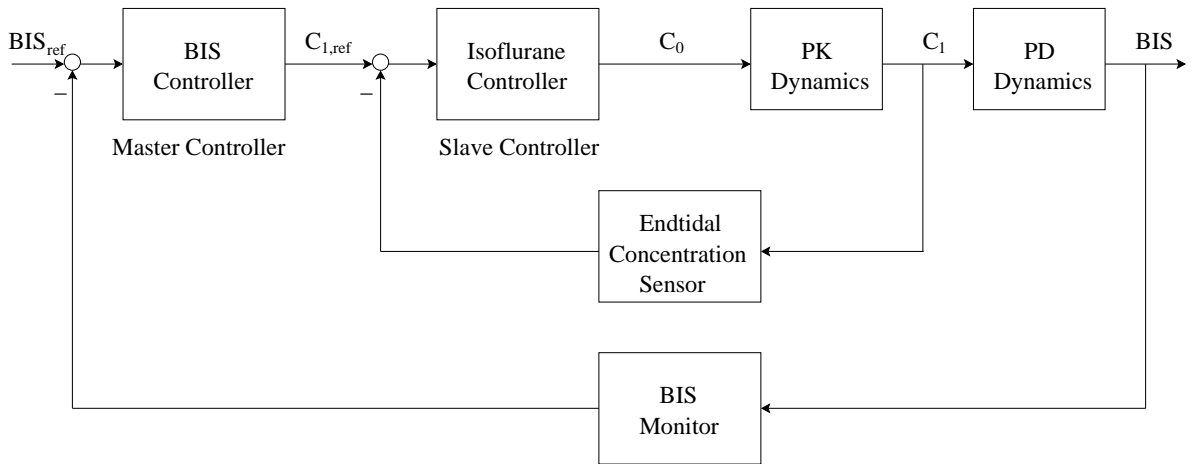


Fig. 4.2. Schematic representation of the CMEC scheme

time constant, τ_{eM} , and modeling error. Then the slave closed-loop observer estimates the modeling error which is a function of estimated time constant for slave

loop, τ_{eS} and the error, e_S which is the difference between measured C_1 and $C_{1,ref}$. With these observations, the slave controller manipulates the isoflurane concentration in inhaled gas, C_0 , which is a function of slave loop closed-loop time constant, τ_{cS} . Maintaining constraints within limits has been taken care within the controller algorithm. One of the drawbacks with the CMEC approach is the need to tune several controller parameters (time constants of the controllers) to obtain the desired response (Alvarez-Ramirez et al. 2002).

4.3.3 Model predictive controller (MPC) design

The detailed description of the MPC scheme for the regulation of hypnosis with isoflurane is provided in section 3.4.4.

4.4 Results and Discussion

This section provides the simulation results of the MPC controller for the control of BIS by manipulating isoflurane. The performance of MPC scheme for BIS regulation has not been reported in the literature. Hence, the MPC performance is considered in this chapter and compared with the recently reported results based on CIMC and CMEC controllers. This section first considers the tuning of the MPC controller. Then the performance of the MPC scheme will be compared with the performances of CIMC (Gentilini et al. 2001a), and CMEC (Puebla & Alvarez-Ramirez 2005) schemes for the control of hypnosis. The comparison will be in terms of set-point tracking, disturbance rejection, uncertainty in the parameters of the model, and rejection of unmeasured noise.

The controller has to maintain BIS between 40 and 60 during the surgery. Also, it is very important to maintain the drug concentration within the acceptable limits in the patient's body. The endtidal concentration, C_1 must be between 0.4 vol.% and 2.2 vol.% (Gentilini et al. 2001a). This is the physiologically acceptable range for

C_1 . The lower limit guarantees a minimum delivery of anesthetic, whereas the upper limit prevents overdosing in the patient's body. C_0 is the manipulated variable which is restricted between 0 and 5 *vol.%* (Gentilini et al. 2001b).

4.4.1 Tuning of MPC

The control execution interval is set as 5 *sec* which is same as the sampling interval for BIS. The same sampling frequency is assumed for the endtidal concentration, C_1 also. Next, the tuning of the proposed MPC controller has been done as follows. The parameters are: M , the input horizon; P , the prediction horizon; S , the weighting matrix for BIS; and R , the input weighting matrix (for the manipulated variable C_0). The prediction horizon P is chosen as 25 sample intervals (approximately equal to the settling time of open-loop response of the system) and the control horizon M is chosen as 2 sample intervals. Here, very low value of M is chosen (relative to P) because the closed-loop system should be robust and we also expect fast closed-loop response. Because the safe regulation of hypnosis level is very crucial during the surgery, the constraints imposed on the inputs and outputs will be hard constraints, *i.e.*, at any time, the controller should not violate the limits imposed on the variables. Hence, to avoid problems associated with the constraints on the output variables, the controller tuning weights should be chosen carefully. The performance of the proposed MPC is calculated based on ITAE values and are calculated for time, $t = 0 - 50$ *min* based on equation (4.1).

$$\text{Integral of the time-weighted absolute error (ITAE)} = \int_0^t t|e(t)|dt \quad (4.1)$$

By considering the performance (ITAE) and % undershoot in BIS, the weights chosen for BIS and input (isoflurane infusion) are 10 and 1, respectively.

4.4.2 Comparison of the performances of MPC, CIMC and CMEC controllers

This section gives the results for the comparison of tracking performance of the proposed MPC controller with CIMC and CMEC. The best performances obtained with the three controllers are provided here. Figure 4.3 shows the variation of endtidal concentration together with the input isoflurane profile for the BIS set-point change from 100 to 50. The values set for the filter time constants λ_2 and λ_1 for the CIMC controller are 0.3 and 1.6, respectively. Also, order of the filters n_2 and n_1 set at 3 and 2, respectively (minimum values which make controllers proper). The values set for the time constants τ_{cM} , τ_{cS} , τ_{eM} and τ_{eS} for the CMEC controller are 4, 0.4, 4 and 0.5, respectively. With all controllers, the reference BIS was tracked within about 12 *min*. From Figure 4.3, we can observe that the settling time with the three controllers is comparable. However, faster initial response is obtained with MPC ($\cong 6$ *min*) when compared to the other two controllers; the smaller undershoot in case of MPC is acceptable in medical practice. The endtidal concentration with all the controllers is maintained within the constraint 0.4 *vol.%* to 2.2 *vol.%* except for the initial phase of induction period ($t = 0 - 5$ *min*). One can further observe from Figure 4.3 that BIS is tracked by increasing the endtidal concentration through isoflurane infusion. The bottom plot in Figure 4.3 shows the variation of input isoflurane concentration with time. All the three controllers maintained the isoflurane concentration within the specified constraints. Here, MPC is aggressive compared to the other two controllers, with more drug infused to the patient to bring BIS quickly to the desired set-point. The CIMC controller is sluggish when compared to the other two controllers. With CMEC controller, the oscillations in the manipulated variable are appreciable and this is not good for the sensitive vaporizer valves.

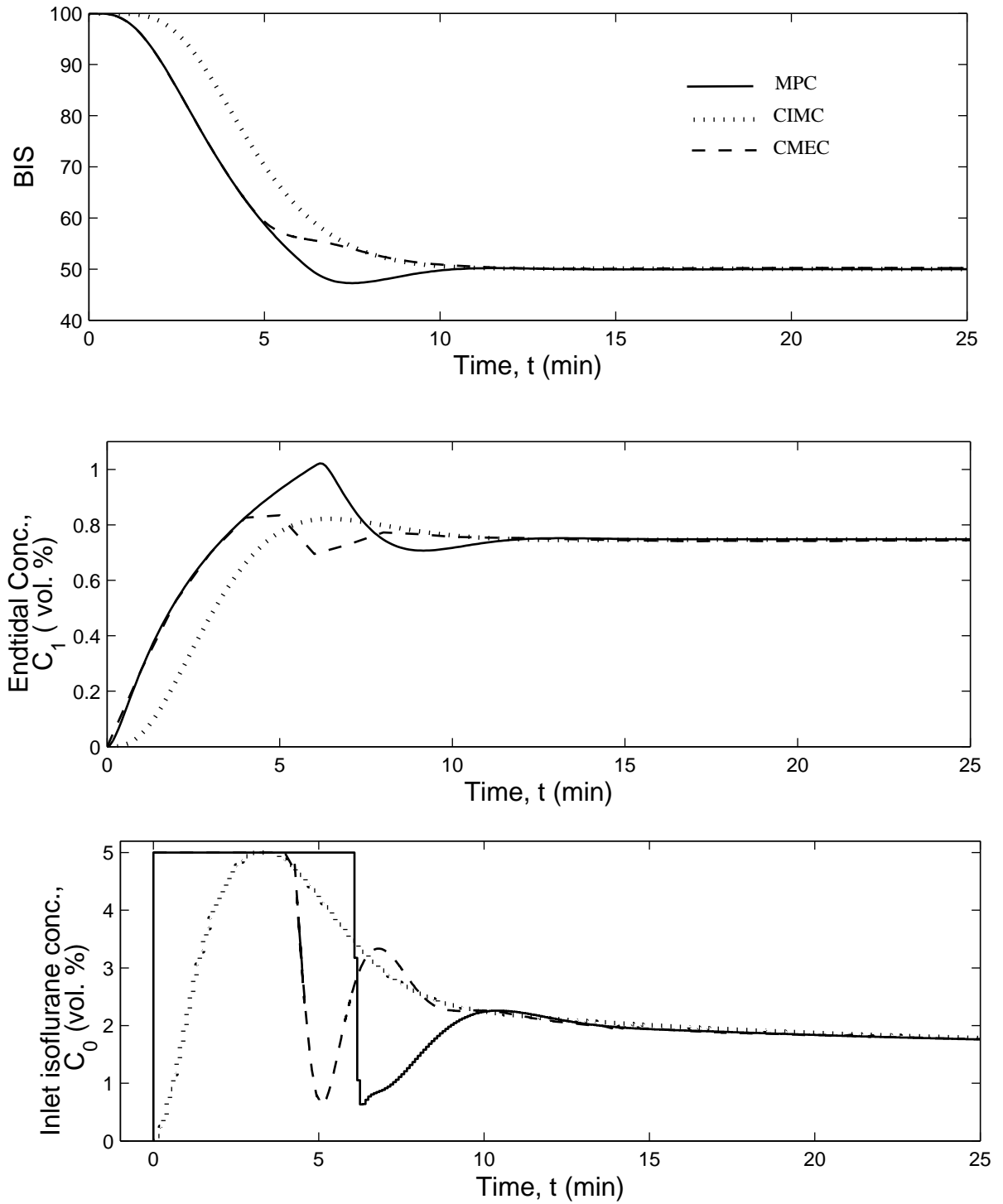


Fig. 4.3. Comparison of the best performances of the MPC, CIMC and CMEC controllers

4.4.3 Robustness comparison

This section discusses the robustness of the three controllers. We would like to test if the three controllers can meet the performance specifications despite significant and reasonable variation in the model parameters (inter- and intra-patient variability). Here, we assume that variability is in both PK and PD model parameters. Open-loop step responses showed that four variables namely frequency of inhalation (f_R), tidal volume (V_T), and volume of the lungs (V_1) from the PK model and concentration of drug at half maximal effect (EC_{50}), from the PD model are the dominant parameters affecting the patient's response. With the range specified for the three PK parameters in Table 3.1, each parameter was varied in three levels (minimum, average, maximum). The single PD parameter was also varied in three levels (0.5146, 0.7478 and 1.0940), thus $3^4 = 81$ patients were obtained. From these patient sets, 27 patients were selected based on covering the entire span of insensitive (higher EC_{50} , V_1 and lower f_R , V_T) to sensitive responses (lower EC_{50} , V_1 and higher f_R , V_T) to the drug. Closed-loop simulations are carried out for these 27 patients with each of the three controllers. The results from these simulations are summarized in Table 4.1.

Table 4.1 shows the best performance obtained for all the 27 patients (rows 2 - 28) with the MPC, CIMC and CMEC controllers which were tuned for the nominal patient (row 1). Figure 4.4 shows the performance of the MPC controller for several sets of parameters shown in Table 4.1. From the top portion of this figure, we can observe that slower response was obtained in all patients (except for the sensitive patients characterized by lower EC_{50} value) when compared to nominal patient (responses also shown in Figure 4.3 and from $t = 0 - 50 \text{ min}$ in Figure 4.5). Also, if f_R and V_T are low and EC_{50} is high compared to their nominal value, the response is too sluggish and this sluggishness decreases with the decrease in V_1 . This is because, if the volume of lungs is very high, the patient needs more drug (higher EC_{50}) and

also the frequency of inhalation and tidal volume are low, the controller should maintain the high isoflurane concentration for a long time to bring the patient to targeted hypnotic level.

Table 4.1
Performance of different controllers

Patient No.	Parameters				Performance (ITAE)		
	f_R	V_T	V_1	EC_{50}	MPC	CIMC	CMEC
1	10	0.6	2.31	0.7478	506	684	566
2	4	0.3	3.02	1.0940	5901	7936	6241
3	4	0.3	2.31	1.0940	3465	4560	3658
4	4	0.3	1.60	1.0940	1986	3050	2145
5	4	0.8	3.02	1.0940	1527	2956	2055
6	4	0.8	2.31	1.0940	1329	2106	1764
7	4	0.8	1.60	0.5146	767	991	884
8	4	1.2	3.02	1.0940	1503	2698	1995
9	4	1.2	2.31	0.7478	544	679	565
10	4	1.2	1.60	1.0940	745	1197	803
11	4	1.2	1.60	0.5146	528	647	554
12	16	0.3	3.02	1.0940	1689	2753	2006
13	16	0.3	1.60	0.5146	638	831	715
14	16	0.8	3.02	0.5146	504	505	506
15	16	0.8	2.31	0.7478	502	720	496
16	16	0.8	1.60	1.0940	997	1214	998
17	16	1.2	3.02	1.0940	1426	2108	1674
18	16	1.2	2.31	0.7478	445	655	415
19	16	1.2	1.60	0.5146	555	607	555
20	25	0.3	3.02	1.0940	1524	2378	1787
21	25	0.3	2.31	0.7478	575	700	585
22	25	0.3	1.60	0.5146	615	724	642
23	25	0.8	3.02	0.5146	492	503	498
24	25	0.8	2.31	0.7478	505	709	476
25	25	0.8	1.60	0.5146	540	610	547
26	25	1.2	3.02	1.0940	1406	2070	1595
27	25	1.2	2.31	0.7478	485	637	469
28	25	1.2	1.60	0.5146	434	494	435
Avg.					1148	1632	1272

From the results shown in the bottom portion of Table 4.1 and responses shown in bottom portion of the Figure 4.4, we can observe that, if f_R is high and EC_{50} is low,

the remaining two variables have less effect on the performance of the controllers. Also, from the results summarized in the top portion of Table 4.1, we can observe that, when f_R is low and both V_1 and EC_{50} are high, the performance of the controller increases with increase in V_T . This is because, even though the frequency of inhalation is less, the high tidal volume compensates for the large volume of lungs. The average ITAE values for all these 28 patients (last row in Table 4.1) shows that the MPC outperforms the other two controllers, and CMEC is better than CIMC. Also, variation of manipulated variable movement is less with MPC compared to CMEC. The manipulated variable responses (not shown) reflect the BIS responses shown in Figure 4.4, as insensitive patient needs more isoflurane infusion and sensitive patient needs less isoflurane infusion.

Out of all 28 patients shown in Table 4.1, the second patient (insensitive patient) shows the worst performance (high ITAE value) regardless of the controller employed (from $t = 0 - 50 \text{ min}$ in Figure 4.6). From this figure, we can observe that all the controllers required more time to bring this patient to the desired hypnotic level (BIS equal to 50). Also, more isoflurane is injected to this patient when compared to the nominal patient (compare Figure 4.6 with Figure 4.3 or Figure 4.5 from $t = 0 - 50 \text{ min}$). This patient is very resistant (insensitive) to isoflurane. This is because, for this patient, the frequency of the inhalation, f_R and the tidal volume, V_T are low and volume of the lung, V_1 and concentration of drug at half maximal effect, EC_{50} are at high value. Because of this reason, the controller designed based on the nominal values give poor performance for this patient when compared to all other patient models. Even on this patient, the MPC controller performed well (quick response with very small undershoot) when compared to the other two controllers. The manipulated variable movement is also minimal with MPC while it is jerky with CMEC.

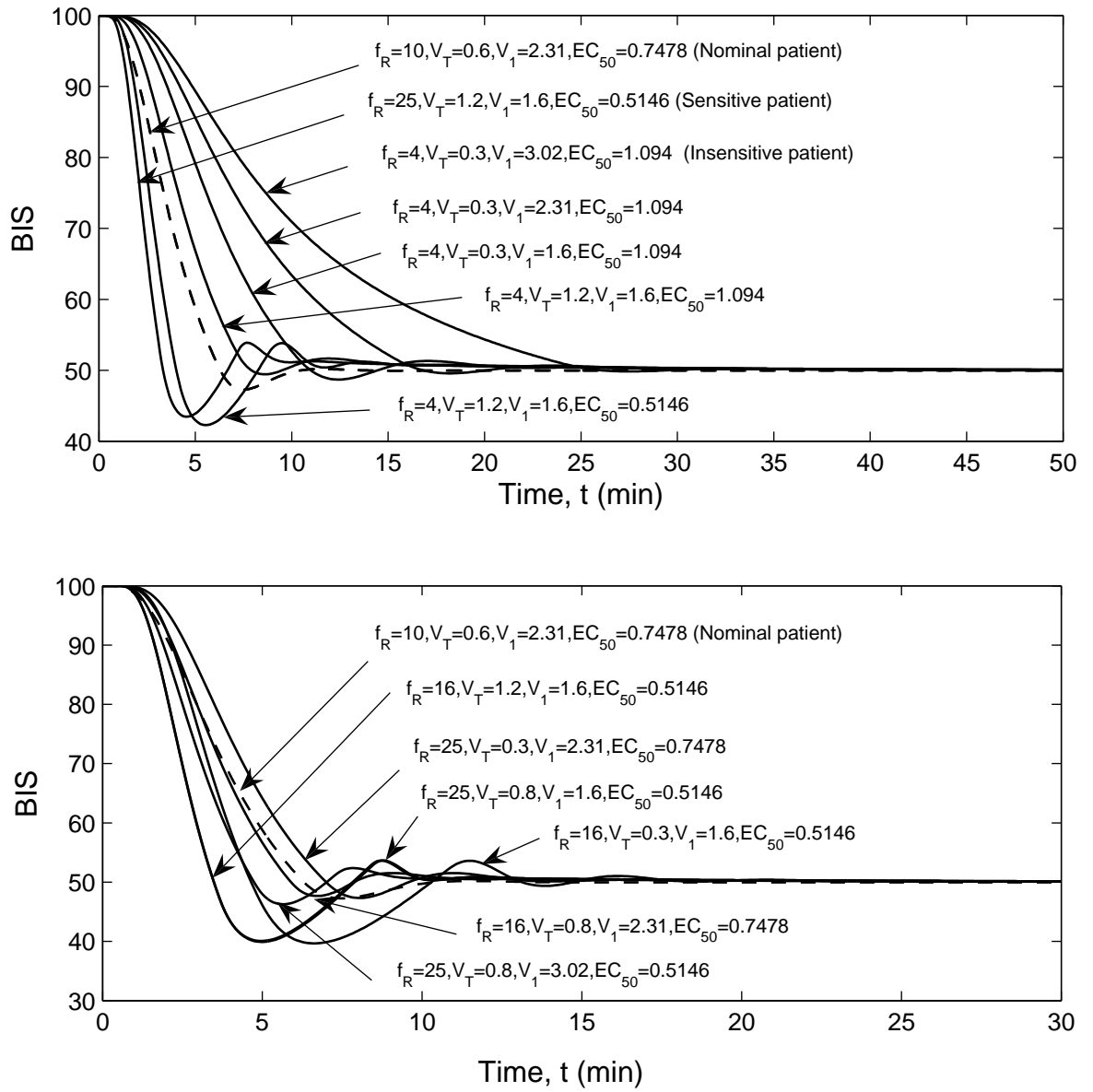


Fig. 4.4. Comparison of the performance of the proposed MPC controller for several patient parameters

The result in Figure 4.7 (from $t = 0 - 50 \text{ min}$) represents patient 28 (sensitive patient) in Table 4.1. Even in this case, CIMC is sluggish and CMEC has more aggressive manipulated variable movement when compared to MPC. From this figure, we can observe that all the controllers took less time to bring the patient to the desired hypnotic level (BIS equal to 50). Also, less isoflurane is injected to this patient when compared to the nominal patient (compare with Figure 4.3 or Figure 4.5 from $t = 0 - 50 \text{ min}$). This patient is very sensitive to isoflurane administration. This is because, for this patient, the frequency of the inhalation, f_R and the tidal volume, V_T are high and the lung volume, V_1 and concentration of drug at half maximal effect, EC_{50} are at low value.

4.4.4 Performance comparison for a step change in BIS and sudden disturbance in Q_0 during the surgery

The three controllers are now tested for a step change in BIS value which may be required at any time during the surgery. This is because, if surgical stimulation is severe at any time during the surgical process, the patient needs to be more unconscious and hence the BIS value should be decreased to some lower value (e.g., 40). Figure 4.5 depicts the performance of the three controllers for a step change in BIS from 50 to 40 at $t = 50 \text{ min}$ for the nominal patient. Here also, performance (with respect to both BIS response and manipulated variable movement) obtained with the MPC is better as compared to CMEC and CIMC. This can be attributed to the inherent online optimization feature embedded in the MPC scheme.

Faults can occur with any of the equipments or variables during surgery. Here, the simulations are carried out for a sudden increase in the flow rate of inspired gas, Q_0 , which is delivered by the pump. Mathematically, this is represented as a step change in Q_0 from 1 to 5 ℓ/min . Figure 4.5 also depicts the performance of all the controllers for the step change in Q_0 at $t = 100 \text{ min}$ for the nominal patient. From

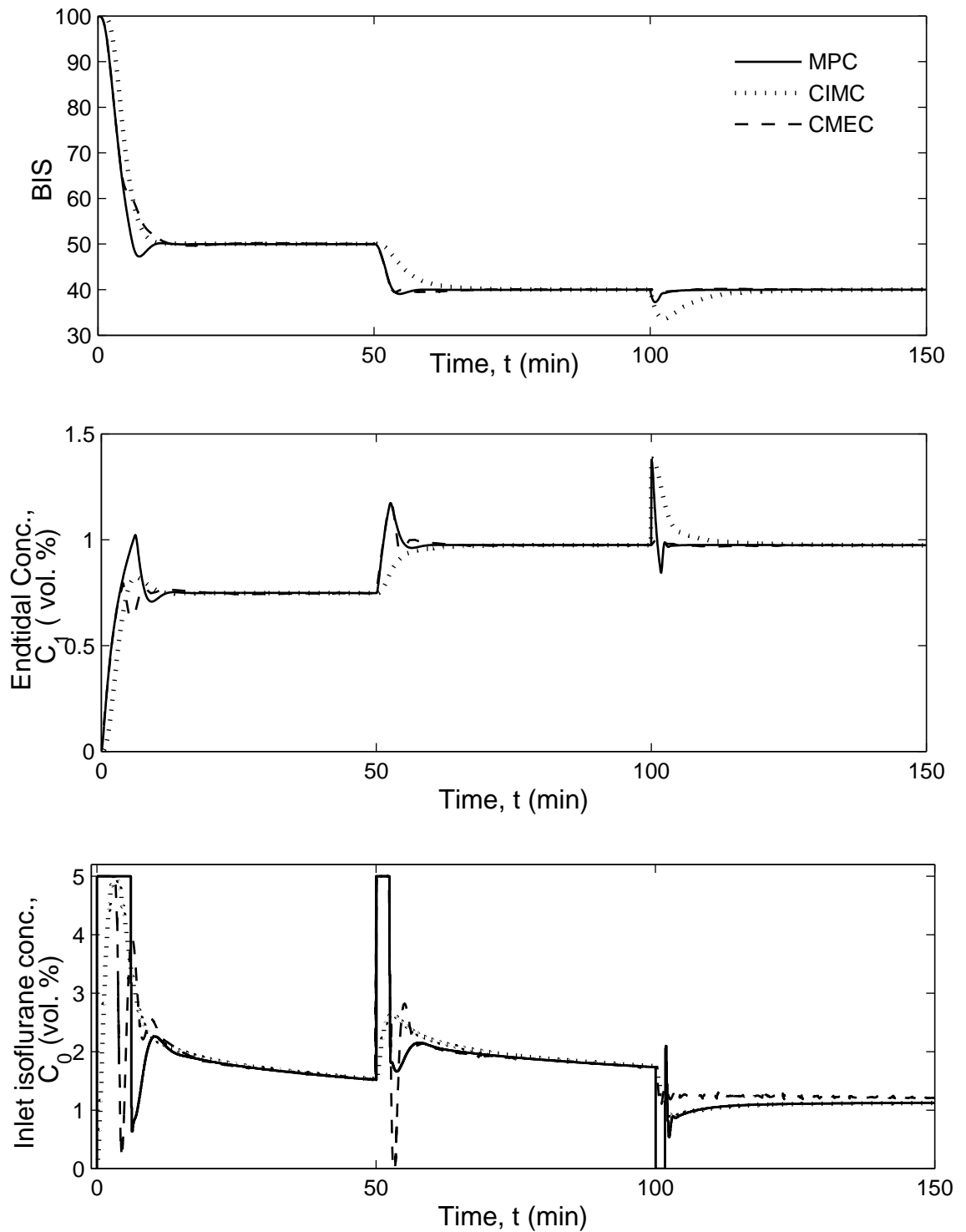


Fig. 4.5. Comparison of the performance of the MPC, CIMC and CMEC controllers to a sudden step change in BIS and to disturbance in Q_0 for the nominal patient

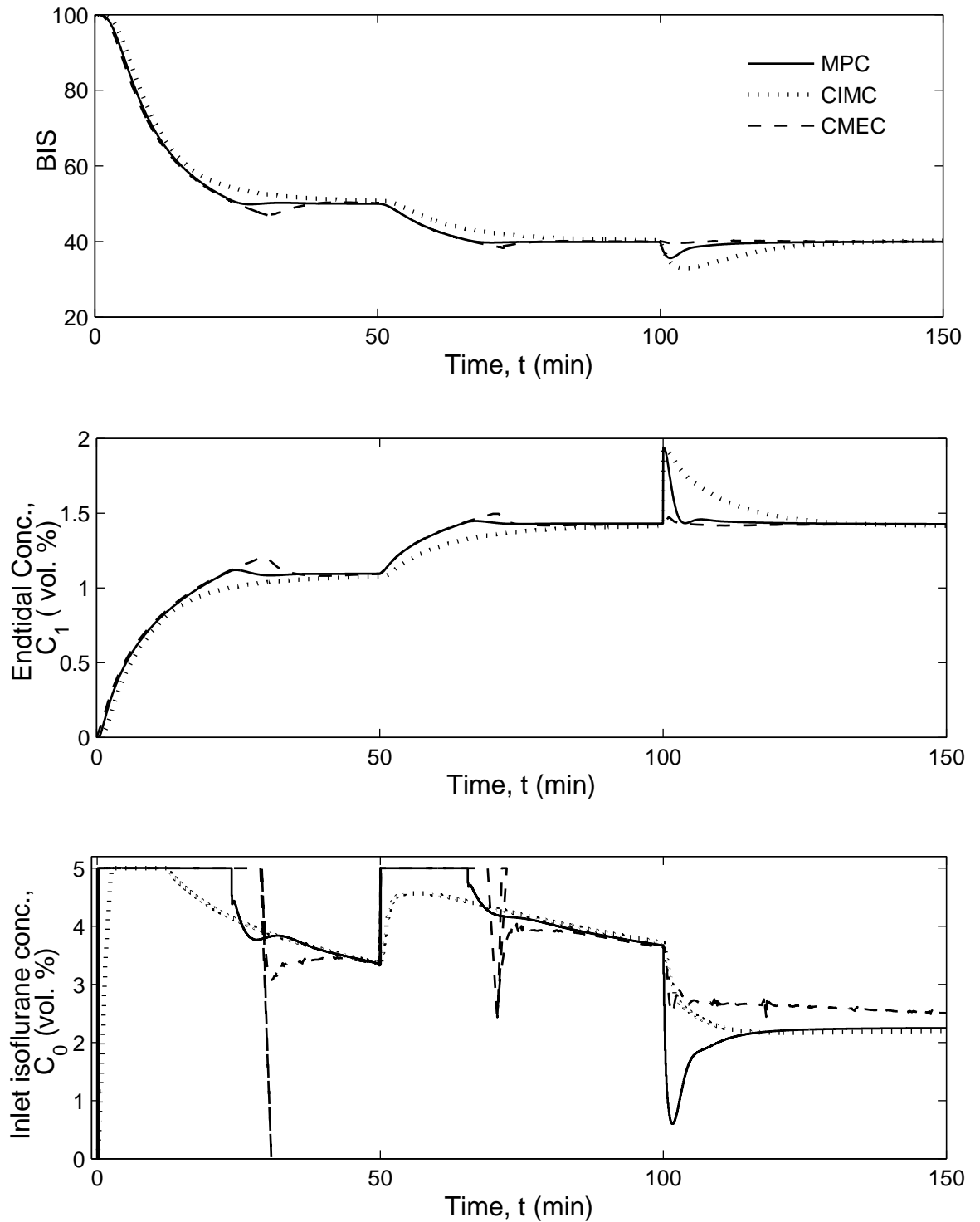


Fig. 4.6. Comparison of the performance of the MPC, CIMC and CMEC controllers to a sudden step change in BIS and to disturbance in Q_0 for insensitive patient

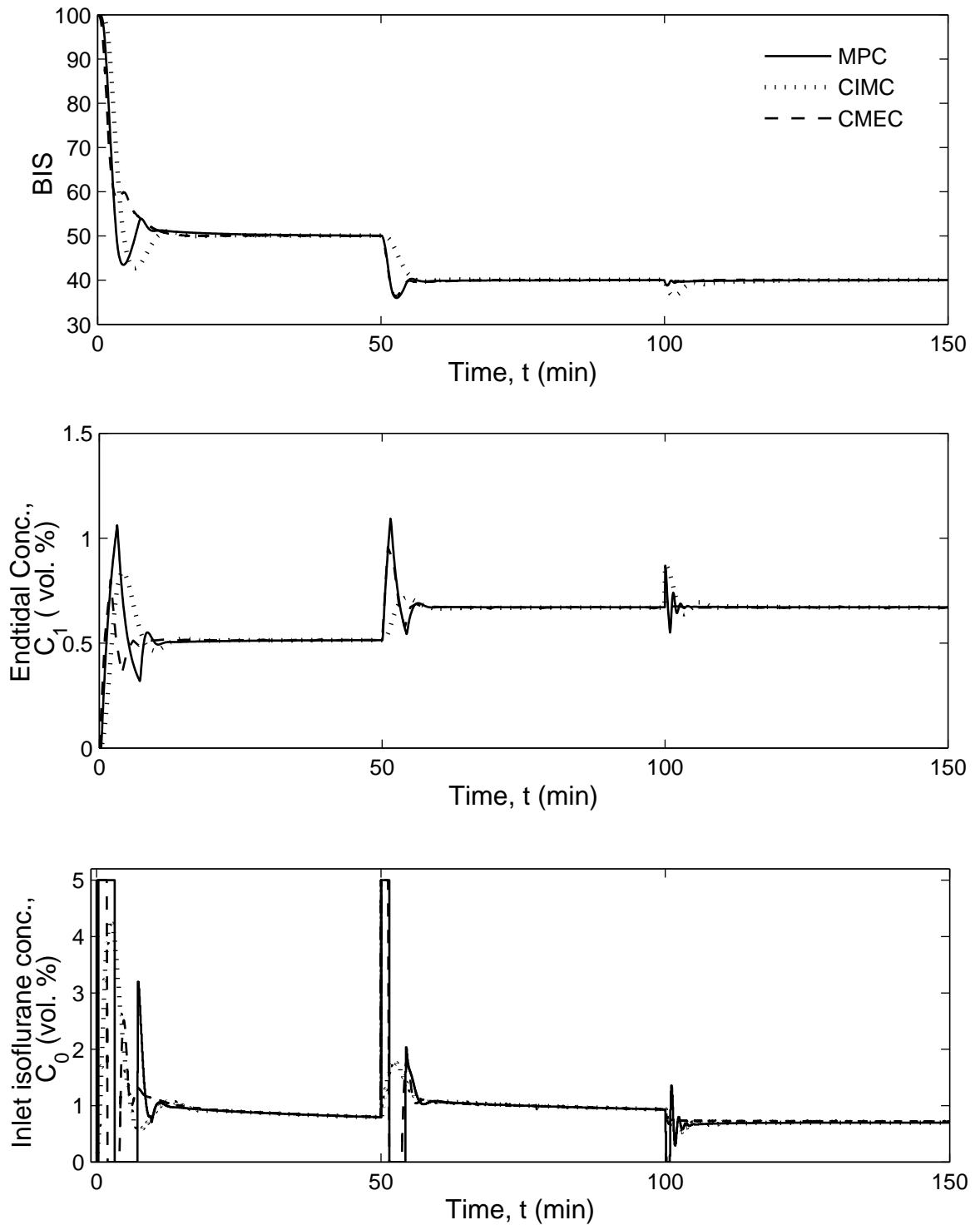


Fig. 4.7. Comparison of the performance of the MPC, CIMC and CMEC controllers to a sudden step change in BIS and to disturbance in Q_0 for sensitive patient

the top part of this figure, we can observe that a small drop in BIS occurs because of sudden increase of flow of gas which carries isoflurane into the lungs. The feedback controllers recovered within 10 *min* with small undershoot in the BIS. Both MPC and CMEC performed better when compared to CIMC with respect to BIS response, but here MPC is more aggressive compared to CMEC in manipulated variable movement (bottom plot of Figure 4.5).

Figures 4.6 and 4.7 show the comparison of performance of three controllers to a step change in BIS at $t = 50$ *min* and to disturbance in Q_0 at $t = 100$ *min* for the insensitive and sensitive patients, respectively. Here also, MPC and CMEC performed well compared to the CIMC which showed a sluggish response. Also, when manipulated variable movement is considered, MPC performed better for BIS set-point change and CMEC performed better for disturbance rejection.

4.4.5 Performance comparison for measurement noise in BIS signal during the surgery

The measured signal used for feedback control (BIS) may be corrupted by artifacts such as measurement noise. BIS artifacts might come from the high impedance of the electrodes, corruption of the EEG with the electromyography (EMG) signal etc. For better control performance, the noise in the feedback signal must be handled appropriately (e.g., filtering). If not, it will be harmful to the patient because unreliable values of the measured signals will result in wrong drug dosage delivered to the patient. If controllers are very aggressive, manipulated variable movement is very rapid because of noise, so care must be taken when tuning the controllers if proper filters are not available to reduce the noise. Figure 4.8 illustrates the behavior of the three controllers (MPC, CIMC and CMEC, respectively) when 2% Gaussian noise is added to the measured BIS signal. Even though the BIS feedback signal has noise, all the three controllers gave very good performance (BIS < 55) without any

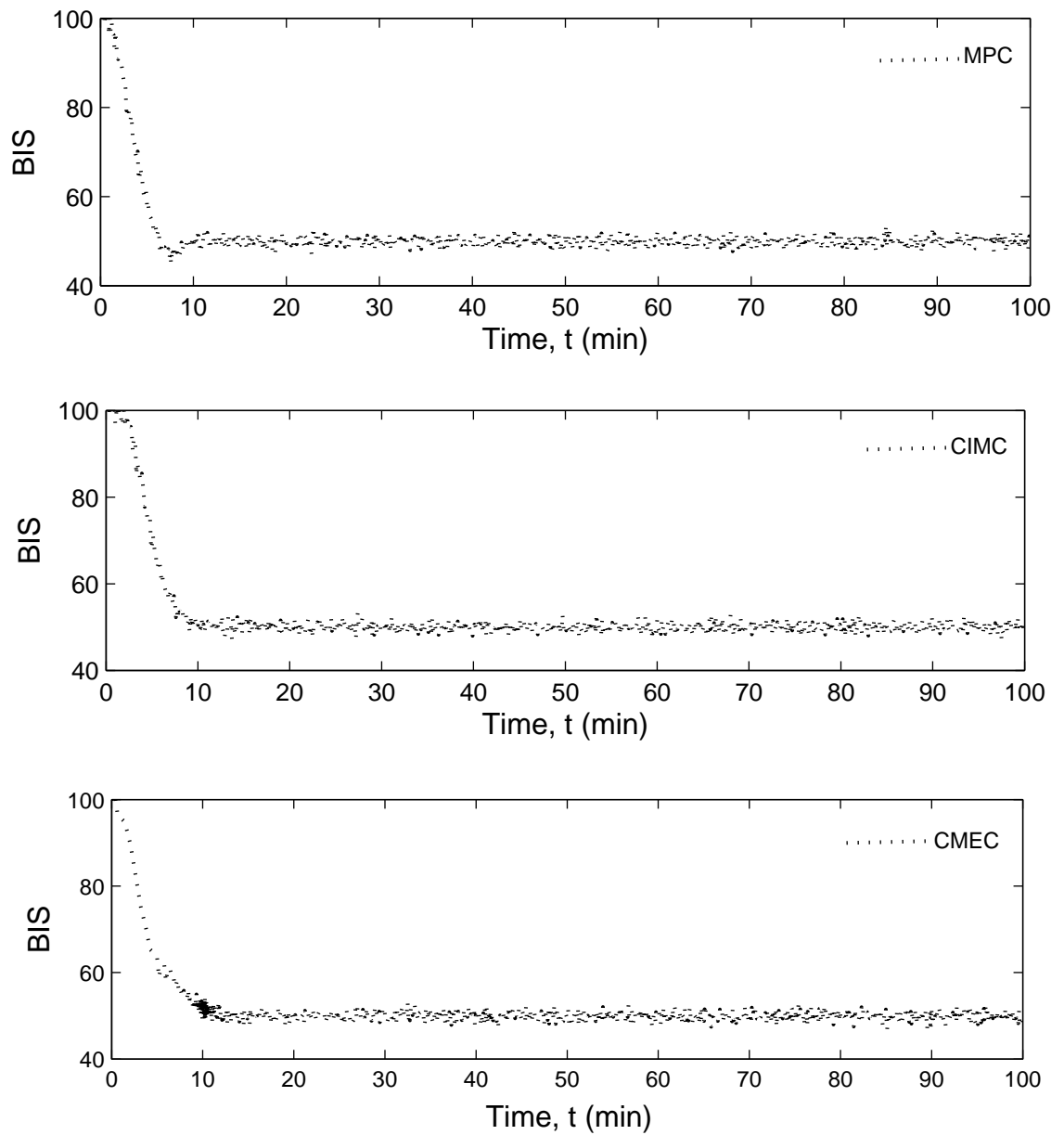


Fig. 4.8. Performance of the MPC, CIMC and CMEC controllers for measurement noise in the BIS feedback signal during the surgery: BIS profiles

further tuning and BIS did not exceed the surgical operating range (from 40 to 60). Also, the remaining two variables (C_1 and C_0) are maintained within constraints.

The endtidal concentration profiles (not shown) reflect the trend of BIS profiles shown in Figure 4.8. Out of three input isoflurane concentration profiles (C_0) for all the controllers (not shown), the one with CMEC is more aggressive, hence the response is oscillatory compared to MPC and CIMC out of which MPC is more aggressive. Due to the non-aggressive nature of CIMC, the isoflurane profile is smooth.

4.5 Conclusions

Good hypnosis regulation, using BIS as the controlled variable, has been achieved through the use of a model predictive control scheme. In comparison with other recently suggested control strategies, namely cascade IMC and cascade modeling error compensation scheme, the MPC provided better performance while respecting the imposed constraints on the manipulated and output variables. The MPC strategy was also found to be more robust to inter-patient variability; it performed well in the presence of disturbances and measurement noise. The MPC is thus recommended as a promising strategy for controlling hypnosis.

Chapter 5

ADVANCED CONTROL STRATEGIES FOR THE REGULATION OF HYPNOSIS WITH PROPOFOL

5.1 Introduction

The present chapter has two main objectives. One objective is to apply and evaluate the promising MEC and IMC approaches for hypnosis regulation using BIS as the controlled variable and manipulating propofol infusion. Another objective is to comprehensively compare the performance of MEC, IMC, MPC, and PID controllers for hypnosis control. Cascade control structure is impractical for propofol-based hypnosis regulation because of unavailability of continuous propofol concentration measurement. Hence, MEC and IMC strategies (and not their cascade versions) are employed here. The four control strategies are applied to the best available PK model (which accurately predicts the experimental plasma propofol concentration) and PD models (which accurately relates the effect-site propofol concentration to BIS) in the literature. Then, extensive simulations are conducted to test the robustness of the four controllers, by considering parameter variations in the selected model to account for patient-model mismatch. The four controllers are tested for set-point changes, disturbances and noise in measured BIS. Then the performance of the MPC and PID controllers is compared with that of RTDA controller for all the scenarios mentioned above. Results of these simulations is used to determine the best controller(s). The study and the findings presented in this chapter have been reported in Sreenivas et al. (2008) and Sreenivas et al. (2009c).

5.2 Mathematical Model for BIS Response to Propofol

The model used for BIS response to propofol consists of two interacting parts: a PK model for estimating the distribution of propofol in the internal organs, and a PD model to describe the effect of propofol on the measured physiological variable, BIS. Figure 5.1 depicts the schematic of the system comprising the propofol delivery circuit and the PK and PD models.

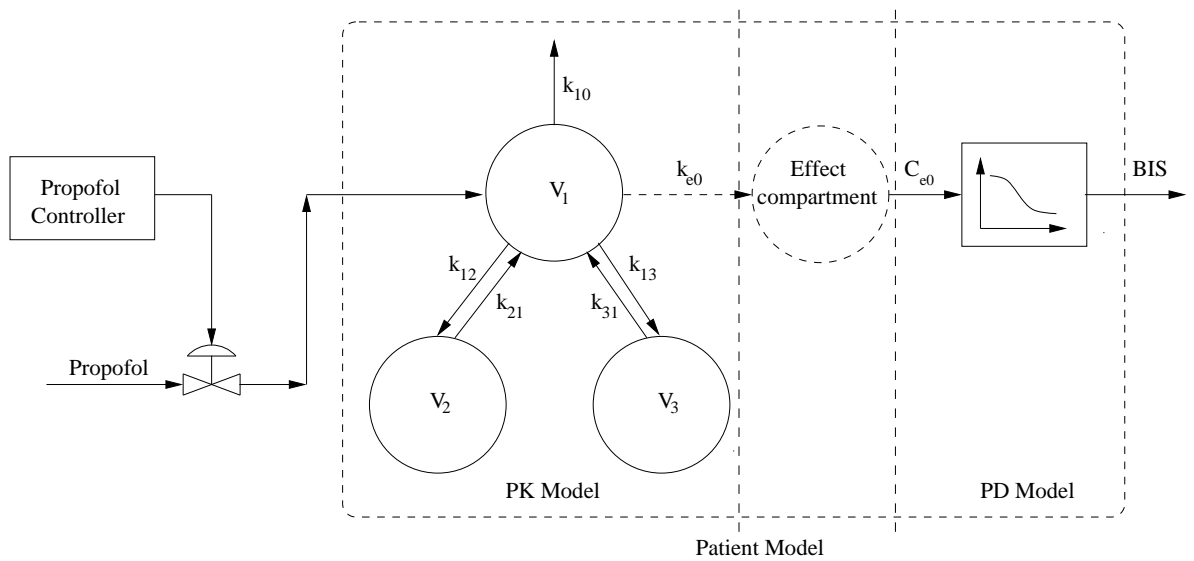


Fig. 5.1. Schematic representation of propofol delivery circuit with PK and PD models

For the distribution of propofol, a linear mammillary three-compartmental PK model is adopted from the literature (Schwilden et al. 1989). The central compartment, V_1 , which is characterized as a plasma compartment in which drug dissolves and is carried to the other compartments. Also, because of metabolism of the drug in the body, elimination of the drug from this compartment is assumed. The second compartment is a shallow peripheral compartment, V_2 , which is characterized by a very rapid movement of the drug from the plasma to this compartment. This is the characteristic of certain tissues which are highly perfused (vessel-rich tissues). The third compartment is a deep peripheral compartment, V_3 , which is

characterized by a slow distribution of the drug from the central compartment to this compartment. This is because of the equilibration of the blood with tissues which are less perfused.

Initially, the PK part assumes that all compartments (Figure 5.1) have a zero initial concentration of the drug (propofol). To achieve rapid target plasma drug concentration (*i.e.*, concentration in V_1), sufficient drug must be given as a bolus dose. If the plasma drug concentration is to be kept constant, the amount of drug entering and leaving the central compartment must be equal. Drug leaves the blood to pass into V_2 and V_3 at a gradually decreasing rate as the concentrations in these compartments increase. Drug (propofol) also leaves the blood because it is metabolized (mainly in the liver) (Tackley et al. 1989, Marsh et al. 1991, Dyck & Shafer 1992). The PD part assumes some lag between the infusion of propofol in the bloodstream and propofol distribution in brain tissue thereby affecting the hypnosis level. This effect on hypnosis level is represented by a nonlinear equation relating the state variables and other system variables to BIS.

5.2.1 Pharmacokinetic model

The PK model for distribution of drug consists of mass balances between the central compartment and the two compartments which are attached to it (Figure 5.1) (Tackley et al. 1989, Marsh et al. 1991, Dyck & Shafer 1992). The main assumptions here are that the central compartment is a well mixed-tank with the plasma propofol concentration being uniform everywhere, and the distribution of propofol is not affected by the presence of other drugs. Hence, the resulting mass balance for propofol in the central compartment is given by:

$$\frac{dC_1}{dt} = \sum_{j=2}^3 \left(k_{j1} C_j \frac{V_j}{V_1} - k_{1j} C_1 \right) - k_{10} C_1 + \frac{\rho}{\alpha V_1} U \quad (5.1)$$

Here C_1 , C_2 and C_3 are concentrations of propofol ($\mu g/ml$) in the first (central), second and third compartments, respectively; V_1 , V_2 and V_3 are the respective volumes (ℓ); k_{12} , k_{13} , k_{21} and k_{31} are the mammillary rate constants (min^{-1}) of the respective compartments, k_{10} is the hepatic metabolism rate constant to represent the elimination rate of propofol from the patient (min^{-1}); $\rho = 10$ (mg/ml) is the available propofol concentration; $\alpha = 60$ (min/hr) is a normalization constant; and U is the infusion rate of propofol (ml/hr). To convert U in ml/hr to u in $mg/kg/hr$ (normalized propofol infusion rate with respect to patient weight), it is multiplied by ρ/w , where w is the weight of the patient in kg . Similarly, for the second and third compartments, the corresponding mass balance is given by:

$$\frac{dC_j}{dt} = k_{1j}C_1 \frac{V_1}{V_j} - k_{j1}C_j \quad (5.2)$$

With the availability of different sets of PK parameters reported by various research groups (Tackley et al. 1989, Marsh et al. 1991, Dyck & Shafer 1992), it is difficult to select a specific PK parameter set from all the available sets (Coetzee et al. 1995). Usually, with the different PK sets, there is a mismatch between predicted and actual concentrations. This mismatch is not so critical as long as

Table 5.1
Rate constants and volumes of the different compartments of the PK model (Marsh model) (Marsh et al. 1991)

Parameter	Value
$k_{10}(min^{-1})$	0.119
$k_{12}(min^{-1})$	0.112
$k_{21}(min^{-1})$	0.055
$k_{13}(min^{-1})$	0.0419
$k_{31}(min^{-1})$	0.0033
V_1 (ℓ)	15.05
V_2 (ℓ)	30.6
V_3 (ℓ)	191.1

the actual concentrations are within the desired therapeutic window. The useful-

ness of target-controlled infusion (TCI) lies in the ability to dose more accurately, to maintain stable drug concentrations (and therefore stable effects), and to make proportional changes to the concentrations. The PK model parameters provided by Marsh et al. (1991) (referred as Marsh model) accurately predict the plasma propofol concentration (Coetzee et al. 1995), and this model is used to check the closed-loop performance of the controllers. Table 5.1 shows the PK parameters mentioned in equations (5.1) and (5.2) for a 34 year old person weighing 66 kg for Marsh model.

5.2.2 Pharmacodynamic model

The above PK model is limited to the representation of distribution kinetics of propofol into different compartments. A PD model is required to relate the effect of drug and the hypnotic level (BIS). The PK model is attached to an effect-site compartment model which represents the time lag between the distribution of drug and its effect on BIS which is given by the nonlinear Hill equation (Bibian et al. 2005). The effect-site compartment accounts for the equilibration time between targeted plasma drug concentration and concentration of drug in the central nervous system (brain). The effect-site concentration and targeted plasma drug concentration are related by a first-order lag given by (Kazama et al. 1999):

$$\frac{dC_e}{dt} = k_{e0}(C_1 - C_e) \quad (5.3)$$

where k_{e0} is used to describe the time course of equilibration between the plasma and the effect-site. The effect-site concentration is related to BIS as (Hill equation) (Bibian et al. 2005):

$$\text{BIS} = 100 - 100 \frac{C_e^\gamma}{C_e^\gamma + EC_{50}^\gamma} \quad (5.4)$$

The detailed description of the parameters in equation (5.4) is provided in section 3.2.3. The nominal values of parameters $k_{e0} = 0.349 \text{ min}^{-1}$, $EC_{50} = 2.65 \text{ } \mu\text{g/ml}$ and $\gamma = 2.561$ are obtained from the pooled analysis (Schnider et al. 1999, Sartori et al. 2005).

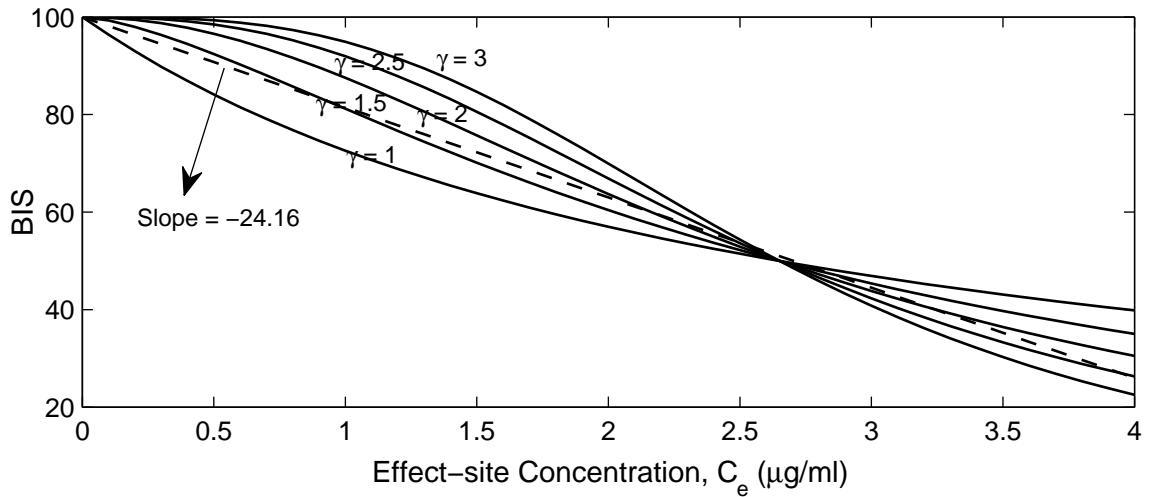


Fig. 5.2. BIS vs effect-site concentration C_e for different values of γ

Nonlinearity exists in equation (5.4) and all the remaining equations (from equations (5.1) – (5.3)) are linear. It comes mainly through the parameter, γ . Figure 5.2 shows the variation of BIS with effect-site concentration, C_e for different γ values according to equation (5.4). From this plot, we can observe that nonlinearity increases with the value of γ and that the linear approximation is acceptable.

5.3 Controller Design

The four control strategies mentioned earlier for the regulation of hypnosis are briefly described in this section.

5.3.1 Proportional-integral-derivative (PID) controller

The PID control structure employed in this study is represented by equation (5.5). The control algorithm is based on standard parameters – proportional gain (K_c), integral time (τ_I), and derivative time (τ_D) (Seborg et al. 2004):

$$p = K_c \epsilon + \frac{K_c}{\tau_I} \int_0^t \epsilon dt + K_c \tau_D \frac{d(CV)}{dt} + p_s \quad (5.5)$$

The proportional term determines the required action to the current error, the integral term determines the required action to the sum of current & past errors and the derivative term determines the required action to the rate at which the controlled variable (CV), *i.e.*, BIS is changing. For this controller, the derivative (D) action acts solely on BIS signal while proportional (P) and integral (I) actions act on the error in BIS. This avoids sudden spikes in the controller output due to step changes in set-points of BIS. Tuning of the three parameters (K_c , τ_I and τ_D) is required to get faster response of BIS without any offset or oscillations. Here, the PID parameters are obtained via optimization so as to get the best performance with this control structure.

5.3.2 Internal model controller (IMC)

The IMC structure to regulate BIS is depicted in Figure 5.3. The blocks P_2 and P_1 together with the nonlinear equation represents the patient's pharmacokinetics and pharmacodynamics, respectively. Here, both P_2 and P_1 are single input-single output (SISO) linear time invariant systems. The corresponding parallel models for the pharmacokinetics and pharmacodynamics are respectively \tilde{P}_2 and \tilde{P}_1 together with the linearization constant k_m . Here, \tilde{P}_2 is a third-order transfer function obtained by combining equations (5.1) and (5.2), \tilde{P}_1 is a first-order transfer function obtained from equation (5.3) and k_m is a constant obtained via linearization of equation (5.4) around the reference concentration $C_e = EC_{50}$ and is given by equation

(3.14). Q is the IMC controller which is obtained by multiplying the low pass filter with the invertible nominal models \tilde{P}_2 , \tilde{P}_1 and k_m .

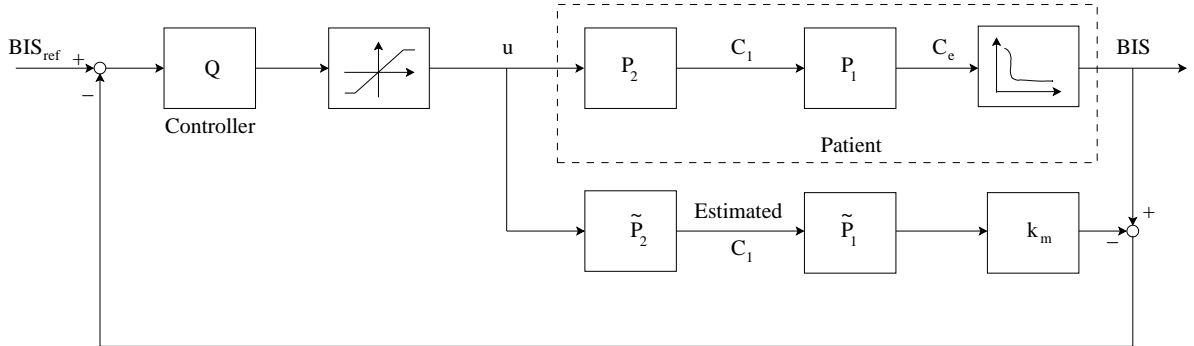


Fig. 5.3. Schematic representation of the IMC structure

In Figure 5.3, the controller Q regulates the BIS by adjusting infusion rate (u) of propofol based on the error between set-point and the difference between actual and predicted BIS. A saturation block is added after the controller Q to keep u within the constraints specified. Because controller Q is the filtered inverse of the nominal patient model, the tuning of the IMC controller depends on the filter time constant, λ and order of the filter, n . Inter-patient variability can be handled by adjusting this filter time constant appropriately to each patient (for robustness) and also for the speed of response. One of the main drawbacks of the linear IMC controller is that it cannot handle open-loop unstable systems and nonlinear models should be linearized for designing the controller (Brosilow & Joseph 2002).

5.3.3 Modeling error compensation (MEC) controller

The central idea in MEC (Alvarez-Ramirez et al. 2002) is to compensate the error due to uncertainty in the parameters of the model by determining the modeling error via patient input and output signals, and using this information for controller design. In addition to normal feedback, an observer is introduced for the modeling error estimation and this feedback action is explicitly proportional to the error resulting

due to parametric uncertainties. As like IMC, this controller also regulates BIS by adjusting infusion rate of propofol (Figure 5.4). The closed-loop

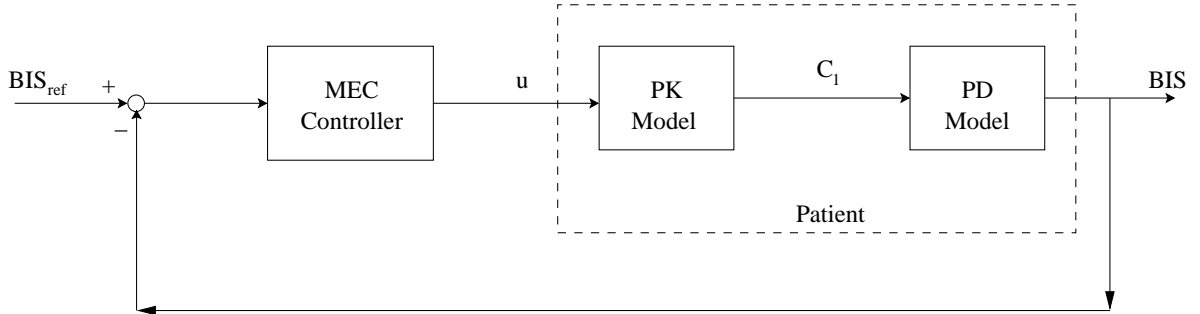


Fig. 5.4. Schematic representation of the MEC scheme

observer in the controller estimates the modeling error which is a function of estimated time constant for the closed-loop, τ_e , and the error, e , which is the difference between measured BIS and the set-point for BIS. With these observations, the controller regulates the infusion rate of propofol, u , which is a function of closed-loop time constant τ_c . Maintaining infusion rate of propofol within constraints has been taken care within the control algorithm via a saturation function added explicitly to the controller. Unlike adaptive control where model parameters are continuously updated based on patient responses, in this approach adaptation is based on the estimation of the trajectory of the modeling error function. Hence, this controller scheme can potentially take care of inter- and intra-patient variability. One of the drawbacks with the MEC approach is the difficulty in tuning the controller parameters (two time constants for each controlled variable) to obtain the desired response.

5.3.4 Model predictive controller (MPC)

The detailed description of the MPC scheme is provided in section 3.4.4. Here, the overall dynamic system for the patient model is a combination of the propofol infusion system, PK and PD models as depicted in Figure 5.1. The propofol infusion system and the PK model are modeled as linear time invariant systems arranged in

series. The linearized form of the PD model is then cascaded to this system to get the overall linear representation in state-space form. The combined state-space model is given in equations (5.6) and (5.7). Here also, k_m is the linearization constant obtained via linearization of equation (5.4) around the reference concentration $C_e = EC_{50}$.

$$\begin{bmatrix} \dot{C}_1 \\ \dot{C}_2 \\ \dot{C}_3 \\ \dot{C}_e \end{bmatrix} = \begin{bmatrix} -(k_{10} + k_{12} + k_{13}) & k_{21} \frac{V_2}{V_1} & k_{31} \frac{V_3}{V_1} & 0 \\ k_{12} \frac{V_1}{V_2} & -k_{21} & 0 & 0 \\ k_{13} \frac{V_1}{V_3} & 0 & -k_{31} & 0 \\ k_{e0} & 0 & 0 & -k_{e0} \end{bmatrix} \begin{bmatrix} C_1 \\ C_2 \\ C_3 \\ C_e \end{bmatrix} + \begin{bmatrix} \frac{\rho}{kV_1} \\ 0 \\ 0 \\ 0 \end{bmatrix} \begin{bmatrix} u \end{bmatrix} \quad (5.6)$$

$$[BIS] = \begin{bmatrix} 0 & 0 & 0 & k_m \end{bmatrix} \begin{bmatrix} C_1 & C_2 & C_3 & C_e \end{bmatrix}^T \quad (5.7)$$

The above continuous state-space model is converted to discrete time finite step response (FSR) model to design the MPC controller.

5.4 Results and Discussion

This section provides the application and evaluation of the MPC, IMC and MEC control strategies, and compares their relative performances among themselves as well as with the PID controller. This section first shows the comparison of closed-loop performance of all the control schemes for the nominal patient model. Later, the remaining performance comparisons will be provided. The performance comparison of controllers will be in terms of ability to handle uncertainty in the model parameters, set-point tracking, and rejection of disturbances and noise. The set-point changes made by anesthetist and disturbances that occur during the surgery cause the relevant physiological changes in the patient. Hence, these events were considered to assess the performance of all the controllers. The performance of all the controllers will be evaluated using integral of the absolute error (IAE) as the metric (equation (3.26)). Also, the performance of all the controllers for different

set-point changes and disturbances during the surgery is evaluated in terms of estimating the percentage of the time the output BIS signal is more than 10 units above or below the specified set-point. Too high or too low BIS values increase the percentage of the time BIS is outside the ± 10 units, which indicates poor control.

5.4.1 Closed-loop performance

The closed-loop performance of all the four controllers will be presented here. Because plasma propofol concentration (C_1) measurement is unavailable, it is estimated through the nominal PK model. BIS is measured online. The controller has to maintain BIS between 40 and 60 during the surgery (Ekman et al. 2004). Initially, it is assumed that the patient is in a fully conscious state ($BIS \approx 100$) and then the controller is turned on and the set-point is changed from 100 to 50. This brings the patient to the surgical operating range ($40 \leq BIS \leq 60$) which must be maintained for the duration of the surgery. The predicted C_1 must be between $0.5 \mu g/ml$ and $5 \mu g/ml$ (the clinically acceptable range for C_1) (Morley et al. 2000, Absalom et al. 2002). The lower bound guarantees a minimum delivery of anesthetic, whereas the upper bound prevents overdosing of the drug for an average subject. The manipulated variable (propofol infusion rate) u is restricted between 0 and $40 mg/kg/hr$ (Krassioukov et al. 1993, Furutani et al. 2005). The upper bound is needed because higher propofol infusion leads to faster increase of propofol concentration in the subject's body and this may lead to hypnotic crisis, cardiac arrhythmia, or even cardiac arrest. The minimum bound on u reflects the impossibility of administering negative concentrations of propofol. For all the four controllers, the control execution interval is set as 5 sec which is also the sampling interval for BIS.

We begin by discussing the design of MPC. First, the MPC controller is designed and tuned on the basis of the Marsh model because this model is the most reliable

one (lower prediction error between predicted and actual plasma propofol concentration) (Coetzee et al. 1995). The tuning parameters are M , the input horizon; P , the prediction horizon; S , the weighting coefficient for BIS; and R , the weighting coefficient for input rate (to penalize the large changes in u). The prediction horizon P is chosen as 12 sampling intervals and the control horizon M is chosen as 2 sampling intervals. Here, very low value of M is chosen (relative to P) because the closed-loop system should be robust and we also expect fast closed-loop response. Because the safe regulation of hypnosis level is very crucial during the surgery, the constraints imposed on the inputs will be hard constraints, *i.e.*, at any time the controller should not violate these limits. By considering performance, the weights S and R for BIS and Δu are chosen as 1 and 0.1, respectively. A higher weight on BIS is chosen because the BIS signal is the only reliable measured signal and the control of BIS has been given higher priority. Also, the plasma propofol concentration is predicted through PK model. From equation (3.14), the value of k_m obtained is -24.16.

Next, we examine the design of the IMC controller. The constraints which were imposed on the MPC controller were also imposed here. But unlike MPC, this controller cannot handle the constraints on variables. Hence, additional saturation block (Figure 5.3) is added to the controller to implement the constraint on the manipulated variable, u . The tuning parameters for the IMC controller are the filter time constant λ which is set at 1.7 and order of the filter n which is set at 2 (minimum value which makes controller proper). Here also, the value of k_m used is -24.16. As in MPC, this controller is also designed and tuned on the basis of the Marsh model. The value chosen for the filter constant is based on the maximum performance (minimum IAE) with no undershoot.

The MEC controller is considered next. Same constraints are imposed. The values set for the tuning parameters, *i.e.*, the time constants τ_c and τ_e for the MEC

controller, are 2.7 and 0.42, respectively (tuned based on Marsh model). The values chosen for the time constants are based on the maximum performance with no undershoot. Because the constraint handling algorithm added explicitly to MEC controller, this algorithm can also handle the constraints imposed on the variables.

With the PID controller (and similar constraints), the settings were $K_c = -0.0598$, $\tau_I = 28.476$, and $\tau_D = 2.368$. As with other controllers, the tuning of this controller is also based on the Marsh model and tuned for maximum performance with no undershoot. As with IMC and MEC, this controller also cannot handle the constraints imposed on the variables. Hence, a saturation block is added to the controller to keep u within the bounds imposed. In summary, three parameters (P , S and R) for MPC (with M kept at a constant value 2), two parameters (λ and n) for IMC, two parameters (τ_c and τ_e) for MEC and three parameters (K_c , τ_I and τ_D) for PID are used for the tuning of the respective controllers.

The comparison of closed-loop performance of all the four controllers is discussed next. Figure 5.5(a) shows that all the four controllers provide a similar performance (IAE value = 217) with respect to BIS. The IAE values are calculated for time, $t = 0 - 50 \text{ min}$ based on equation (3.26). Even though response is faster with PID controller than with the other controllers, a small offset persists throughout the simulation time. Figure 5.5(b) shows the predicted plasma propofol concentration, where it is seen that all the controllers result in overshoot (higher with PID controller) but are still maintained within the constraints. From Figure 5.5(c), one can observe that the controllers follow different infusion profile patterns. Because all the four controllers show similar performance (IAE values are almost identical), further studies are needed to check the robustness of these controllers.

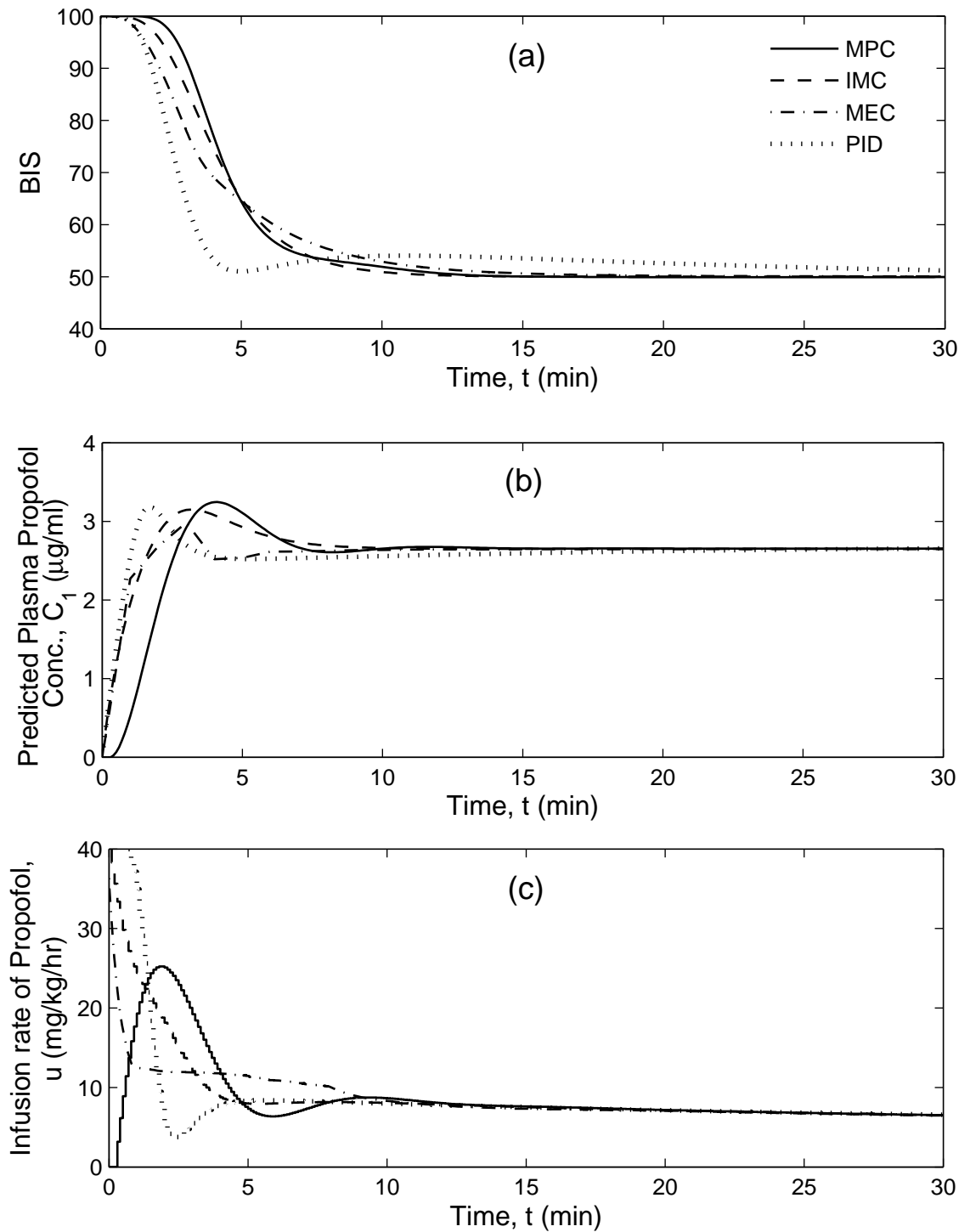


Fig. 5.5. Performance of MPC, IMC, MEC and PID controllers for the Marsh model

5.4.2 Robustness comparison

This section discusses the robustness of all the four controllers for many parameter variations based on Marsh's pharmacokinetic model. We would like to test if the four controllers are able to meet performance specifications despite significant and reasonable variation in the model parameters (inter-patient variability). Here, we assume that variability is in both the PK (based on age and weight) and PD (based on patient's sensitivity to the drug) model parameters. There is a variation of 25% in PK model parameters (Schnider et al. 1998, Schttler & Ihmsen 2000) and a possible range of PD parameters (Schnider et al. 1999, Wakeling et al. 1999). Our open-loop simulations showed that the variability in PD parameters have more impact on BIS than the variability in PK parameters. First, each PK parameter (k_{10} , k_{12} , k_{21} , k_{13} , k_{31} , V_1 , V_2 and V_3) is assumed to vary over three levels (minimum, average, maximum). This gave, $3^8 = 6561$ combinations of patients, and closed-loop simulations for a step change of 100 to 50 are carried out for these patients with MPC. Simulations showed that changes in volumes of the compartments (V_1 , V_2 and V_3) has very less effect on the performance (IAE values). Hence, these three parameters were kept constant and the simulations are carried out by changing only the remaining five parameters and this gave $3^5 = 243$ combinations of patients. Closed-loop simulations with MPC controller showed that IAE values varied only in the small range of 201 – 243. Hence, from these 243 combinations, six parameter sets which span the entire IAE range were selected. With these six parameter sets, three PD parameters were varied in three levels and this gave $6 \times 3^3 = 162$ combinations of patients. Closed-loop simulations with MPC controller showed that IAE values varied in the range of 168 – 372. From the 162 parameter combinations, 17 sets were selected to cover the entire span of IAE. The values of the parameters for the selected 17 patient sets are given in Table 5.2. These 17 patient sets are arranged in the decreasing order of their BIS sensitivity to propofol infusion. For the insensitive patient, depletion rate constants of the central compartment (k_{10} , k_{12} and k_{13}) are

high (0.149, 0.14 and 0.052, respectively) and absorption rate constants (k_{21} and k_{31}) are low (0.041 and 0.002, respectively). In the PD parameters, higher EC_{50} (3.7) indicates the need for more drug to get the same hypnosis level, higher γ (3.12) represents higher nonlinearity and lower k_{e0} (0.239) indicates sluggishness in response. For the sensitive patient k_{10} , k_{12} and k_{13} are low (0.089, 0.084 and 0.031, respectively) and k_{21} , k_{31} are high (0.069 and 0.004, respectively). In the PD parameters, lower EC_{50} (1.6) indicates the need of less drug to get the same hypnosis level, lower γ (2) represents lower nonlinearity, and higher k_{e0} (0.459) indicates faster response. Also, since k_{e0} represents the process gain, higher k_{e0} (higher gain) represents faster response and lower k_{e0} (lower gain) represents slower response of the process. With these 17 “patients”, robustness of all the remaining controllers were tested.

Table 5.2
 Values of the parameters for the 17 patient sets arranged in the decreasing order of their BIS sensitivity to propofol infusion

Patient No.	Parameter							
	k_{10}	k_{12}	k_{21}	k_{13}	k_{31}	k_{e0}	EC_{50}	γ
1 (Sensitive)	0.08925	0.084	0.06875	0.031425	0.004125	0.459	1.6	2
2	0.14875	0.14	0.04125	0.052375	0.004125	0.239	1.6	2
3	0.14875	0.112	0.04125	0.0419	0.004125	0.239	1.6	3.122
4	0.14875	0.14	0.04125	0.052375	0.004125	0.239	1.6	3.122
5	0.08925	0.084	0.04125	0.052375	0.002475	0.459	2.65	2.561
6	0.08925	0.084	0.06875	0.031425	0.002475	0.349	2.65	2.561
7	0.14875	0.112	0.06875	0.031425	0.002475	0.459	2.65	2.561
8 (Nominal)	0.119	0.112	0.055	0.0419	0.0033	0.349	2.65	2.561
9	0.119	0.112	0.055	0.0419	0.0033	0.239	2.65	2
10	0.119	0.112	0.055	0.0419	0.0033	0.239	2.65	2.561
11	0.08925	0.084	0.06875	0.031425	0.002475	0.459	3.7	2
12	0.14875	0.112	0.06875	0.031425	0.002475	0.349	3.7	2.561
13	0.08925	0.084	0.06875	0.031425	0.002475	0.239	3.7	2.561
14	0.08925	0.084	0.06875	0.031425	0.002475	0.239	3.7	3.122
15	0.08925	0.084	0.04125	0.052375	0.002475	0.239	3.7	3.122
16	0.14875	0.14	0.04125	0.052375	0.004125	0.349	3.7	2.561
17 (Insensitive)	0.14875	0.14	0.04125	0.052375	0.002475	0.239	3.7	3.122

Figure 5.6 depicts the closed-loop performance of the MPC controller for the 17 different patient parameter sets. Figure 5.6(a) shows the tracking performance with respect to BIS set-point equal to 50. For all these sets, BIS reached the set-point with a small undershoot (for sensitive patients) and with some time delay (for insensitive patients). Insensitive patient (IAE = 372) has sluggish response, whereas sensitive patient (IAE = 168) has faster response when compared to the response of the nominal patient (IAE = 217). Figure 5.6(b) represents the predicted plasma propofol concentration, C_1 using the nominal (and not the actual) patient model. For the sensitive patient, nominal patient model predicts lesser concentration than the actual concentration because it infuses less drug based on the larger gain BIS response to propofol infusion. Similarly, for the insensitive patient, higher C_1 is predicted with the nominal patient model than the actual concentration because more drug is infused based on the smaller gain BIS response to propofol infusion. However, the predicted C_1 remained within the constraints and with a small overshoot for all the 17 patient sets. Figure 5.6(c) represents the propofol infusion rate, u . As discussed above, more drug is infused to the insensitive patient and less drug is infused to the sensitive patient when compared to the nominal patient.

Figure 5.7 depicts the closed-loop performance of the IMC controller with 17 different patient parameter sets. Figure 5.7(a) shows the performance in tracking the set-point change of -50 units in BIS. For all these “patients”, the set-point was reached but with undershoot that was higher than with MPC controller and with time delay that depended on the patient’s sensitivity to the drug. Despite the undershoot noticed with some of the patient sets, the BIS set-point was tracked with this controller without violating the constraints. Figure 5.7(a) also shows the sluggish response of the insensitive patient (IAE = 396) and faster response of the sensitive patient (IAE = 122) when compared to the nominal patient (IAE = 218). The IMC shows some overshoot in C_1 for some of the patient sets (not shown), but all variables were maintained within constraints. Even here, more drug is injected

to the insensitive patient and less drug is injected to the sensitive patient when compared to the nominal patient (Figure 5.7(b)).

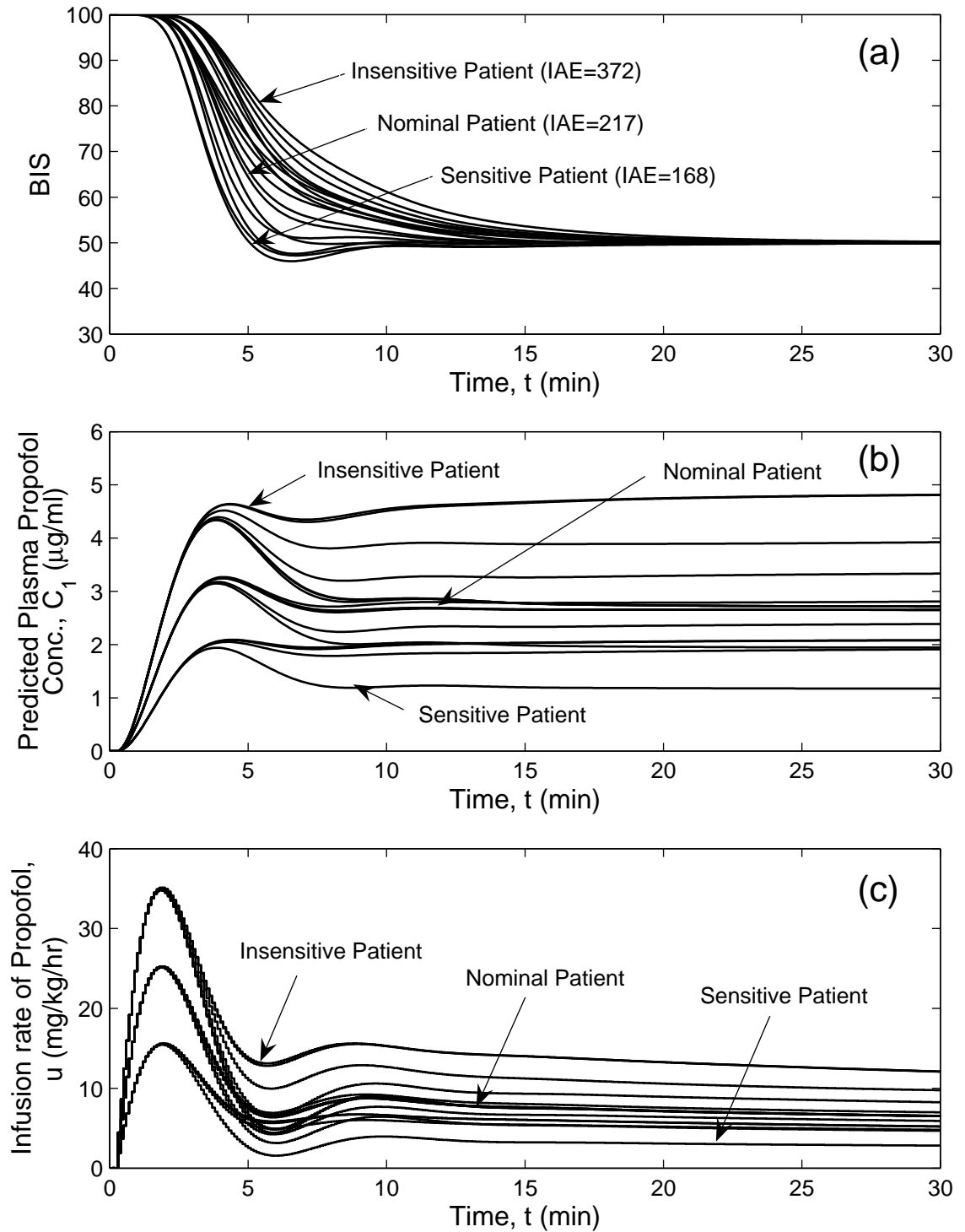


Fig. 5.6. Performance of MPC controller for 17 patients

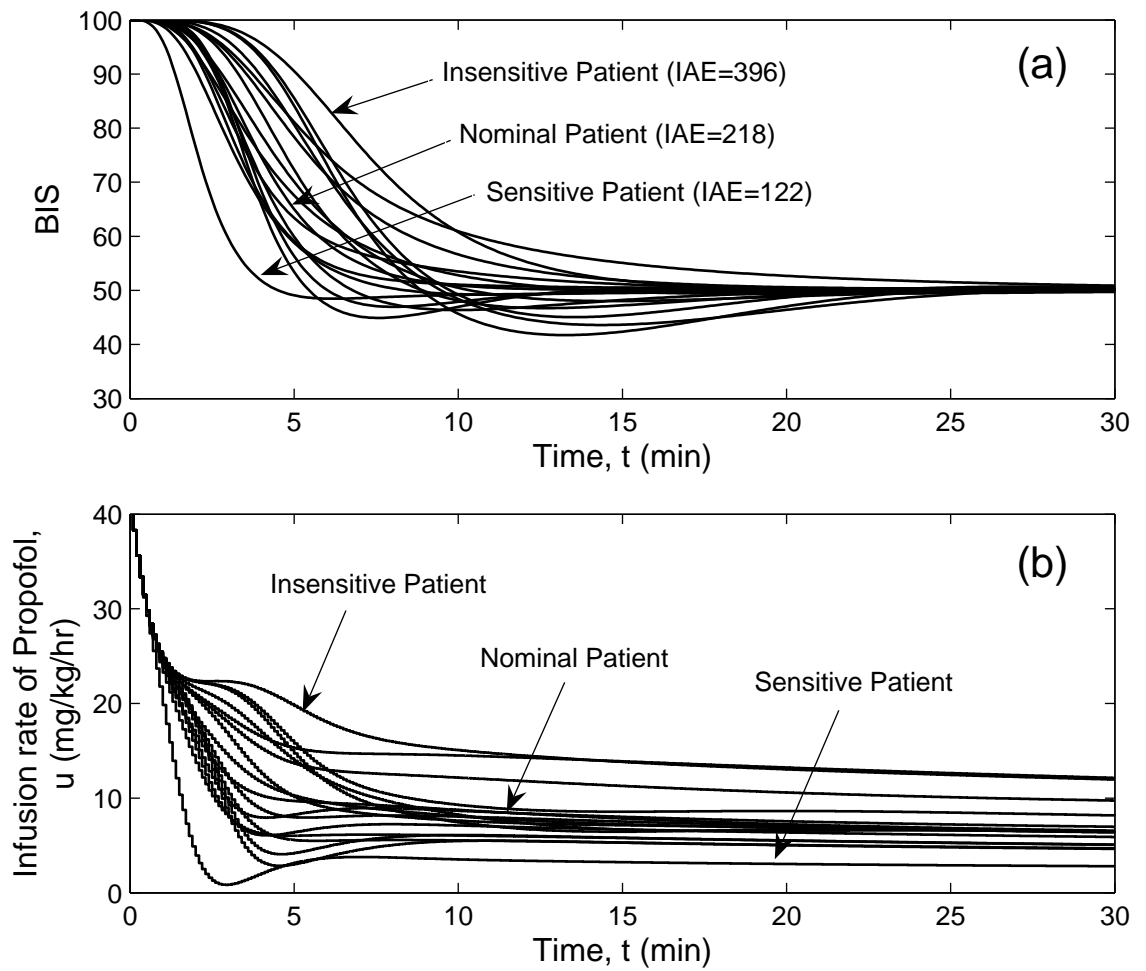


Fig. 5.7. Performance of IMC controller for 17 patients

When the simulations were done with MEC controller (Figure 5.8), IAEs of 438, 97 and 217 were obtained for the insensitive, sensitive and nominal patients, respectively. When compared to MPC and IMC, MEC gave a higher IAE value for the insensitive patient and lower IAE value for the sensitive patient. Also, with MEC controller, output BIS has no undershoot when compared with MPC and IMC. With the PID controller (Figure 5.9), IAEs for insensitive, sensitive and nominal patients are 384, 166 and 217, respectively. With the PID controller, output BIS has higher undershoot for a few patient models and also has offset when compared to the remaining three controllers.

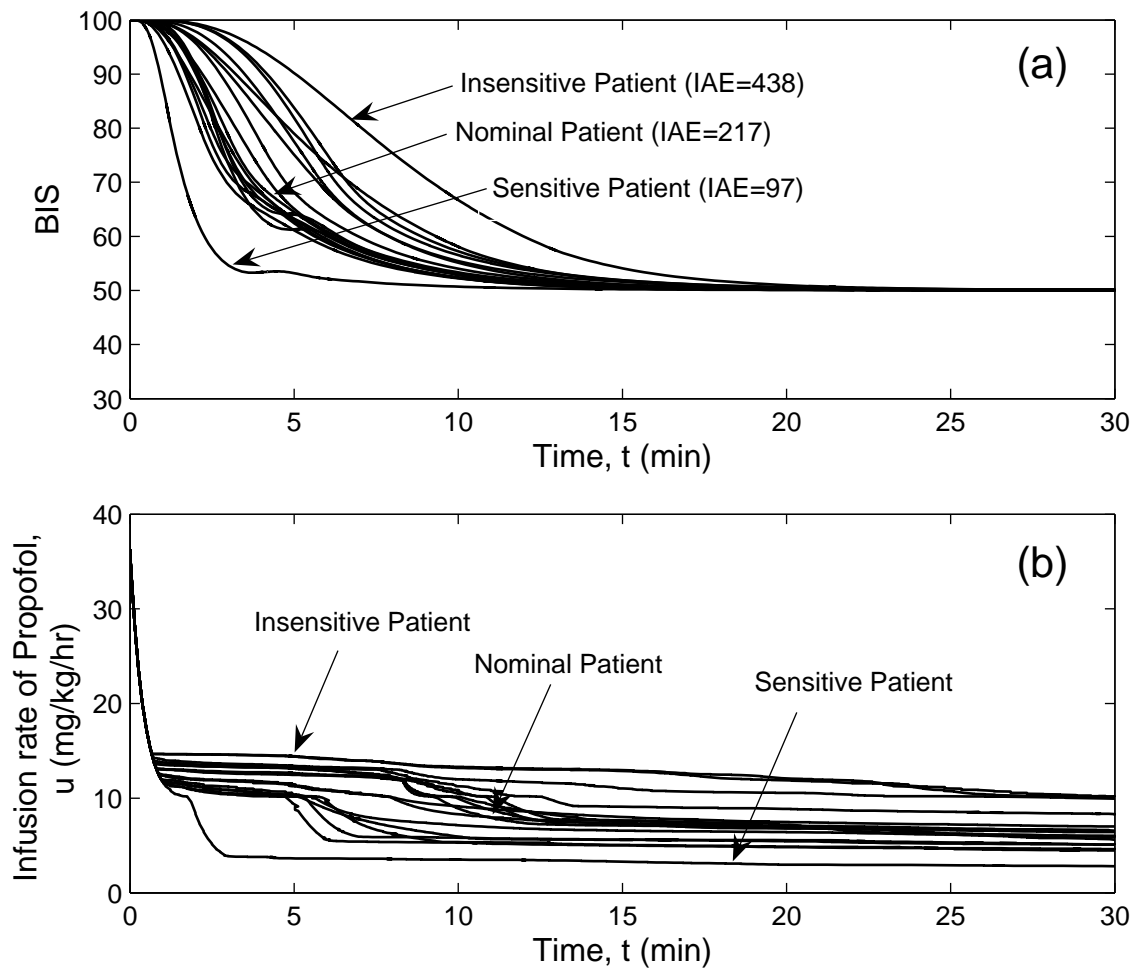


Fig. 5.8. Performance of MEC controller for 17 patients

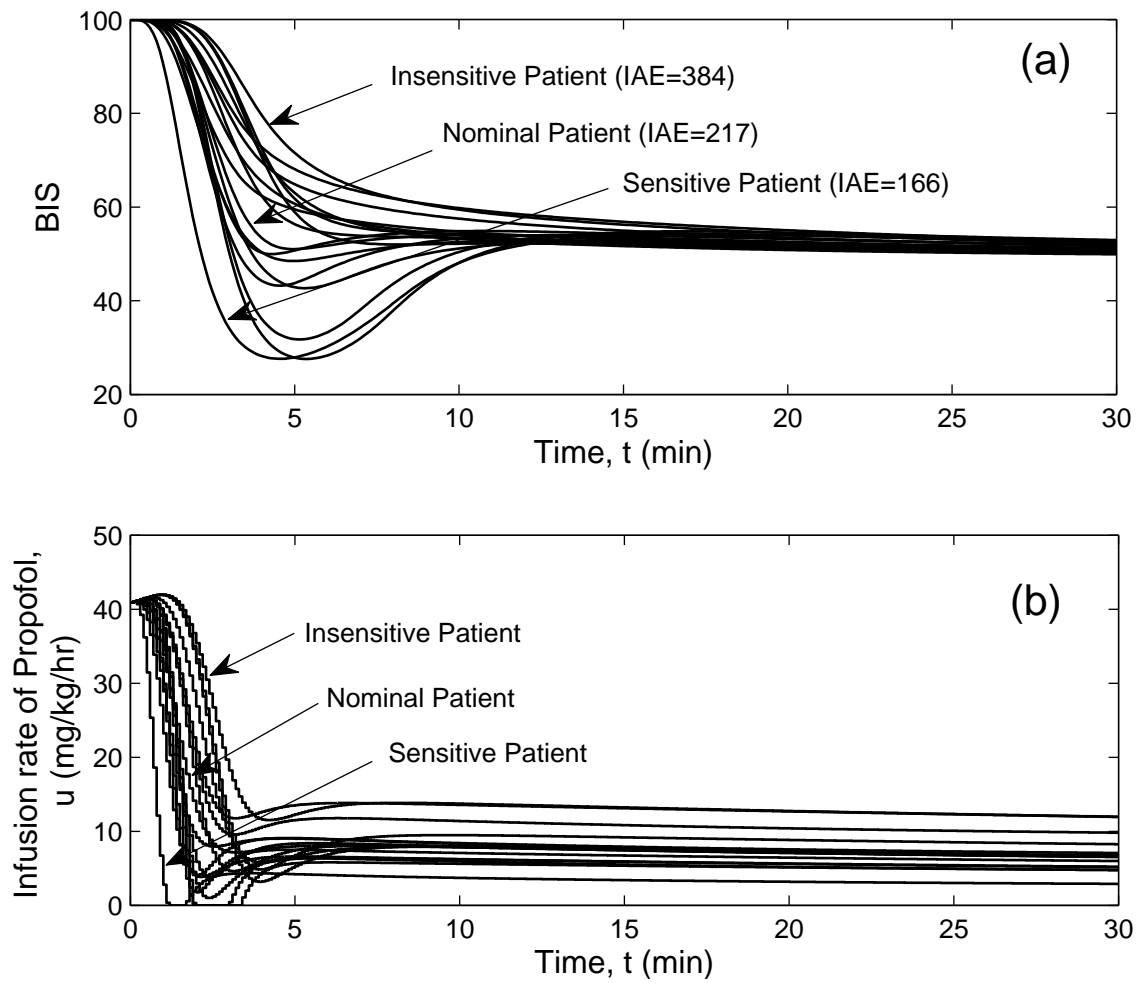


Fig. 5.9. Performance of PID controller for 17 patients

Figure 5.10 shows the comparison of IAE values of all the four controllers for BIS set-point change from 100 to 50 for these 17 patient sets. The average IAE values for MPC, IMC, MEC and PID are 237, 267, 249 and 267, respectively. The standard deviation in IAE values are 57, 83, 81 and 65, respectively. From these we can see that, by considering both average IAE and standard deviation in IAE, the MPC controller provides better robust performance when compared to the other three controllers. Even though the PID controller performs similar to MEC and IMC, the undershoot and offset in output BIS signal are of some practical concern.

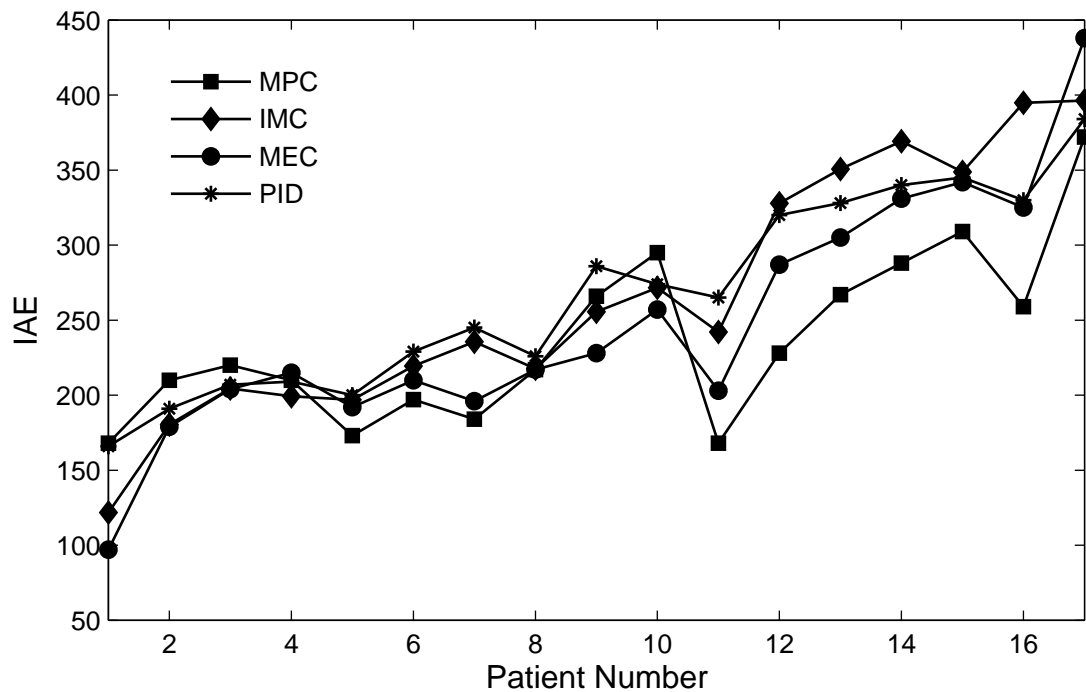


Fig. 5.10. IAE for all the 17 patients for set-point change from 100 to 50

5.4.3 Performance comparison for disturbances and measurement noise in the BIS signal

BIS signal may be corrupted by artifacts such as measurement noise and stimulus of different strengths. The artifacts in BIS signal might come from the high impedance of the electrodes, corruption of the EEG with the electromyography signal (EMG), etc. Disturbances in BIS signal may come from changes in strengths of

surgical stimuli based on different surgical circumstances which cause arousal reflex. For better control performance, the noise and disturbances in the BIS signal must be handled appropriately (for example, filtering noise). If not, it will be harmful to the patient because unreliable values of the measured signals will result in wrong drug dosage delivered to the patient. Here, the simulations are carried out by adding 2% Gaussian noise to the BIS signal and for disturbances, a standard stimulus profile (Struys et al. 2004) is applied from $t = 70 - 130 \text{ min}$ to all the “patients”. The total stimulation time of 60 *min* includes virtual inductions of different strengths and different periods up to the time of skin closure. Figure 5.11 depicts the corresponding stimulus profile (dotted line). The detailed description of the stimulus profile is provided in section 3.5 (also shown in Figure 3.7).

Figure 5.11 depicts the performance of the MPC controller with noise and disturbance in the BIS signal for the nominal patient. Figure 5.11(a) shows the measured BIS profile with the BIS set-point set at 50. The dashed line includes the disturbance signal added to output BIS. Even though the BIS signal has noise, the controller regulates the BIS signal well. But, a strong disturbance for a longer duration of time causes the BIS signal to cross the limits imposed during the period of disturbance. Figure 5.11(b) shows the predicted plasma propofol concentration profile. Whenever BIS increases, controller increases C_1 by increasing propofol infusion rate to bring back BIS to its original set-point. Unlike BIS, the controller maintains predicted C_1 within the constraints imposed and this is very important for patient safety. Figure 5.11(c) shows the propofol infusion rate profile and this correlates very well with the C_1 profile. Even though the BIS signal is corrupted with noise, the MPC controller maintained a smooth infusion profile for propofol.

Figure 5.12 depicts the performance of the IMC controller with noise and disturbance in the BIS signal for the nominal patient. This controller also maintained the predicted C_1 within constraints. Unlike MPC, the noise in BIS signal leads to

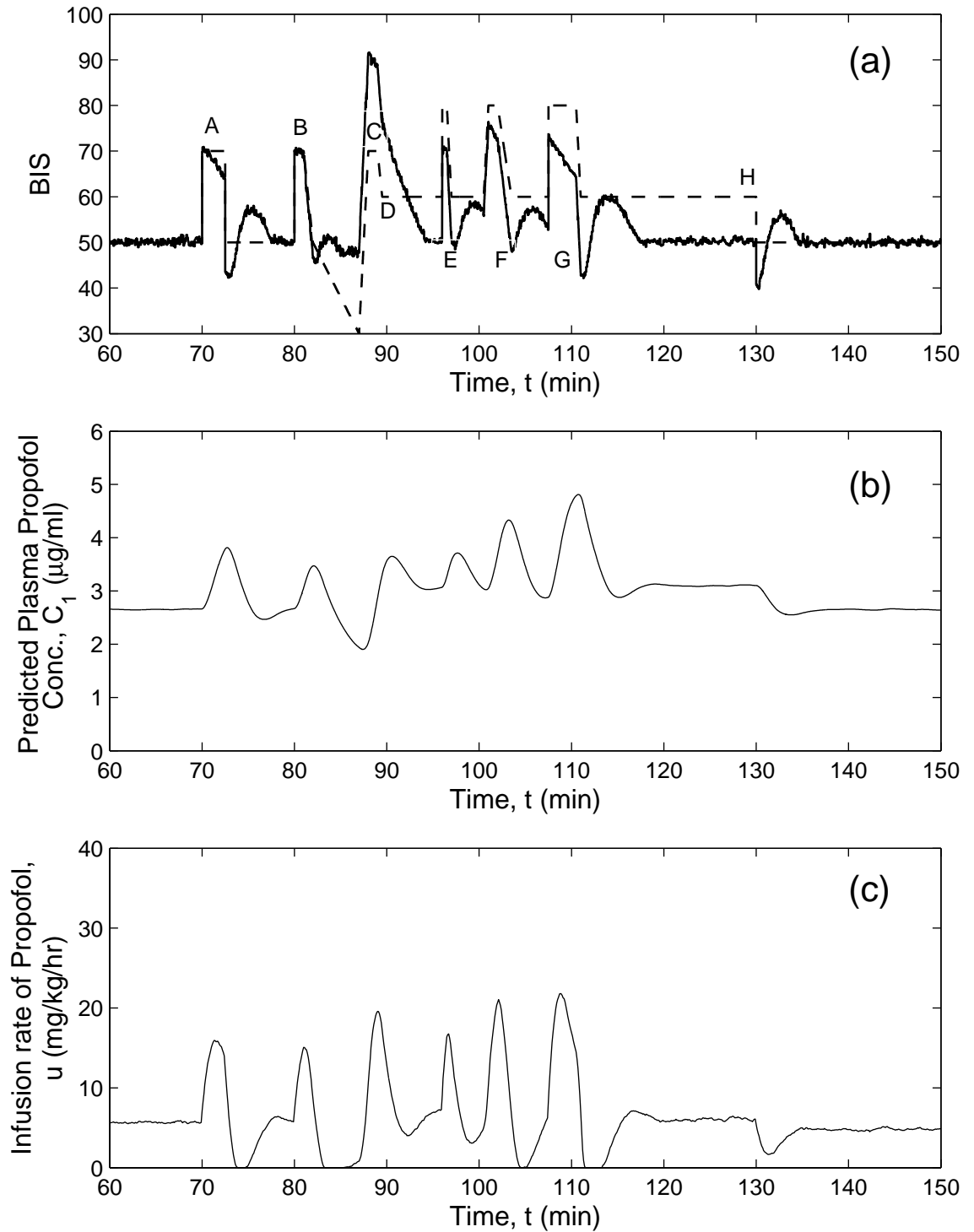


Fig. 5.11. Performance of the MPC controller for measurement noise and disturbances during the surgery

small fluctuations in the propofol infusion rate with IMC (Figure 5.12(b)). This is perhaps not good for the actuator element (control valve). Figure 5.13(a) depicts the performance of the MEC controller for the same scenario in the BIS signal for the nominal patient. Predicted C_1 maintained by this controller is within the constraints imposed. The profile of the propofol infusion rate (Figure 5.13(b)) is very noisy compared to MPC and IMC. This indicates the sensitivity of the MEC controller to noise, which can cause frequent movement of the control valve. This can be a problem in practical applications. Figure 5.14 depicts the performance of the PID controller. The regulatory performance is sluggish (Figure 5.14(a)), and hence the PID performance is lower than the other controllers. The propofol infusion profile (Figure 5.14(b)) is less noisy when compared to MEC controller but more noisy when compared to MPC and IMC controllers.

The performance (IAE values) of all four controllers is tested on the 17 different patient sets for the noise and disturbance in output BIS, and the results obtained are summarized in Figure 5.15. The average performance is high for the MPC controller (IAE = 461) and less for the PID controller (IAE = 528). Average IAE values with MEC and IMC are 489 and 470, respectively. The standard deviation in IAE values for MPC, IMC, MEC and PID are 21, 22, 19 and 29, respectively.

Figure 5.16 shows the performance of the four controllers for the percentage of the time, the output BIS value is outside ± 10 units of the set-point for all 17 patient models for disturbances in output BIS (Struys et al. 2004). The performance is evaluated for the disturbance period from 70 to 150 *min*. The comparison shows the poor average performance with the PID controller (28%) and high average performance with the MPC controller (21%). MEC and IMC gave similar average performance of 23% and 23%, respectively. These percentages are somewhat higher because of the large magnitudes of disturbance pulses introduced within a short

period of time. The standard deviation in the above percent times is small (2 – 3%) for all the four controllers tested.

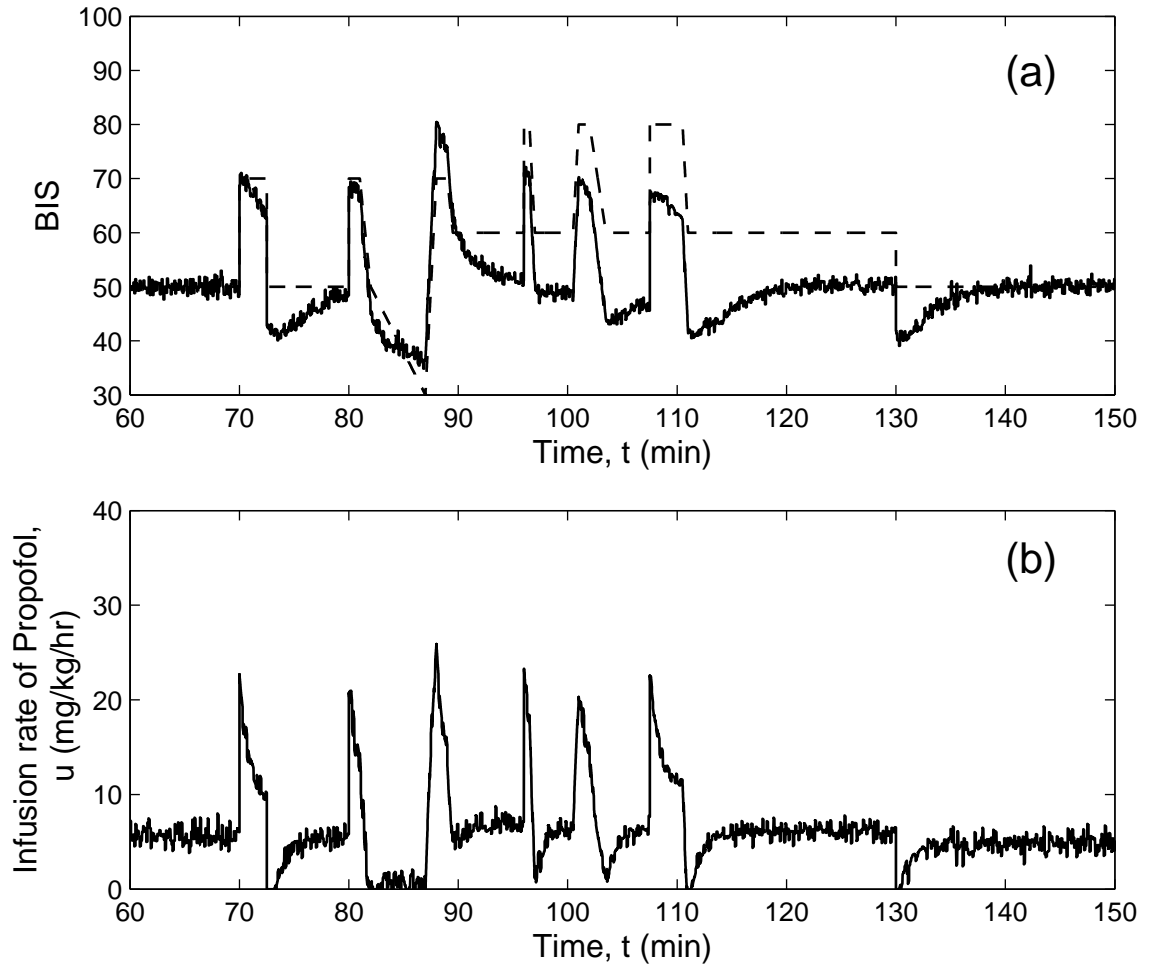


Fig. 5.12. Performance of the IMC controller for measurement noise and disturbances during the surgery

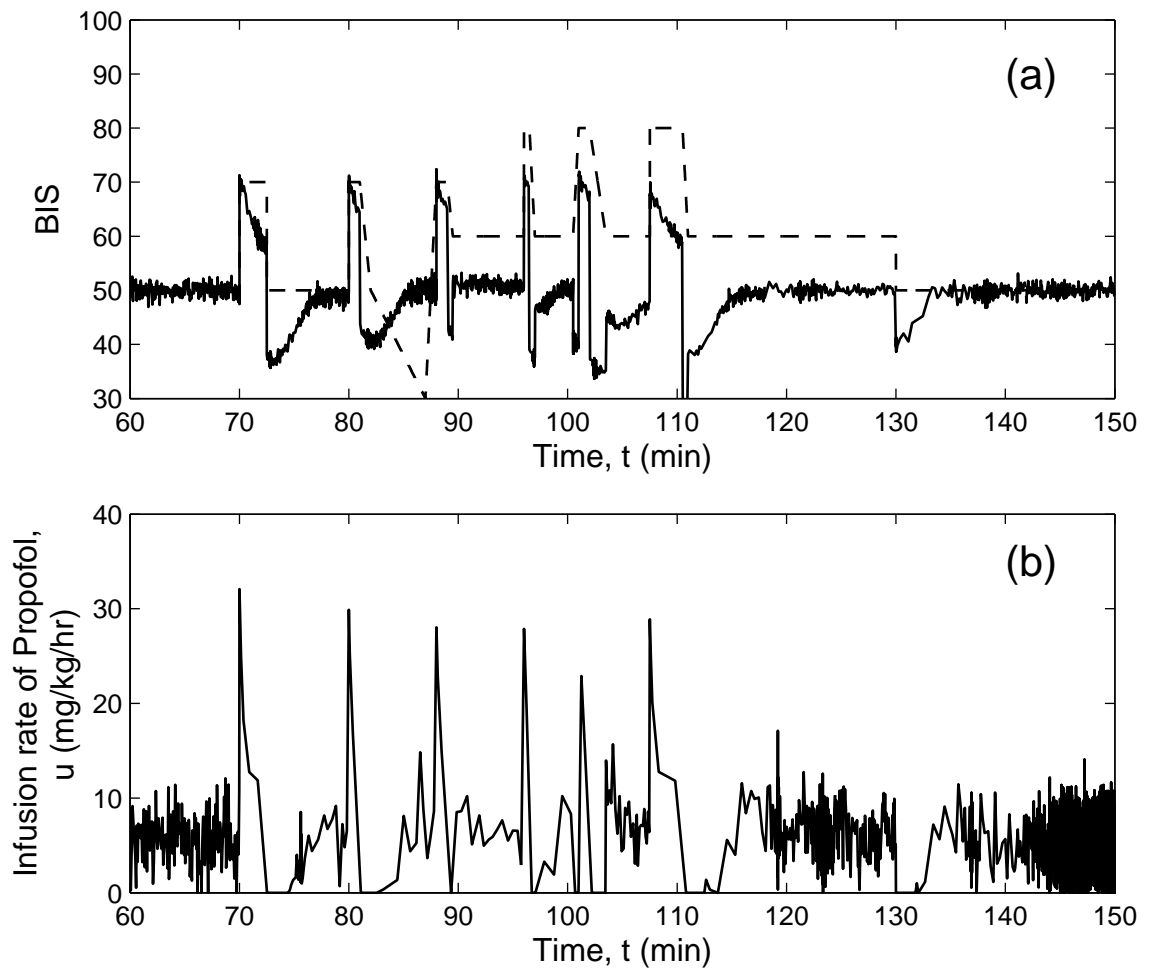


Fig. 5.13. Performance of the MEC controller for measurement noise and disturbances during the surgery

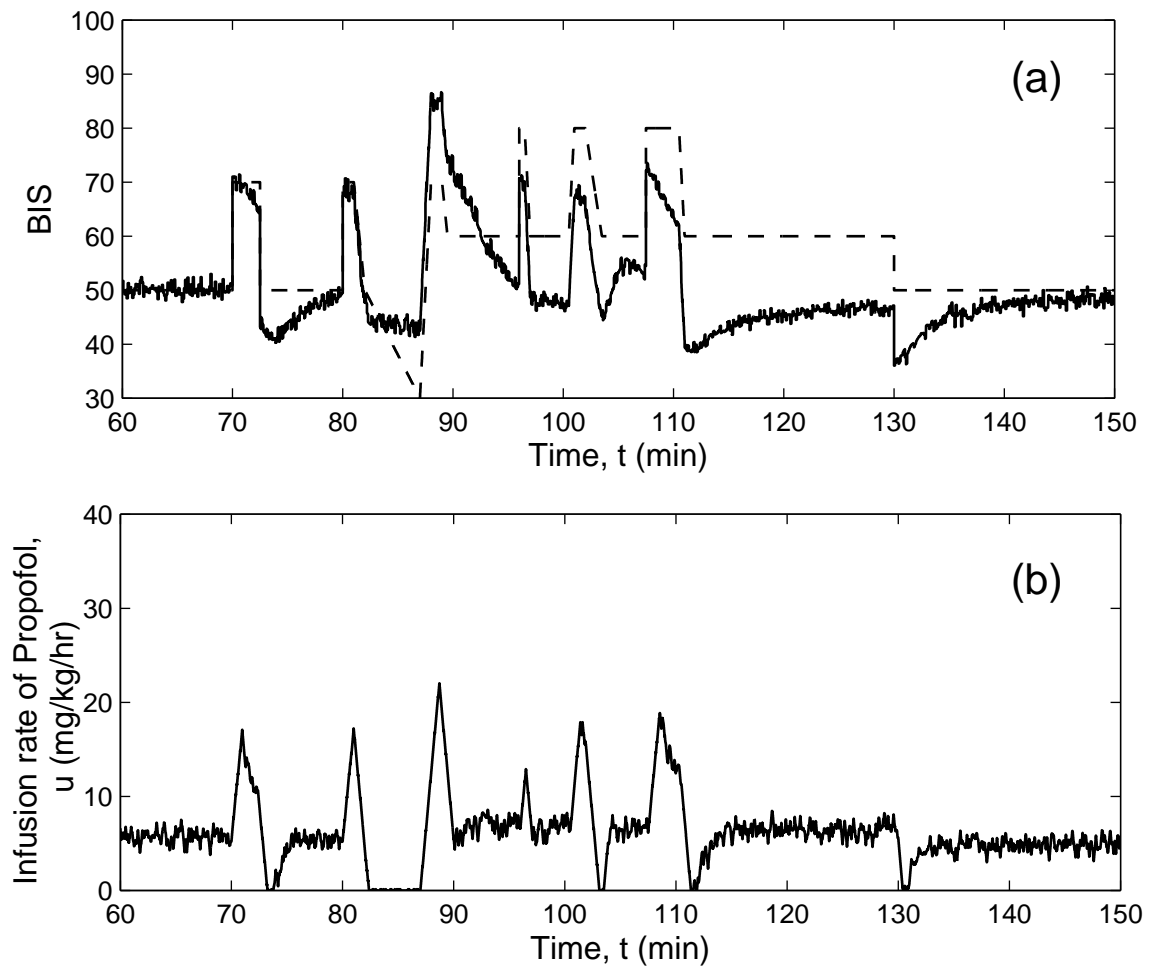


Fig. 5.14. Performance of the PID controller for measurement noise and disturbances during the surgery

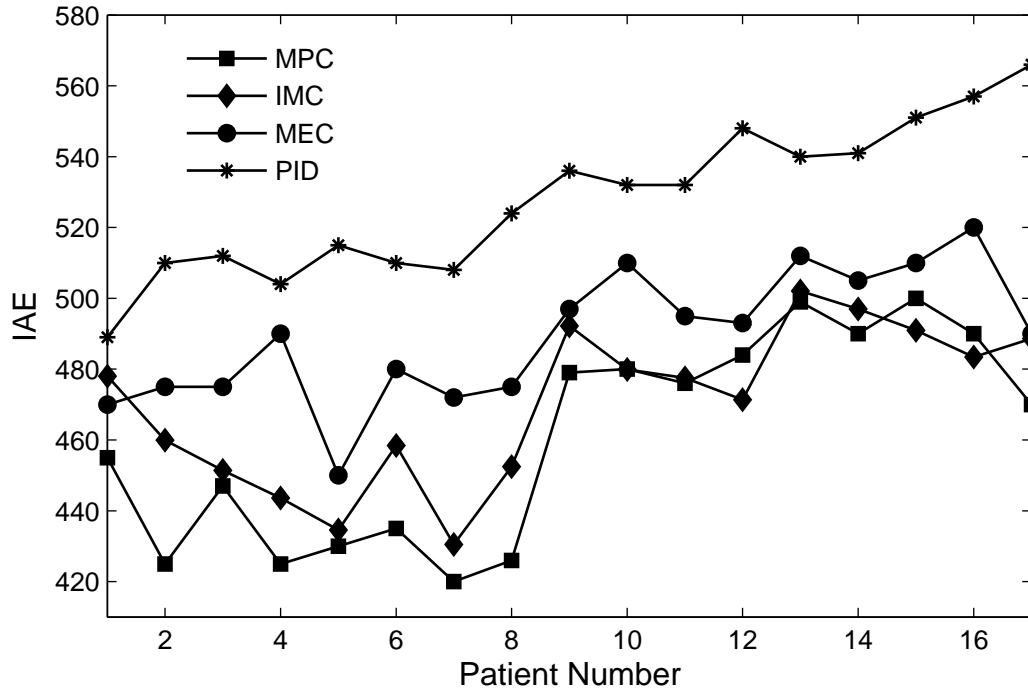


Fig. 5.15. IAE for all the 17 patient models for noise and disturbances in BIS signal

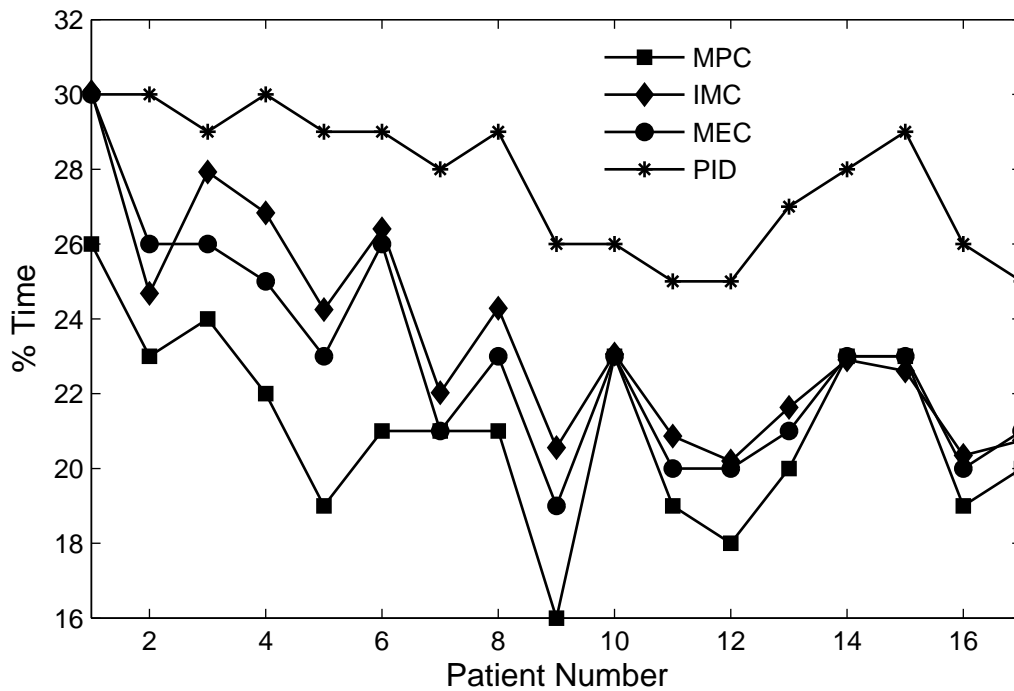


Fig. 5.16. Percentage of the time output BIS value is outside ± 10 units of the set-point for all 17 patient models for disturbances in the BIS signal

5.4.4 Performance comparison for set-point changes in BIS during surgery

Anesthesiologists can anticipate periods that require more stimulation and also periods during which light sedation is required during the surgery and accordingly adjust the BIS set-point. Hence, the four controllers are now tested for different set-point changes in BIS value which may be required at any time based on the extent of surgery. For example, if surgical stimulation is severe at any time during the surgical process, the patient needs to be more unconscious and hence the BIS value should be decreased to some lower value (e.g., 40). Afterward, toward the end of the surgery, the patient needs to be less unconscious and the BIS set-point may be increased from 40 to say, 70. Figures 5.17 – 5.20 depict the performance of the four controllers (MPC, IMC, MEC and PID, respectively) for a step change in BIS from 50 to 40 at $t = 30 \text{ min}$, from 40 to 70 at $t = 60 \text{ min}$, and from 70 to 50 at $t = 90 \text{ min}$ for the nominal patient. In these simulations, 2% Gaussian noise is added to the output BIS signal.

Plot (a) of Figures 5.17 – 5.20 depicts the performance of four controllers for different set-point changes during the surgery. Despite the noise in the output BIS signal, all controllers perfectly regulate the BIS near to the specified set-point. The PID controller gives offset in output BIS signal (Figure 5.20(a)) – this is not observed with the remaining three controllers. Figure 5.17(b) shows the smooth predicted C_1 profile with the MPC controller. The similar smooth predicted C_1 profiles are observed with the remaining three controllers. The propofol infusion profile obtained with the MPC controller is shown in Figure 5.17(c) and is smoother than the profiles obtained with the remaining three controllers which are shown in Figures 5.18(b), 5.19(b) and 5.20(b). Out of all these, infusion profile obtained with MEC controller is very aggressive and is deemed not good in a surgical setting.

The performance of all the four controllers is tested with the 17 different patients for the set-point changes mentioned above and the IAE values obtained are depicted

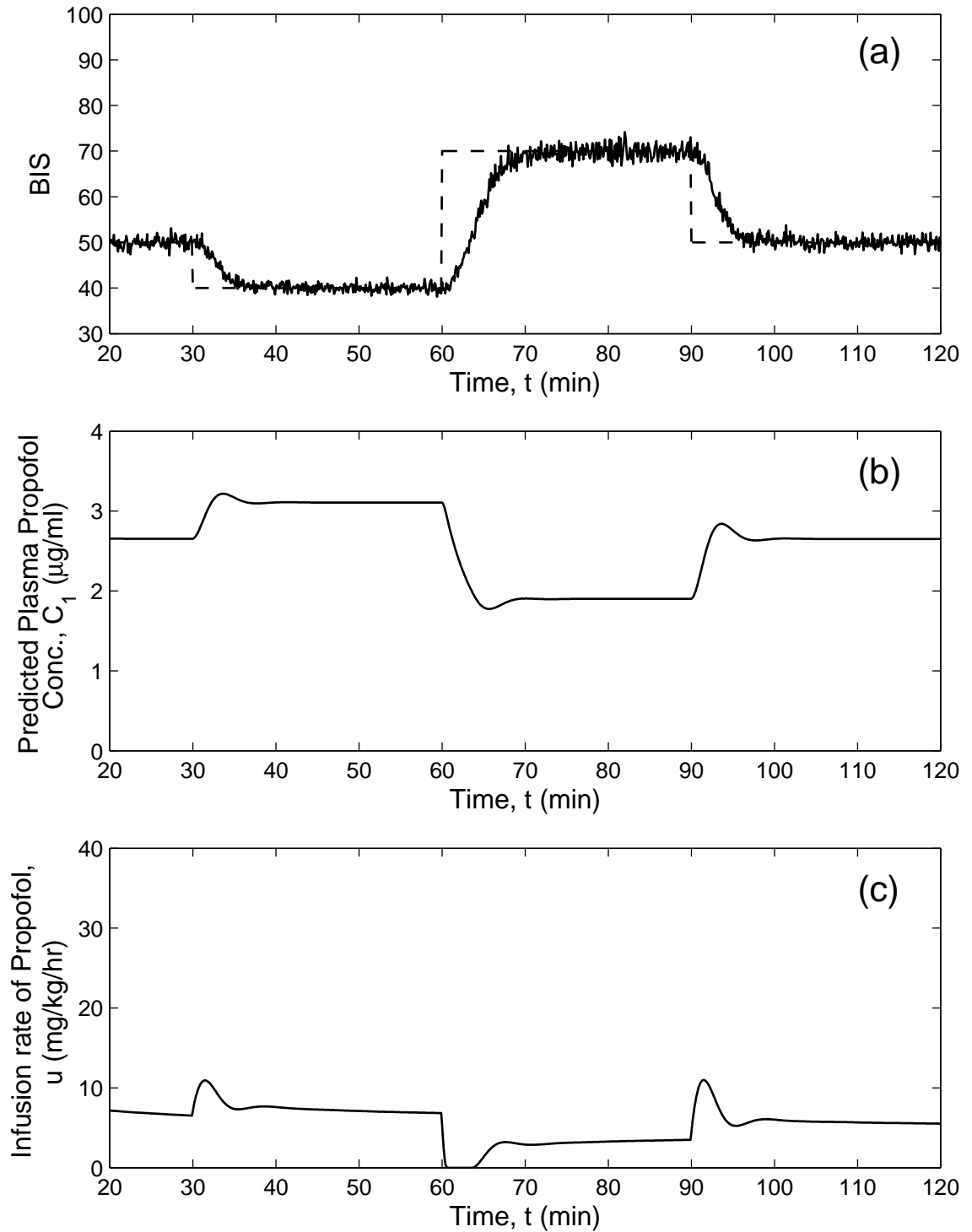


Fig. 5.17. Performance of the MPC controller for different set-point changes in BIS during the surgery

in Figure 5.21. The average performance is high for the MPC controller (IAE = 324) and poor for the PID controller (IAE = 405). MEC and IMC gave average IAE values of 337 and 340, respectively. The standard deviation in IAE values for MPC, IMC, MEC and PID are 27, 36, 29 and 42, respectively.

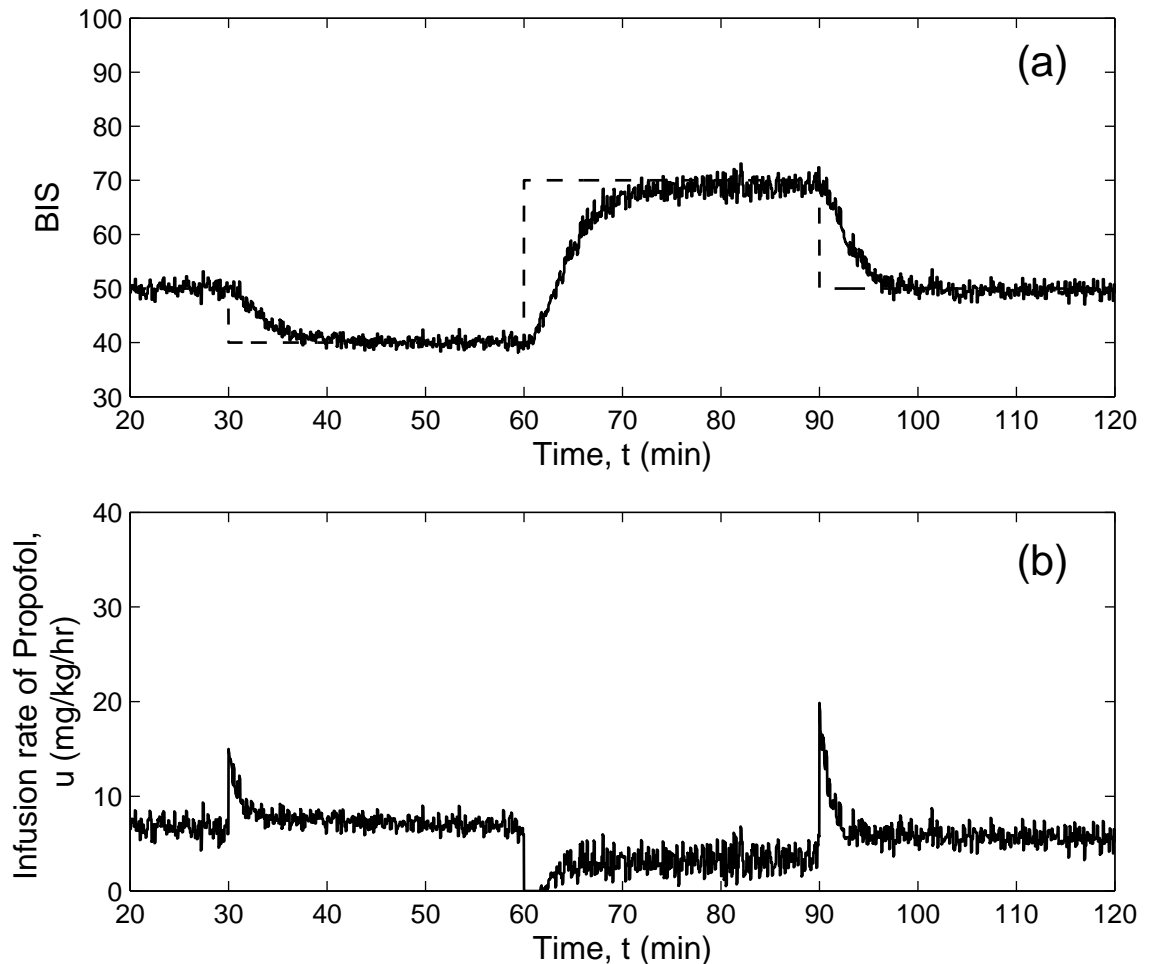


Fig. 5.18. Performance of the IMC controller for different set-point changes in BIS during the surgery

Figure 5.22 shows the performance of the four controllers for the percentage of the time output BIS value is outside ± 10 units from the set-point for all 17 patient models for different set-point changes in BIS (Struys et al. 2004). The performance is evaluated for the time period from 30 to 120 *min*. This comparison also shows the poor average performance with the PID controller (13%) and high average performance with the MPC controller (10%). MEC and IMC gave similar average

performance of 11%. The standard deviation in these percent times is 1% for all the four controllers tested.

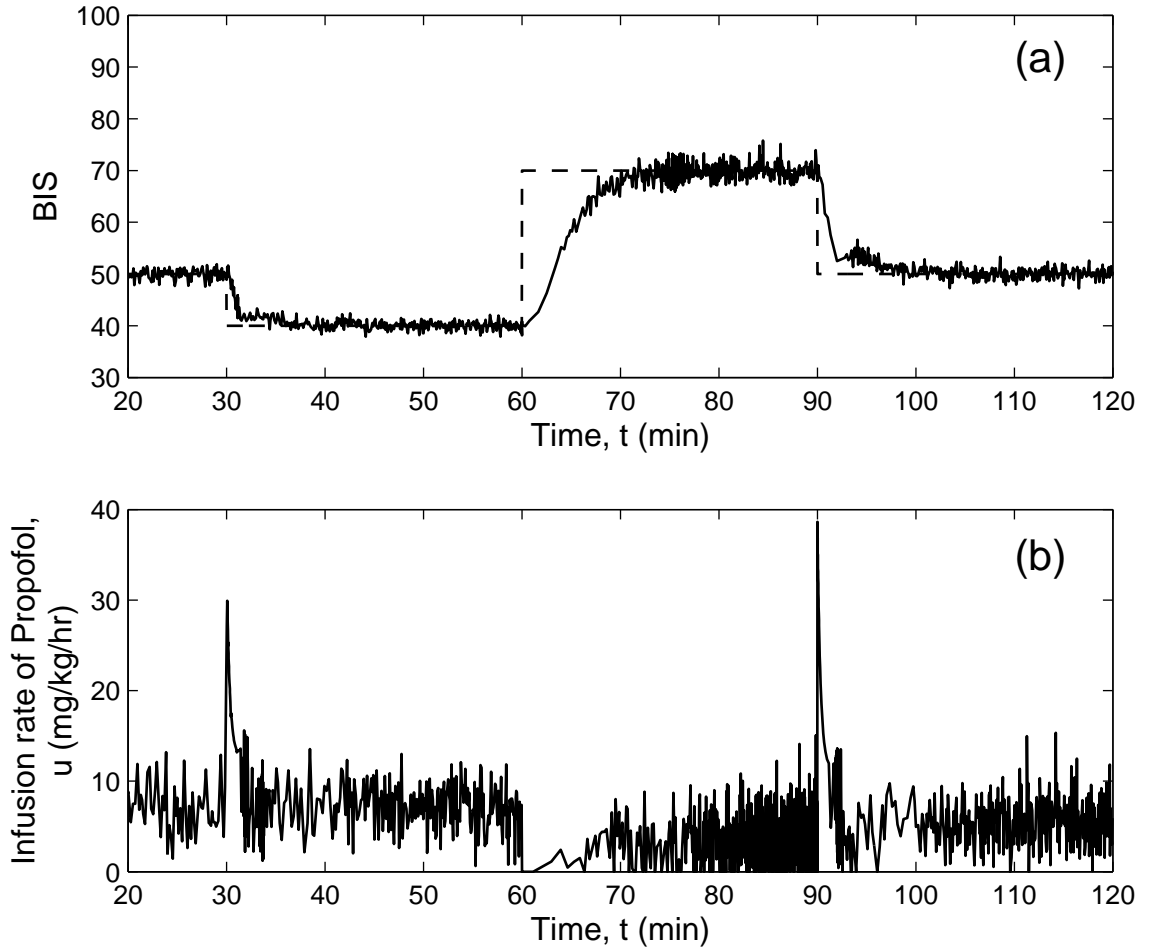


Fig. 5.19. Performance of the MEC controller for different set-point changes in BIS during the surgery

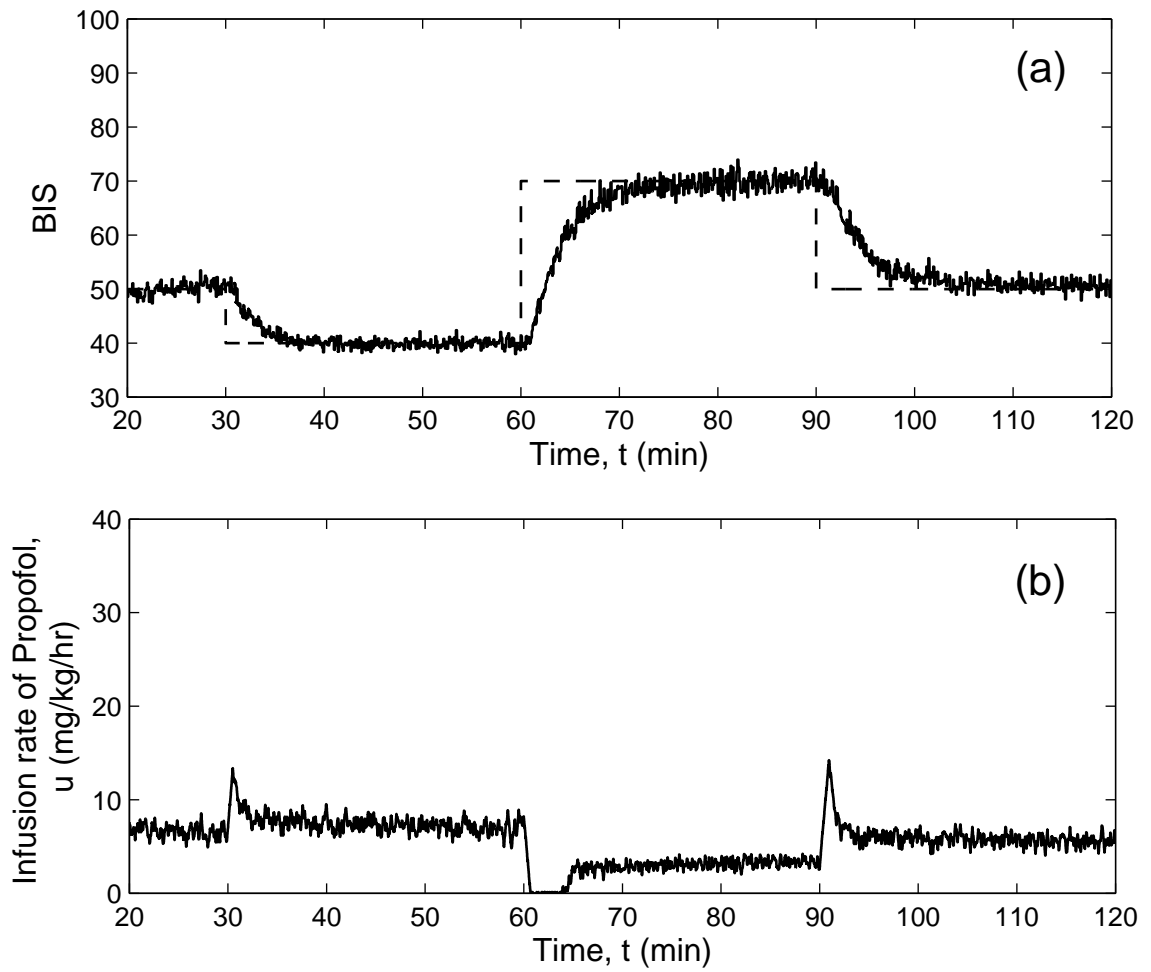


Fig. 5.20. Performance of the PID controller for different set-point changes in BIS during the surgery

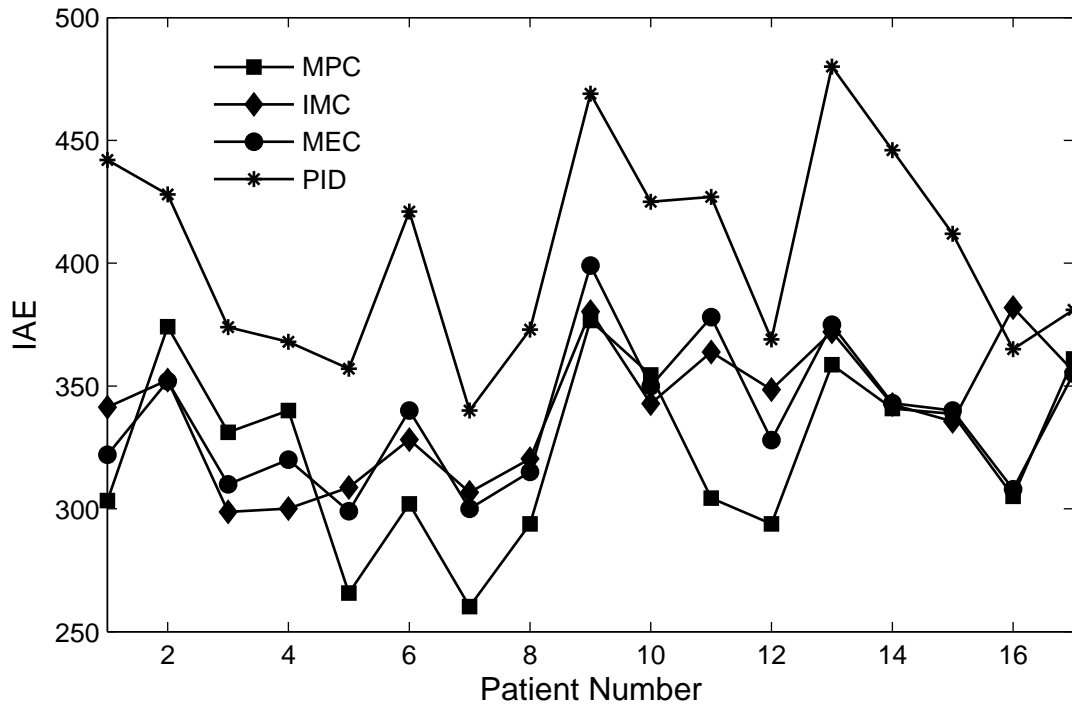


Fig. 5.21. IAE for all the 17 patient models for set-point changes

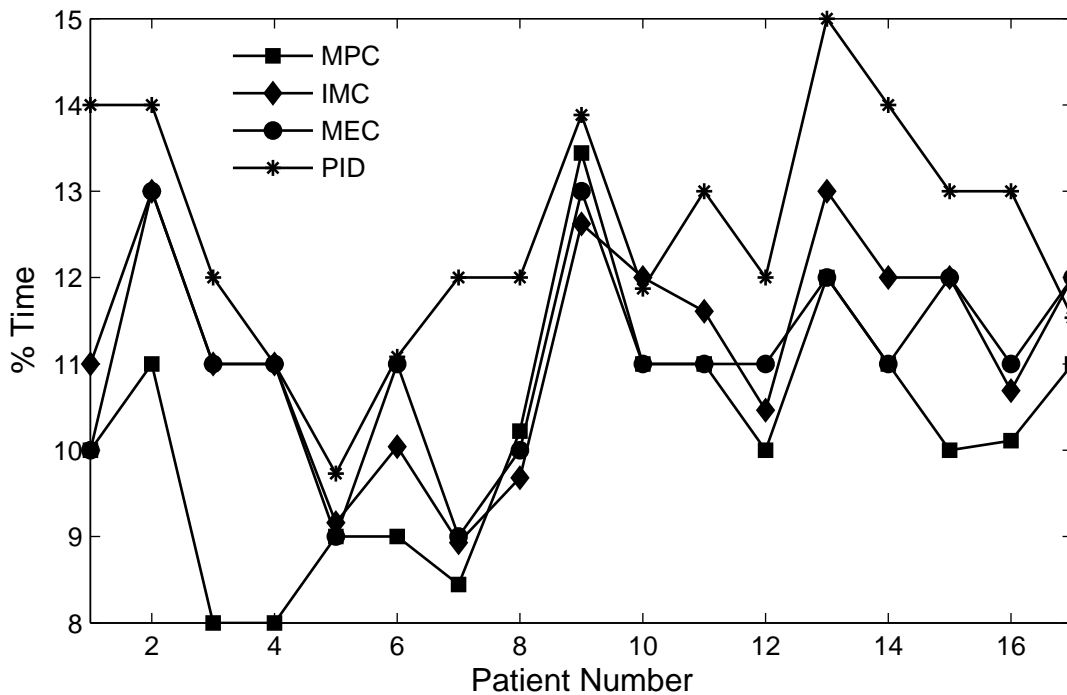


Fig. 5.22. Percentage of the time output BIS value is outside ± 10 units from the set-point for all 17 patient models for different set-point changes

5.5 Comparison of the performance with the RTDA Controller

This section provides a comparison between the performances of RTDA, MPC and PID controllers. Because, FOPTD model is used to design and tune RTDA controller, the four state, nonlinear patient model is approximated to FOPTD model through process reaction curve method. Figure 5.23 depicts the degree of approximation obtained. The four parameters of this controller are tuned using the direct

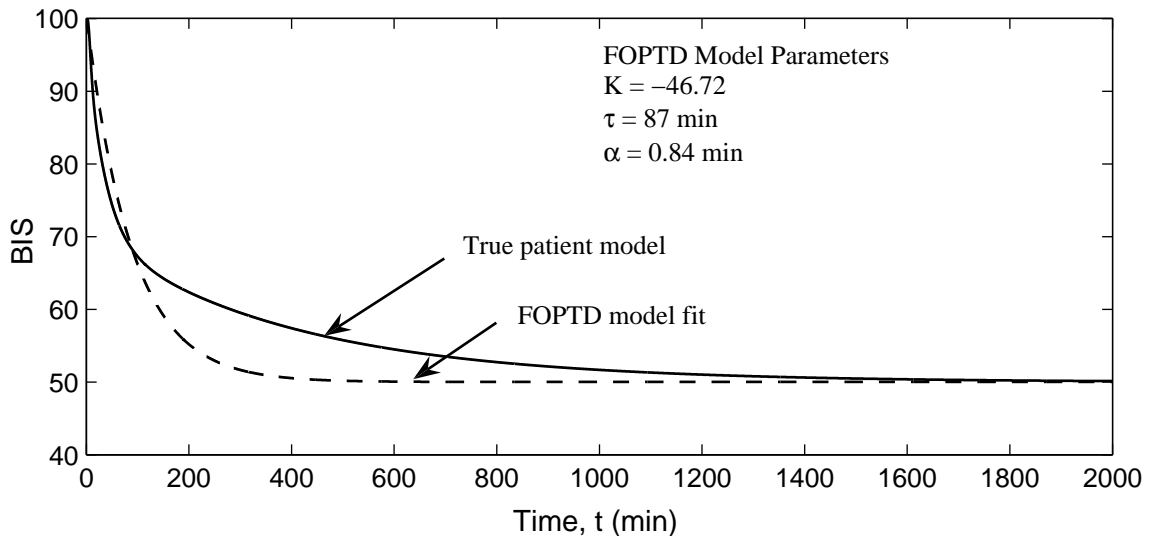


Fig. 5.23. FOPTD model fit to true patient model response

search optimization algorithm for the best performance *i.e.*, minimum IAE value (equation (3.26)) based on set-point changes to BIS from 100 to 50 (the BIS value recommended during surgery). The BIS response obtained through these settings gave a small undershoot, hence further fine tuning was carried out using different values of θ_T (tuning parameter which track the set-point changes) while keeping the remaining tuning parameters constant. Figure 5.24 depicts the performance of the RTDA controller for different values of θ_T and based on the performance, a value of 0.044 is selected. These settings ($\theta_R = 0.037$, $\theta_D = 0.937$, $\theta_A = 0.812$ and $\theta_T =$

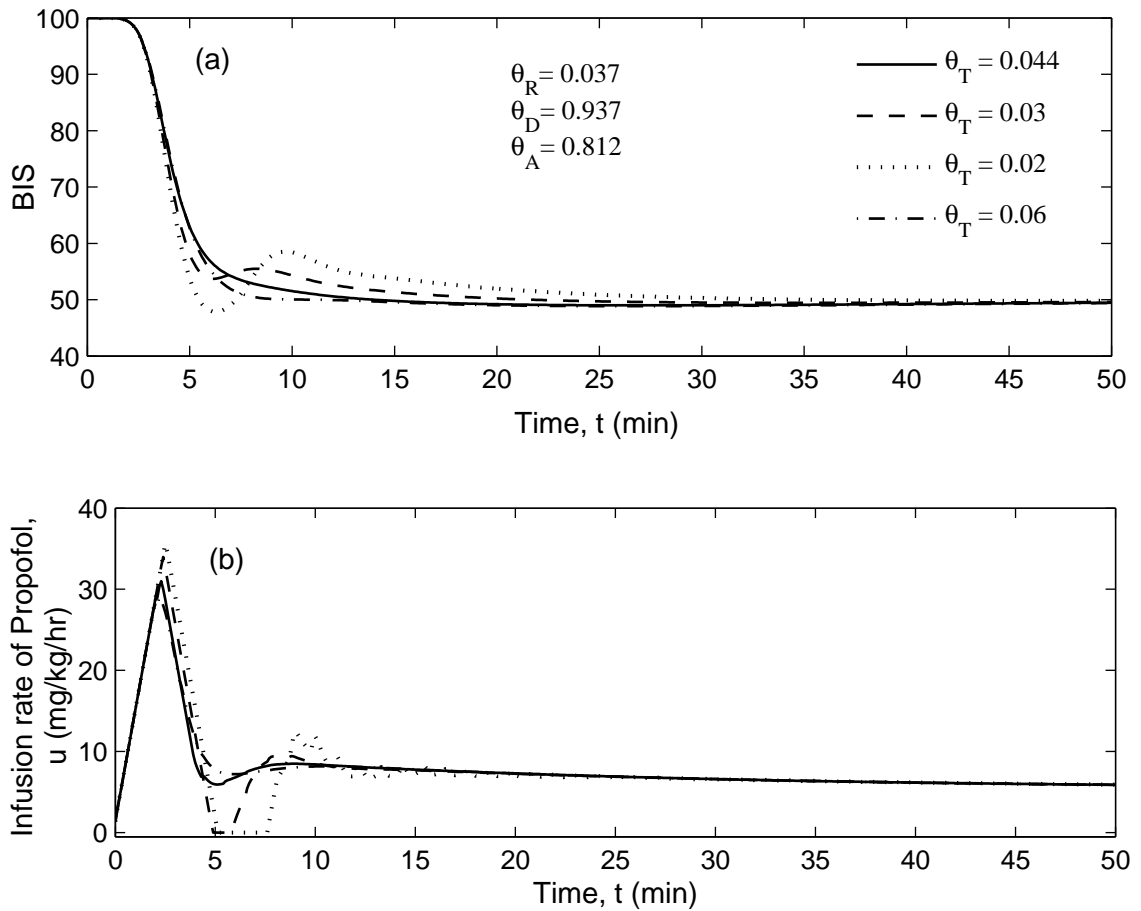


Fig. 5.24. Performance of the RTDA controller for different values of θ_T

0.044) will be used for further performance comparisons. The sampling time of all the controllers is set to 0.0833 *min* which is equal to the sampling time of BIS.

5.5.1 Performance comparison for a step change in BIS during surgery

The three controllers are tested for different step changes in BIS value on the nominal patient. Figure 5.25 depicts the performance of the three controllers for a step change in BIS from 50 to 40 at $t = 50$ *min* and from 40 to 60 at $t = 100$ *min*. Better transition of the BIS is obtained with RTDA and MPC controllers when compared to PID controller. Also, the PID controller has a relatively longer settling time.

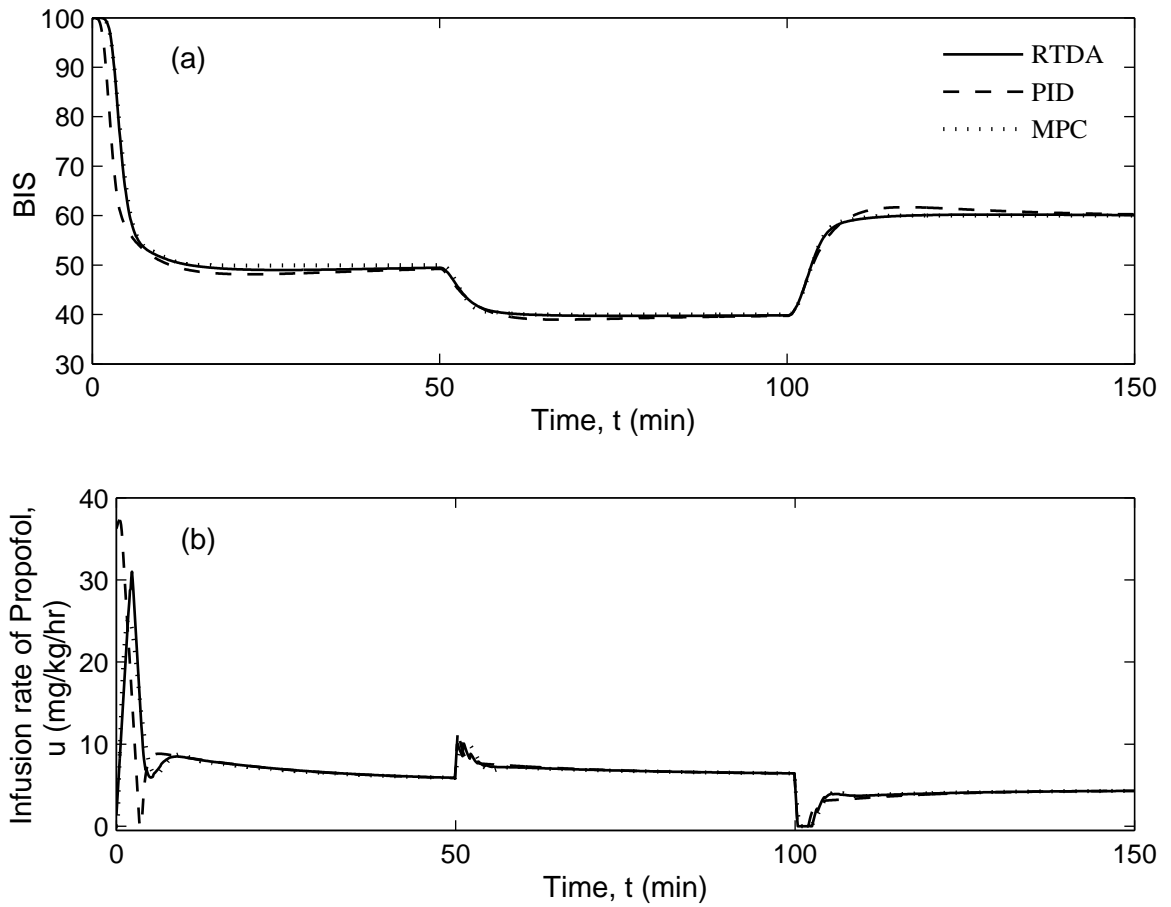


Fig. 5.25. Performance of the RTDA, MPC and PID controllers for different set-point changes during the surgery

5.5.2 Robustness comparison

This section discusses the robustness of the RTDA, MPC and PID controllers based on the IAE values. After a sensitivity test of the parameters, 17 patients (representing the *population* of patients) are selected (Table 5.2) and used for comparing the robustness of the three controllers. Figure 5.26 depicts the closed-loop performance of the RTDA controller with 17 patient sets. Figure 5.26(a) shows the tracking performance with respect to BIS set-point 50. With all these sets, the BIS

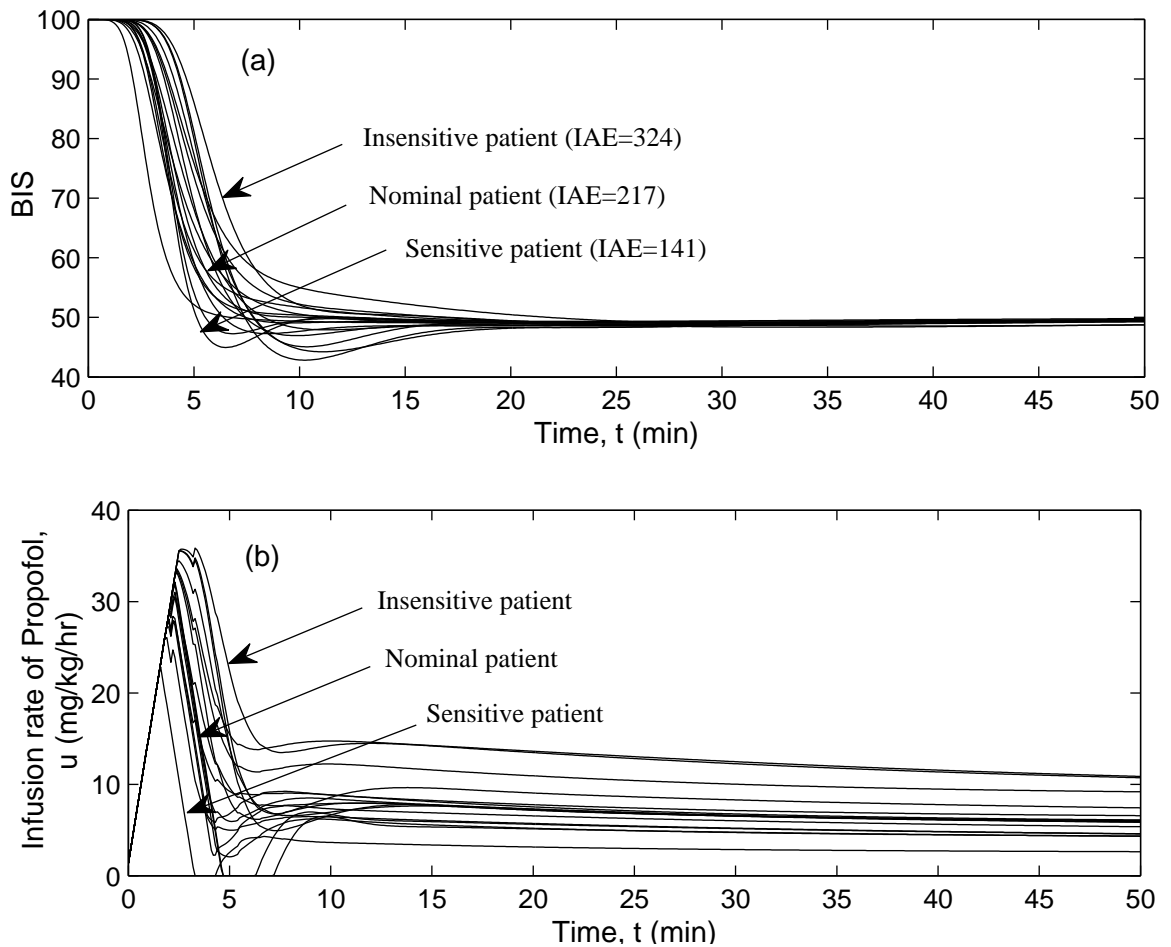


Fig. 5.26. Robust performance of the RTDA controller for different sets of patient model parameters

value reached the set-point with some undershoot and time delay based on the patient's sensitivity to the drug. Insensitive patient (IAE = 324) has sluggish response whereas sensitive patient (IAE = 141) has faster response when compared to the

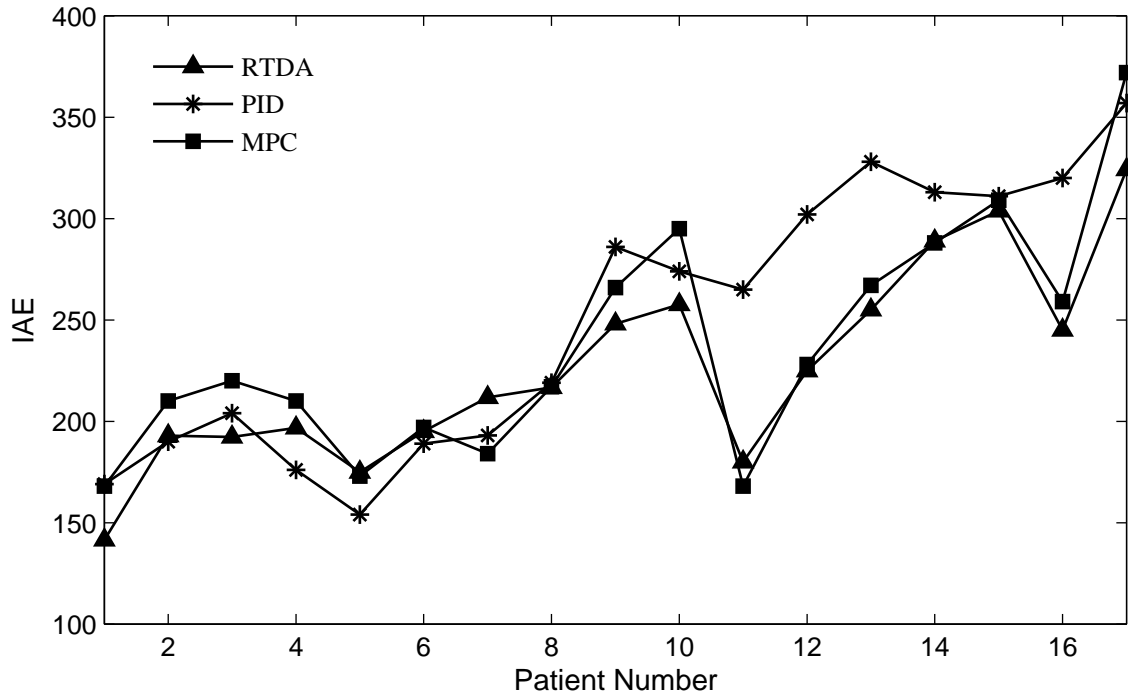


Fig. 5.27. IAE for all the 17 patient models for BIS set-point 50

response of the nominal patient ($IAE = 217$). Figure 5.26(b) represents the propofol infusion rate, u . In line with the above observations, more drug is injected to the insensitive patient and less drug is infused into the sensitive patient as compared to the nominal patient. Figure 5.27 shows the comparison of the performance (IAE values) of all the three controllers for BIS set-point 50 for these 17 patient models. In this plot, the average IAE value is lower for the RTDA controller ($IAE = 226$) and highest for the PID controller ($IAE = 250$). The IAE value for the MPC controller is 237 - this is slightly higher than that obtained for the RTDA controller.

5.5.3 Performance comparison for a sudden disturbance in BIS signal

The three controllers are tested for sudden disturbances which can occur at any-time during the surgery. Here, simulations are carried out by adding a disturbance pulse of strength 20 in the BIS signal from $t = 50 - 80 \text{ min}$. Figure 5.28 depicts the performance of all the three controllers with disturbance in the BIS signal for

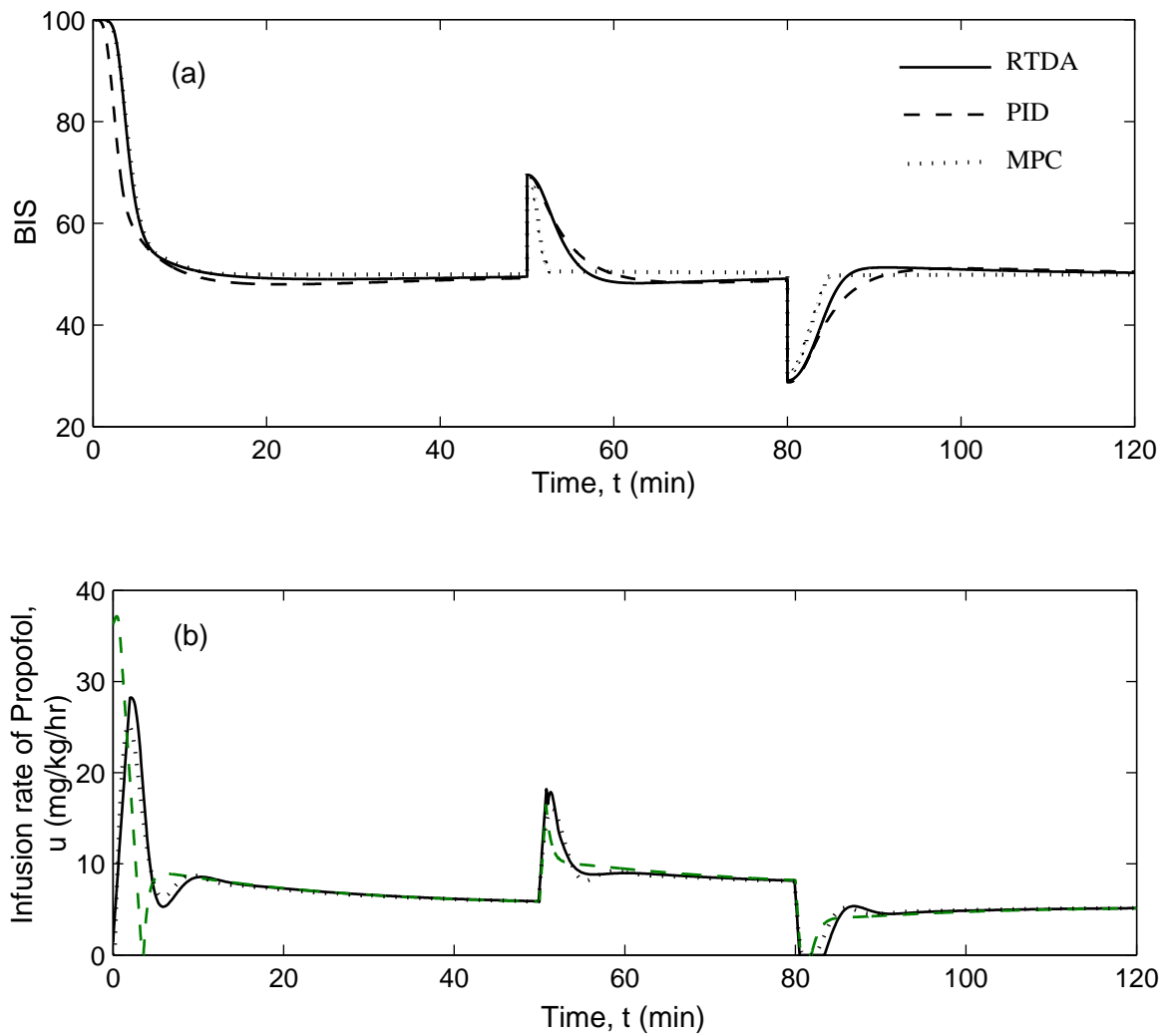


Fig. 5.28. Performance of the RTDA, MPC and PID controllers for disturbance during the surgery

the nominal patient. Figure 5.28(a) shows the BIS signal (BIS set-point = 50) and Figure 5.28(b) shows the propofol infusion rate profile. Here also, the performance of RTDA controller (IAE = 403) is slightly better than MPC (IAE = 407) performance. The PID controller performs poorly (IAE = 450) compared to RTDA and MPC.

5.6 Conclusions

In this chapter, three advanced control strategies (model predictive control, internal model control, controller with modeling error compensation) for regulation of hypnosis using BIS as the controlled variable have been evaluated thoroughly. The performance of these controllers are considered along with the performance of the conventional PID controller. In comparison with the PID controller, the advanced, model-based controllers are found to be robust to inter-patient variability, better at handling disturbances and measurement noise. Even though the performance of the MEC controller is approximately equal to the MPC controller's performance, the noise in the BIS signal causes excessive fluctuations in the valve movement with the MEC controller and is not acceptable for surgical applications. The performance of the IMC controller is less than that of MPC and MEC controllers, but there is very small movement of the control valve with this controller. Among the four controllers, the MPC is found to perform the best. Finally, the performance of MPC and PID controllers is compared with the novel RTDA controller. The RTDA controller performs significantly better than the PID controller and does slightly better than the MPC controller in regulating hypnosis when tested on patient models. It also appears to be robust to variation in patient parameters.

Chapter 6

SIMULTANEOUS REGULATION OF HYPNOSIS AND ANALGESIA USING MODEL PREDICTIVE CONTROL

6.1 Introduction

The objective of this chapter is to design and thoroughly evaluate, through simulation, a model predictive controller (MPC) for optimal infusion rates of both hypnotic and analgesic drugs such that the patient's hypnotic and analgesic states (measured by BIS and MAP, respectively) are well regulated and the side effects (due to over-dosage) are minimized. The present study is the first one on two-input two-output MPC of BIS and MAP using propofol and remifentanyl. Manual administration of neuromuscular blocking drug is assumed for the skeletal muscle relaxation. Extensive simulations are conducted to test the robustness of the proposed controller, by considering parameter variations in the PK and PD models (to account for patient-model mismatch) and typical set-point changes and disturbances during surgical operations. Results show that the MPC provides better performance in comparison with two (decentralized) PID controllers.

The chapter is organized as follows. Section 6.2 includes the description of the modeling of BIS response to infusion of propofol & remifentanyl and MAP response to infusion of remifentanyl. Section 6.3 includes the detailed description of MPC and PID control structures used in this chapter. Section 6.4 includes the tuning of controllers, and the evaluation of performances for MPC and PID controllers for the set-point changes and disturbances that may occur during the surgery. Individual

differences in model parameters are also considered to evaluate the performance of controllers in handling inter-patient variability.

6.2 Modeling Hypnosis and Analgesia

The model used for BIS and MAP responses to propofol/remifentanyl consists of two interacting parts: a PK model for estimating the distribution of propofol/remifentanyl in the internal organs, and a PD model to describe the effect of propofol/remifentanyl on the measured physiological variables, *i.e.*, BIS and MAP. Figure 6.1 is a schematic of the system comprising of propofol/remifentanyl delivery circuit, and the PK & PD models. Note that, propofol affects BIS only, whereas remifentanyl affects both BIS and MAP. In this figure, subscripts 'p' and 'r' refer to the respective variables for propofol and remifentanyl.

For the distribution of the drug (propofol or remifentanyl), a linear mammillary three-compartmental PK model is adopted from the literature (Schwilden et al. 1989). The central compartment, V_1 , represents blood plasma in which drug dissolves and is carried to the other compartments. Also, because of the drug metabolism in the body, elimination of the drug from the central compartment is assumed. The second compartment is a shallow peripheral compartment, V_2 , which is characterized by a very rapid movement of the drug from the plasma to this compartment. This is the characteristic of certain tissues which are highly perfused (*i.e.*, vessel-rich tissues). The third compartment is a deep peripheral compartment, V_3 , which is characterized by a slow distribution of the drug from the central compartment to this compartment. This is because of the equilibration of the blood with tissues which are less perfused.

The PK part assumes that all compartments (Figure 6.1) have a zero initial concentration of the drug (propofol or remifentanyl). To achieve rapid target plasma drug concentration (*i.e.*, concentration in V_1), sufficient drug must be given as a

bolus dose. If the plasma drug concentration is to be kept constant, the amount of drug entering and leaving the central compartment must be equal. Drug leaves the blood (V_1) to pass into V_2 and V_3 at a gradually decreasing rate as the concentrations in these compartments increase. Drug also leaves the blood because it is metabolized (mainly in the liver) (Marsh et al. 1991). The PD part assumes some lag between the infusion of drug in the bloodstream and its distribution to corresponding tissues (brain or nerve) before affecting the hypnosis and analgesia levels. This effect on hypnosis level is represented by a nonlinear equation, and on analgesia level by a linear equation relating the state variables and other system variables to BIS and MAP, respectively.

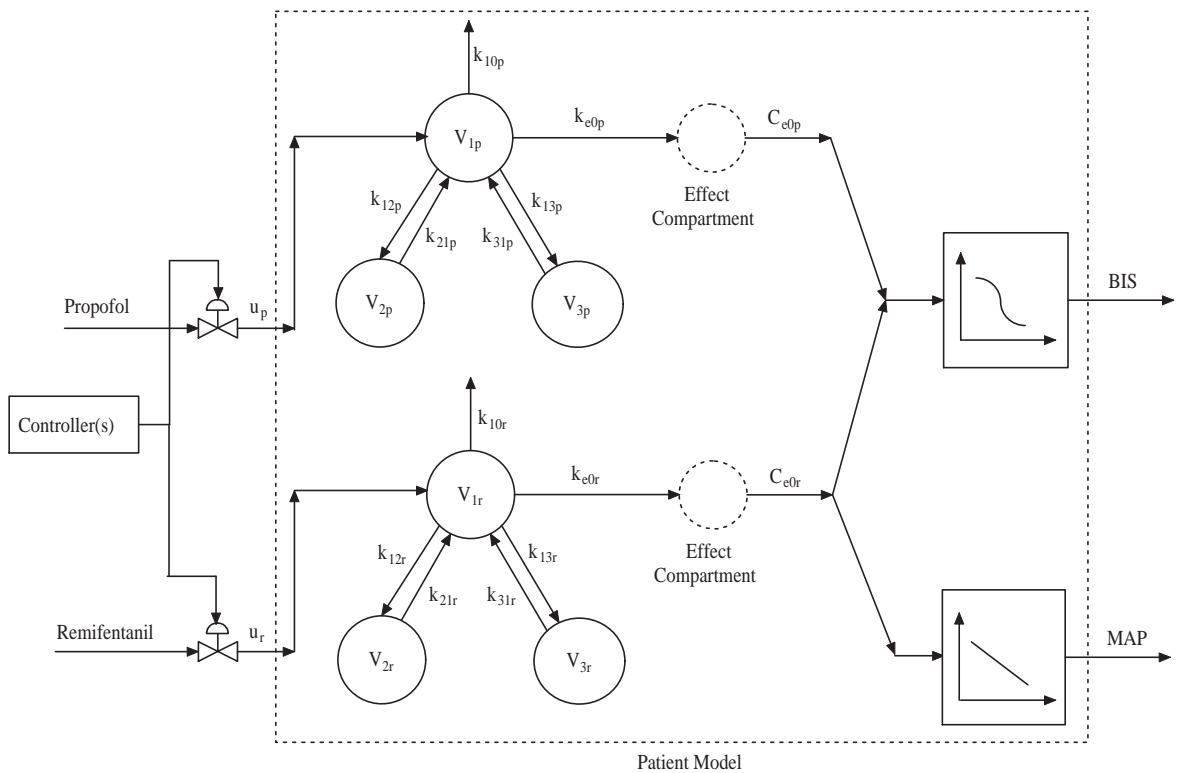


Fig. 6.1. Schematic representation of propofol and remifentanyl delivery circuit with PK and PD models

6.2.1 Pharmacokinetic model

Figure 6.1 shows the PK model for distribution of drug (propofol/remifentanil) which is described by mass balances around each of the three compartments. The main assumptions here are that the central compartment is a well mixed tank with the plasma propofol/remifentanil concentration uniform everywhere, and the distribution of these drugs are not affected by the presence of other drugs. Hence, the resulting mass balance for propofol/remifentanil in the central compartment is given by equation (6.1).

$$\frac{dC_1}{dt} = \sum_{j=2}^3 \left(k_{j1} C_j \frac{V_j}{V_1} - k_{1j} C_1 \right) - k_{10} C_1 + \frac{\rho}{\alpha V_1} U \quad (6.1)$$

Here, C_1 , C_2 and C_3 are concentrations of the drug (propofol, $\mu\text{g}/\text{ml}$, or remifentanil, ng/ml) in the first (central), second and third compartments, respectively; V_1 , V_2 and V_3 are the respective volumes (ℓ); k_{12} , k_{13} , k_{21} and k_{31} are the mammillary rate constants (min^{-1}) of the respective compartments, k_{10} is the hepatic metabolism rate constant representing the elimination rate of drugs from the patient (min^{-1}); $\rho = 10$ (mg/ml) and 5×10^2 ($\mu\text{g}/\text{ml}$) are the available propofol and remifentanil concentrations, respectively; normalization constant, $\alpha = 60$ (min/hr) for propofol and 1 (min/min) for remifentanil; and U is the infusion rate of propofol in ml/hr and remifentanil in ml/min . Clinically, infusion rates of propofol, u_p and remifentanil, u_r are expressed in $\text{mg}/\text{kg}/\text{hr}$ and $\mu\text{g}/\text{kg}/\text{min}$ (normalized drug infusion rates with respect to patient's body weight), respectively. To convert U to u_p in $\text{mg}/\text{kg}/\text{hr}$ and u_r in $\mu\text{g}/\text{kg}/\text{min}$, it is multiplied by respective $\frac{\rho}{w}$, where w is the weight of the patient in kg . Similarly, for the second and third compartments, the corresponding mass balance is given by:

$$\frac{dC_j}{dt} = k_{1j} C_1 \frac{V_1}{V_j} - k_{j1} C_j, \quad j = 2, 3 \quad (6.2)$$

The PK model parameters provided by Marsh et al. (1991) are used for propofol and those by Minto et al. (1997) are used for remifentanil. As equations (6.1) and (6.2) refers to both propofol and remifentanil, indexes 'p' and 'r' are omitted to avoid or minimize notation overload. Table 6.1 shows the PK parameters for propofol and remifentanil mentioned in equations (6.1) and (6.2) for a 34 year old person weighing 66 kg.

Table 6.1
Rate constants and volumes of the different compartments (Marsh et al. 1991, Minto et al. 1997) of the PK model

Parameter	Drug	
	Propofol	Remifentanil
$k_{10}(min^{-1})$	0.1190	0.509
$k_{12}(min^{-1})$	0.1120	0.362
$k_{21}(min^{-1})$	0.0550	0.195
$k_{13}(min^{-1})$	0.0419	0.013
$k_{31}(min^{-1})$	0.0033	0.014
$V_1 (\ell)$	15.050	4.409
$V_2 (\ell)$	30.600	8.184
$V_3 (\ell)$	191.10	4.323

6.2.2 Pharmacodynamic interaction model for BIS response to propofol and remifentanil

The above PK model is limited to the representation of distribution kinetics of propofol and remifentanil into different compartments. A PD model is required to calculate the effect of each drug on the anesthetic level. The detailed description of the PD model is provided in sections 3.2.3 and 5.2.2.

The nominal values of the parameters, $k_{e0p} = 0.349 \text{ min}^{-1}$, $EC_{50p} = 2.65 \text{ } \mu\text{g/ml}$ and $\gamma_p = 2.561$ for propofol (Sartori et al. 2005) and $k_{e0r} = 0.516 \text{ min}^{-1}$, $EC_{50r} = 11.2 \text{ ng/ml}$ and $\gamma_r = 2.51$ for remifentanyl (Minto et al. 1997) are obtained from the pooled analysis.

The model represented in equation (5.4) is limited to denote the individual effect of each drug on BIS response. To represent the effect of combination of synergistically interacting drugs on BIS response, an interaction model is needed. Minto et al. (2000) described an approach based on response surface methodology for characterizing drug-drug interactions between several intravenous anesthetic drugs. This model can characterize the entire dose-response relation between combinations of anesthetic drugs and is mathematically consistent with models of the concentration-response relation of single drugs. Nieuwenhuijs et al. (2003) also used this methodology to investigate propofol-remifentanyl interaction on cardiorespiratory control and BIS and concluded that the model can capture the synergistic interaction between these two drugs. The interaction model developed by Minto et al. (2000), which is also supported by Bruhn et al. (2003), considered in this study is described below.

Initially, the concentrations were normalized to their respective potencies, *i.e.*, the effect concentration at half the maximal effect:

$$U_p = \frac{Ce_p}{EC_{50p}}, \quad U_r = \frac{Ce_r}{EC_{50r}} \quad (6.3)$$

where Ce_p and Ce_r are the respective effect-site concentrations of propofol and remifentanyl. The additive interaction is represented with the “effective” concentration, which is normalization of sum of individual concentrations and is described in equation (6.4).

$$\text{BIS} = \text{BIS}_0 \left(1 - \frac{U_p + U_r}{1 + U_p + U_r} \right) \quad (6.4)$$

Deviation from a purely additive interaction is modeled by changing the potency of the drug mixture depending on the ratio of the interacting drugs. This gives

$$\theta = \frac{U_p}{U_p + U_r} \quad (6.5)$$

By definition, θ ranges from 0 (remifentanil only) to 1 (propofol only). Thus, the concentration-response relationship for any ratio of the two drugs can be described as

$$\text{BIS} = \text{BIS}_0 \left(1 - \frac{\left(\frac{U_p + U_r}{U_{50}(\theta)} \right)^{\gamma(\theta)}}{1 + \left(\frac{U_p + U_r}{U_{50}(\theta)} \right)^{\gamma(\theta)}} \right) \quad (6.6)$$

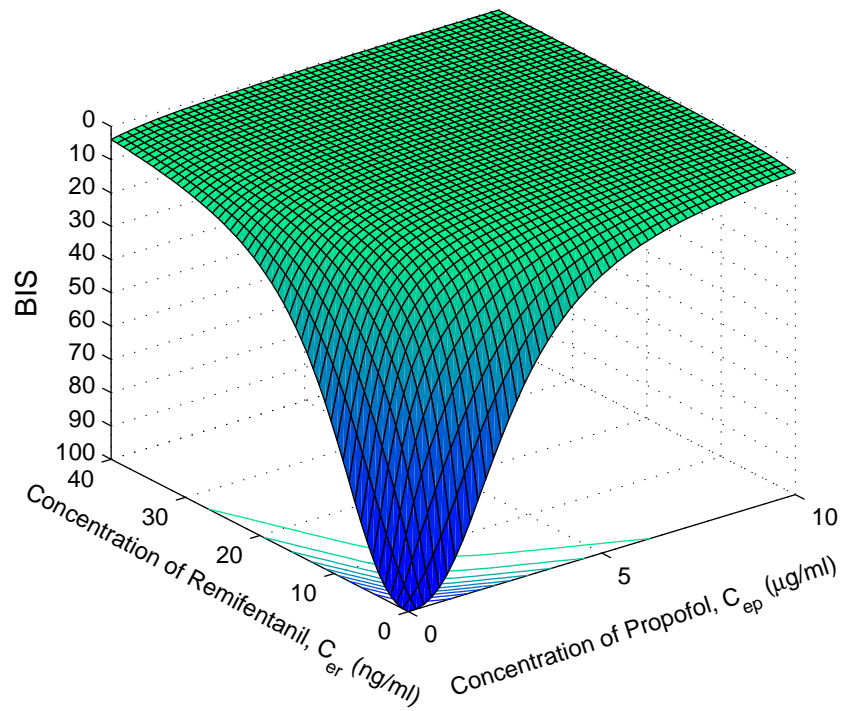
where $\gamma(\theta)$ is the steepness of the concentration-response relation, and $U_{50}(\theta)$ is the number of units (U) associated with 50% of maximum effect at ratio θ . According to Minto et al. (2000), the equation for potency as a function of θ can be simplified to a quadratic polynomial:

$$U_{50}(\theta) = 1 - \beta_{2,U_{50}}\theta + \beta_{2,U_{50}}\theta^2 \quad (6.7)$$

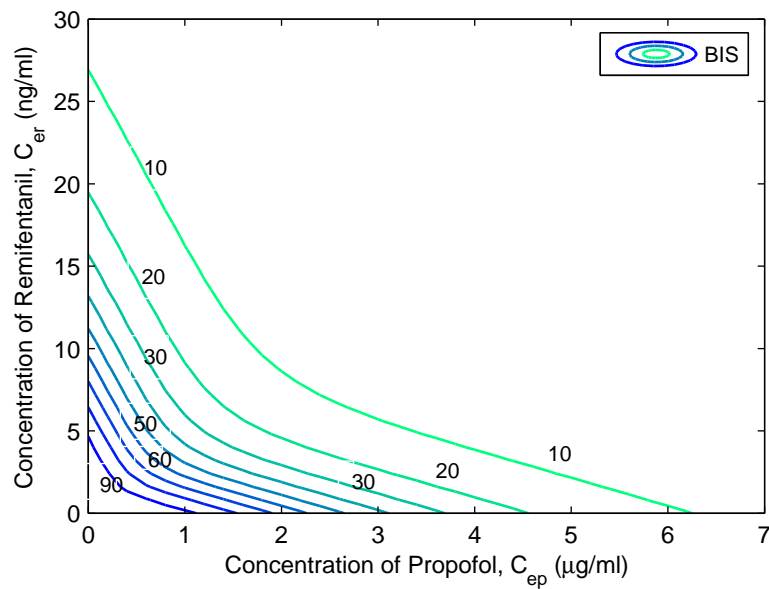
The value of $\beta_{2,U_{50}}$ obtained according to Bruhn et al. (2003) is 1.44. The model for the steepness term, $\gamma(\theta)$ can be described as

$$\gamma(\theta) = \gamma_r + (\gamma_p - \gamma_r)\theta \quad (6.8)$$

Figure 6.2(a) is the response surface plot, where the left and rightmost edges of the surface are the individual sigmoid concentration-response relation for remifentanil and propofol, respectively. Figure 6.2(b) shows the sigmoid concentration-response relation for different ratios of propofol and remifentanil. From Figure 6.2, it is evident that the PD interaction between propofol and remifentanil is very nonlinear (Glass 1998).



(a) Response Surface Plot



(b) Contour Plot

Fig. 6.2. Nonlinear PD interaction between propofol and remifentanyl

6.2.3 Pharmacodynamic model for MAP response to remifentanyl

Skin incision and intubation during the surgery may increase MAP. These MAP changes must be minimized during surgery by infusing sufficient amount of opiate. The success of closed-loop control of MAP lies in the use of reliable models in controller design (Furutani et al. 1995). The PK model for distribution of remifentanyl is described earlier. A PD model that relates effect-site concentration of remifentanyl to MAP is not available in the literature. Hence, based on the MAP responses obtained with remifentanyl infusion (Warner et al. 1996, Doyle et al. 2001) and also from the information obtained for other similar opioids (Gentilini et al. 2002) which are closely related to remifentanyl, a linear model between effect-site concentrations of remifentanyl and MAP is assumed with a negative gain equivalent to $-0.1762 \text{ mmHg}/(\text{ng/ml})$. The sign of the gain guarantees that the infusion rate will decrease when MAP is low and increase when MAP is high.

6.3 Controllers Studied

Design of model predictive and decentralized PID control strategies for the regulation of hypnosis and analgesia are described briefly in this section.

6.3.1 Model predictive controller (MPC)

The MPC scheme for simultaneous regulation of hypnosis and analgesia is shown in Figure 6.3. The detailed description of the MPC scheme is provided in section 3.4.4. The patient model is used to predict the current values of the output variables (BIS and MAP). The difference between measured outputs from the patient and the respective model outputs are called residuals, and serves as feedback signal to the prediction block. The predictions are used in control calculations subject to suitable constraints on the inputs u_p & u_r and output variables BIS & MAP. That is, the

control calculations are based on the current measurements and predictions of the future values of outputs.

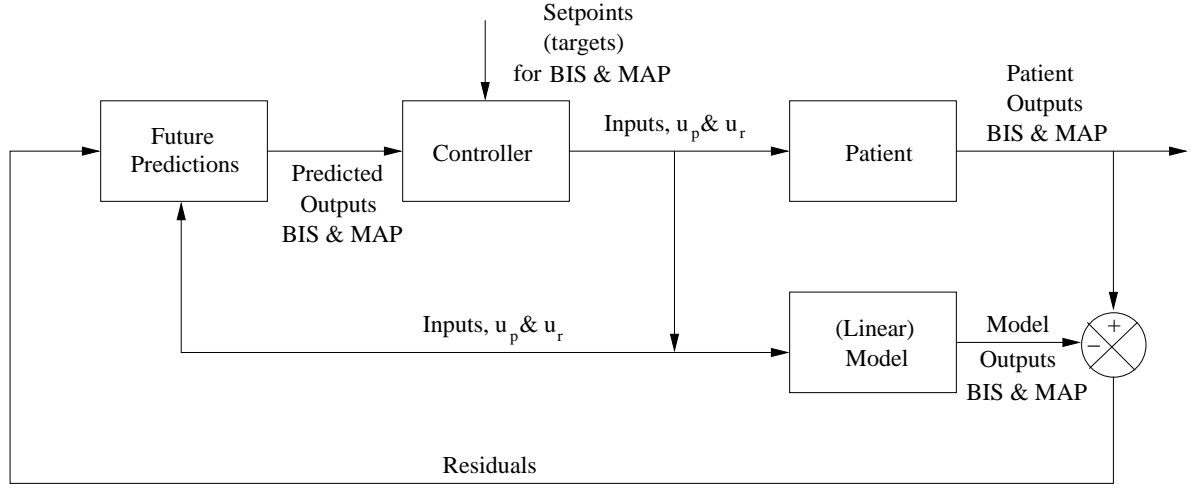


Fig. 6.3. Schematic representation of the MPC scheme for simultaneous regulation of BIS and MAP

The expression for quadratic objective function for the MPC scheme is

$$\min_{\Delta u_k, \Delta u_{k+1}, \dots, \Delta u_{k+M-1}} J(P, M) = \sum_{i=k+1}^{k+P} e_i^T S e_i + \sum_{i=k}^{k+M-1} \Delta u_i^T R \Delta u_i \quad (6.9)$$

subject to absolute and rate constraints on the manipulated variables

$$\begin{aligned} u_{min} &\leq u_i \leq u_{max} && \text{(for } i = k, k+1, \dots, k+M-1) \\ u_{i-1} - \Delta u_{max} &\leq u_i \leq u_{i-1} + \Delta u_{max} && \text{(for } i = k, k+1, \dots, k+M-1) \end{aligned}$$

where, at each sampling instant i , $\Delta u_i = u_{i+1} - u_i$ is the vector of manipulated variable deviations, $e_i = r_i - y_i$ is the vector of model predicted errors, r_i is the desired set-point, y_i is the vector of predicted future values of BIS and MAP. The length of these vectors depends on the prediction (output) horizon P . Also, S and R are the diagonal weighting matrices for outputs (BIS and MAP) and variation in inputs (propofol and remifentanil infusion rates, u_p and u_r), respectively. These weighting matrices can be used to tune the MPC controller to achieve the desired tradeoff between output performance and manipulated variable movement. The

prediction horizon P is chosen on the basis of open-loop settling time whereas control horizon M is chosen based on the tradeoff between faster response (large value of M) and robustness (small value of M). Generally, the chosen value for M will be very small compared to P .

A linear MPC requires an internal linear time-invariant model (e.g., a linear step response model) to estimate the future output values using the past and future values of the inputs (Seborg et al. 2004). Here, the overall dynamic system for the patient model is a combination of the propofol and remifentanil infusion systems, and the PK & PD models as depicted in Figure 6.1. The propofol and remifentanil infusion systems and the corresponding PK models are modeled as linear time invariant systems arranged in series. The nonlinear PD interaction model which is linearized at specific operating points (say BIS at 50 and MAP at 80) is then cascaded to this system to get the overall linear representation in state-space form. The combined state-space model is given in equation (6.10).

$$\begin{aligned} \dot{x} &= Ax + Bu \\ y &= Cx \end{aligned} \tag{6.10}$$

where, $x = \left[C_{1p} \ C_{2p} \ C_{3p} \ C_{ep} \ C_{1r} \ C_{2r} \ C_{3r} \ C_{er} \right]^T$

$$A = \begin{bmatrix} -k_{1p} & k_{21p} \frac{V_{2p}}{V_{1p}} & k_{31p} \frac{V_{3p}}{V_{1p}} & 0 & 0 & 0 & 0 & 0 \\ k_{12p} \frac{V_{1p}}{V_{2p}} & -k_{21p} & 0 & 0 & 0 & 0 & 0 & 0 \\ k_{13} \frac{V_{1p}}{V_{3p}} & 0 & -k_{31p} & 0 & 0 & 0 & 0 & 0 \\ k_{e0p} & 0 & 0 & -k_{e0p} & 0 & 0 & 0 & 0 \\ 0 & 0 & 0 & 0 & -k_{1R} & k_{21r} \frac{V_{2r}}{V_{1r}} & k_{31r} \frac{V_{3r}}{V_{1r}} & 0 \\ 0 & 0 & 0 & 0 & k_{12r} \frac{V_{1r}}{V_{2r}} & -k_{21r} & 0 & 0 \\ 0 & 0 & 0 & 0 & k_{13} \frac{V_{1r}}{V_{3r}} & 0 & -k_{31r} & 0 \\ 0 & 0 & 0 & 0 & k_{e0r} & 0 & 0 & -k_{e0r} \end{bmatrix}$$

where, $k_{1p} = k_{10p} + k_{12p} + k_{13p}$, and $k_{1R} = k_{10r} + k_{12r} + k_{13r}$

$$B = \begin{bmatrix} \frac{\rho_p}{\alpha_p V_{1p}} & 0 & 0 & 0 & 0 & 0 & 0 & 0 \\ 0 & 0 & 0 & 0 & \frac{\rho_r}{\alpha_r V_{1r}} & 0 & 0 & 0 \end{bmatrix}^T, \quad C = \begin{bmatrix} 0 & 0 & 0 & k_{mp} & 0 & 0 & 0 & k_{mr1} \\ 0 & 0 & 0 & 0 & 0 & 0 & 0 & k_{mr2} \end{bmatrix}$$

$$u = \begin{bmatrix} u_p & u_r \end{bmatrix}^T \text{ and } y = \begin{bmatrix} BIS & MAP \end{bmatrix}^T$$

where k_{mp} and k_{mr1} are the linearization constants with respect to BIS and k_{mr2} is the linearization constant with respect to MAP. The above continuous state-space model is converted to discrete time finite step response (FSR) model for designing the MPC controller (Seborg et al. 2004).

6.3.2 Proportional-integral-derivative (PID) controller

Figure 6.4 shows the schematic representation of the two decentralized PID controllers for the simultaneous regulation of hypnosis and analgesia. The detailed description of the PID controller scheme is provided in section 5.3.1. Here also, the PID parameters are obtained via optimization so as to get the best performance with the decentralized control structure.

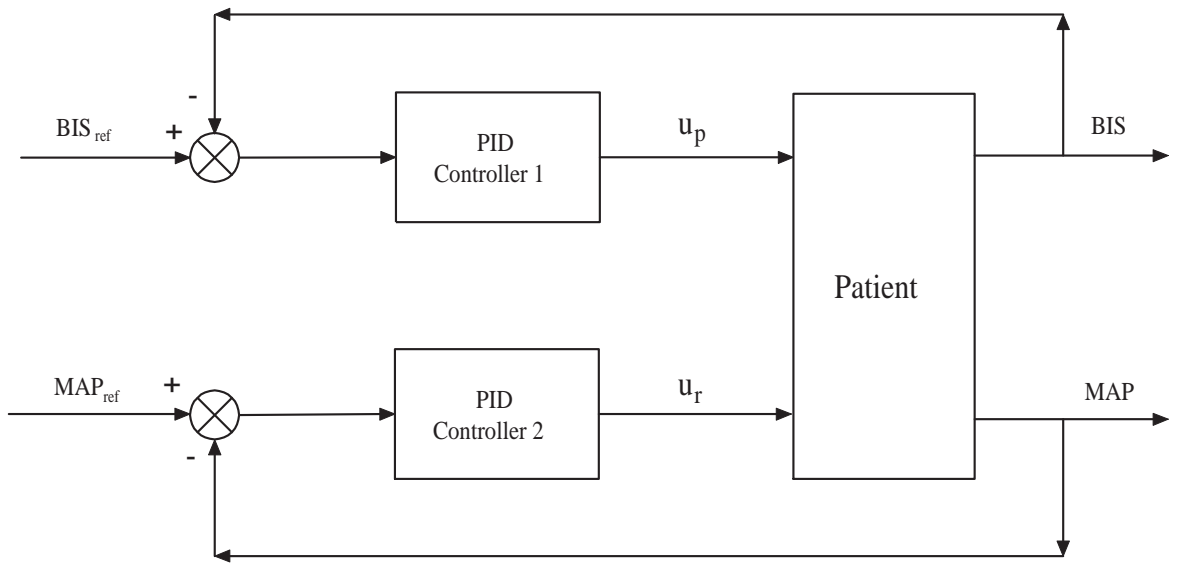


Fig. 6.4. Schematic representation of the PID controller scheme for simultaneous regulation of BIS and MAP

6.4 Results and Discussion

This section provides the simulation results of the multi input-multi output (MIMO) MPC and two single input-single output (SISO) PID controllers (decentralized) for the control of BIS and MAP by simultaneous regulation of propofol and remifentanyl. Tuning of the MPC and decentralized PID controllers is first presented. Later, the performance of the two controllers will be evaluated and compared in terms of ability to handle uncertainty in the model parameters, set-point tracking, and rejection of disturbances, all in the presence of measurement noise. Integral of the absolute error (IAE) and control effort are employed as the metrics for performance evaluation.

The controller has to maintain BIS between 40 and 60 during the surgery (Ekman et al. 2004). Initially, it is assumed that the patient is in a fully conscious state (BIS \approx 100) and average MAP is at 100 mm Hg. Then, the controller is turned on and the set-point of BIS is changed from 100 to 50 and MAP from 100 to 80. This brings the patient to the surgical operating range ($40 \leq \text{BIS} \leq 60$ & $70 \leq \text{MAP} \leq 110$) that must be maintained for the duration of the surgery. The set-point for MAP is kept at a lower value to reduce the blood loss and to compensate the sudden increase in blood pressure. The predicted C_{1p} must be between $0.5 \mu\text{g/ml}$ and $5 \mu\text{g/ml}$ and C_{1r} between 0.5ng/ml and 10ng/ml (clinically acceptable ranges) (Absalom et al. 2002); note that these are not measured and they are estimated using the nominal patient model. The lower bound guarantees a minimum delivery of the drug, whereas the upper bound prevents overdosing of the drug for an average subject. It is important to maintain C_{1r} within the limits because remifentanyl is hemodynamically stable and increasing its concentration in the plasma may not decrease MAP unlike C_{1p} which directly affects BIS response.

The manipulated variables u_p and u_r (propofol and remifentanyl infusion rates) are restricted between 0 and 20 $mg/kg/hr$ (Sawaguchi et al. 2008) and from 0 to 1 $\mu g/kg/min$ (Struys et al. 2001), respectively. The upper bound is needed because higher propofol and remifentanyl infusions lead to faster increase of drug concentrations in the subject's body and may lead to hypnotic crisis, cardiac arrhythmia, or even cardiac arrest. The minimum bound on u_p and u_r reflects the impossibility of administering negative concentrations of propofol and remifentanyl. It is very important to maintain the drug concentrations and infusion rates within the acceptable limits, and the designed controller should not violate these constraints. The control execution interval is set as 5 *sec* which is also the sampling time for BIS and the same is assumed for MAP also.

6.4.1 Tuning of controllers

This section begins with the discussion on the design and tuning of MPC for the nominal patient model (parameters mentioned in section 6.2). The tuning parameters in the MPC are: M , the input horizon; P , the prediction horizon; S_1 , the weighting coefficient for BIS; S_2 , the weighting coefficient for MAP; R_1 , the weighting coefficient for propofol rate; and R_2 , the weighting coefficient for remifentanyl rate (to penalize the large changes in u_p and u_r). The prediction horizon P is chosen as 30 sampling intervals and the control horizon M is chosen as 2 sampling intervals. Simulations showed that further increase in P does not affect the performance of the controller, and hence it is fixed at that value. Also, very low value of M is chosen (relative to P) because the closed-loop system should be robust and also expect fast closed-loop response. Because the safe regulation of hypnosis and analgesia levels are very crucial during the surgery, the constraints imposed on the inputs will be hard constraints *i.e.*, at any time controller should not violate these limits. At the same time, smooth control action would be required to avoid sudden large fluctuations in control valve movement. Hence, to avoid problems associated with

the constraints, the controller tuning weights should be chosen carefully. Table 6.2 shows the performance of the MPC with different weights on the measured output variables and on the input rates. Here, IAE values are calculated for time, $t = 0 - 50$ min based on equation (3.26). Another measure of the controller performance, the required control effort is computed by calculating the total variation (TV) of the manipulated input, u given by equation (3.31). The TV of $u(t)$ is the sum of all up and down control moves. Thus, it is a good measure of the smoothness of the manipulated input signal. It is desired that TV be as small as possible.

Table 6.2
Tuning Parameters

Weights		Performance			
R_1	R_2	IAE _{BIS}	IAE _{MAP}	TV _P	TV _R
0	0	176	82	20.29	1.36
1	0	214	82	14.10	1.36
0	1	196	102	21.56	0.93
1	1	221	102	13.88	0.93
0.2	0.6	196	91	21.10	1.21
0.6	0.2	202	83	15.93	1.33
0.5	0.5	196	89	17.41	1.24

The performance of the MPC controller for different tuning weights on the output variables and input variable rates are depicted in Figure 6.5. Plots (a) and (b), respectively show the transient responses of BIS and MAP and plots (c) and (d), respectively show the infusion rates of propofol and remifentanyl. Equal preference has been given for the control of BIS and MAP by keeping equal weights ($S_1 = S_2 = 1$) on each of these variables. Next, tuning has been done by varying the weights on input rates (R_1 and R_2). From all these plots, one can observe that, if weights on input rates are low, performance is good (lower IAE) but control effort

is more (higher TV). Also, if weights on input rates are high, performance is poor (higher IAE) but control effort is less (lower TV). By compromising between these contradicting situations, equal medium value on weights are chosen for each input rate (*i.e.*, $R_1 = R_2 = 0.5$).

Next, the tuning of the two decentralized PID controllers are discussed here. Each PID controller infuses the respective drug (either propofol or remifentanyl) based on BIS and MAP levels. The two PID controllers are simultaneously tuned for minimizing IAE and control effort (TV) with respect to BIS and also to MAP for time, $t = 0 - 50 \text{ min}$ based on equations (3.26) and (3.31) by using direct search optimization algorithm. The final tuned settings for the two PID controllers are given in Table 6.3. Also, plots (a) and (b) in Figure 6.6 show the transient responses of BIS and MAP and plots (c) and (d), respectively show the infusion rates of propofol and remifentanyl. By considering the performance (minimum IAE) of both the PID controllers, setting 3 is selected for the remaining performance evaluations. Also, for the selected PID settings, IAE values are comparable with the values of the selected MPC controller so that a fair comparison can be made between MPC and decentralized PID.

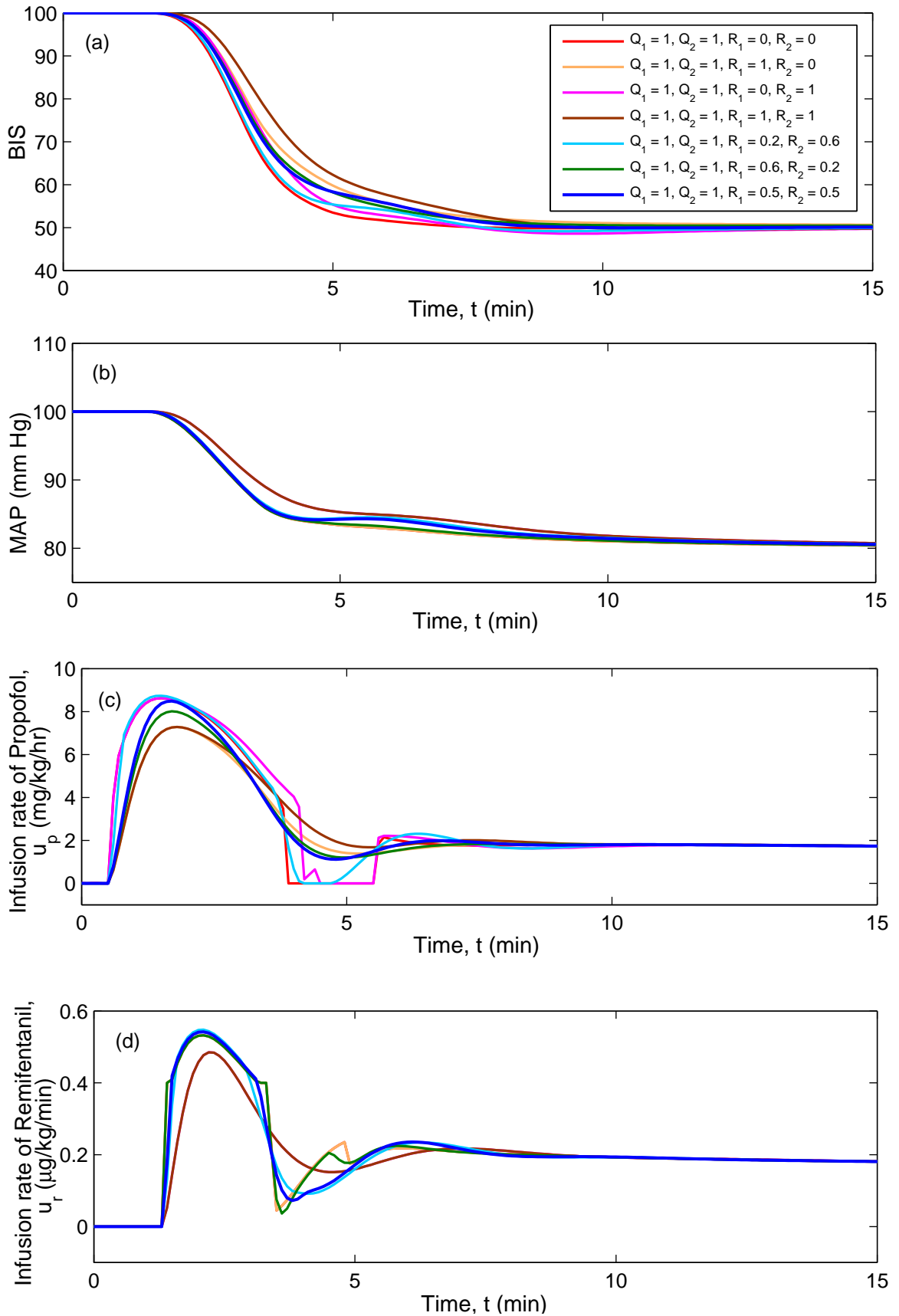


Fig. 6.5. Performance of the MPC controller for different weights (see Table 6.2)

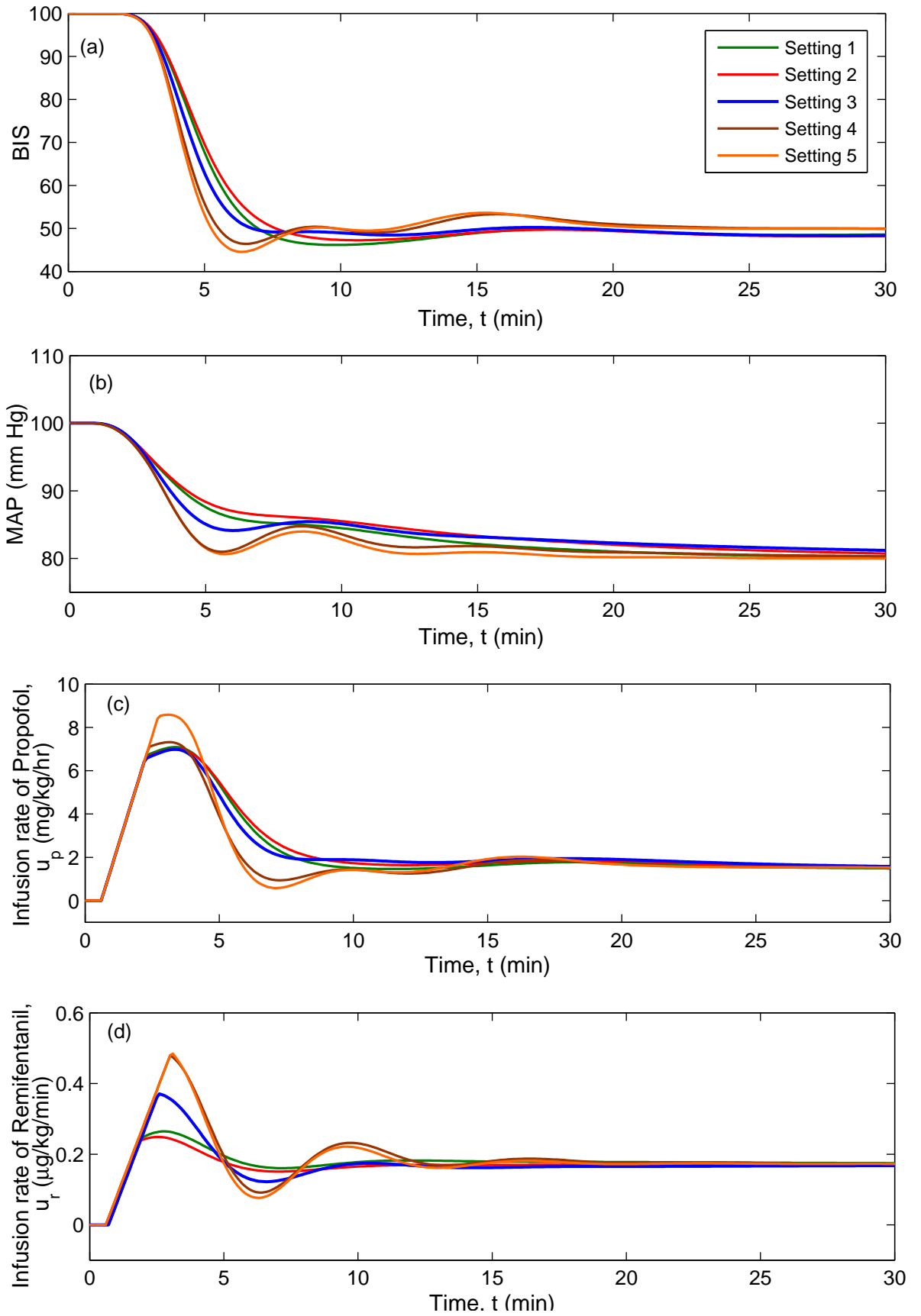


Fig. 6.6. Performance of the decentralized PID controller for different tuning parameters (see Table 6.3)

Table 6.3
Decentralized PID controller settings

Setting	PID Controller 1			PID Controller 2			Performance			
	K_c	τ_I	τ_D	K_c	τ_I	τ_D	IAEBIS	IAEMAP	TVP	TVR
1	-0.8225	11.9723	0.0228	-0.2327	7.1600	0.2037	220	110	16.9	1.95
2	-0.8141	12.2421	0.0254	-0.2147	9.2543	0.1439	226	115	15.8	1.74
3	-0.9051	11.1192	0.0198	-0.2589	6.9225	0.0263	201	91	18.7	2.2
4	-0.8815	15.6294	0.0000	-0.4619	6.4153	0.0000	210	97	17.8	1.98
5	-1.0459	17.5782	0.0004	-0.4570	9.8704	0.0138	232	110	14.6	1.94

6.4.2 Performance of MPC and PID for step type set-point changes in BIS and MAP during surgery

Set-point changes in BIS and blood pressure are often made depending on the surgical procedure being performed (Doyle et al. 2007). Anesthesiologist can anticipate the periods that would require more stimulation and also the periods in which light sedation is required during the surgery. For example, if surgical stimulation is severe at any time during the surgical process, the patient needs to be more unconscious and hence the BIS value should be decreased to some lower value (e.g., 40). Similarly, surgical stimulation increases the blood pressure, and hence it should be compensated by decreasing the set-point for MAP. Afterwards, towards the end of the surgery, the patient needs to be less unconscious and BIS set-point may be increased, say from 40 to 70. Table 6.4 shows the set-point changes and their time of introduction for BIS and MAP. Also, these two signals are generally corrupted by measurement noise, which might come from the high impedance of

Table 6.4
Series of intraoperative set-point changes for BIS and MAP

Time (<i>min</i>)	BIS Set-Point Change	MAP Set-Point Change (<i>mm Hg</i>)
30	50 to 40	–
60	40 to 50	–
90	–	80 to 70
120	–	70 to 80
150	50 to 60	–
180	–	80 to 90
210	60 to 70	90 to 100

the electrodes, corruption of the EEG and MAP with the electromyography (EMG) signal etc. Hence, to simulate the realistic situations, 2% Gaussian noise is added to BIS and MAP signals.

The performance of designed MPC controller is compared with the performance of decentralized PID controllers designed separately for regulation of BIS and MAP. The responses obtained with the two controllers are compared in Figures 6.7 and 6.8 for the set-point changes mentioned in Table 6.4, for the nominal PK-PD model parameters described in section 6.2. Because of unavailability of plasma propofol and remifentanil concentrations (C_{1p} and C_{1r}), they are predicted using the nominal (and not the actual) patient model. To reduce the variation in the manipulated variable (*i.e.*, to reduce valve movements) because of noise in BIS and MAP, these signals were passed through filters with a time constant of 1 *min* each. The IAE and TV values are calculated for the maintenance period $t = 30 - 280$ *min* and are given in Table 6.5. Hence, for the nominal patient, the IAE values for both controllers are comparable although control effort with the PID controller is high for both the drugs compared to MPC. This is because, although MPC is aggressive compared to decentralized PID, noise in BIS and MAP signals caused the higher variation in propofol and remifentanil infusions with decentralized PID compared to MPC.

Table 6.5
Performance of MPC and PID for nominal patient for the set-point changes during the maintenance period

Controller	IAE _{BIS}	IAE _{MAP}	TV _P	TV _R
MPC	808	295	28.1	2.67
PID	815	307	34.5	6.20

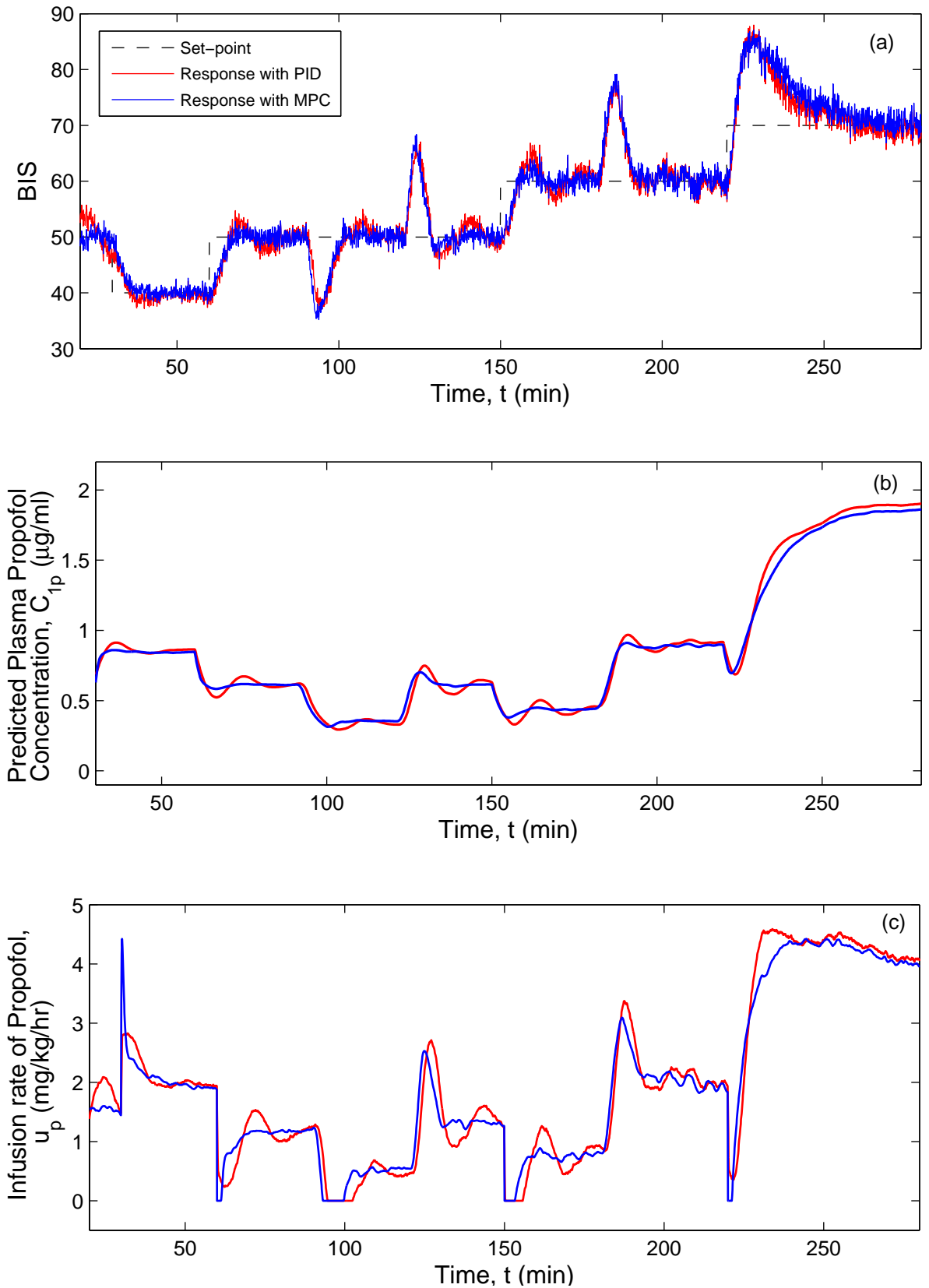


Fig. 6.7. Performance of MPC and PID controllers for set-point changes during the maintenance period $t = 30 - 280$ min: BIS, predicted propofol concentration in the plasma and propofol infusion rate

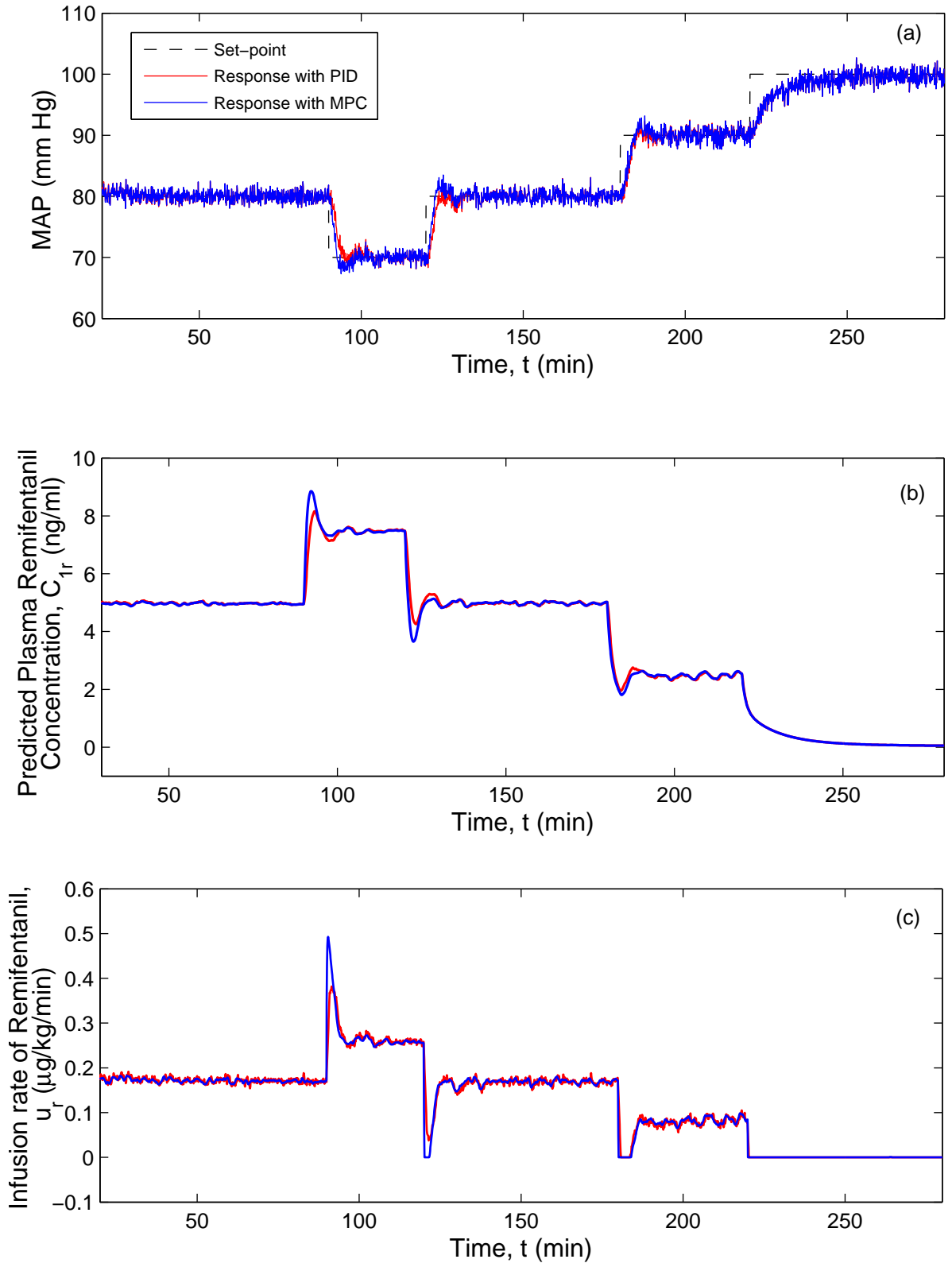


Fig. 6.8. Performance of MPC and PID controllers for set-point changes during the maintenance period $t = 30 - 280$ min: MAP, predicted remifentanyl concentration in the plasma and remifentanyl infusion rate

Next, tests are conducted to check if these two controllers (MPC and decentralized PID) are able to meet performance specifications despite significant and reasonable variation in the model parameters (inter-patient variability) based on PK-PD model described in section 6.2. Here, assumption is that variability is in both the PK (based on age and weight) and PD (based on patient's sensitivity to the drug) model parameters. There is a variation of 25% in PK model parameters (Schttler & Ihmsen 2000) and a possible range of PD parameters for both the drugs (Schnider et al. 1999). Open-loop simulation studies showed that the variability in PD parameters have more impact on BIS than the variability in PK parameters. Also, volumes of the compartments (V_{1p} , V_{2p} , V_{3p} , V_{1r} , V_{2r} and V_{3r}) have negligible effect on the BIS performance. Hence, the remaining PK parameters (k_{10p} , k_{12p} , k_{21p} , k_{13p} , k_{31p} , k_{10r} , k_{12r} , k_{21r} , k_{13r} and k_{31r}) are assumed to vary over three levels (minimum, average, maximum) and are given in Table 6.6. This gave, $3^{10} = 59049$ combinations of patients and closed-loop simulations with MPC for the maintenance period are carried out for these patients. Simulations showed that IAE values varied from 831 to 1049. Hence, from these 59049 combinations, 12 parameter sets which span the entire IAE range were selected. With these 12 parameter sets, 7 PD parameters were varied in 3 levels and this gave $12 \times 3^7 = 26244$ combinations of patients. Closed-loop simulations with MPC controller showed that IAE values varied in the range 662 to 1210. From the 26244 parameter combinations, 28 sets were selected to cover the entire span of IAE. These 28 patient sets are arranged in the decreasing order of their BIS sensitivity to propofol and remifentanyl infusions (given in Table 6.7).

An insensitive patient requires relatively more drug dosage and also responds slowly to the drug. For the insensitive patient, depletion rate constants of the central compartment (k_{10p} , k_{12p} , k_{13p} , k_{10r} , k_{12r} and k_{13r}) are high (0.14875, 0.14, 0.052375, 0.63625, 0.4525 and 0.01625, respectively) and absorption rate constants (k_{21p} , k_{31p} , k_{21r} and k_{31r}) are low (0.04125, 0.002475, 0.14625 and 0.0105, respectively). In the PD parameters, higher EC_{50p} and EC_{50r} (3.7 and 14.56, respectively) indicate the

Table 6.6
Variation in parameters in PK/PD models

Parameter	Lower Limit ~ Mean ~ Upper Limit
k_{10p} (min^{-1})	0.08925 ~ 0.119 ~ 0.14875
k_{12p} (min^{-1})	0.084 ~ 0.112 ~ 0.140
k_{21p} (min^{-1})	0.04125 ~ 0.055 ~ 0.06875
k_{13p} (min^{-1})	0.031425 ~ 0.0419 ~ 0.052375
k_{31p} (min^{-1})	0.002475 ~ 0.0033 ~ 0.004125
k_{e0p} (min^{-1})	0.239 ~ 0.349 ~ 0.459
EC_{50p} ($\mu g/ml$)	1.6 ~ 2.65 ~ 3.7
γ_p	2 ~ 2.561 ~ 3.122
k_{10r} (min^{-1})	0.38175 ~ 0.509 ~ 0.63625
k_{12r} (min^{-1})	0.2715 ~ 0.362 ~ 0.4525
k_{21r} (min^{-1})	0.14625 ~ 0.195 ~ 0.24375
k_{13r} (min^{-1})	0.00975 ~ 0.013 ~ 0.01625
k_{31r} (min^{-1})	0.0105 ~ 0.014 ~ 0.0175
k_{e0r} (min^{-1})	0.3612 ~ 0.516 ~ 0.6708
EC_{50r} (ng/ml)	7.84 ~ 11.2 ~ 14.56
γ_r	1.757 ~ 2.51 ~ 3.263
k_r ($mmHg/(ng/ml)$)	-0.12334 ~ -0.1762 ~ -0.22906

need for more drug to get the same hypnosis and analgesia levels, higher γ_p and γ_r (3.122 and 3.263, respectively) represent higher nonlinearity, and lower k_{e0p} and k_{e0r} (0.239 and 0.3612, respectively) indicate sluggishness in response. For the sensitive patient k_{10p} , k_{12p} , k_{13p} , k_{10r} , k_{12r} and k_{13r} are low (0.08925, 0.084, 0.031425, 0.38175, 0.2715 and 0.00975, respectively) and k_{21p} , k_{31p} , k_{21r} and k_{31r} are high (0.06875,

Table 6.7
28 patients and their associated PK and PD parameters

Patient No.	k_{10p}	k_{12p}	k_{21p}	k_{13p}	k_{31p}	k_{e0p}	EC_{50p}	γ_p	k_{10r}	k_{12r}	k_{21r}	k_{13r}	k_{31r}	k_{e0r}	EC_{50r}	γ_r	k_r
1 (Sensitive)	0.08925	0.084	0.06875	0.031425	0.004125	0.459	1.60	2.000	0.38175	0.2715	0.24375	0.00975	0.0175	0.6708	7.840	1.757	-0.12334
2	0.11900	0.112	0.05500	0.041900	0.003300	0.239	2.65	2.000	0.38175	0.2715	0.24375	0.00975	0.0175	0.6708	7.840	1.757	-0.12334
3	0.08925	0.084	0.06875	0.031425	0.002475	0.459	1.60	2.000	0.50900	0.3620	0.24375	0.01625	0.0105	0.6708	7.840	1.757	-0.22906
4	0.14875	0.112	0.06875	0.031425	0.002475	0.459	2.65	2.561	0.50900	0.3620	0.24375	0.01625	0.0105	0.6708	7.840	1.757	-0.22906
5	0.08925	0.084	0.04125	0.052375	0.002475	0.459	2.65	2.561	0.50900	0.4525	0.24375	0.01625	0.0105	0.6708	14.56	2.510	-0.12334
6	0.11900	0.112	0.05500	0.041900	0.003300	0.239	2.65	2.561	0.38175	0.2715	0.14625	0.00975	0.0140	0.5160	7.840	1.757	-0.12334
7	0.08925	0.084	0.06875	0.031425	0.002475	0.459	3.70	2.000	0.38175	0.4525	0.19500	0.01625	0.0140	0.5160	11.20	2.510	-0.17620
8	0.11900	0.112	0.05500	0.041900	0.003300	0.239	2.65	2.000	0.63625	0.2715	0.24375	0.01300	0.0140	0.6708	7.840	1.757	-0.17620
9	0.14875	0.112	0.06875	0.031425	0.002475	0.349	3.70	2.561	0.50900	0.4525	0.24375	0.01625	0.0105	0.6708	14.56	2.510	-0.12334
10	0.08925	0.084	0.06875	0.031425	0.002475	0.349	2.65	2.561	0.50900	0.3620	0.14625	0.00975	0.0140	0.5160	14.56	1.757	-0.22906
11	0.14875	0.140	0.04125	0.052375	0.004125	0.239	1.60	2.000	0.63625	0.2715	0.24375	0.01300	0.0140	0.6708	7.840	1.757	-0.17620
12	0.08925	0.084	0.06875	0.031425	0.002475	0.239	3.70	3.122	0.63625	0.2715	0.24375	0.01300	0.0140	0.6708	7.840	1.757	-0.17620
13 (Nominal)	0.11900	0.112	0.05500	0.041900	0.003300	0.349	2.65	2.561	0.50900	0.3620	0.19500	0.01300	0.0140	0.5160	11.20	2.510	-0.17620
14	0.14875	0.140	0.04125	0.052375	0.004125	0.349	3.70	2.561	0.50900	0.3620	0.19500	0.01300	0.0140	0.5160	11.20	2.510	-0.17620
15	0.14875	0.140	0.04125	0.052375	0.004125	0.239	1.60	3.122	0.63625	0.2715	0.24375	0.01300	0.0140	0.6708	7.840	1.757	-0.17620
16	0.11900	0.112	0.05500	0.041900	0.003300	0.239	2.65	2.000	0.50900	0.4525	0.24375	0.01625	0.0105	0.6708	14.56	2.510	-0.12334
17	0.08925	0.084	0.06875	0.031425	0.002475	0.239	3.70	2.561	0.63625	0.4525	0.19500	0.01300	0.0175	0.6708	14.56	2.510	-0.12334
18	0.11900	0.112	0.05500	0.041900	0.003300	0.239	2.65	2.000	0.50900	0.3620	0.14625	0.00975	0.0140	0.5160	14.56	1.757	-0.22906
19	0.14875	0.112	0.04125	0.041900	0.004125	0.239	1.60	3.122	0.50900	0.4525	0.24375	0.01625	0.0105	0.6708	14.56	2.510	-0.12334
20	0.08925	0.084	0.04125	0.052375	0.002475	0.239	3.70	3.122	0.63625	0.2715	0.14625	0.01625	0.0175	0.5160	11.20	1.757	-0.22906
21	0.08925	0.084	0.04125	0.052375	0.002475	0.239	3.70	3.122	0.50900	0.3620	0.14625	0.00975	0.0140	0.5160	14.56	1.757	-0.22906
22	0.11900	0.112	0.05500	0.041900	0.003300	0.239	2.65	2.561	0.38175	0.3620	0.19500	0.00975	0.0105	0.3612	11.20	1.757	-0.22906
23	0.08925	0.084	0.06875	0.031425	0.002475	0.239	3.70	3.122	0.38175	0.3620	0.19500	0.00975	0.0105	0.3612	11.20	1.757	-0.22906
24	0.14875	0.140	0.04125	0.052375	0.004125	0.239	1.60	2.000	0.50900	0.2715	0.14625	0.00975	0.0105	0.3612	14.56	2.510	-0.22906
25	0.11900	0.112	0.05500	0.041900	0.003300	0.239	2.65	2.561	0.50900	0.2715	0.14625	0.00975	0.0105	0.3612	14.56	2.510	-0.22906
26	0.08925	0.084	0.04125	0.052375	0.002475	0.239	3.70	3.122	0.50900	0.2715	0.14625	0.00975	0.0105	0.3612	14.56	2.510	-0.22906
27	0.14875	0.112	0.04125	0.041900	0.004125	0.239	1.60	3.122	0.63625	0.4525	0.14625	0.01625	0.0175	0.3612	14.56	3.263	-0.22906
28 (Insensitive)	0.14875	0.140	0.04125	0.052375	0.002475	0.239	3.70	3.122	0.63625	0.4525	0.14625	0.01625	0.0105	0.3612	14.56	3.263	-0.22906

0.004125, 0.24375 and 0.0175, respectively). In the PD parameters, lower EC_{50p} and EC_{50r} (1.6 and 7.84, respectively) indicate that less drug is required to get the same hypnosis and analgesia levels, lower γ_p and γ_r (2 and 1.757, respectively) represent lower nonlinearity, and higher k_{e0p} and k_{e0r} (0.459 and 0.6708, respectively) indicate faster response. Inverse of k_{e0p} and k_{e0r} represent lag in the response with higher values of these parameters representing faster response and lower values representing slower response of the process.

Table 6.8 shows the performance comparison of MPC and decentralized PID controllers for sensitive and insensitive patients together with their control efforts. For both the controllers, high IAE values for the insensitive patient indicate the sluggish response (needs more drug) whereas low IAE values for the sensitive patient indicate the faster response (needs less drug) when compared to the IAE values for

Table 6.8
Performance of MPC and PID for sensitive and insensitive patients
for the set-point changes during the maintenance period

Controller	Insensitive Patient				Sensitive Patient			
	IAE _{BIS}	IAE _{MAP}	TV _P	TV _R	IAE _{BIS}	IAE _{MAP}	TV _P	TV _R
MPC	1210	344	37.8	2.98	662	261	25.8	2.46
PID	1246	388	40.8	6.38	711	271	28.6	6.00

the nominal patient given in Table 6.5. Also, as mentioned earlier, C_{1p} and C_{1r} are predicted using the nominal patient model. For the sensitive patient, nominal patient model predicts lesser concentration than the actual concentration because it infuses less drug based on the larger gain BIS response to propofol and remifentanyl infusions. Similarly, for the insensitive patient, higher C_{1p} and C_{1r} are predicted with the nominal patient model than the actual concentration because more drug is infused based on the smaller gain BIS and MAP responses to propofol and remifen-

tanil infusions. Even though predicted concentrations are different from the actual concentrations for these patients, the constraints imposed are not exceeded.

Figure 6.9 shows the performance comparison of MPC and PID controllers for the maintenance period, $t = 30 - 280 \text{ min}$ for the 28 patients. Figures 6.9(a) and (b) show the comparison of IAE values with respect to BIS and MAP, respectively and Figures 6.9(c) and (d) show comparison of controller effort with respect to propofol and remifentanyl, respectively. Table 6.9 shows the average performance and control effort of both controllers for the 28 patients together with corresponding standard deviations. Here, IAE_{BIS} values are high compared to IAE_{MAP} because changes in MAP affects the BIS response and not vice versa; possible reasons for

Table 6.9
Average performance of MPC and PID for the set-point changes during the maintenance period, for 28 patients

Controller	Mean IAE_{BIS} (SD)	Mean IAE_{MAP} (SD)	Mean TV_{P} (SD)	Mean TV_{R} (SD)
MPC	905 (165)	299 (23)	30.1 (2.84)	2.76 (0.12)
PID	948 (169)	325 (26)	34.5 (3.05)	6.23 (0.09)

this are: (a) propofol affects BIS only whereas remifentanyl affects both BIS and MAP, and (b) nonlinear relation between effect concentration and BIS (see section 6.2.2). Hence, by considering average IAE and control efforts, controlling BIS is critical compared to controlling MAP. Also, increase in remifentanyl infusion adds like an additive disturbance to BIS response - therefore, propofol infusion needs to be changed to bring BIS to the specified set-point. From Table 6.9, it is clear that the average performance of MPC controller is better compared to PID controller both in terms of set-point tracking and control effort. Further, Figure 6.9 shows that MPC performance is better than that of PID controller except for a few patients for whom IAE_{BIS} is comparable for both the controllers.

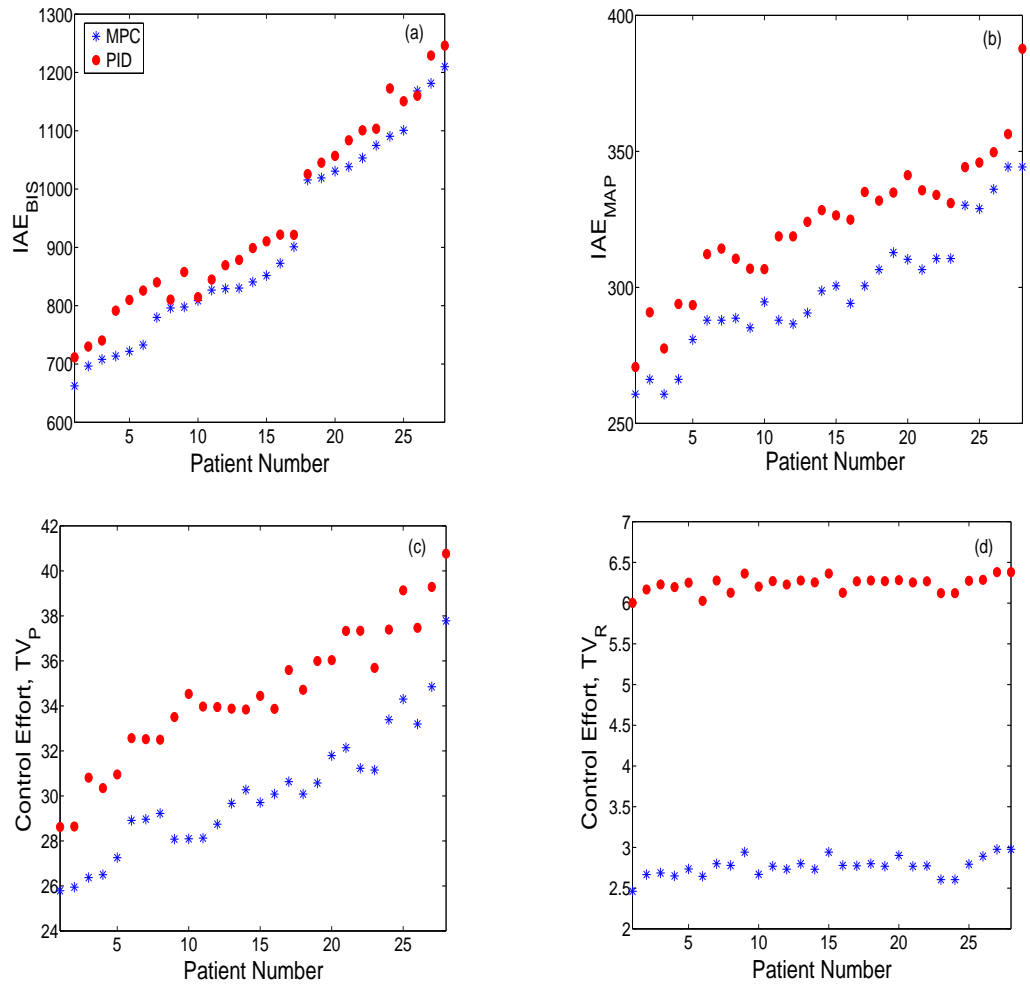


Fig. 6.9. Performance of MPC and PID for all the 28 patients for set-point changes during the maintenance period $t = 30 - 280 \text{ min}$

6.4.3 Performance of MPC and PID for disturbance rejection in BIS and MAP during surgery

Surgical stimulation can cause arousal reflex in the patient leading to disturbances in BIS and MAP during surgery. Strength of these disturbances is directly proportional to the nature of surgical stimulus, and these disturbances increase both BIS and MAP (Derighetti et al. 1997, Frei et al. 2000). Also, in typical operating conditions, BIS and MAP signals are corrupted by noise as mentioned in section 6.4.2. For better control performance, noise and disturbances in the BIS and MAP signals must be handled appropriately (e.g., filtering noise). If not, it will be harmful to the patient due to wrong drug dosage delivered to the patient. Here, the simulations are carried out by adding 2% Gaussian noise to the BIS and MAP signals. Noise in BIS and MAP signals cause fluctuations in propofol and remifentanyl infusion rates leading to higher valve movement. Hence, filters are added to feedback BIS and MAP signals to get smoother drug infusion profiles. For the disturbance, a typical stimulus profile (Struys et al. 2004) for BIS and MAP signals is applied from $t = 280 - 400 \text{ min}$ to all the patients.

Figure 6.10 depicts the responses of MPC and PID controllers for disturbances in the BIS and MAP signals for the nominal patient. Figures 6.10(a) and (b) shows the regulation of BIS and MAP at set-point of 50 and 80, respectively for the nominal patient. Both the controllers maintained the BIS and MAP within the operating range in spite of noise in both signals. However, higher disturbance magnitudes with higher frequency for longer duration of time causes the BIS and MAP signals to cross the respective surgical operating range ($40 \leq \text{BIS} \leq 60$ & $70 \leq \text{MAP} \leq 110$) during the period of disturbance. From these figures, one can observe that the disturbance in BIS (at $t = 280 \text{ min}$) does not affect the MAP response but disturbance in MAP (at $t = 310 \text{ min}$) affects the BIS response because of the effect of remifentanyl infusion change to counteract the disturbance in MAP, on BIS. This

is the same case with the disturbances in the remaining time period, $t = 340 - 400$ min. Also, when disturbance occurs, MAP settles very fast relative to BIS. This is because propofol and remifentanyl have to cross many barriers within the body to affect BIS compared to remifentanyl alone on MAP. Whenever BIS and MAP increase due to disturbances, the controller will increase the corresponding plasma drug concentrations, C_{1p} and C_{1r} (not shown) by increasing the infusion rates of propofol and remifentanyl (Figures 6.10(c) and (d)) to bring back BIS and MAP to their original set-points. Even when BIS and MAP went out of their limits, the controller maintained C_{1p} and C_{1r} within the constraints imposed and this is very important for patient safety. Noise in BIS and MAP has very little effect on predicted drug concentrations.

The performance of both controllers is checked for the remaining 27 patients and the IAE and TV values are provided in Table 6.10 for the insensitive, nominal and sensitive patients. Here also, response for the sensitive patient is faster (less drug usage) and response for the insensitive patient is sluggish (high drug usage) compared to response with the nominal patient. Figure 6.11 shows the performance

Table 6.10
Performance of MPC and PID controllers during disturbances for sensitive, nominal and insensitive patients

Controller	MPC				PID			
	IAE _{BIS}	IAE _{MAP}	TV _P	TV _R	IAE _{BIS}	IAE _{MAP}	TV _P	TV _R
Insensitive Patient	847	788	39.7	9.96	1152	802	35.2	7.78
Nominal Patient	695	665	29.7	8.22	803	755	24.4	6.81
Sensitive Patient	617	641	24.2	7.42	726	733	21.0	6.25

comparison of MPC and PID controllers in the disturbance period, $t = 280 - 440$ min for the 28 patients. Table 6.11 compares the average performance and control

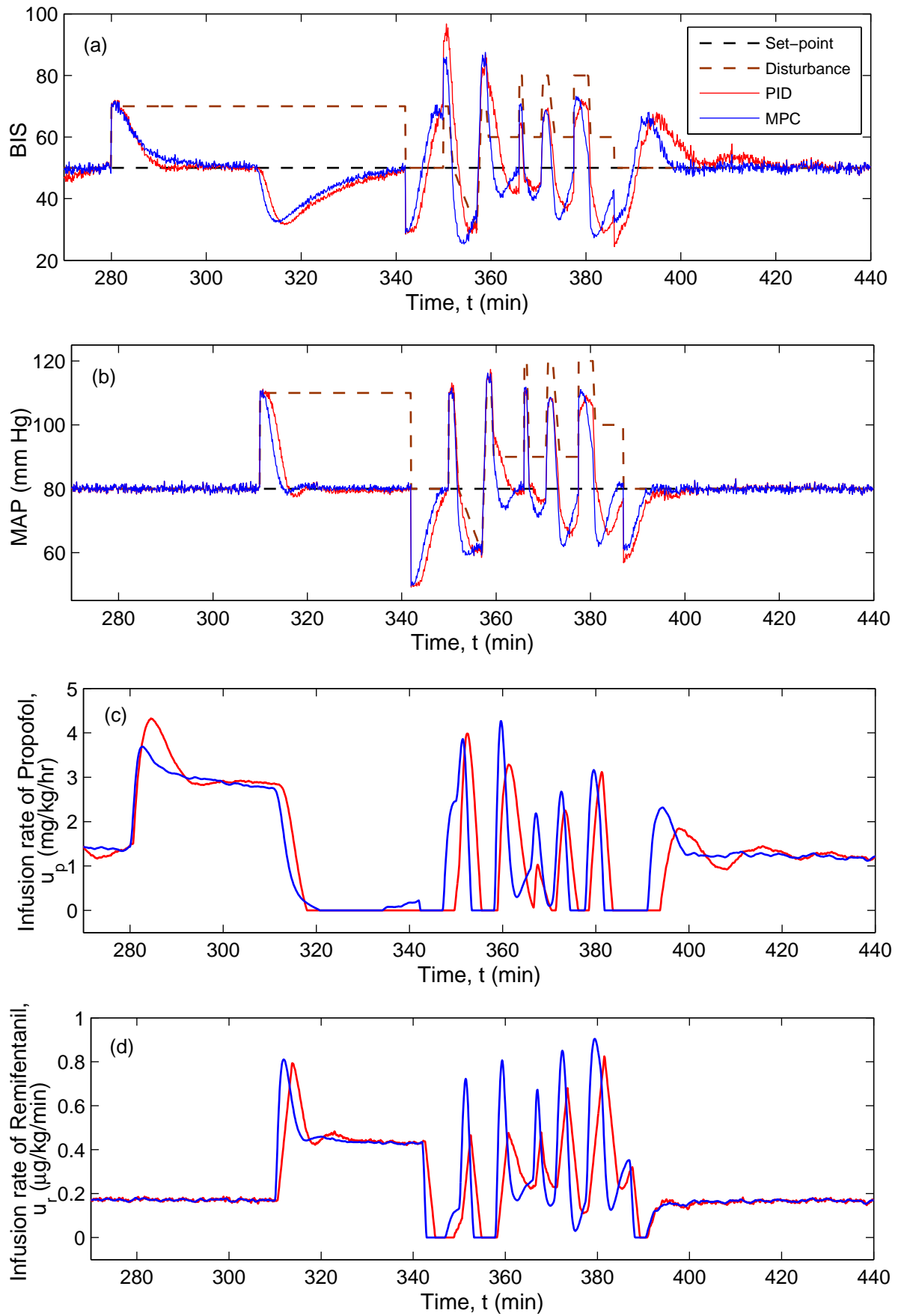


Fig. 6.10. Performance of MPC and PID controllers for disturbance rejection

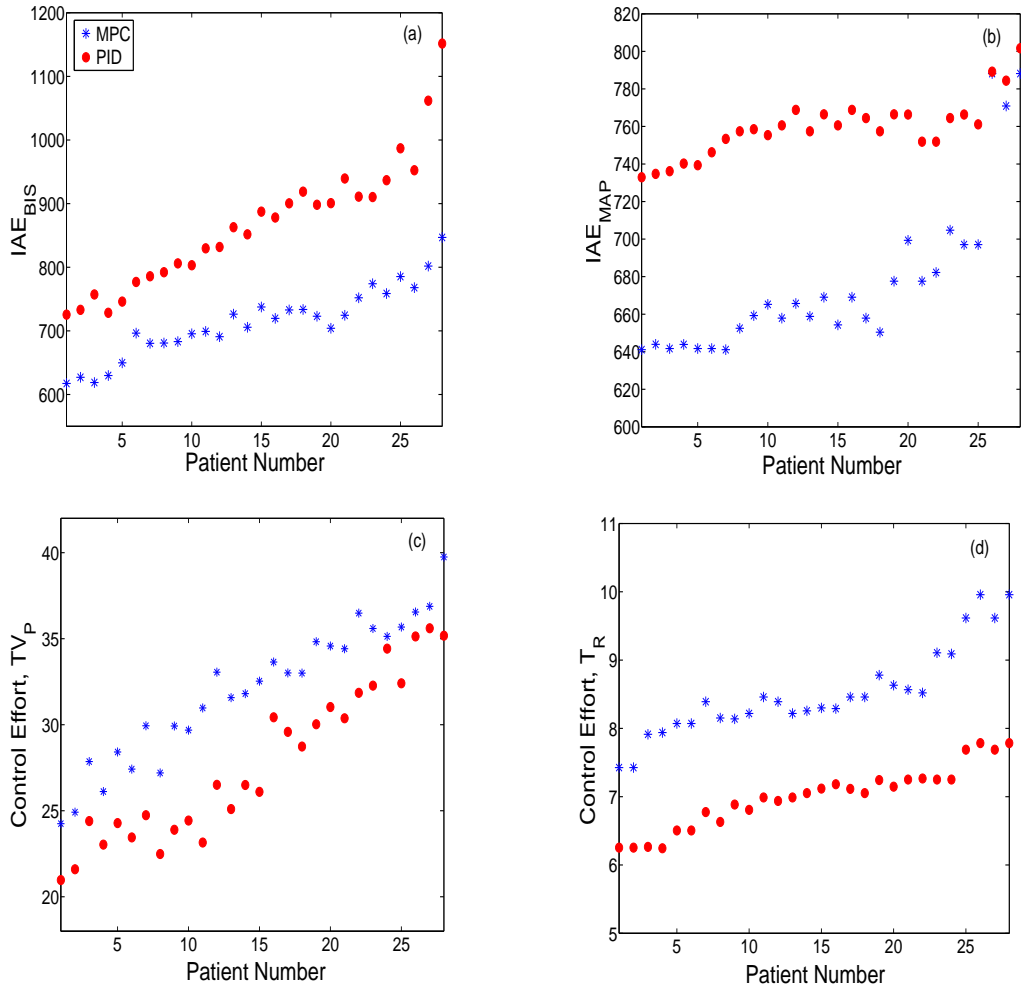


Fig. 6.11. Performance of MPC and PID for all the 28 patients for disturbances in BIS and MAP

Table 6.11
Average performance of MPC and PID controllers during disturbances for the 28 patients

Controller	Mean IAE_{BIS} (SD)	Mean IAE_{MAP} (SD)	Mean TV_P (SD)	Mean TV_R (SD)
MPC	716 (54)	668 (31)	32.4 (3.16)	8.66 (0.54)
PID	861 (83)	760 (15)	27.7 (3.91)	6.97 (0.43)

effort of both controllers together with their corresponding standard deviations. From Figure 6.11 and Table 6.11, one can clearly conclude that the performance of MPC is better than that of PID controller. The average control effort with MPC is

higher compared to PID – this clearly shows the aggressive nature of MPC compared to PID. This is not the case with set-point changes made during the maintenance period discussed earlier. Here, larger disturbances cause higher valve movement leading to higher control effort with MPC. These disturbance effects dominate the effect of noise in BIS and MAP signals which mostly affect the performance and control effort of decentralized PID compared to MPC.

6.5 Conclusions

Simultaneous automatic regulation of multiple drugs has more advantages when compared to the automatic regulation of a single drug and manual administration of other drugs. In this study, an advanced control strategy (model predictive control) for simultaneous regulation of hypnosis and analgesia using BIS and MAP as respective controlled variables has been developed. The performance of the MPC controller is compared with the performance of the decentralized PID control scheme. Both the controllers were designed for the nominal patient model, and then tested for their efficacy and robustness on 28 patient models covering sensitive to insensitive patients and operating conditions via simulation. The MPC controller is capable of improving hypnosis and analgesia regulation by 10 to 15% compared to decentralized PID controller, and also displays better robustness in set-point tracking and disturbance rejection when implemented on different patient profiles.

Chapter 7

CONCLUSIONS AND RECOMMENDATIONS

The previous chapters in this thesis described the application and simulation results of several advanced feedback control techniques applied for regulating two anesthetic components (hypnosis and analgesia) during surgery. General control strategies such as PI, PID, PID-P and PID-PI as well as advanced model based control strategies such as IMC, MEC (also in their cascade versions), RTDA and MPC were considered in this work. The following concluding remarks are drawn from the present study conducted on feedback control of hypnosis and analgesia.

7.1 Conclusions

Chapter 3 demonstrated the automatic control of hypnosis using bispectral index (BIS) as the controlled variable and isoflurane infusion as the manipulated variable. The main objective of this chapter was to design and evaluate the performance of MPC and the RTDA control strategies. Further, the performance of these two model based controllers was compared with the performance of SISO PI & PID and also cascade PID-P & PID-PI controllers. The performance comparison of these six controllers was conducted by considering parameter variations in the patient model to account for patient-model mismatch, set-point changes and disturbances during the surgery. For realistic assessment, measurement noise (white noise with zero mean and SD of ± 3) was added to the BIS signal in the simulations. These performance validations were done on a set of 16 patient profiles that were constructed based on different isoflurane sensitivities. MPC and RTDA controllers performed better and were also found to more robust compared to PI/PID controllers. When compared to

PI/PID, cascade controllers provided better and robust performance but not as good as MPC or RTDA. Also, to cope with the possible loss of BIS signal during surgery, estimation of a patient-specific EC_{50} value (based on BIS and endtidal concentration measurements in the induction period) and its use for estimating BIS for subsequent feedback was proposed, and its effectiveness was shown via simulation with all the six controllers.

The automatic control of hypnosis using BIS as the controlled variable by manipulating isoflurane infusion is further studied in chapter 4. The performance of the devised model predictive controller (MPC) was comprehensively compared with the performances of cascade internal model control (CIMC) and cascade modeling error compensation (CMEC) approaches available in the literature. The proposed MPC used the approximate linear PK-PD model in the controller design which was obtained by linearization of the nonlinear model around the operating point (BIS equal to 50). A set of 28 patient profiles (by varying PK-PD model parameters) was constructed to represent patients with different drug sensitivities. MPC scheme provided better performance compared to other two control schemes while respecting the imposed constraints on the manipulated and output variables. It is also more robust to inter-patient variability and performed well in the presence of disturbances and measurement noise in BIS signal.

The studies in chapters 3 and 4 were on closed-loop regulation of hypnosis with the inhalational drug isoflurane. The study in chapter 5 evaluated the performances of MPC, IMC and MEC controllers for closed-loop regulation of hypnosis using intravenous drug propofol with BIS as the controlled variable. Cascade control structures used for closed-loop regulation of isoflurane in chapters 3 and 4 are impractical with propofol because of unavailability of continuous plasma propofol concentration measurement. Hence, instead of their cascade versions, SISO MEC and IMC strategies were employed in this chapter. The performance of these model-based controllers

were considered along with that of the conventional PID controller. A well-accepted propofol PK-PD model taken from the literature and a set of 17 patient profiles (obtained by varying PK-PD model parameters) was constructed to represent patients with different propofol sensitivities. Extensive simulations were conducted to test the performance of the four controllers for robustness, set-point tracking, disturbance and noise rejection characteristics. Here also, model-based controllers (MPC, IMC and MEC) showed robust performance, and were found to be better at handling disturbances and measurement noise in comparison with the PID controller. Excessive manipulated variable movement was observed with MEC controller (because of noise) when compared to MPC controller even though performances of both the controllers appeared to be similar. With IMC controller, small manipulated movement was observed but its performance turned out to be poorer compared to that of the remaining two model-based controllers. Among the four controllers, MPC performed better. Finally, the performance of MPC and PID controllers was compared with that of the novel RTDA controller. The RTDA controller performance was found to be better than the PID controller and even slightly better than the MPC when tested on the same patient models. The RTDA controller appears to be more robust compared to MPC and PID.

While studies in chapters 3 to 5 were limited to regulation of hypnosis by infusing either isoflurane or propofol, the study in chapter 6 investigated the simultaneous closed-loop regulation of hypnosis and analgesia by infusing intravenous drugs propofol and remifentanil. This chapter demonstrated the design and thorough evaluation of a MPC controller for optimal infusion of both propofol and remifentanil to regulate patient's hypnotic and analgesic states (measured by BIS and MAP respectively). Extensive simulations were conducted to test the robustness of the proposed MPC controller, by considering parameter variations in the PK and PD models (28 patient models covering the entire spectrum of sensitive to insensitive patients) and typical set-point changes and disturbances during surgical operations. Also, the per-

formance of the MPC controller was compared with that of the decentralized PID control scheme for all the above mentioned scenarios. Results show that the MPC controller provides better performance when compared to decentralized PID controller, and also displayed better robustness in set-point tracking and disturbance rejection when implemented on different patient profiles. When compared to results in chapter 5, less propofol was infused for the same BIS set-point change (because of synergistic interaction of propofol and remifentanyl) and hence propofol overdose was limited. This is good for the patient's rehabilitation as less time will be spent in postoperative care leading to a reduction in the cost of surgery.

All the above studies indicated that the model-based controllers work well, more robust and suitable in surgical settings. Out of all the controllers studied, MPC showed robust performance in all the scenarios tested and is therefore recommended as a promising strategy for controlling hypnosis as well as simultaneous control of hypnosis and analgesia. In general, comprehensive simulations and evaluations performed in this study provide greater confidence on closed-loop control of anesthesia and its benefits. Also, the patient profiles developed and used in the present study will be useful in future studies on anesthesia control.

7.2 Recommendations for Future Work

In this section several important topics on modeling and control of anesthesia are outlined for further investigation.

7.2.1 Simultaneous control of hypnosis, analgesia and skeletal muscle relaxation

During general anesthesia, drugs are administered to provide hypnosis, ensure analgesia and skeletal muscle relaxation. As discussed in the previous chapters, hypnosis is controlled by administration of hypnotic drugs (e.g., isoflurane, propofol),

analgesia is maintained by administration of opioids (e.g., remifentanyl, alfentanil) and muscle relaxation is controlled using neuromuscular blocking agents (e.g., midazolam, mivacurium and rocuronium). Up to now, very few control strategies were studied for simultaneous regulation of hypnosis and analgesia with limited combination of hypnotic and analgesic drugs (e.g., propofol and remifentanyl). These control strategies can be extended to other combinations of hypnotic and analgesic drugs also (e.g., isoflurane and remifentanyl, isoflurane and alfentanil, propofol and alfentanil etc.). Although volatile hypnotic agents like isoflurane have slower onset and require actuators which are difficult to handle than actuators for intravenous drugs such as propofol, their concentrations in the central compartment can be measured online. Also, opioids (e.g., remifentanyl, alfentanil) can potentiate the hypotensive effects of isoflurane, and hence further decrease in opioids infusion can be achieved to get the same level of MAP. For some of the surgeries, skeletal muscle relaxation should be maintained within acceptable limits. The administered neuro muscular blocking agents to maintain skeletal muscle relaxation will also affect the properties of both hypnotics and analgesics. Up to now, there is little or no work done on the simultaneous regulation of hypnosis, analgesia and skeletal muscle relaxation. Hence, it is desirable to develop and study a control strategy to regulate all these three anesthesia components simultaneously. The available interaction models for the drug combinations involving propofol, alfentanil and midazolam (e.g., Minto et al. (2000)) can be used for such a study.

7.2.2 Fault-tolerant control

Occasionally, measurement artifacts deteriorate the controller's performance and can be harmful to the patient. These artifacts could arise due to noise in the measurement signals as well as due to disconnection of the sensors from the patient. The designed controller should handle all these typical types of artifacts to assure patient's safety. For this, a multivariable controller can be designed for simultaneous

regulation of all anesthetic components and hemodynamic variables (e.g., cardiac output (CO), blood pressure (BP) etc.). This controller should perform satisfactorily even when any of the controlled output signals (e.g., BIS, MAP, CO and BP) have artifacts. For example, when artifacts are present in the MAP signal, one should not use MAP as the controlled variable but use the reliable measurements like CO or BP as the controlled variable. To detect artifacts in any of the measured signals, an observer based control algorithm (e.g., Noura et al. (2009)) can be developed based on signal quality index (SQI). This algorithm will alert the controller on which signal is reliable for use with the control algorithm to regulate the controlled outputs.

7.2.3 Nonlinear model-based control

The models developed for the drug effects and the effect of combination of drugs are nonlinear. On the other hand, many of the developed control algorithms use linearized models. Hence, the designed controller may not perform well. Nonlinear controllers (e.g., Ricker & Lee (1995)) for anesthesia regulation can be developed to further improve the patient's safety and rehabilitation during surgery.

7.2.4 Clinical validation

Although, this thesis has highlighted the superior performance of several model-based controllers for anesthesia regulation using simulations, their clinical applicability and performance need to be demonstrated. Hence, clinical tests must be conducted before the developed control system can be used by the clinical staff in a surgical theater. This important aspect should be investigated in detailed multi-center studies.

REFERENCES

- Absalom, A. R., & Kenny, G. N. C. (2003). Closed-loop control of propofol anaesthesia using bispectral index: Performance assessment in patients receiving computer-controlled propofol and manually controlled remifentanyl infusions for minor surgery. *British Journal of Anaesthesia*, *90*(6), 737–741.
- Absalom, A. R., Sutcliffe, N., & Kenny, G. N. (2002). Closed-loop control of anaesthesia using Bispectral index: Performance assessment in patients undergoing major orthopedic surgery under combined general and regional anaesthesia. *Anesthesiology*, *96*(1), 67–73.
- Alvarez-Ramirez, J., Alvarez, J., & Morales, A. (2002). An adaptive cascade control for a class of chemical reactors. *International Journal of Adaptive Control and Signal Processing*, *16*(10), 681–701.
- Ausems, M. E., Hug, C. C., Stanski, D. R., & Burm, A. G. L. (1986). Plasma-concentrations of alfentanil required to supplement nitrous-oxide anaesthesia for general-surgery. *Anesthesiology*, *65*(4), 362–373.
- Ausems, M. E., Vuyk, J., Hug, C. C., & Stanski, D. R. (1988). Comparison of a computer-assisted infusion versus intermittent bolus administration of alfentanil as a supplement to nitrous-oxide for lower abdominal-surgery. *Anesthesiology*, *68*(6), 851–861.
- Bailey, J. M., & Haddad, W. M. (2005). Drug dosing control in clinical pharmacology. *IEEE Control Systems Magazine*, *25*(2), 35–51.
- Bailey, J. M., Haddad, W. M., Jeong, J. I., Hayakawa, T., & Nagel, P. A. (2006). Adaptive and neural network adaptive control of depth of anaesthesia during

- surgery. In *Proceedings of the American Control Conference*, Minneapolis, MN, USA, pp. 3409–3414.
- Beck, C., Lin, H.-H., & Bloom, M. (2007). Modeling and control of anesthetic pharmacodynamics. In *Lecture Notes in Control and Information Sciences - Biology and Control Theory: Current Challenges*, Vol. 357, Springer-Verlag: Berlin, Heidelberg, pp. 263–289.
- Bequette, B. W. (2003). *Process Control: Modeling, Design and Simulation*. Prentice Hall PTR: New Jersey.
- Bibian, S., Ries, C. R., Huzmezan, M., & Dumont, G. A. (2003). Clinical anesthesia and control engineering: Terminology, concepts and issues. In *Proceedings of the European Control Conference*, Cambridge, UK, pp. 2465–2474.
- Bibian, S., Ries, C. R., Huzmezan, M., & Dumont, G. A. (2005). Introduction to automated drug delivery in clinical anesthesia. *European Journal of Control*, 11(6), 535–557.
- Bibian, S., Zikov, T., Dumont, G., Ries, C., Puil, E., Ahmadi, H., Huzmezan, M., & MacLeod, B. (2001). Estimation of the anesthetic depth using wavelet analysis of electroencephalogram. In *Proceedings of the 23rd Annual International Conference of the IEEE Engineering in Medicine and Biology Society*, Vol. 1, Istanbul, Turkey, pp. 951–955.
- Bouillon, T. W., Bruhn, J., Radulescu, L., Andresen, C., Shafer, T. J., Cohane, C., & Shafer, S. L. (2004). Pharmacodynamic interaction between propofol and remifentanyl regarding hypnosis, tolerance of laryngoscopy, bispectral index, and electroencephalographic approximate entropy. *Anesthesiology*, 100(6), 1353–1372.
- Brosilow, C., & Joseph, B. (2002). *Techniques of Model-Based Control*. Prentice Hall PTR: New Jersey.

- Bruhn, J., Bouillon, T. W., Radulescu, L., Hoeft, A., Bertaccini, E., & Shafer, S. L. (2003). Correlation of approximate entropy, bispectral index, and spectral edge frequency 95 (SEF95) with clinical signs of “anesthetic depth” during coadministration of propofol and remifentanyl. *Anesthesiology*, *98*(3), 621–627.
- Camacho, E. F., & Bordons, C. (2004). *Model Predictive Control*. Springer-Verlag: London.
- Cardoso, N., & Lemos, J. M. (2008). Model predictive control of depth of anaesthesia: Guidelines for controller configuration. In *Proceedings of the 30th Annual International Conference of the IEEE Engineering in Medicine and Biology Society (EMBS)*, pp. 5822–5825.
- Chen, D., & Seborg, D. E. (2002). PI/PID controller design based on direct synthesis and disturbance rejection. *Industrial and Engineering Chemistry Research*, *41*(19), 4807–4822.
- Chien, I.-L., & Fruehauf, P. S. (1990). Consider IMC tuning to improve controller performance. *Chemical Engineering Progress*, *86*(10), 33–41.
- Ch’ng, K. L., & Lakshminarayanan, S. (2006). Performance assessment and sensitivity test of novel regulatory RTD-A controller. In *Proceedings of the 6th Asian Control Conference*, Bali, Indonesia, pp. 273–282.
- Coetzee, J. F., Glen, J. B., Wium, C. A., & Boshoff, L. (1995). Pharmacokinetic model selection for target controlled infusions of propofol: Assessment of three parameter sets. *Anesthesiology*, *82*(6), 1328–1345.
- Derighetti, M., Frei, C. W., Buob, M., Zbinden, A. M., & Schnider, T. W. (1997). Modeling the effect of surgical stimulation on mean arterial blood pressure. In *Proceedings of the Annual International Conference of the IEEE Engineering in Medicine and Biology*, Vol. 5, pp. 2172–2175.

- Doi, M., Gajraj, R. J., Mantzaridis, H., & Kenny, G. N. (1997). Effects of cardiopulmonary bypass and hypothermia on electroencephalographic variables. *Anaesthesia*, *52*(11), 1048–1055.
- Doyle, F., Jovanovic, L., Seborg, D., Parker, R. S., Bequette, B. W., Jeffrey, A. M., Xia, X., Craig, I. K., & McAvoy, T. (2007). A tutorial on biomedical process control. *Journal of Process Control*, *17*(7), 571–594.
- Doyle, P. W., Coles, J. P., Leary, T. M., Brazier, P., & Gupta, A. K. (2001). A comparison of remifentanyl and fentanyl in patients undergoing carotid endarterectomy. *European Journal of Anaesthesiology*, *18*(1), 13–19.
- Dua, P., & Pistikopoulos, E. N. (2005). Modelling and control of drug delivery systems. *Computers & Chemical Engineering*, *29*, 2290–2296.
- Dyck, J. B., & Shafer, S. L. (1992). Effects of age on propofol pharmacokinetics. *Seminars in Anesthesia*, *11*, 2–4.
- Egan, T. D. (2000). Pharmacokinetics and pharmacodynamics of remifentanyl: An update in the year 2000. *Current Opinion in Anaesthesiology*, *13*(4), 449–455.
- Ekman, A., Lindholm, M.-L., Lennmarken, C., & Sandin, R. (2004). Reduction in the incidence of awareness using BIS monitoring. *Acta Anaesthesiologica Scandinavica*, *48*(1), 20–26.
- Epple, J., Kubitz, J., Schmidt, H., Motsch, J., Bttiger, B. W., Martin, E., & Bach, A. (2001). Comparative analysis of costs of total intravenous anaesthesia with propofol and remifentanyl vs. balanced anaesthesia with isoflurane and fentanyl. *European Journal of Anaesthesiology*, *18*(1), 20–28.
- Frei, C. W., Derighetti, M., Morari, M., Glattfelder, A. H., & Zbinden, A. M. (2000). Improving regulation of mean arterial blood pressure during anesthesia through estimates of surgery effects. *IEEE Transactions on Biomedical Engineering*, *47*(11), 1456–1464.

- Friman, M., & Waller, K. V. (1997). Two-channel relay for autotuning. *Industrial and Engineering Chemistry Research*, *36*(7), 2662–2671.
- Furutani, E., Araki, M., & Maetani, S. (1995). Blood pressure control during surgical operations. *IEEE Transactions on Biomedical Engineering*, *42*(10), 999–1006.
- Furutani, E., Sawaguchi, Y., Shirakami, G., Araki, M., & Fukuda, K. (2005). A hypnosis control system using a model predictive controller with online identification of individual parameters. In *Proceedings of the IEEE International Conference on Control Applications*, Vol. 1, Toronto, Canada, pp. 154–159.
- Gentilini, A., Rossoni-Gerosa, M., Frei, C. W., Wymann, R., Morari, M., Zbinden, A. M., & Schnider, T. W. (2001a). Modeling and closed-loop control of hypnosis by means of bispectral index (BIS) with isoflurane. *IEEE Transactions on Biomedical Engineering*, *48*(8), 874–889.
- Gentilini, A., Frei, C. W., Glattfedler, A. H., Morari, M., Sieber, T. J., Wymann, R., Schnider, T. W., & Zbinden, A. M. (2001b). Multitasked closed-loop control in anesthesia. *IEEE Engineering in Medicine and Biology Magazine*, *20*(1), 39–53.
- Gentilini, A. L. (2001c). *Feedback control of hypnosis and analgesia in humans*. PhD thesis. Swiss Federal Institute of Technology (ETH).
- Gentilini, A., Schaniel, C., Morari, M., Bieniok, C., Wymann, R., & Schnider, T. (2002). A new paradigm for the closed-loop intraoperative administration of analgesics in humans. *IEEE Transactions on Biomedical Engineering*, *49*(4), 289–299.
- Glass, P. S. (1998). Anesthetic drug interactions: An insight into general anesthesia—Its mechanism and dosing strategies. *Anesthesiology*, *88*(1), 5–6.
- Glass, P. S., Bloom, M., Kearse, L., Rosow, C., Sebel, P., & Manberg, P. (1997). Bispectral analysis measures sedation and memory effects of propofol, midazolam, isoflurane, and alfentanil in healthy volunteers. *Anesthesiology*, *86*(4), 836–847.

- Glass, P. S., & Rampil, I. J. (2001). Automated anesthesia: Fact or fantasy? *Anesthesiology*, *95*(1), 1–2.
- Grieder, P., Gentilini, A., Morari, M., & Schnider, T. W. (2001). Robust adaptive control of hypnosis during anesthesia. In *Proceedings of the 23rd Annual International Conference of the IEEE Engineering in Medicine and Biology Society*, Vol. 2. Istanbul, Turkey, pp. 2055–2058.
- Habibi, S., & Coursin, D. B. (1996). Assessment of sedation, analgesia, and neuromuscular blockade in the perioperative period. *International Anesthesiology Clinics*, *34*(3), 215–241.
- Haeri, M. (2005). PI design based on DMC strategy. *Transactions of the Institute of Measurement and Control*, *27*(1), 21–36.
- Huang, J. W., Lu, Y.-Y., Nayak, A., & Roy, R. J. (1999). Depth of anesthesia estimation and control. *IEEE Transactions on Biomedical Engineering*, *46*(1), 71–81.
- Isaka, S., & Sebald, A. V. (1993). Control strategies for arterial blood pressure regulation. *IEEE Transactions on Biomedical Engineering*, *40*(4), 353–363.
- Johnson, K. B., Syroid, N. D., Gupta, D. K., Manyam, S. C., Egan, T. D., Huntington, J., White, J. L., Tyler, D., & Westenskow, D. R. (2008). An evaluation of remifentanyl propofol response surfaces for loss of responsiveness, loss of response to surrogates of painful stimuli and laryngoscopy in patients undergoing elective surgery. *Anesthesia & Analgesia*, *106*(2), 471–479.
- Johnson, T. W., & Luscombe, F. E. (1992). Patient controlled analgesia—assessment of machine feedback to patients. *Anaesthesia*, *47*(10), 899–901.
- Kaplan, A. J. (1993). *Cardiac Anesthesia*. Philadelphia, PA: Saunders.

- Kazama, T., Ikeda, K., Morita, K., Kikura, M., Doi, M., Ikeda, T., Kurita, T., & Nakajima, Y. (1999). Comparison of the effect-site k_{e0} s of propofol for blood pressure and EEG bispectral index in elderly and younger patients. *Anesthesiology*, *90*(6), 1517–1527.
- Kenny, G. N., & Mantzaridis, H. (1999). Closed-loop control of propofol anaesthesia. *British Journal of Anaesthesia*, *83*(2), 223–228.
- Kenny, G., & Ray, D. (1993). *Validation of monitoring anesthetic depth by closed-loop control*. Englewood Cliffs, NJ: Prentice Hall.
- Kenny, G., & Ray, D. (1995). *Adaptive control of intravenous anesthesia by evoked potentials*. Berlin: Springer-Verlag.
- Kern, S. E., Xie, G., White, J. L., & Egan, T. D. (2004). Opioid-hypnotic synergy: A response surface analysis of propofol-remifentanyl pharmacodynamic interaction in volunteers. *Anesthesiology*, *100*(6), 1373–1381.
- Kissin, I. (2000). Depth of anesthesia and bispectral index monitoring. *Anesthesia & Analgesia*, *90*(5), 1114–1117.
- Kochs, E., Bischoff, P., Pichlmeier, U., & am Esch, J. S. (1994). Surgical stimulation induces changes in brain electrical activity during isoflurane/nitrous oxide anesthesia. A topographic electroencephalographic analysis. *Anesthesiology*, *80*(5), 1026–1034.
- Krassioukov, A. V., Gelb, A. W., & Weaver, L. C. (1993). Action of propofol on central sympathetic mechanisms controlling blood pressure. *Canadian Journal of Anesthesia*, *40*(8), 761–769.
- Lichtenbelt, B.-J., Mertens, M., & Vuyk, J. (2004). Strategies to optimise propofol-opioid anaesthesia. *Clinical Pharmacokinetics*, *43*(9), 577–593.
- Linkens, D. (1994). *Introduction to intelligent control paradigms and system modelling*. Bristol, PA: Taylor & Francis.

- Linkens, D. A. (1992). Adaptive and intelligent control in anesthesia. *IEEE Control Systems Magazine*, 12(6), 6–11.
- Linkens, D. A., & Hacisalihzade, S. S. (1990). Computer control systems and pharmacological drug administration: A survey. *Journal of Medical Engineering & Technology*, 14(2), 41–54.
- Liu, F.-Y., & Northrop, R. (1990). A new approach to the modeling and control of postoperative pain. *IEEE Transactions on Biomedical Engineering*, 37(12), 1147–1158.
- Locher, S., Stadler, K. S., Boehlen, T., Bouillon, T., Leibundgut, D., Schumacher, P. M., Wymann, R., & Zbinden, A. M. (2004). A new closed-loop control system for isoflurane using bispectral index outperforms manual control. *Anesthesiology*, 101(3), 591–602.
- Mahfouf, M. (2006). *Intelligent Systems Modeling and Decision Support in Bioengineering*. Artech House, Inc. MA.
- Mahfouf, M., Asbury, A., & Linkens, D. (2003). Unconstrained and constrained generalised predictive control of depth of anaesthesia during surgery. *Control Engineering Practice*, 11(12), 1501–1515.
- Mahfouf, M., Nunes, C. S., Linkens, D. A., & Peacock, J. E. (2005). Modelling and multivariable control in anaesthesia using neural-fuzzy paradigms. Part II. Closed-loop control of simultaneous administration of propofol and remifentanyl. *Artificial Intelligence in Medicine*, 35(3), 207–213.
- Marchetti, G., Barolo, M., Jovanovi, L., Zisser, H., & Seborg, D. E. (2008). A feedforward-feedback glucose control strategy for type 1 diabetes mellitus. *Journal of Process Control*, 18(2), 149–162.

- Marsh, B., White, M., Morton, N., & Kenny, G. N. (1991). Pharmacokinetic model driven infusion of propofol in children. *British Journal of Anaesthesia*, *67*(1), 41–48.
- Mendonca, T., Nunes, C., Magalhaes, H., Lemos, J. M., & Amorim, P. (2006). Predictive adaptive control of unconsciousness - Exploiting remifentanil as an accessible disturbance. In *Proceedings of the IEEE International Conference on Control Applications*, Munich, Germany, pp. 205–210.
- Mertens, M. J., Olofsen, E., Engbers, F. H. M., Burm, A. G. L., Bovill, J. G., & Vuyk, J. (2003). Propofol reduces perioperative remifentanil requirements in a synergistic manner: Response surface modeling of perioperative remifentanil-propofol interactions. *Anesthesiology*, *99*(2), 347–359.
- Milne, S. E., Kenny, G. N. C., & Schraag, S. (2003). Propofol sparing effect of remifentanil using closed-loop anaesthesia. *British Journal of Anaesthesia*, *90*(5), 623–629.
- Minto, C. F., Schnider, T. W., Egan, T. D., Youngs, E., Lemmens, H. J., Gambus, P. L., Billard, V., Hoke, J. F., Moore, K. H., Hermann, D. J., Muir, K. T., Mandema, J. W., & Shafer, S. L. (1997). Influence of age and gender on the pharmacokinetics and pharmacodynamics of remifentanil. I. Model development. *Anesthesiology*, *86*(1), 10–23.
- Minto, C. F., Schnider, T. W., Short, T. G., Gregg, K. M., Gentilini, A., & Shafer, S. L. (2000). Response surface model for anesthetic drug interactions. *Anesthesiology*, *92*(6), 1603–1616.
- Morari, M., & Gentilini, A. (2001). Challenges and opportunities in process control: Biomedical processes. *AIChE Journal*, *47*(10), 2140–2143.
- Morari, M., & Lee, J. H. (1999). Model predictive control: Past, present and future. *Computers & Chemical Engineering*, *23*(4-5), 667–682.

- Morari, M., & Zafriou, E. (1989). *Robust process control*. Englewood Cliffs, N.J.: Prentice Hall.
- Morley, A., Derrick, J., Mainland, P., Lee, B. B., & Short, T. G. (2000). Closed loop control of anaesthesia: An assessment of the bispectral index as the target of control. *Anaesthesia*, *55*(10), 953–959.
- Mortier, E., Struys, M., Smet, T. De, Versichelen, L., & Rolly, G. (1998). Closed-loop controlled administration of propofol using bispectral analysis. *Anaesthesia*, *53*(8), 749–754.
- Mukati, K., & Ogunnaiké, B. (2004). Stability analysis and tuning strategies for a novel next generation regulatory controller. In *Proceedings of the American Control Conference*, Vol. 5. Boston, MA, USA, pp. 4034–4039.
- Nayak, A., & Roy, R. J. (1998). Anesthesia control using midlatency auditory evoked potentials. *IEEE Transactions on Biomedical Engineering*, *45*(4), 409–421.
- Nieuwenhuijs, D. J. F., Olofsen, E., Romberg, R. R., Sarton, E., Ward, D., Engbers, F., Vuyk, J., Mooren, R., Teppema, L. J., & Dahan, A. (2003). Response surface modeling of remifentanyl-propofol interaction on cardiorespiratory control and bispectral index. *Anesthesiology*, *98*(2), 312–322.
- Noura, H., Theilliol, D., Ponsart, J.-C., & Chamseddine, A. (2009). *Fault-tolerant Control Systems – Design and Practical Applications*. Springer-Verlag: London.
- Nunes, C. S., Mahfouf, M., Linkens, D. A., & Peacock, J. E. (2005). Modelling and multivariable control in anaesthesia using neural-fuzzy paradigms. Part I. Classification of depth of anaesthesia and development of a patient model. *Artificial Intelligence in Medicine*, *35*(3), 195–206.
- Nunes, C. S., Mendonca, T. F., Magalhaes, H., Lemos, J. M., & Amorim, P. (2006). Predictive adaptive control of the bispectral index of the EEG (BIS) – Using the intravenous anaesthetic drug propofol. In *Lecture Notes in Computer Science*

- *Knowledge-Based Intelligent Information and Engineering Systems*, Vol. 4252, Springer-Verlag: Berlin, Heidelberg, pp. 1248–1255.
- Ogunnaike, B. A., & Mukati, K. (2006). An alternative structure for next generation regulatory controllers. Part I: Basic theory for design, development and implementation. *Journal of Process Control*, 16(5), 499–509.
- Ogunnaike, B. A., & Ray, W. H. (1994). *Process Dynamics, Modeling, and Control*. Oxford University Press, New York.
- O'Hara, D. A., Bogen, D. K., & Noordergraaf, A. (1992). The use of computers for controlling the delivery of anesthesia. *Anesthesiology*, 77(3), 563–581.
- Parker, R. S., Doyle, F.J., I., & Peppas, N. A. (1999). A model-based algorithm for blood glucose control in type I diabetic patients. *IEEE Transactions on Biomedical Engineering*, 46(2), 148–157.
- Pinsker, M. (1986). Anesthesia: A pragmatic construct. *Anesthesia & Analgesia*, 65(7), 819–820.
- Pomfrett, C. J. (1999). Heart rate variability, BIS and depth of anaesthesia. *British Journal of Anaesthesia*, 82(5), 659–662.
- Prys-Roberts, C. (1987). Anaesthesia: a practical or impossible construct? *British Journal of Anaesthesia*, 59, 1341–1345.
- Puebla, H., & Alvarez-Ramirez, J. (2005). A cascade feedback control approach for hypnosis. *Annals of Biomedical Engineering*, 33(10), 1449–1463.
- Qin, S. J., & Badgwell, T. A. (2003). A survey of industrial model predictive control technology. *Control Engineering Practice*, 11(7), 733–764.
- Rampil, I. J. (1998). A primer for EEG signal processing in anesthesia. *Anesthesiology*, 89(4), 980–1002.

- Rampil, I. J., & Laster, M. J. (1992). No correlation between quantitative electroencephalographic measurements and movement response to noxious stimuli during isoflurane anesthesia in rats. *Anesthesiology*, *77*(5), 920–925.
- Rao, R. R., Bequette, B. W., & Roy, R. J. (2000). Simultaneous regulation of hemodynamic and anesthetic states: A simulation study. *Annals of Biomedical Engineering*, *28*(1), 71–84.
- Rao, R. R., Palerm, C. C., Aufderheide, B., & Bequette, B. W. (2001). Automated regulation of hemodynamic variables. *IEEE Engineering in Medicine and Biology Magazine*, *20*(1), 24–38.
- Ricker, N. L., & Lee, J. H. (1995). Nonlinear model predictive control of the Tennessee Eastman challenge process. *Computers & Chemical Engineering*, *19*(9), 961–981.
- Rosow, C. E. (1997). Anesthetic drug interaction: An overview. *Journal of Clinical Anesthesia*, *9*(6 Suppl), 27S–32S.
- Sakai, T., Matsuki, A., White, P. F., & Giesecke, A. H. (2000). Use of an EEG-bispectral closed-loop delivery system for administering propofol. *Acta Anaesthesiologica Scandinavica*, *44*(8), 1007–1010.
- Sartori, V., Schumacher, P. M., Bouillon, T., Luginbuehl, M., & Morari, M. (2005). On-line estimation of propofol pharmacodynamic parameters. In *Proceedings of the 27th Annual International Conference of the IEEE Engineering in Medicine and Biology*, Shanghai, China, pp. 74–77.
- Sawaguchi, Y., Furutani, E., Shirakami, G., Araki, M., & Fukuda, K. (2008). A model-predictive hypnosis control system under total intravenous anesthesia. *IEEE Transactions on Biomedical Engineering*, *55*(3), 874–887.
- Schnider, T. W., Minto, C. F., Gambus, P. L., Andresen, C., Goodale, D. B., Shafer, S. L., & Youngs, E. J. (1998). The influence of method of administration and

- covariates on the pharmacokinetics of propofol in adult volunteers. *Anesthesiology*, 88(5), 1170–1182.
- Schnider, T. W., Minto, C. F., Shafer, S. L., Gambus, P. L., Andresen, C., Goodale, D. B., & Youngs, E. J. (1999). The influence of age on propofol pharmacodynamics. *Anesthesiology*, 90(6), 1502–1516.
- Schraag, S., Flaschar, J., Schleyer, M., Georgieff, M., & Kenny, G. N. C. (2006). The contribution of remifentanyl to middle latency auditory evoked potentials during induction of propofol anesthesia. *Anesthesia & Analgesia*, 103(4), 902–907.
- Schuttler, J., & Ihmsen, H. (2000). Population pharmacokinetics of propofol: A multicenter study. *Anesthesiology*, 92(3), 727–738.
- Schwilden, H., Schuttler, J., & Stoeckel, H. (1987). Closed-loop feedback control of methohexital anesthesia by quantitative EEG analysis in humans. *Anesthesiology*, 67(3), 341–347.
- Schwilden, H., & Schuttler, J. (1995). *Model-based adaptive control of volatile anesthetics by quantitative EEG*. Berlin: Springer-Verlag.
- Schwilden, H., & Stoeckel, H. (1993). Closed-loop feedback controlled administration of alfentanil during alfentanil-nitrous oxide anaesthesia. *British Journal of Anaesthesia*, 70(4), 389–393.
- Schwilden, H., Stoeckel, H., & Schuttler, J. (1989). Closed-loop feedback control of propofol anaesthesia by quantitative EEG analysis in humans. *British Journal of Anaesthesia*, 62(3), 290–296.
- Seborg, D. E., Edgar, T. F., & Mellichamp, D. A. (2004). *Process Dynamics and Control*. John Wiley & Sons: New York.
- Sigl, J. C., & Chamoun, N. G. (1994). An introduction to bispectral analysis for the electroencephalogram. *Journal of Clinical Monitoring*, 10(6), 392–404.

- Sreenivas, Y., Lakshminarayanan, S., & Rangaiah, G. P. (2008). Advanced regulatory controller for automatic control of anesthesia. In *IFAC Proceedings*, Vol. 17, pp. 11636–11641.
- Sreenivas, Y., Lakshminarayanan, S., & Rangaiah, G. P. (2009a). A comparative study of three advanced controllers for the regulation of hypnosis. *Journal of Process Control*, *19*, 1458–1469.
- Sreenivas, Y., Yeng, T. W., Rangaiah, G. P., & Lakshminarayanan, S. (2009b). A comprehensive evaluation of PID, cascade, model-predictive, and RTDA controllers for regulation of hypnosis. *Industrial and Engineering Chemistry Research*, *48*(12), 5719–5730.
- Sreenivas, Y., Lakshminarayanan, S., & Rangaiah, G. P. (2009c). Advanced control strategies for the regulation of hypnosis with propofol. *Industrial and Engineering Chemistry Research*, *48*(8), 3880–3897.
- Stoelting, R., & Hillor, S. (2006). *Handbook of Pharmacology & Physiology in anesthetic practice*. 2 ed. Lippincott Williams & Wilkins, Philadelphia, Pennsylvania.
- Struys, M. M. R. F., Jensen, E. W., Smith, W., Smith, N. T., Rampil, I., Dumortier, F. J. E., Mestach, C., & Mortier, E. P. (2002). Performance of the ARX-derived auditory evoked potential index as an indicator of anesthetic depth: a comparison with bispectral index and hemodynamic measures during propofol administration. *Anesthesiology*, *96*(4), 803–816.
- Struys, M. M. R. F., Mortier, E. P., & Smet, T. De (2006). Closed loops in anaesthesia. *Best Practice & Research Clinical Anaesthesiology*, *20*(1), 211–220.
- Struys, M. M. R. F., Smet, T. De, Greenwald, S., Absalom, A. R., Bing, S., & Mortier, E. P. (2004). Performance evaluation of two published closed-loop control systems using bispectral index monitoring: A simulation study. *Anesthesiology*, *100*(3), 640–647.

- Struys, M. M. R. F., Vereecke, H., Moerman, A., Jensen, E. W., Verhaeghen, D., Neve, N. D., Dumortier, F. J. E., & Mortier, E. P. (2003). Ability of the bispectral index, autoregressive modelling with exogenous input-derived auditory evoked potentials, and predicted propofol concentrations to measure patient responsiveness during anesthesia with propofol and remifentanyl. *Anesthesiology*, *99*(4), 802–812.
- Struys, M. M., Smet, T. De, Versichelen, L. F., Velde, S. V. D., den Broecke, R. V., & Mortier, E. P. (2001). Comparison of closed-loop controlled administration of propofol using Bispectral Index as the controlled variable versus “standard practice” controlled administration. *Anesthesiology*, *95*(1), 6–17.
- Tackley, R. M., Lewis, G. T., Prys-Roberts, C., Boaden, R. W., Dixon, J., & Harvey, J. T. (1989). Computer controlled infusion of propofol. *British Journal of Anaesthesia*, *62*(1), 46–53.
- Viertio-Oja, H., Maja, V., Sarkela, M., Talja, P., Tenkanen, N., Tolvanen-Laakso, H., Paloheimo, M., Vakkuri, A., Yli-Hankala, A., & Merilainen, P. (2004). Description of the entropy algorithm as applied in the Datex-Ohmeda S/5 entropy module. *Acta Anaesthesiologica Scandinavica*, *48*(2), 154–161.
- Vuyk, J. (1997). Pharmacokinetic and pharmacodynamic interactions between opioids and propofol. *Journal of Clinical Anesthesia*, *9*(6), 23S–26S.
- Vuyk, J. (2001). Clinical interpretation of pharmacokinetic and pharmacodynamic propofol-opioid interactions. *Acta Anaesthesiologica Belgica*, *52*(4), 445–451.
- Vuyk, J., Mertens, M. J., Olofsen, E., Burm, A. G., & Bovill, J. G. (1997). Propofol anesthesia and rational opioid selection: determination of optimal EC_{50} - EC_{95} propofol-opioid concentrations that assure adequate anesthesia and a rapid return of consciousness. *Anesthesiology*, *87*(6), 1549–1562.

- Wakeling, H. G., Zimmerman, J. B., Howell, S., & Glass, P. S. (1999). Targeting effect compartment or central compartment concentration of propofol: What predicts loss of consciousness? *Anesthesiology*, *90*(1), 92–97.
- Wang, L. (2004). Discrete model predictive controller design using Laguerre functions. *Journal of Process Control*, *14*(2), 131–142.
- Wang, L., & Young, P. C. (2006). An improved structure for model predictive control using non-minimal state space realisation. *Journal of Process Control*, *16*(4), 355–371.
- Warner, D. S., Hindman, B. J., Todd, M. M., Sawin, P. D., Kirchner, J., Roland, C. L., & Jamerson, B. D. (1996). Intracranial pressure and hemodynamic effects of remifentanyl versus alfentanil in patients undergoing supratentorial craniotomy. *Anesthesia & Analgesia*, *83*(2), 348–353.
- Wojsznis, W. K., Blevins, T. L., & Thiele, D. (1999). Neural network assisted control loop tuner. In *Proceedings of the IEEE International Conference on Control Applications*, Vol. 1. Kohala Coast, HI, USA, pp. 427–431.
- Yasuda, N., Lockhart, S. H., Eger, E. I., Weiskopf, R. B., Liu, J., Laster, M., Taheri, S., & Peterson, N. A. (1991). Comparison of kinetics of sevoflurane and isoflurane in humans. *Anesthesia & Analgesia*, *72*(3), 316–324.
- Zhang, X.-S., Roy, R. J., & Huang, J. W. (1998). Closed-loop system for total intravenous anesthesia by simultaneously administering two anesthetic drugs. In *Proceedings of the 20th Annual International Conference of the IEEE Engineering in Medicine and Biology Society*, Hong Kong, pp. 3052–3055.

Appendix A

Presentations and Publications of the Author

Journal Publications

- Sreenivas Yelneedi, Lakshminarayanan S., and Rangaiah, G. P., “Advanced control strategies for the regulation of hypnosis with propofol,” *Industrial & Engineering Chemistry Research*, 48(8), pp. 3880–3897, April 2009.
- Yelneedi Sreenivas, Tian Woon Yeng, G. P. Rangaiah, and S. Lakshminarayanan, “A comprehensive evaluation of PID, cascade, model predictive and RTDA controllers for regulation of hypnosis,” *Industrial & Engineering Chemistry Research*, 48(12), pp. 5719–5730, June 2009.
- Sreenivas Yelneedi, Lakshminarayanan S., and Rangaiah, G. P., “A comparative study of three advanced controllers for the regulation of hypnosis,” *Journal of Process Control*, 19(9), pp. 1458–1469, October 2009.
- Sreenivas Yelneedi, Rangaiah, G. P., and Lakshminarayanan S., “Simultaneous regulation of hypnosis and analgesia using model predictive control,” under review.

Peer Reviewed Conference Papers

- Sreenivas Yelneedi, Lakshminarayanan S., and Rangaiah, G. P., “Advanced regulatory controller for automatic control of anesthesia,” *Proceedings of the 17th World Congress - The International Federation of Automatic Control (IFAC)*, July 6–11, 2008, Seoul, South Korea, vol. 17, pages 11636–11641.
- Yelneedi Sreenivas, S. Lakshminarayanan and G. P. Rangaiah, “A model predictive control strategy for the regulation of hypnosis,” *IFMBE Proceedings - World Congress on Medical Physics and Biomedical Engineering, August 27–September 1, 2006*, Seoul, South Korea, vol. 14, pages 77–81, 2007.
- Yelneedi Sreenivas, S. Lakshminarayanan and G. P. Rangaiah, “Automatic regulation of anesthesia by simultaneous administration of two anesthetic drugs using model predictive control,” *IFMBE Proceedings - World Congress on Medical Physics and Biomedical Engineering, August 27–September 1, 2006*, Seoul, South Korea, vol. 14, pages 82–86, 2007.

Conference Presentations

- “Adaptive model predictive control for automatic regulation of anesthesia by simultaneous administration of two intravenous drugs,” *AIChE Annual Meeting*, November 4–9, 2007, Salt Lake City, Utah, USA.
- “Analysis of sleep EEG signals by parametric modeling methods,” *12th International Conference on Biomedical Engineering (ICBME)*, December 7–10, 2005, Singapore.
- “Analysis of sleep EEG signals by parametric modeling methods,” *2nd Annual Graduate Student Symposium, National University of Singapore*, October 6, 2005, Singapore.

Conference Posters

- “A comprehensive evaluation of PID, cascade and model predictive controllers for isoflurane administration using BIS as the controlled variable,” *International Conference on Advanced Control of Industrial Processes (ADCONIP)*, May 4–7, 2008, Alberta, Canada.
- “Model predictive control strategy for the automatic regulation of anesthesia by simultaneous administration of two intravenous drugs,” *Graduate Student Symposium in Biological and Chemical Engineering, National University of Singapore*, September 14, 2007, Singapore.

Appendix B

Curriculum Vitae of the Author

YELNEEDI SREENIVAS

E5-03-30, Dept. of Chemical & Biomolecular Engineering, 4 Engineering Drive 4,
National University of Singapore, Singapore - 117576

E-mail: g0403168@nus.edu.sg *and* yelneedi@gmail.com

Tel: +65-91683957 (Mobile), +65-65165802 (Office)

Website: <http://cheed.nus.edu.sg/~chels/DACSPHOTOS/SREENIVASHP.html>

Education

- Doctor of Philosophy, Chemical Engineering 2004 – 2009
National University of Singapore, Singapore
Dissertation: Advanced Control Strategies for Automatic Drug Delivery to Regulate Anesthesia during Surgery
- Master of Technology, Chemical Engineering 1999 - 2001
Indian Institute of technology Madras, Chennai, India
- Bachelor of Technology, Chemical Engineering 1995 - 1999
Andhra University Engineering College, Visakhapatnam, India

Awards & Achievements

- Graduate Research Scholarship, NUS (August 2004–July 2008)
- Mico Bosch Medal for best project (Energy Conservation), Department of Chemical Engineering, Indian Institute of Technology Madras, Chennai, India (1999-2001)
- CGPA 8.97/10 in M.Tech. (top 5 out of 40)
- MHRD-GATE Scholarship by Government of India in M.Tech.
- 74th rank (top 4%) in GATE - 1999 (National Level Technical Examination, India)
- 407th rank (top 0.5%) in EAMCET - 1995 (State Level Technical Examination, Andhra Pradesh, India)

Professional Experience

- Research Assistant (part time: 4 months 2006/07) - ChemBioSys group, NUS: Systems Biomedical Engineering - worked on modeling transdermal drug delivery.
- Teaching Assistant (one semester: 2005/06) - Department of Chemical & Biomolecular Engineering, NUS: Tutor for one under graduate module (Process Modeling and Numerical Simulation).

- Grader (four semesters: 2005/06, 2006/07, 2007/08) - Design Project (HYSYS), Process Dynamics and Control, Numerical Methods, Process Systems Engineering for undergraduates; Mathematical Methods for Chemical & Environmental Engineering for graduates; and Data Based Process Characterization for both graduates and undergraduates. Helped several students in finishing their simulation works in MATLAB and HYSYS. Mentored two undergraduate students in their research projects.
- Lecturer (July 2001 - July 2004) - Department of Chemical Engineering, R.V.R. & J.C. College of Engineering, Guntur, Andhra Pradesh, India: Floated new projects in Aspen Plus, setup new experiments in Mass Transfer and Process Control Laboratories, supervised 12 students for undergraduate projects.

Research/Professional Interests

- First Principles and Data based Process Modeling, Design of Experiments
- Design and Tuning of PID and other control loops
- Multivariable Model Predictive Control
- Nonlinear State Estimation with Kalman Filtering
- Nonlinear Model Predictive Control
- Optimization of Chemical Processes
- Statistical Process Control

Computational Skills

- Process Modeling: Design of experiments, Data based process modeling
- Process Control Schemes: Model Predictive Control, Dynamic Matrix Control, IMC, PID etc.
- Software Packages: MATLAB, SIMULINK, HYSYS, HYSYS DYNAMICS, ASPEN PLUS, HX-NET, PRO II, FORTRAN, C, C++
- Operating Systems: Windows 2000/XP, UNIX, LINUX

Publications

1. Sreenivas Yelneedi, Lakshminarayanan S., and Rangaiah, G. P., "Advanced control strategies for the regulation of hypnosis with propofol," *Industrial & Engineering Chemistry Research*, 48(8), pp. 3880–3897, April 2009.
2. Yelneedi Sreenivas, Tian Woon Yeng, G. P. Rangaiah, and S., Lakshminarayanan, "A comprehensive evaluation of PID, cascade, model predictive and RTDA controllers for regulation of hypnosis," *Industrial & Engineering Chemistry Research*, 48(12), pp. 5719–5730, June 2009.

3. Sreenivas Yelneedi, Lakshminarayanan S., and Rangaiah, G. P., “A comparative study of three advanced controllers for the regulation of hypnosis,” *Journal of Process Control*, 19(9), pp. 1458–1469, October 2009.
4. Sreenivas Yelneedi, Rangaiah, G. P., and Lakshminarayanan S., “Simultaneous regulation of hypnosis and analgesia using model predictive control,” under review.

Peer Reviewed Conference Papers

1. Sreenivas Yelneedi, Lakshminarayanan S., and Rangaiah, G. P., “Advanced regulatory controller for automatic control of anesthesia,” *Proceedings of the 17th World Congress - The International Federation of Automatic Control (IFAC)*, Seoul, South Korea, vol. 17, pages 11636–11641, 2008.
2. Yelneedi Sreenivas, S. Lakshminarayanan and G. P. Rangaiah, “A model predictive control strategy for the regulation of hypnosis,” *IFMBE Proceedings - World Congress on Medical Physics and Biomedical Engineering 2006*, Seoul, South Korea, vol. 14, pages 77-81, 2007.
3. Yelneedi Sreenivas, S. Lakshminarayanan and G. P. Rangaiah, “Automatic regulation of anesthesia by simultaneous administration of two anesthetic drugs using model predictive control,” *IFMBE Proceedings - World Congress on Medical Physics and Biomedical Engineering 2006*, Seoul, South Korea, vol. 14, pages 82-86, 2007.

Conference Presentations

1. Sreenivas Yelneedi, Lakshminarayanan S., and Rangaiah G. P., “Adaptive model predictive control for automatic regulation of anesthesia by simultaneous administration of two intravenous drugs,” Presented in *AICHE Annual Meeting*, 2007, Salt Lake City, Utah, USA.
2. Yelneedi S., Chiu M. S., Lakshminarayanan S., Karimi I. A., Lee D. Y., Rao R. K., Rangaiah G. P., “Systems engineering approach for human body temperature regulation - a review,” Presented in *3rd WACBE World Congress on Bioengineering*, 2007, Bangkok, Thailand.
3. Y. Sreenivas, S. Lakshminarayanan, G. P. Rangaiah, “Analysis of sleep EEG signals by parametric modeling methods,” Presented in *12th International Conference on Biomedical Engineering (ICBME)*, 2005, Singapore.
4. Sreenivas Yelneedi, Meena V., “Studies on fermentation of glucose using different bioreactors,” Presented in *National Seminar on Modern Biology*, 2003, Nagarguna Nagar, India.

Conference Posters

1. Tian Woon Yeng, Yelneedi Sreenivas, G. P. Rangaiah, and S. Lakshminarayanan. “A comprehensive evaluation of PID, cascade and model predictive controllers for isoflurane administration using BIS as the controlled variable,” Presented in *International Conference on Advanced Control of Industrial Processes (AD-CONIP)*, 2008, Alberta, Canada.

Additional Training

- *Presentation Skills Workshop*, September 18-25, 2006.
- *Training Course for Teaching Assistants*, May 18-19, 2005, National University of Singapore.
- *Analytical and Numerical Methods in Modeling and Simulation of Engineering Systems*, January 12-16, 2004, Department of Chemical Engineering, Indian Institute of Technology Madras, Chennai, India.
- *Modeling, Simulation and analysis of Enhanced Distillation Processes*, May 12-16, 2003, Department of Chemical Engineering, Indian Institute of Technology Madras, Chennai, India.
- Done Project work on “*Material Balances, Energy Balances of Ammonia Plant and Calculation of Catalyst Activity*,” during January 1-18, 1998 in Nagarjuna Fertilizers and Chemicals Limited (NFCL), Kakinada, India.

Extra Curricular Activities

- Student member of the Graduate Students Association (GSA), Department of Chemical & Biomolecular Engineering, NUS (2005-2006) - served as Web Master: developed HTML scripts to maintain Department’s GSA website.

Personal Particulars

Nationality : Indian
Marital Status : Married
Languages : English, Hindi and Telugu

REFERENCES

Prof. G. P. Rangaiah (Thesis Advisor)

Deputy Head, Student and Academic Affairs
Department of Chemical & Biomolecular Engineering
4 Engineering Drive, 4
National University of Singapore, Singapore - 117576.
E-mail: chegpr@nus.edu.sg
Tel: +65 - 6516 2187, Fax: +65 - 6516 1936

Dr. S. Lakshminarayanan (Thesis Advisor)

Department of Chemical & Biomolecular Engineering
4 Engineering Drive, 4
National University of Singapore, Singapore - 117576
E-mail: chels@nus.edu.sg
Tel: +65 - 6516 8484, Fax: +65 - 6516 1936